UNIVERSITÀ DEGLI STUDI DI MILANO

Dipartimento di Biotecnologie mediche e medicina molecolare

Corso di Dottorato in

Biotecnologie Applicate alle Scienze Mediche
XXVI Ciclo

DUAL ROLE OF SNAP-25 AT PRE- AND POST-SYNAPTIC LEVEL DURING DEVELOPMENT

Bio/14

Tesi di Dottorato di:

Giuliana FOSSATI

Matricola R09293

Direttore del corso: Prof. Alessandro GIANNI

Tutor: Prof.ssa Michela MATTEOLI

Co-tutor: Dott.ssa Elisabetta MENNA

Anno accademico 2012 / 2013

TABLE OF CONTENTS

1) *Antonucci F, Corradini I, Morini R,* **Fossati G**, *Menna E, Pozzi D, Pacioni S, Verderio C, Bacci A, Matteoli M (2013) Reduced SNAP-25 alters short-term plasticity at developing glutamatergic synapses. EMBO reports* **14:** *645-651*

2) *Menna E, Zambetti S, Morini R, Donzelli A, Disanza A, Calvigioni D, Braida D, Nicolini C, Orlando M,* **Fossati G**, *Cristina Regondi M, Pattini L, Frassoni C, Francolini M, Scita G, Sala M, Fahnestock M, Matteoli M (2013) Eps8 controls dendritic spine density and synaptic plasticity through its actin-capping activity. EMBO J* **32:** *1730-1744*

3) *Menna E,* **Fossati G**, *Scita G, Matteoli M (2011) From filopodia to synapses: the role of actin-capping and anti-capping proteins. The European journal of neuroscience* **34:** *1655-1662*

ABSTRACT

Impairment of synaptic function can lead to neurological and psychiatric disorders collectively referred to as synaptopathies. SNAP-25, a SNARE protein controlling synaptic vesicle exocytosis and fundamental presynaptic functions, is implicated in several brain pathologies and, indeed, brain areas of psychiatric patients often display reduced SNAP-25 expression.

We observed that halved SNAP-25 levels at 13–14DIV not only fail to impair synaptic transmission, but instead enhance evoked glutamatergic neurotransmission. This effect is probably dependent on presynaptic voltage-gated calcium channel activity and it is not followed by changes in spontaneous quantal events or in the pool of readily releasable synaptic vesicles. Notably, synapses of neurons with reduced SNAP-25 levels show paired-pulse depression as opposed to paired-pulse facilitation occurring in their wild-type counterpart. These phenotypes disappear with synapse maturation, where instead a reduction of evoked glutamatergic transmission and mEPSC amplitude emerge in heterozygous neurons thus suggesting the onset of a postsynaptic defect. In fact, it has been recently reported that a peculiar postsynaptic SNARE complex is required for long-term potentiation; however, the role of SNAP-25 in this process is not completely understood. We recently demonstrated that acute down-regulation of SNAP-25 in vitro affects spine morphogenesis through binding to p140Cap, thus suggesting that the protein may exert a structural role at the postsynaptic level. Here we demonstrate that in vivo acute down-regulation of SNAP-25 in CA1 hippocampal neurons affects spine number and morphology and causes a specific reduction of the postsynaptic protein PSD-95. Consistently, hippocampal neurons from SNAP-25 het mice show a flawed maturation of postsynaptic specializations, reduced densities of dendritic spines and defective PSD-95 clustering. These effects do not stem from impaired presynaptic function, but as a direct consequence of reduced SNAP-25 levels in the postsynaptic compartment. By co-immunoprecipitation and LUMIER Assay, we show that SNAP-25, PSD-95 and p140Cap are part of the same molecular complex in the brain, with p140Cap being intrinsically capable to bind either to SNAP-25 and PSD-95. These data provide new mechanistic insights as to SNAP-25 involvement in synaptopathies that go beyond the protein's known roles in presynaptic function.

INTRODUCTION

1- THE SYNAPSE

Chemical synapses are complex cellular junctions specialized for communication between neurons. Charles Sherrington originally introduced the term 'synapse' more than 100 years ago.

For the most part, synapses are formed as either axo-dendritic or axo-somatic contacts, in which the axon of the cell of origin makes its functional contact with the dendrite or the soma of the target cell; contacts between adjacent cell bodies (soma-somatic) or overlapping dendrites (dendro-dendritic) are more rare. The synapse is a complex of a presynaptic element, a postsynaptic element and a cleft. Information arrives at a presynaptic terminal in the form of an action potential and is transmitted to the postsynaptic cell via a chemical neurotransmitter.

Synapses are the most complex subcellular compartments of neurons, indeed. The synapse proteome - the set of proteins in the presynaptic and postsynaptic compartments - is much more complex than anticipated based on earlier pharmacological and electrophysiological studies. Proteomic studies show that between 1,000 and 2,000 proteins are present in rodent synapses, and these are organized into multi-protein complexes and molecular networks. This molecular complexity is also found in human synapses. Synapses are also greatly complex cell biological machines. Synaptic transmission is dependent on a spatially and temporally coordinated cascade of biochemical and cell biological processes that control presynaptic action potential generation, ion channel activation, synaptic vesicle trafficking and fusion, neurotransmitter receptor activation, and postsynaptic signal propagation, as well as numerous other collateral processes that are necessary to establish synapses, to modify their efficacy on short-term and long-term time scales, and to provide them with the necessary metabolic support.

Nowadays it is accepted that the correct development and functioning of the synapse requires the fundamental role of glia. The concept of "tripartite synapse" began with a series of evidences that revealed the existence of bidirectional communication between

neurons and astrocytes (Bezzi and Volterra 2001; Perea et al. 2009). The signaling pathway between neurons and astrocytes at the "tripartite synapse" is reciprocal; astrocytes sense neuronal activity by increasing intracellular levels of calcium and respond by releasing a variety of different molecules (Santello et al., 2012). However, not all the synapses are tripartite, in the hippocampus only 40% is enfolded by astrocytes (Perea *et al*., 2009, Halassa *et al*., 2009)

.
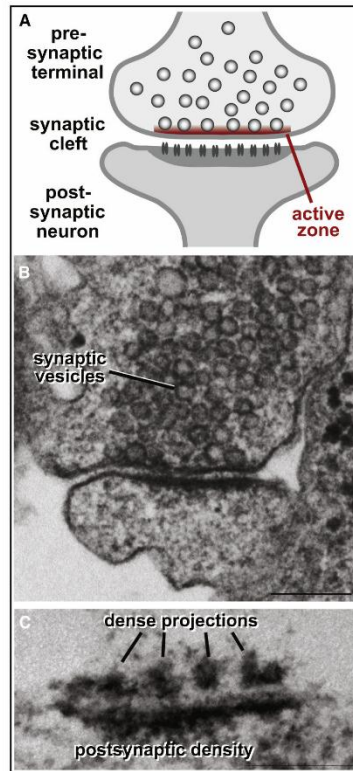
Fig. 1: A) Cartoon of a synapse. B) Hippocampal synapse at electron microscopy. C) Visualization of pre- and postsynaptic specializations. From Sudhof, 2012.

1.1 THE PRESYNAPTIC TERMINAL

At the presynaptic terminal, neurotransmitters are packaged into synaptic vesicles (SVs); when an action potential opens presynaptic voltage-gated Ca2.1 channels, the neurotransmitters are released by calcium-triggered exocytosis into the synaptic cleft thus leading to postsynaptic receptors activation. SV exocytosis is restricted to the small section of the presynaptic plasma membrane containing an electrondense material called the "active zone", which contains clustered Cav2 (P/Q and N-type) voltage-gated Ca2.1

channels (Benarroch, 2013). Presynaptic active zones perform four principal functions in neurotransmitter release. First, they dock and prime synaptic vesicles; note, however, that SNARE and synaptic membrane (SM) proteins which are the core fusion proteins of synaptic vesicles, are not enriched in the active zone. Second, active zones recruit voltage-gated Ca^{2+} channels to the presynaptic membrane to allow fast synchronous excitation/release coupling. Third, active zones contribute to the precise location of pre- and postsynaptic specializations exactly opposite to each other via trans-synaptic cell-adhesion molecules. Finally, active zones mediate much of the short- and long-term presynaptic plasticity observed in synapses, either directly, by responding to second messengers such as Ca^{2+} or diacylglycerol whose production causes plasticity, or indirectly, by recruiting other proteins that are responsible for this plasticity. All of these functions aim to finely control neurotransmitter release and allow presynaptic vesicle exocytosis, which occurs with the required speed and plasticity needed for the information transfer and computational function of a synapse (Owald and Sigrist, 2009; Sudhof, 2012).

When a nerve terminal is stimulated, not all vesicles can be released immediately. The existence of two distinct presynaptic pools of transmitter, a "readily releasable" fraction, which is depleted at high frequencies of stimulation, and a "non-readily releasable" fraction has been indeed demonstrated. Current research suggests that the *readily releasable pool* (RRP) is the vesicle sub-population that is immediately available for release upon stimulation (usually being thought to include vesicles docked at the active zone and primed for release). A much bigger population of vesicles constitutes the *reserve pool* (RP); these vesicles are thought of residing at some distance away from the active zone, and requiring some form of transport or change in docking state to become fusion competent (for reviews see Rodesch and Broadie, 2000; Rizzoli and Betz, 2003; Neher and Sakaba, 2008).

All presynaptic functions, directly or indirectly, involve synaptic vesicles. Synaptic vesicles undergo a trafficking cycle in the nerve terminal that can be divided into sequential steps: First, neurotransmitters are actively transported into synaptic vesicles (step 1), and synaptic vesicles cluster in front of the active zone (step 2). Then synaptic vesicles dock at the active zone (step 3), where the vesicles are primed (step 4) to convert them into a state of competence for Ca^{2+}-triggered fusion-pore opening (step 5). After fusion-pore opening, synaptic vesicles are recycled probably by three alternative pathways: (*a*) Vesicles are reacidified and refilled with neurotransmitters without

undocking, thus remaining in the RRP (step 6, called "kiss-and-stay"); (*b*) vesicles undock and recycle locally (step 7, called "kiss-and-run") to reacidify and be refilled with neurotransmitters (back to steps 1 and 2); or (*c*) vesicles are taken up via clathrin-coated pits (step 8) and reacidified and refilled with neurotransmitters either directly or after passing through an endosomal intermediate (step 9) (Sudhof, 2004; JahnandFasshauer, 2012).
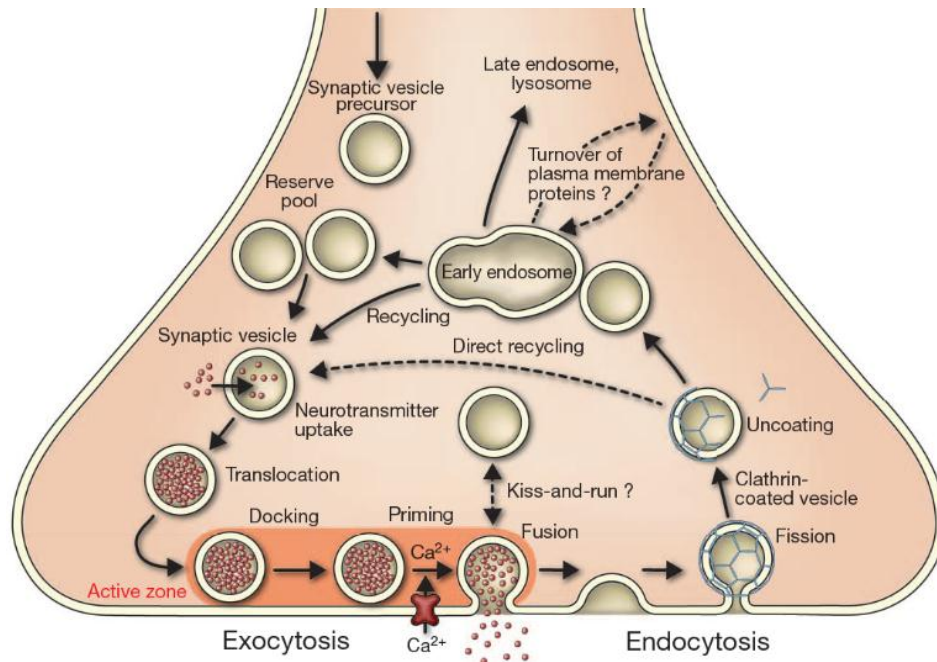

Fig. 2: The synaptic vesicles cycle: synaptic vesicles are filled with neurotransmitter. Active vesicles dock to release sites in the active zone. Vesicles are primed to acquire release readiness of the exocytotic complex. After exocytosis, the vesicle proteins probably remain clustered and they are then retrieved by endocytosis. Synaptic vesicles are regenerated within the nerve terminal, probably involving a passage through an endosomal intermediate. Actively recycling vesicles are in slow exchange with the reserve pool. From Jahn and Fasshauer, 2012.

1.2 THE POSTSYNAPTIC TERMINAL

Studies around the postsynaptic compartment began in 1907, when the British physiologist J. Langley introduced the concept of receptor molecules to explain the specific and potent actions of certain chemicals on muscle and nerve cells (Purves et al., Neuroscience, 3rd ed., 2004). Neurotransmitters released from the presynaptic terminal of a chemical synapse bind to receptors in the postsynaptic membrane. The receiving synapse can be excitatory or inhibitory. On the postsynaptic side of the most part of excitatory synapses, multiprotein complexes make up a region known as the postsynaptic density (PSD) which mediate clustering of receptors and cell-adhesion

molecules and orchestrate the coupling of diverse signaling components (Kim and Sheng, 2004).

Ongoing research has focused on the identification of the protein components that are part of this huge macromolecular signaling complex. In general, one can subdivide these proteins into classes of (1) cell-adhesion proteins, (2) cytoskeletal proteins, (3) scaffolding and adaptor proteins, (4) membrane-bound receptors and channels, (5) G-proteins and modulators and (6) signaling molecules including kinases/phosphatases (Sala et al., 2008). Large PSDs are especially characteristic of glutamatergic excitatory synapses. PSDs are either located directly on the dendritic shaft or at the tip of tubular, thin, stubby or mushroom-shaped dendritic spines and lie just below the postsynaptic membrane. They form a 30nm- to 40nm-thick protein meshwork with a diameter of a few hundred nanometers (Boeckers, 2006). The maintenance of the synaptic structure requires a constant replacement of proteins, lost by degradation, with newly synthesized ones. During constitutive replacement, however, the synaptic strength must be preserved, which is particularly important when it relates to the exchange of scaffold proteins such as PSD-95 (see below), because these proteins offer the necessary binding sites that regulate the receptor number at synapses. In line with these observations, synaptic PSD-95 clusters may be stable for days, yet individual PSD-95 molecules exchange with a half-life of less than one hour (Gray et al., 2006).

Throughout the brain and spinal cord, the amino acid glutamate mediates the vast majority of excitatory neurotransmission. Glutamate acts on various membrane receptors, in particular ionotropic glutamate receptors (iGluRs), which form cation-permeable ion channel receptors and can be subdivided into three large families: AMPA receptors (α-amino-3-hydroxy-5-methyl-4-isoxazolepropionic acid), kainate receptors and NMDA receptors (N-methyl-D-aspartate) (Paoletti et al., 2013). These receptors show a different permeability to Na^+ or Ca^{2+} related to the family and the subunit composition of the receptor. Another group of receptors called metabotropic receptors act through secondary messengers (mGluR).

NMDA receptors require, to be activated, a strong AMPAR-mediated membrane depolarization, to remove the Mg^{2+} that blocks the resting channels (Dingledine *et al.*, 1999). To date, seven different subunits have been identified. The GluN1 subunit, four distinct GluN2 subunits (GluN2A, GluN2B, GluN2C and GluN2D), which are encoded by four different genes, and a pair of GluN3 subunits (GluN3A and GluN3B), arising

from two separate genes (Paoletti et al., 2013). Different combinations of these subunits produce a variety of postsynaptic responses.

In the mammalian central nervous system, AMPA-type glutamate receptors are responsible for fast excitatory synaptic transmission. AMPARs are tetramers made up of combinations of four subunits: GluA1, GluA2, GluA3, and GluA4 (Dingledine et al., 1999, Isaac et al., 2007).

Kainate-type glutamate receptors are expressed throughout the mammalian central nervous system (CNS) and affect neural circuit activity through the modulation of excitatory and inhibitory tone, neuronal excitability, synaptic development and various other aspects of brain function (Copits and Swanson, 2013).

Metabotropic receptors are composed by a 7-fold transmembrane peptide (mGlu1-8). They are coupled to G-proteins and act through second messengers into the cytoplasm. Metabotropic glutamate receptors can also modulate the release and/or actions (directly or indirectly) of other neurotransmitters (Coutinho and Knopfel, 2002).

It is widely believed that synapses constitute key loci for modifying neuronal network function and glutamate receptors are fundamental players in the establishment of synaptic plasticity, classically defined as a series of changes in the strength of synaptic connections, resulting in the final adaptations of neural networks to several stimuli (Bliss et al., 1973). Many synapses in the mammalian CNS exhibit long-lasting forms of synaptic plasticity that are plausible substrates for more permanent changes in behavior. Synaptic plasticity is thus believed to be the cellular correlate of learning and memory. Long-term potentiation (LTP) and long-term depression (LTD) at glutamate excitatory synapses represent the most widely studied mechanisms of synaptic plasticity, and provide either a learning-based synapse reinforcement or a weakening, respectively (Isaevoli et al., 2013). LTP is induced by AMPA-mediated depolarization that results in Mg^{2+} elimination from the NMDA channel. Removal of Mg^{2+} allows Ca^{2+} to enter the postsynaptic neuron and the resulting increase in Ca^{2+} concentration within the dendritic spines of the postsynaptic cell turns out to be the trigger for LTP (Malenka and Bear, 2004). Long-lasting changes have been described to occur by means of PSD scaffolding proteins. Although scaffolding proteins may not directly modify the amplitude or the frequency of excitatory post-synaptic currents, they have been found to affect synaptic strength (Iasevoli et al., 2013)
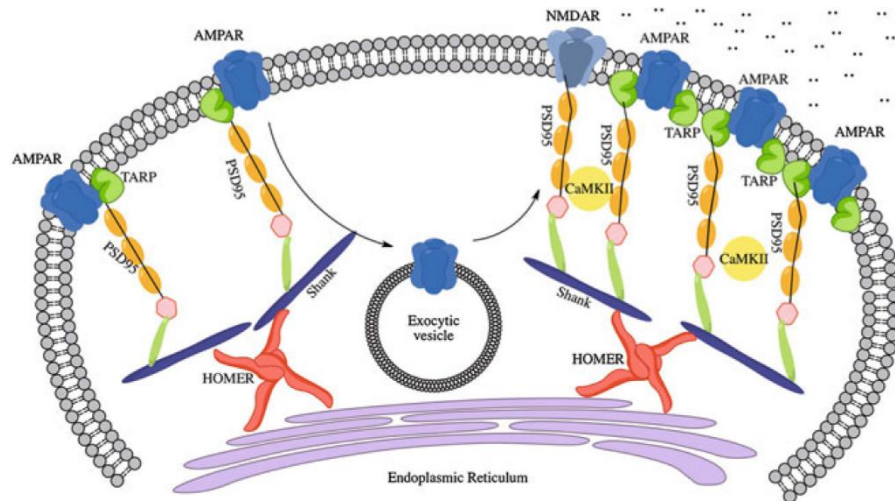
Fig. 3: LTP guides clustering of receptors in the membrane following AMPA-mediated depolarization. The stimulus activate NMDA receptors and induce LTP. Scaffold proteins such as PSD-95 are responsible for the postsynaptic remodeling. From Iasevoli et al., 2013.

1.3 DENDRITIC SPINES

Dendritic spines are the specialized subcellular compartments that characterize dendritic arbors. They are the main site of synaptic input for excitatory neurons. Spines act as subcellular compartment that locally control the signaling mechanisms and they are crucially involved in receiving and processing synaptic information. Neurotransmitter receptors are largely restricted to the surface of spines and concentrated in the membrane area facing the presynaptic element (Halbach, 2009). Concerning the hippocampus, it has been shown that dendritic spines are the predominant sites of excitatory synapses on CA1 pyramidal neurons (Megias al., 2001), where most spines are contacted by a single presynaptic bouton (Andersen, 1990). Thus, hippocampal spines rarely have inhibitory or peptidergic modulatory synapses, instead, the modulatory synapses tend to be located on neighboring dendritic shafts or cell soma (Sorra and Harris, 2000).

From a structural point of view, a dendritic spine consists of a head that is connected to the dendritic shaft by a narrow neck. Depending on the shape, the dendritic spines can be subdivided into different categories. 1) Mushroom spines with a large head and a narrow neck. 2) Thin spines with a smaller head and a narrow neck. 3) Stubby spines without an obvious constriction between the head and the attachment to the shaft (Peters

8

and Kaiserman- Abramof, 1970; Halbach, 2009; Rochefort and Konnerth, 2012). Spine neck allows the formation of an isolated biochemical and electrical compartment, which enables each synapse on a single spine to function and be regulated independently (Lai and Ip, 2013). By using glutamate uncaging on single spines, it has been demonstrated that spine morphology correlates directly with the number of AMPA receptors, and that the spine–neck geometry is an important determinant of NMDA receptor-dependent calcium signalling in spine head and dendritic shaft (Rochefort and Konnerth, 2012). The size of dendritic spines varies among brain areas, as well as between species (Rochefort and Konnerth, 2012). Interestingly, spines are present at the squid giant synapses (Young, 1973) but are rarely found in other lower organisms, suggesting that they may have developed early in evolution in order to implement more complex nervous systems functions (Sala et al., 2008).

Although de novo formation of dendritic spines in adult mice has been described, most spines are thought to arise from dendritic filopodia during early postnatal life. Filopodia are more prominent in the developing brain at early postnatal stages and diminish with adulthood. One prevailing view is that filopodia represent the spine precursors during synapse formation. The long necks of filopodia would render them highly mobile and hence facilitate the search for presynaptic partners during synaptogenesis (Lai and Ip, 2013). Dendritic filopodia have a network-like organization of actin filaments (Korobova and Svitkina, 2010), which provide the structural basis for spine formation and elimination (Cingolani and Goda, 2008). When a presynaptic terminal encounters a filopodium, a cluster of actin filaments appears at the contact site in the filopodium. The stabilization of filopodia to form new synaptic contacts is based on a rapid and persistent reorganization of the spine actin cytoskeleton (Luscher et al, 2000; Jourdain et al, 2003; Nikonenko et al, 2003; Honkura et al, 2008). This mainly consists of a reduced depolymerization rate from the pointed end of the filament, at the core of the spine, with polymerization continuing at the barbed end, in the spine periphery (Okamoto et al, 2004; Ramachandran and Frey, 2009). Early spines are often very long and have filopodia-like shape but, later during development, their mean length decreases and the number of filopodia is greatly reduced. Three major changes can be observed during the maturation process: an increase in spine density, a decrease in overall length and a decrease in the number of dendritic filopodia with a simultaneous decrease in spine motility (Sala et al., 2008).

It is well known that the morphological changes of dendritic spines occurring both during development and plasticity phenomena require the active remodeling of actin cytoskeleton. In a recent work to which I contributed, it has been shown that proteins involved in the regulation of the actin cytoskeleton dynamics affect the spine growth. These proteins act as actin anti-capping or capping proteins. These proteins, which are fundamental in orchestrating the processes which control neuronal connectivity and plasticity, have been recently detected in dendritic spines (Menna et al., 2011). In particular, we found a prominent role of the actin capping protein Eps8, which absence impairs spine enlargement and plasticity (Menna et al., 2013). Many other different proteins are involved in spine dynamics, for reviews see Sala et al., 2008 and Koleske, 2013.

Dendritic spines are not static; they change morphology continuously, even throughout adulthood, reflecting the plastic nature of synaptic connections. Activity patterns that induce LTP cause enlargement of spine heads, suggesting that changes in dendritic spine morphology play an important role in memory formation (Houtulainen and Hoogenrad, 2010).

One mechanism which regulates spine morphology is the local addition or removal of synaptic membrane and turnover of postsynaptic receptors, which associates with the rapid formation of new spines depending on NMDA receptor activation. This is confirmed in dissociated hippocampal neurons upon the induction of chemically-induced LTP (cLTP) with glycine (Lu et al., 2001), a protocol which triggers rapid enlargement of the spine heads. Spine enlargement precedes the increase in AMPA receptor insertion and larger spines are associated with larger postsynaptic densities, greater glutamate-induced currents and calcium influx (Lai and Ip, 2013). Therefore, during LTP, activation of NMDA receptors increases connectivity of specific neurons through modulation of dendritic spines in three different ways: the enlargement of pre-existing spines, the stabilization of newly-formed spines, and the formation of new spines (Lai and Ip, 2013).

Enlargement of dendritic spines is not the only morphological modification observed after LTP. For example, mobilization of recycling endosomes and vesicles and amorphous vesicular clumps into spines have been observed within minutes after the induction of LTP (Park et al., 2006). Electron microscopy analysis has shown that the size of the PSD is perfectly correlated with the size of the presynaptic bouton and the

number of vesicles it contains (Harris et al. 1992). Therefore, PSD enlargement induced by LTP might presumably induce an enlargement of the presynaptic active zone and increase in the number of presynaptic vesicles (Sala et al., 2008).
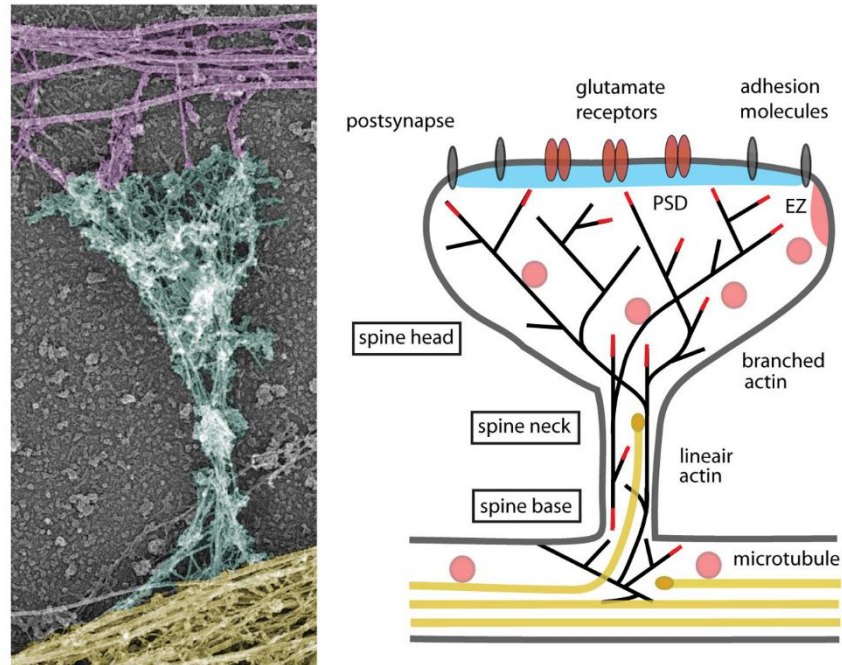

Fig. 4: Left, actin and microtubule cytoskeleton organization in a mature dendritic spine from cultured hippocampal neurons visualized by platinum replica electron microscopy. Axonal cytoskeleton, purple; dendritic shaft, yellow; dendritic spine, cyan. Right, diagram of a mature mushroom-shaped spine showing the postsynaptic membrane containing the postsynaptic density (PSD; blue), adhesion molecules (gray) and glutamate receptors (reddish brown), the actin (black lines) and microtubule (yellow) cytoskeleton, and organelles. Dendritic spines exhibit a continuous network of both straight and branched actin filaments (black lines). Modified from Houtulainen and Hoogenraad, 2010.

1.4 PSD-95

PSD-95 (95kDa) is the most abundant protein of the postsynaptic density; it forms the core of the scaffold at excitatory synapses (Boeckers, 2006).

PSD-95/SAP90 is a member of the membrane-associated guanylate kinase family (MAGUK), which has master-organizing roles in the multimerization and clustering of protein complexes within the PSD. PSD-95 protein contains in its structure three repeated PDZ (PSD-95/disc large/zonula occludens-1) domains, one SH3 (Src homology 3), and one guanylate kinase (GUK) domain (Zhang et al., 2013). PDZ domains are peptide-binding domains located at the C-terminus of MAGUK proteins, which may enable PSD-95 to interact with several binding partners within the PSD, such as NMDAR and serotonin receptor subunits, as well as other tyrosine kinase

receptors and ion channels, cell adhesion molecules, and cytoplasmic proteins (de Bartolomeis et al., 2013). Thus, by assembling in multimers with other PSD proteins, PSD-95 enables the formation of extensive protein complexes that organize receptors and signal transduction proteins in the PSD. Indeed, affinity-purified PSD-95 complexes have been described to include (AMPAR) subunits (GluA1, GluA2, GluA3, GluA4), NMDAR subunits (GluN1, GluN2A, GluN2B), scaffolding proteins (PSD-93, Shank2, Shank3, Homer, SAPAP1, SAPAP2, SAPAP4), G-protein regulators (such as SynGAP or BRAG1), and other PSD proteins (Dosemeci et al., 2007). PSD-95 is thus well positioned to link and coordinate multiple pathways regulating synapse structure and function, such as those that control activity-dependent spine growth and protein trafficking. Given its functions, PSD-95 has been implicated in synaptic plasticity processes and in the interplay among glutamatergic, dopaminergic, and serotonergic signaling pathways (de Bartolomeis et al., 2013).

Furthermore, PSD-95 is highly stable at the synapse, consistent with a role in forming and maintaining the PSD (Bresler et al., 2001 and 2004; Gray et al., 2006; Sturgill et al., 2009). Overexpression of PSD-95 increases spine maturation and stability (Nikonenko et al., 2008). Consistently, acute knockdown of PSD-95 arrests the functional and morphological development of glutamatergic synapses (Ehrlich et al., 2007), while PSD-95 mutant mice exhibit variations in spine densities in several brain regions (Vickers et al., 2006). In addition, PSD-95 has also been proposed to affect synapse maturation and stabilization and, thus, synapse number (El-Husseini et al., 2000; Ehrlich et al., 2007). Activity-dependent spine growth is positively and negatively regulated by PSD-95, phosphorylated at Ser73 site by CaMKII (calcium calmoduline kinase II), which has been reported to slow down both the growth of apical spines and the strength of synaptic currents (Steiner et al., 2008).

A growing number of studies have implicated PSD-95 in animal models of psychosis, and in the pathophysiology of schizophrenia, as demonstrated by postmortem human brain analyses. Early works demonstrated an increase in thalamic PSD-95 gene expression in schizophrenic patients, with a concurrent decrease in NMDAR NR1 subunits in the same region (Clinton et al., 2003). Postmortem studies indicated that young schizophrenic patients have decreased PSD-95 thalamic levels and increased NMDAR NR2B subunits (Clinton et al., 2004). No diagnostic changes for NR1 were found in any area while a region-specific decrease in PSD-95 was found in the dentate molecular layer of the hippocampus in both schizophrenia and bipolar disorder relative

to major depressive disorder (Toro and Daikin, 2005). Moreover, it has been observed that pluripotent stem cells from peripheral fibroblasts of schizophrenia patients show decreased PSD-95 protein amounts and reduced neurite number when differentiated into neurons (Brennand et al., 2011). Different studies suggest the implication of PSD-95 also in autism spectrum disorders (Feyder et al., 2011).

Fig. 5: Three-dimensionally reconstructed dendritic segment. Black: PSD-95 at the tip of the spines. Modified from Nikonenko et al., 2008.

2- SYNAPTOPATHIES

The highly organized synaptic structure results from a protracted developmental program in the course of which synapses are assembled and stabilized in the mature brain, while retaining sufficient flexibility to exhibit plasticity of structure and function. The ability of synapses to maintain their individual characteristics is very much dependent on the network of interactions within these complexes. The accumulation of synapses on neuronal processes indicates that synapses, although well served by transport links, operate remotely from the biosynthetic processes occurring at the cell body. Owing to this 'isolation', a number of underpinning processes evolved at synapses. These include local membrane and protein turnover, high efficient local mRNA translation, compartmentalized metabolic capability and a host of local modulatory signal cascades supported by synaptic protein scaffolds, which together compose a picture of staggering molecular complexity. In spite of their partial autarky, synapses are still dependent on the biosynthetic and metabolic support of the cell body. Therefore, more general cellular dysfunctions can become manifest as perturbed synaptic function and thus represent synaptopathies, although synapse function itself is not primarily affected (Brose et al., 2010). Synaptopathies can arise from large numbers of mutations in the *synaptome* and disruption of these genes play a role in a remarkable number of brain diseases (Bayes et al., 2011).

Here I will only give some examples of postsynaptic proteins involved in synaptopathies.

SHANK3, a synaptic scaffolding protein enriched in the postsynaptic density of excitatory synapses, and Neuroligin 3 and 4, cell-adhesion proteins on the postsynaptic membrane that mediate the formation and maintenance of synapses between neurons, are two major proteins found mutated in autism (see for a review Sudhof, 2008 and Guilmatre et al., 2013) a pathology which affects about 0.7% of children, characterized by deficits in social communication, absence or delay in language, and stereotyped and repetitive behaviors.

Polymorphisms and frame shift mutations of Disrupted in schizophrenia 1 (DISC1) have been linked to schizophrenia. DISC1 protein is known to interact with several regulators of spine morphogenesis. It has also a function as molecular organizer in spines and provides a structural link between surface receptors, including glutamatergic receptors, and intracellular signaling networks (Hayashi-Takagi et al., 2010).

A clear modification in spines shape and density also accompanies alterations of cognitive functions (Penzes et al., 2011). Post-mortem human brains of patients affected by autism showed an increase in spine density on apical dendrites of pyramidal neurons from frontal, temporal and parietal lobes (Hutsler et al., 2010). Similar to autism, in another form of intellectual disability, the fragile X syndrome, the brain is characterized by elevated spine density (Pfeiffer et al., 2010). Gray matter loss, which is accelerated during periadolescence, and a consequent reduction in spine density (Selemon et al., 1999) occur in schizophrenia. Finally, in AD, dendritic spine loss is observed in the hippocampus and throughout the cortex, the principal areas affected by Alzheimer's disease–related pathologies (Walsh et al., 2004).
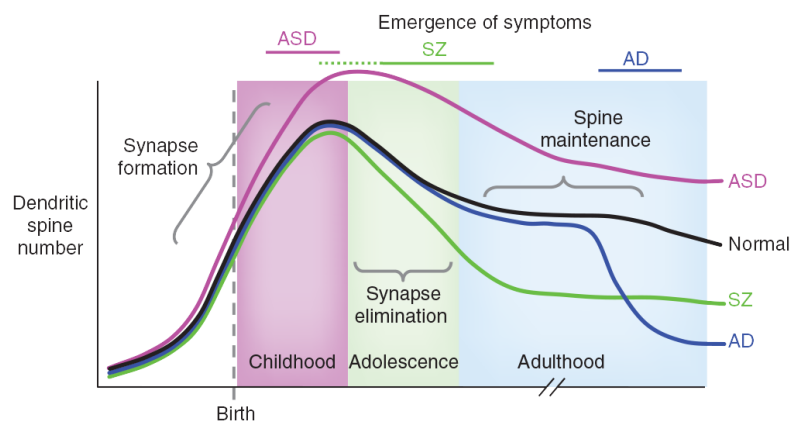

Fig. 6: Estimated lifetime of dendritic spines number in the in a normal subject (black), in autism (ASD, pink), in schizophrenia (SZ, green) and in Alzheimer's disease (AD, blue). Bars indicate the beginning of the disease. It is possible to observe in ASD an excessive number of spines, due to incomplete pruning or

exaggerated spine formation. On the contrary, in schizophrenia there is an exaggerated elimination of spines during adolescence. In AD, spines are lost in late adulthood, suggesting alterations in mechanisms of spine maintenance. From Penzes et al., 2011.

3- SNAP-25

SNAP-25 is a SNARE protein controlling neurotransmitter release and negatively modulating voltage gated calcium channels (Stein et al, 2009; Verderio et al., 2004, Pozzi et al., 2008). Moreover, SNAP-25 has been recently found to play a crucial role in the postsynaptic compartment (Selak et al., 2009, Lau et al., 2010, Jurado et al., 2013, Tomasoni et al., 2013).

3.1- PROTEIN STRUCTURE

SNAP-25 is a hydrophilic protein of 206 amino acids abundantly expressed in mouse brain but not in non-neuronal tissue (Oyler *et al.*, 1989). SNAP-25 has been demonstrated to be extensively, but differently distributed both in the nervous system as well as in endocrine and neuroendocrine cells (Jacobsson *et al.*, 1994, Bark *et al.*, 1995; Jacobsson *et al.*, 1996; Gonelle- Gispert *et al.*, 1999; Jacobsson *et al.*, 1999). The gene expression is correlated to neuronal maturation (Catsicas *et al.*, 1991). SNAP-25 associates with the plasmamembrane through palmitoyl residues that are thioester-linked to four closely spaced cysteine residues at the center of the protein. The amino- and carboxy-terminal domains are highly conserved. The *SNAP-25* gene is a single gene covering more than 80kb of genomic DNA and the polypeptide is encoded for by eight different exons spaced by large intron sequences (Bark, 1993). Obligate alternative splicing of exon 5 generates SNAP-25a or SNAP-25b mRNA (Bark and Wilson, 1994). The nine amino acids that distinguish SNAP-25b from SNAP-25a are included in the SNAP-25 region that spans the last part of the N-terminal SNARE motif and the first part of the linker that separates the N- and C-terminal α-helices. Thus, the different amino acids participating in forming the four α-helix coil–coil structure in the SNARE complex could possibly interfere with SNARE complex stability or ability to interact with accessory proteins (Bark, 1993; Bark and Wilson, 1994). Studies of gene

expression of the alternative SNAP-25 variants in mouse brain have demonstrated that the two mRNAs are differently expressed during development and have a distinct neuroanatomical distribution. SNAP-25a is mostly expressed at early stages of brain development (Oyler *et al.*,1991; Bark *et al.*, 1995; Boschert *et al.*, 1996), while in the postnatal period, when developing axons approach their target cells, SNAP-25b expression is noticeably up regulated (Catsicas *et al.*, 1991; Oyler *et al.*, 1991; Bark *et al.,* 1995; Boschert *et al.*, 1996), consistent with its well-known role in neurite outgrowth and in synaptogenesis (Osen-Sand *et al.*, 1993; Shirasu *et al.*, 2000).

3.2- SNAP-25 IN NEUROTRANSMITTER RELEASE:
ROLE AS A SNARE PROTEIN

SNAP-25 plays a key role in neurotransmitter release by participating to the formation of the SNARE (soluble *N*-ethylmaleimidesensitive factor attachment protein receptor) complex through its SNARE motifs. The synaptic proteins synaptobrevin (also referred to as VAMP2), syntaxin1 and SNAP-25 belong to the SNARE protein family. Their defining feature is an extended coiled-coil stretch, which is referred to as a SNARE motif. In syntaxin, synaptobrevin and in most of the other SNAREs, the SNARE motifs are connected by a short linker to a carboxy-terminal transmembrane region (TMR). SNAP-25 deviates from this general structure: two of its SNARE motifs are connected by a linker region that is palmitoylated, whereas a TMR is lacking. SNAP-25 has been primarily studied in the presynaptic plasma membrane. At this site, on contact, SNARE proteins complex is initiated amino-terminally and proceeds towards the C terminus in a zipper-like fashion, thus pulling the synaptic vesicle and the presynaptic membranes together (Stein et al., 2009; Jahn and Fasshauer, 2012).
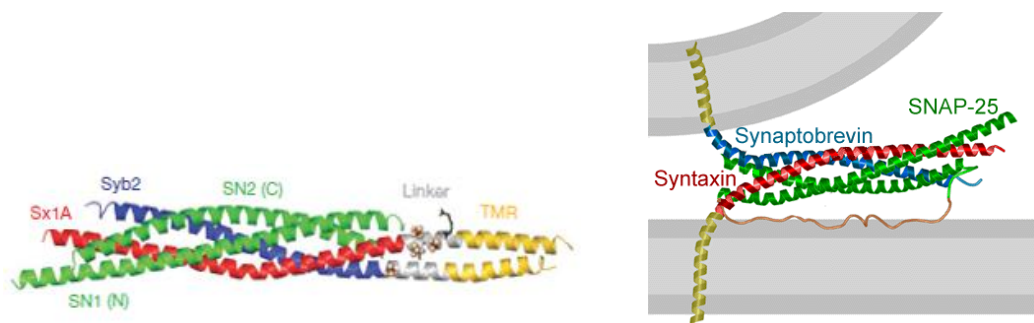
Fig. 7: Left, ribbon plot of the synaptic SNARE complex. Adapted from Stein et al., 2009. Right, SNARE proteins bound to permit the docking of vesicles to the membrane. From Fasshauer et al., *Neuronal SNARE proteins*, 2013.

Although the formation of the SNARE complex is the first step leading to vesicles fusion, it is not sufficient *per se* to generate the release of the neurotransmitter: indeed other proteins (i.e. Munc13, Munc18; Rim, Rab3) and cofactors (i.e. NSF, α/βSNAP) are required (Chua et al., 2010), but their role will not be discussed here.

A special mention, instead, regards synaptotagmin, a synaptic vesicle protein that functions as Ca^{2+}-sensor for fast Ca^{2+}-triggered exocytosis. Synaptotagmin contains two domains that mediate Ca^{2+}-dependent binding directly to both membrane lipids and SNAP-25, one located around the center and another at the C-terminal end of the SNARE bundle (Chua et al., 2010; Mohrmann et al., 2013). Recently it has been discovered that the interaction with the central SNARE motifs of SNAP-25 is essential for vesicle docking, priming, and fast fusion-triggering exocytosis. Mutations in this interaction site led to more pronounced phenotypes in the context of the adult neuronal isoform SNAP-25b than in the embryonic isoform SNAP-25a. Moreover, the C-terminal binding interface only plays a subsidiary role in triggering, but is required for the full size of the readily releasable pool (Mohrmann et al., 2013).

3.3- SNAP-25 IN NEUROTRANSMITTER RELEASE: ROLE AS A CALCIUM CHANNELS MODULATOR

Multiple evidences indicate an additional function of SNAP-25 in the modulation of various ion channels. In particular, the interaction of SNAP-25 with different types of voltage-gated calcium channels (VGCCs), including N-type (Sheng et al., 1996), P/Q-type (Rettig et al., 1996; Martin-Moutot et al., 1996) and L-type (Wiser et al., 1999) has been demonstrated in non-neuronal cells.

These interactions occur through a specific channel region known as the *syn*aptic *pr*otein *int*eraction (*synprint*) site. This interaction has been shown to alter channel function by reducing N-type channel current (Wiser et al.,1996), inhibiting L-type channel currents (Ji et al., 2002), or reducing the activity of P/Q type Ca^{2+} channels by negatively shifting the steady state voltage dependence of inactivation (Zhong et al., 2001).
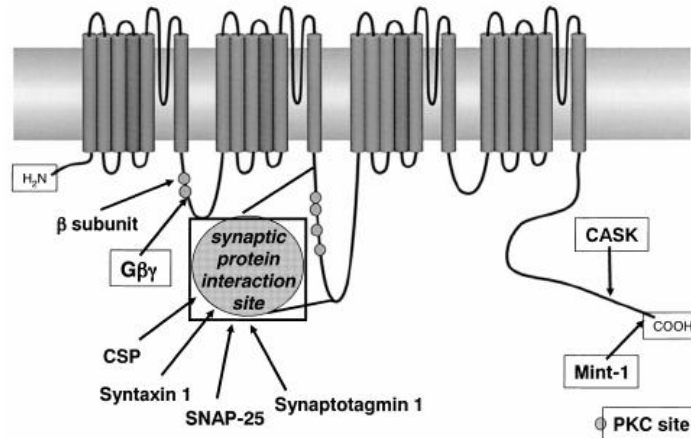
Fig. 8: Transmembrane topology of the N-type calcium channel α1- subunit illustrating major protein interactions sites. The domain II – III linker region of vertebrate N-type channels contains a synaptic protein interaction site that interacts with syntaxin1, synaptotagmin1, and SNAP-25. From Zamponi et al., 2003.

In Verderio et al. 2004, it was reported for the first time the occurrence of a correlation between the levels of SNAP-25 and the extent of depolarization-induced neuronal calcium influx. Indeed, it was demonstrated that SNAP-25 is expressed at almost undetectable levels in GABAergic neurons, which are instead characterized by a higher calcium responsiveness to depolarization. Moreover, exogenous expression of SNAP-25 in GABAergic neurons was found to reset the calcium responsiveness to levels comparable to those of glutamatergic neurons. These data suggests that different levels of SNAP-25 expression in excitatory versus inhibitory neurons may profoundly modulate neuronal responses to synaptic stimuli in a dose-dependent manner, and that SNAP-25 is involved in the regulation of neuronal excitability (Verderio et al., 2004).
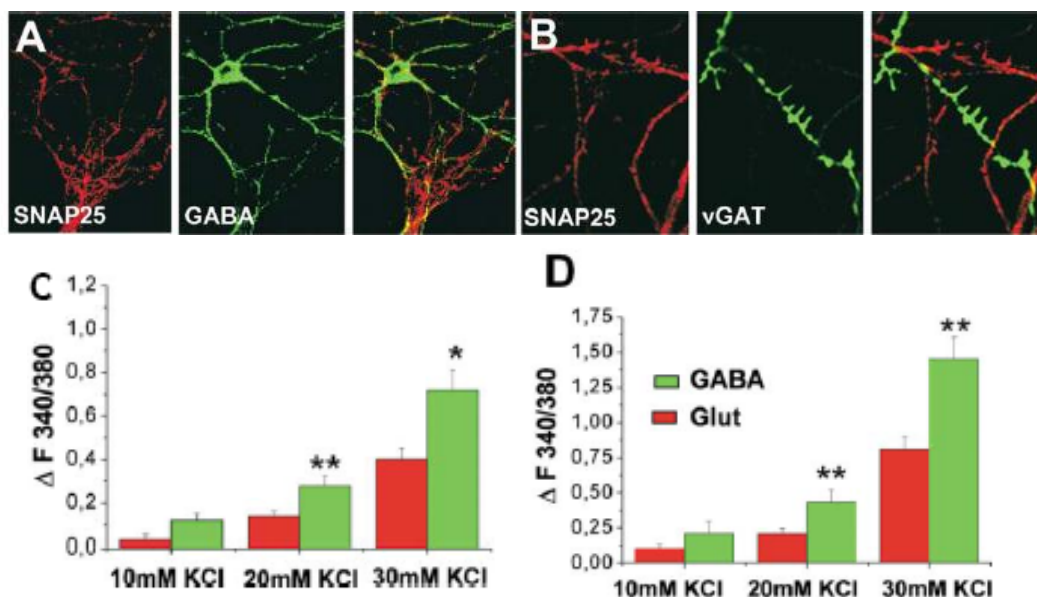
Fig. 9: A-B) Double labeling of hippocampal neurons for SNAP-25 and for GABA (A) or the vesicular GABA transporter v-GAT (B). SNAP-25 immunoreactivity is lacking from neuronal processes positive for GABA or for v-GAT. C-D) Quantitative analysis of $[Ca^{2+}]i$ responses recorded in the dendrites (C) and soma (D) of glutamatergic and GABAergic neurons after exposure to 10-20-30mM KCl. Modified from Verderio et al., 2004.

In a subsequent paper from our laboratory, Pozzi et al. studied how variations of the endogenous levels of SNAP-25 could modulate calcium responsiveness, using primary hippocampal cultures from SNAP-25 wild-type and transgenic mice. Immunocytochemistry and western blotting analysis revealed that cultures from SNAP-25 heterozygous mutants display levels of SNAP-25 intermediate between SNAP-25 KO and wild-type neurons, confirming previously reported data (Washbourne et al., 2002). As hypothesized, the magnitude of calcium response following a depolarizing stimulus was found to be inversely proportional to the amount of SNAP-25.
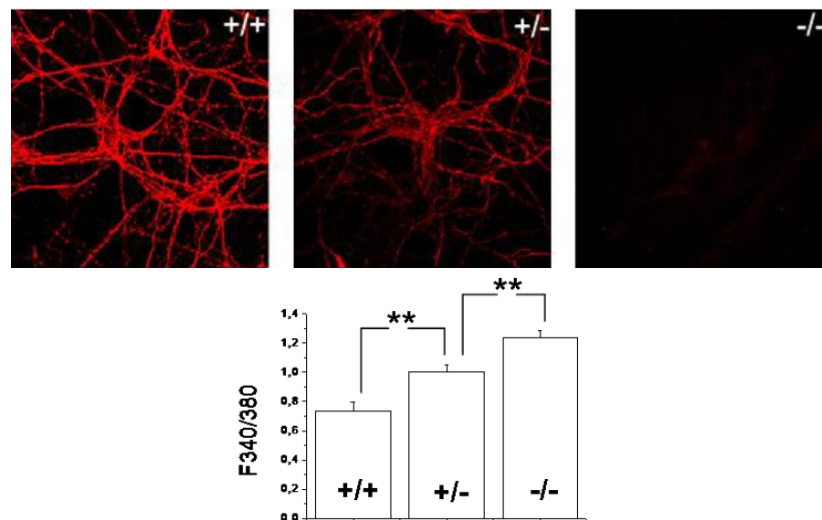
Fig. 10: Top, immunofluorescence for SNAP-25 (red) in hippocampal cultures established from Wt (+/+), heterozygous (+/-), and KO (-/-) mice. Bottom, analysis of calcium responses measured in cultures upon 30mM KCl depolarization. Notably, the increase in responses is inversely proportional to SNAP-25 levels. From Pozzi et al., 2008.

SNAP25 phosphorylation of the serine in position 187 (Ser187) by PKC was found to be crucial for the negative regulation of VGCCs (Pozzi et al., 2008). Because Ser187 phosphorylation is transiently induced by neuronal activity (Pozzi et al. 2008), these data revealed that SNAP-25 provides a negative feedback mechanism for controlling neuronal excitability.

Fig. 11: Left, western blot analysis of SNAP-25 phosphorylation in hippocampal cultures in control conditions or after stimulation with 1μM PMA (PKC activator) for 30 min. Right, time course of SNAP-25 phosphorylation in cultures exposed to 30mM KCl for 5 min, immediately solubilized (KCl), or washed and solubilized after 30 or 60 min. From Pozzi et al., 2008.
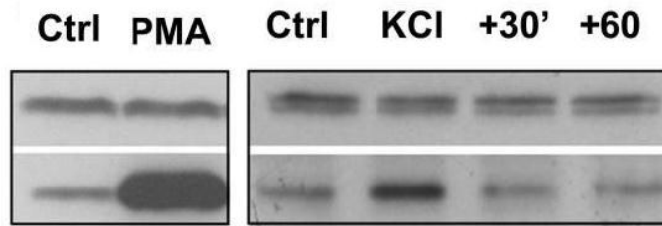
Cultured glutamatergic and GABAergic neurons showed markedly different VGCC properties, which are affected by SNAP25 level of expression, confirming the hypothesis that the regulation of SNAP-25 may have a crucial role in the control of neuronal network activity (Condliffe et al., 2010). It is also possible that the effects of reducing endogenous SNAP-25 expression have a greater impact on VGCC regulation than on the function of the protein as a SNARE. Several finding where reduction of SNAP-25 do not affect SNARE-dependent neurotransmission (Bronk et al., 2007; Delgado-Martinez et al., 2007) support this idea.

Finally, we have recently demonstrated that halved SNAP-25 levels at 13-14 DIV hippocampal neurons enhance evoked glutamatergic neurotransmission possibly, due to increased presynaptic VGCCs activity, and affect short-term presynaptic plasticity. Indeed, synapse between heterozygous neurons show paired-pulse depression as opposed to paired-pulse facilitation occurring in their wild-type counterparts (Antonucci et al., 2013; see also Result section of this thesis).

3.4- A NOVEL POSTSYNAPTIC ROLE FOR SNAP-25

Despite the established role at the presynaptic compartment, new roles are emerging for SNAP-25 at the postsynaptic terminal in the last years.

The protein lacks a selective pre- or postsynaptic distribution, being instead more diffusely localized throughout the neuronal plasma membrane; some recent evidence locate SNAP-25 in the postsynaptic terminal either by immunofluorescence (Selak et al., 2009, Tomasoni et al., 2013), or ground state depletion (GSD) microscopy which allows protein localization with a precision up to 20nm (Tomasoni et al., 2013). SNAP-

25 immunoreactivity can be detected, although it is not specifically enriched, in dendritic protrusions of cultured hippocampal neurons. Also by coimmunoprecipitation, bimolecular fluorescence complementation (BiFC) and biochemical fractionation it is possible to appreciate a relation with postsynaptic proteins (Selak et al., 2009; Tomasoni et al., 2013 but see Kerti et al., 2012).
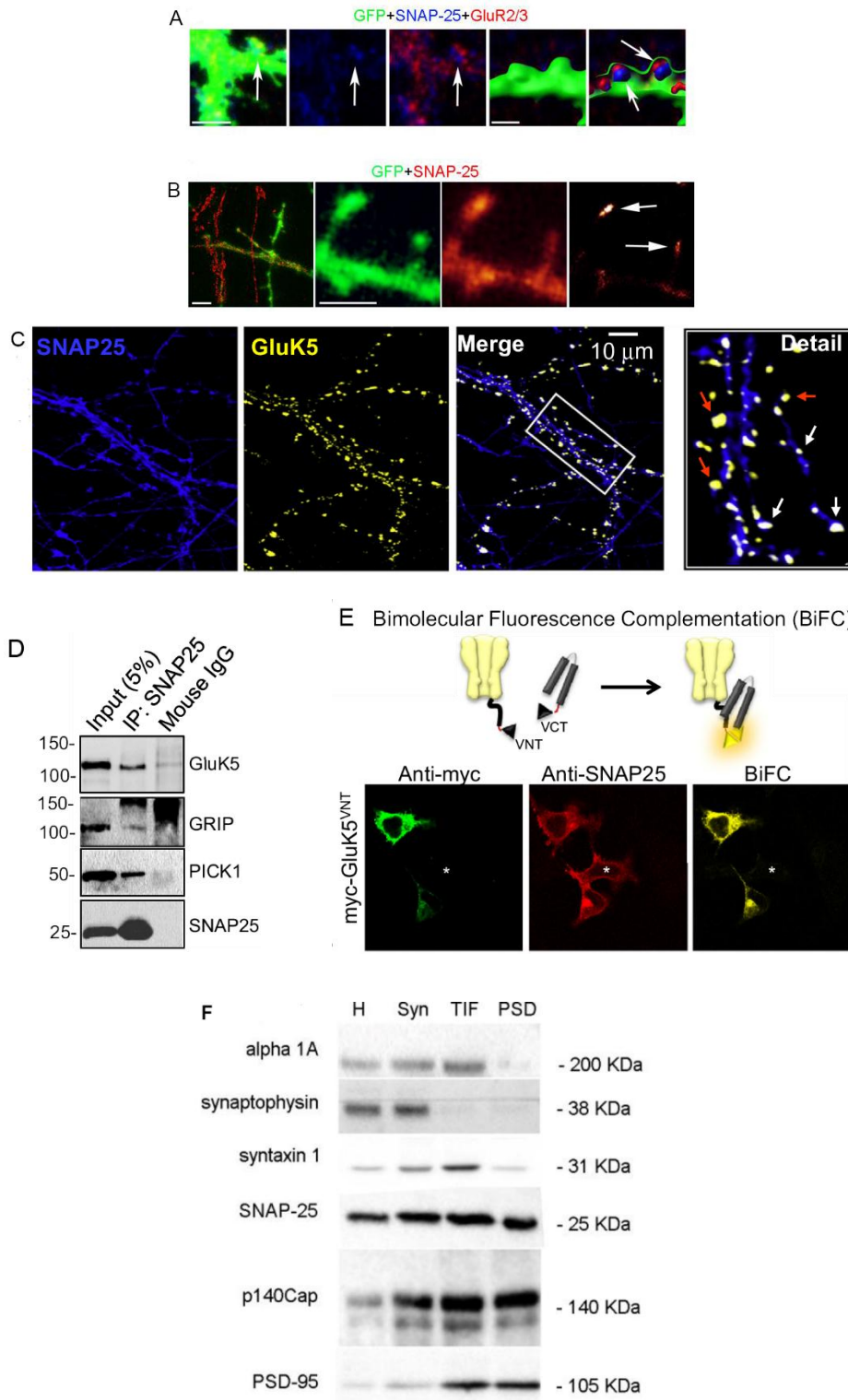
Fig. 12: A) Labeling of hippocampal cultures, transfected with GFP, for SNAP-25 (blue) and for the post-synaptic marker GluR2/3 (red). Scale bar 1µm (three left panels) and scale bar 2.5µm (two right panels). B) Ground State Depletion images displaying endogenous SNAP-25 immunoreactivity. Left panel: axonal and dendritic processes labeled for SNAP-25 in neurons transfected with GFP. Scale bar 3µm. High magnification panels show SNAP-25 immunoreactivity in dendritic protrusions. Scale bar 1.5µm. Modified from Tomasoni et al., 2013. C) In mature hippocampal neurons, SNAP-25 (blue) and GluK5 (yellow) colocalize in roughly 50% of immunolabeled puncta. D) SNAP-25 coimmunoprecipitated GluK5, GRIP and PICK1 from hippocampus homogenate. E) Demonstration of SNAP25-GluK5 interaction by bimolecular fluorescence complementation (BiFC). BiFC takes advantage of the fact that when the two non-fluorescent amino- and carboxy-terminal fragments of yellow fluorescent protein (YFP) are brought into close apposition they interact leaving to the irreversible formation of a fluorescent protein. HEK cells were cotransfected with GluK5 and SNAP-25 fusion proteins to which the N-terminal (VNT) and C-terminal (VCT) domains of the YFP. Double immunolabeling, using antibodies against myc (green) and SNAP-25 (red), was also performed to check for the levels of protein expression. Single confocal images showing that cotransfection of GluK5VNT and SNAP-25VCT leads to the reconstitution of Venus in those cells where both proteins are expressed. Modified from Selak et al., 2009. F) SNAP-25 as well as markers of the presynaptic (synaptophysin, alpha 1A subunit of calcium channels) and postsynaptic (PSD-95) compartment were analyzed by western blotting in various subcellular compartments. H, Homogenate; Syn, synaptosomes; TIF, Triton X-100 Insoluble Fraction; PSD, Post-Synaptic Density.

Nowadays a number of studies demonstrate a functional role of SNAP-25 in the postsynaptic terminal. Selak and colleagues showed that SNAP-25 regulates the membrane insertion and removal of the kainate receptor (KAR) containing the subunit GluK5. The interaction of SNAP-25 with GluK5 and PICK1 reduces the GluK5 stability on the membrane, favoring KAR internalization. Indeed, postsynaptic long-term depression (LTD) of KAR-mediated excitatory postsynaptic currents was prevented by disrupting the interaction between SNAP-25 and GluK5 (Selak et al., 2009). The mechanism by which SNAP-25 exerts its function on KAR is not however completely understood, even if the SNARE function seems not to be involved. A working hypothesis is that PICK1 may favor GluK5 phosphorylation by PKC, which may induce a conformational change facilitating the association of GluK5 with SNAP-25, while decreasing GRIP binding affinity (Selak et al., 2009). Since SNAP-25 and GluK5 co-localize almost exclusively in the association with the plasma membrane, it is even possible that SNAP-25 could play a role in the lateral movement or sorting of activated KARs into the lateral plasma membrane invaginations representing endocytic ''hot spots'' (Lu et al., 2007).
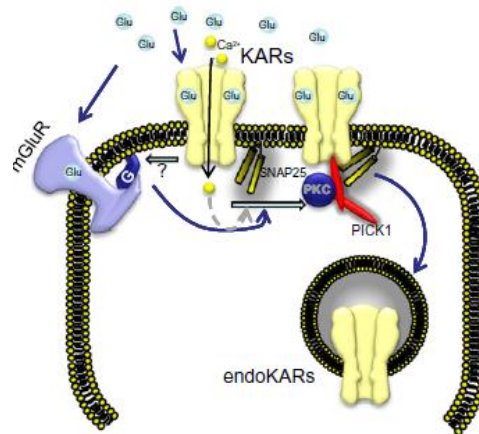
Fig. 13: Cartoon to illustrate the putative role of mGluRs, SNAP-25, PICK1 and PKC in long-term synaptic kainate receptor internalization. From Selak et al., 2009.

Another key study revealed the importance of SNAP-25 in regulating NMDA receptor insertion in the membrane, through PKC-mediated phosphorylation (Lau et al., 2010). It is known that PKC enhances NMDA receptor (NMDAR)-mediated currents and promotes NMDAR delivery to the cell surface via SNARE-dependent exocytosis. SNAP-25 has been discovered to be a target of PKC on its residue Ser187 and favors NMDAR incorporation into the membrane through its SNARE properties. SNAP-25 is therefore involved in the potentiation of the synapse. Given that LTP-inducing protocols can induce SNAP-25 phosphorylation (Genoud et al., 1999), high frequency stimulation protocols may act via phosphorylation of SNAP-25 to promote insertion of NMDARs thus eliciting LTP.

Based on these results, it is conceivable that postsynaptic SNAP-25 may be important for regulating a dynamic equilibrium among the glutamate receptors at a given synapse, thereby leading to adequate tuning of neurotransmission also at postsynaptic level.

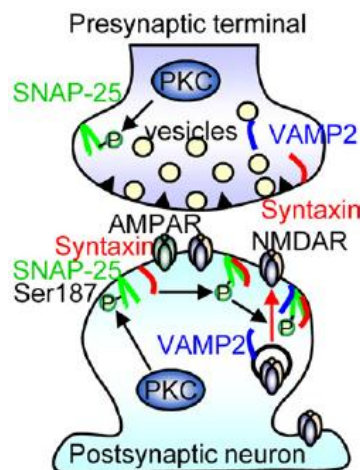**Fig. 14:** Proposed model showing that activation of PKC phosphorylates SNAP-25 and promotes insertion of new NMDA-, but not AMPA-, channels at the cell surface. This is consistent with trafficking of AMPARs and NMDARs in distinct postsynaptic vesicles and delivery to the plasma membrane via distinct pathways of exocytosis. From Lau et al., 2010.

Interestingly, the effects on KAR and NMDAR specifically require SNAP-25 phosphorylation, without implication of SNAP-23. SNAP-23 shows 58% aminoacidic identity with SNAP-25 and it is ubiquitously expressed. Similarly to SNAP-25, SNAP-23 is localized to the plasma membrane (Wang *et al.*, 1997). SNAP-23 regulates a wide variety of diverse membrane-membrane fusion events outside of the CNS, such as exocytosis from mast cells, insulin-dependent GLUT-4 release from adipocytes and degranulation in platelets (Suh et al., 2010). Nevertheless, SNAP-23 has also been detected in cortical neurons and in purified synaptic vesicles (Takamori et al. 2006, Bragina et al. 2007). SNAP-23 can support synaptic vesicle fusion in the absence of SNAP-25 and may function in a SNARE complex driving asynchronous and/or spontaneous neurotransmitter release (Chieregatti et al., 2004). SNAP-23 is enriched in dendritic spines, co-localizes with constituents of the postsynaptic density in neurons and has a role in the postsynaptic glutamate receptor trafficking. In fact, surface NMDAR and NMDA receptor currents are reduced in SNAP-23 heterozygous mice, in particular SNAP-23 reduction suppresses plasma membrane expression of NR2B by inhibiting the recycling of internalized receptors, without interacting directly with the NMDAR (Suh et al., 2010). However SNAP-23 roles do not seem to overlap with SNAP-25 ones, for example, differently from SNAP-25, SNAP-23 is not required for AMPA-mediated LTP in both slices and cultured neurons (Jurado et al., 2013).

It has recently been shown that acute SNAP-25 downregulation results in LTP impairment, possibly due to defective NMDA receptors trafficking (Jurado et al., 2013; see also Lau et al., 2010). It is noteworthy that a similar reduction of SNAP-25 expression does not detectably impair presynaptic neurotransmitter release, probably because the presynaptic SNAP-25 concentrations far exceed the needs of the presynaptic release machinery (Sharma et al., 2011).

Because postsynaptic SNAP-25 may be critical for NMDAR trafficking, it was correctly hypothesized that the SNAP-25 knock down (KD) impaired LTP by reducing the surface levels of NMDAR. In fact, reduced levels of NMDARs were found in the dendrites of SNAP-25 KD cells. Furthermore, AMPAR/NMDAR ratios in SNAP-25 KD in acute slices were significantly higher than in control cells (Jurado et al., 2013).
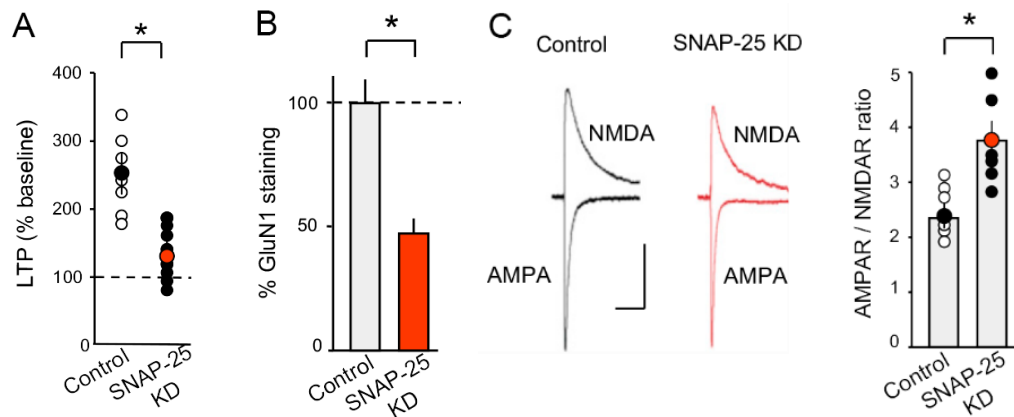
Fig. 15: A) Scatter plot of individual LTP experiments in control and SNAP-25 KD CA1 pyramidal cells. B) Normalized levels of GluN1 on dendrites of hippocampal cultured neurons. C) Ratio of AMPAR- to NMDAR-mediated EPSCs is increased in SNAP-25 KD cells. Representative EPSCs recorded at -60mV and +40mV are shown. Modified from Jurado et al., 2013.

Interestingly, Jurado and colleagues indicated SNAP-47 as the protein responsible for AMPAR delivery during LTP. In neurons, SNAP-47 shows a widespread distribution on intracellular membranes and it is also enriched in synaptic vesicle fractions. In vitro, SNAP-47 can functionally substitute for SNAP-25 in SNARE complex formation and it also substituted for SNAP-25 in proteoliposome fusion. However, neither complex assembly nor fusion was as efficient as with SNAP-25 (Holt et al., 2006). Importantly, the SNAP-47 KD did not alter basal AMPAR- or NMDAR-mediated synaptic responses or basal AMPAR surface expression. SNAP-47 specifically participates in the fusion machinery during LTP and the interaction of SNAP-47 with other SNARE proteins to form SNARE complexes is critical for AMPAR exocytosis during LTP, but not for constitutive basal AMPAR exocytosis (Jurado et al., 2013). Thus, several evidence accumulated indicating that SNAP25 may exerts a fundamental role at the postsynaptic compartment by affecting glutamate receptors insertion.

A recent paper of our group suggested that SNAP-25 might have also a structural role in the postsynaptic compartment. In fact, acute down-regulation of the protein expression in vitro was found to lead to an immature phenotype of dendritic spines (Tomasoni et al., 2013). Conversely, over-expression of SNAP-25 resulted in an increase in the density of mature spines. The regulation of spine morphogenesis by SNAP-25 depends on the protein's ability to bind both the plasma membrane and the adaptor protein p140Cap (Tomasoni et al., 2013). p140Cap has been discovered as a regulator of Src tyrosine kinase, which associates with microtubules and with the actin binding protein,

cortactin. Consistently, p140Cap plays a crucial role in regulating actin cytoskeleton and spine formation (Jaworski et al., 2009). There is the possibility that SNAP-25, present at the plasma membrane of new dendritic spines, allows pl40Cap relocalization at a site where, in the presence of the appropriate molecular components necessary for spine formation, the process of spine morphogenesis may start.
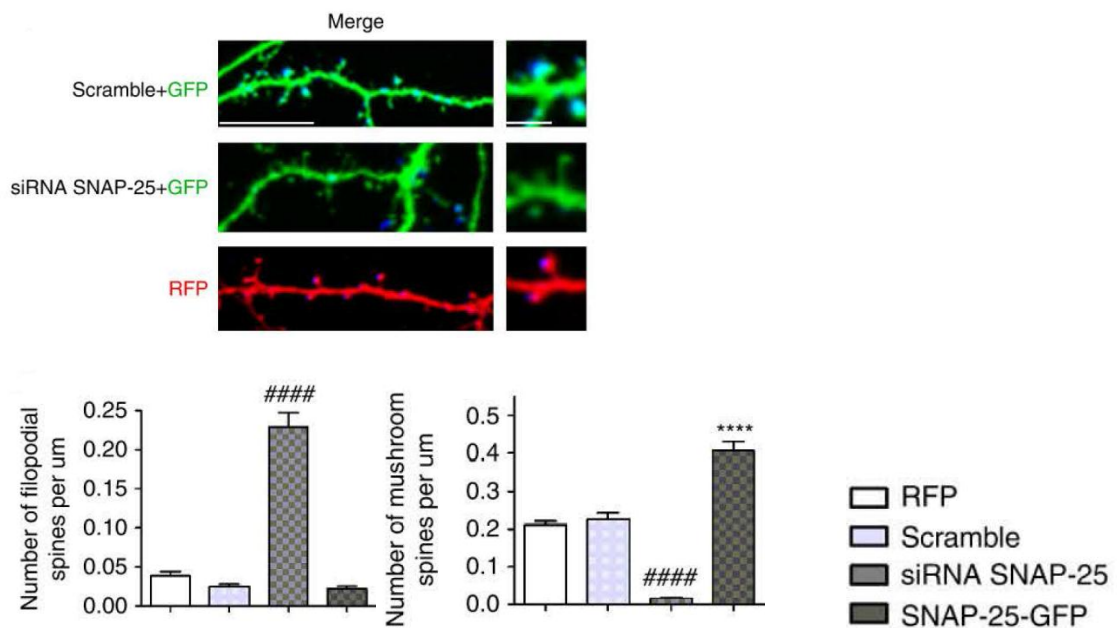
Fig. 16: Top, PSD-95 immunocytochemical staining of rat hippocampal cultures silenced for SNAP-25 and transfected with a scramble or silencing sequence for SNAP-25 and GFP; RFP alone or SNAP-25-GFP and RFP, Scale bar 10μm (scale bar inset 2.5μm). Bottom, quantitative analysis of spine density, subdivided in filopodia-like or mushroom type. Modified from Tomasoni et al., 2013.

3.5- SNAP-25 IN NEUROPSYCHIATRIC DISORDERS

In the last years, data accumulated suggesting that SNAP-25 is involved in different neuropsychiatric and neurological disorders; alterations in SNAP-25 isoform expression have been linked to diseases with developmental onset such as schizophrenia, attention deficit/hyperactivity disorder and epilepsy. Recent genetic studies of human populations and of some mice models suggested that alterations in *SNAP-25* gene structure, expression and/or function might contribute directly to these distinct neuropsychiatric and neurological disorders. Further studies are required to clarify if the changes in SNAP-25 expression may represent a cause or a consequence of such pathologies.

ADHD

Attention-deficit/hyperactivity disorder (ADHD) is one of the most prominent neuropsychiatric disorders developing during childhood, which affects roughly 3% - 7% school-aged children in the U.S. (CDC 2013). It is a psychiatric disorder of the neurodevelopmental age characterized by significant problems of attention, hyperactivity and/or impulsivity that are not appropriate for a person's age. Nowadays it is know that the disorder is marked by disruption of catecholamine signaling, with mainstay treatments for the disorder targeting the dopamine and noradrenaline transporters and the α2a adrenoreceptor (Arnstenet al., 2011). Also the genetic component is non deniable, in fact ADHD is clearly inheritable (Faraone et al., 2005) and genetic association studies suggest that allelic variations in the *SNAP-25* gene might confer susceptibility to ADHD (Barr et al., 2000; Feng et al., 2005; Caylak, 2012). A latest study shows that DNA variations at *SNAP-25* confers risk to ADHD and reduces the expression of the transcript in the inferior frontal gyrus, a region of the brain that is critical for the regulation of attention and inhibition (Hawi et al., 2013).

The Coloboma mouse model has been fundamental to unveil the role of *SNAP-25* as a susceptibility gene for ADHD. The Coloboma mouse bears a semi-dominant mutation (cm/+) in which the heterozygous form results in the mutant type while the homozygous is lethal. The mutation is a 0.2Cm deletion encompassing genes including *SNAP-25* 5 (Hess et al., 1994) and it is used as a model for ADHD (Wilson 2000; Faraone et al. 2005; Russell, 2007). In Coloboma mutant mice (Cm/+), deletion of the *SNAP-25* gene results in 50% lower amounts of the SNAP-25 mRNA and protein expression compared to wild-type mice. Coloboma mice exhibit normal circadian rhythm and, as children with ADHD, they are hyperactive during their active phase, with locomotor activity averaging three fold the activity of control littermates (Hess et al.,1992).

Notably, a similar phenotype has been observed in mice heterozygous for SNAP-25. At seven postnatal weeks, SNAP-25 het mice show a moderate hyperactivity, which, however, disappears in adult animals, which are instead characterized by impairments in associative learning and memory (Corradini et al., 2012). ADHD children display impaired associative implicit learning, mediated by frontal-striatal-cerebellar circuits, but normal spatial contextual learning depending upon the medial temporal lobes (Barnes et al., 2010). Under this respect, an analysis of the structure and function of the synapses where SNAP-25 expression is in fact lower, using SNAP-25 heterozygous

mice, , could be useful for identifying the substrate of impaired forward signaling even if compensated by later network maturation (Corradini et al., 2012).

SCHIZOPHRENIA

Schizophrenia is a mental disorder characterized by problems with thought processes and by poor emotional response, affecting approximately 24 million of the population worldwide (WHO 2013), with the onset of symptoms in late adolescence or early adulthood. Schizophrenia is often described in terms of positive and negative symptoms. Positive symptoms include hallucinations, delusions, disordered thoughts and speech. Negative symptoms include reduced interest or motivation and cognitive impairment. The neuropathophysiology of the disorder remains unclear, although, as in the case of ADHD, alterations in dopaminergic and serotoninergic circuitry, as well as in glutamatergic transmission, have been strongly implicated. The morphological correlates of schizophrenia are subtle, and range from a slight reduction in brain size to localized alterations in the morphology and molecular composition of specific neuronal, synaptic, and glial populations in the hippocampus, dorsolateral prefrontal cortex, and dorsal thalamus (Harrison and Weinberger, 2005).

Twin studies show unequivocally that schizophrenia is predominantly a genetic disorder, with estimated risk of heritability around 80% (Harrison and Weinberger, 2005). However, neither a gene has been found to be a causative allele nor the mechanism by which it predisposes to schizophrenia has been identified. Many genes have been recognized as susceptibility genes in this disease because of genome-wide association studies (Giusti-Rodriguez and Sullivan, 2013). Among them, the chromosome region which includes the *SNAP-25* gene (20p12.3-11) emerged as a strong candidate region for schizophrenia (Lewis et al., 2003; Corradini et al., 2009). Consistently, SNAP-25 levels are lower in the hippocampus (Young et al. 1998; Thompson et al. 2003) and in the frontal lobe (Thompson et al., 1998) of patients with schizophrenia. Decreases in the mRNA level were also found in various parts of the brains in post mortem studies of patients with bipolar affective disorder (Scarr et al., 2006).

Recently, more attention has been given to polymorphisms associated with the disease. Point of variation or polymorphisms are the source of genetic variation that contribute to differences between individuals. There are several types of polymorphisms, one commonly studied type are the single-nucleotide polymorphisms (SNPs). A SNP

consists in a DNA sequence variation that occurs when a single nucleotide (A,T,C,or G) in the genome sequence is altered; to be classified as polymorphism, the variation must occur in at least 1% of the population. Carroll and colleagues demonstrated that ADHD and schizophrenia shares the same SNPs mutations of *SNAP-25* (Carroll et al., 2009). Recent studies have found another SNP mutated in the 3'UTR *SNAP-25* gene, which alteration is supposed to influence NMDA receptors trafficking (Kovács-Nagy et al., 2009; Lochmann et al., 2013).

EPILEPSY

Epilepsy is one of the most common neurological disorders that affects 50 million people worldwide of all ages (WHO 2012). It is a common and diverse set of chronic neurological disorders characterized by seizures. It is a paroxysmal behavioral generally caused by an excessive disorderly discharge of cortical nerve cells of the brain and can range from clinically undetectable (electrographic seizures) to convulsions. In many cases, a cause cannot be identified; however, factors that are associated include brain trauma, strokes, brain cancer, drug and alcohol misuse among others. Clinical manifestations of epilepsy are varied and despite availability of a number of antiepileptic drugs, about one-third of epileptic patients are resistant to treatment.

As for schizophrenia or other psychiatric disorders, also for epilepsy it is difficult to find a genetic correlate, but some animal models provides some insights that alterations in SNAP-25 could be involved in the insurgence of epilepsy. The mutant mouse Coloboma (*Cm/+*), already discussed as a model of ADHD, display robust cortical-cortical spike-wave discharges and increased thalamic T-type currents (Zhang et al., 2004), two typical features of absence epilepsy (Tsakiridou et al., 1995; Coenen and Van Luijtelaar, 2003).

SNAP-25 is expressed at much higher levels at excitatory respect to inhibitory synapses (Verderio et al., 2004; Bragina et al., 2007). Thus, hyperexcitability could result from perturbations of the processes that balance the developmental assembly of inhibitory and excitatory circuits.

Since the phosphorylation of SNAP-25 plays an important role in synaptic function, a mutant mouse, substituting Ser187 of SNAP-25 with Ala (Kataoka et al., 2011) was generated. The most striking phenotype of SNAP-25 S187A/S187A mice was the abnormal behavior possibly attributed to increased anxiety. SNAP-25 S187A/S187A mice froze very readily in response to environmental change. Dopamine and serotonin

release in amygdala was markedly decreased in SNAP-25 S187A/S187A mice, possibly due to a lack of phosphorylation-dependent enhancement of monoamine release. In addition, the mutant mice sometimes exhibited spontaneously occurring convulsive seizures.

A recent study from our lab revealed behavioral alterations in SNAP-25 heterozygous mice. In particular, SNAP-25 reduction was found to be associated with diffuse network hyper-excitability, which does not lead to spontaneous convulsive behavior (Corradini et al., 2012). The data are in line with the significantly higher incidence of epilepsy in pathologies characterized by SNAP-25 alterations. In particular, the incidence of epilepsy is about six times higher in schizophrenic patients than in controls (Chang et al. 2011) and ADHD children are 3 fold more likely to have epilepsy (Davis et al. 2010), also showing higher occurrence of subclinical epileptiform activity (Richer et al. 2002; Becker et al. 2004).

AIM OF THE PROJECT

SNAP-25 is a member of the SNARE protein complex that participates in synaptic vesicle exocytosis. Previous studies of our group have demonstrated that SNAP-25, which is expressed at high levels in glutamatergic, but not GABAergic terminals of hippocampal neurons (Verderio et al., 2004), regulates intracellular calcium dynamics by negatively modulating neuronal voltage-gated calcium channels upon SNAP-25 activity-dependent phosphorylation on Ser187 (Pozzi et al., 2008, Condliffe et al., 2010). The regulation of the intracellular calcium concentration at the presynaptic level is fundamental for neurotransmission. In the last years, evidence are accumulating suggesting that SNAP-25 might also play a crucial role at the postsynaptic level. In particular it has been shown that SNAP-25 promotes NMDA receptors insertion in the postsynaptic membrane via SNARE-dependent exocytosis upon NMDA application (Lau et al., 2010), and it is also critical for the synaptic removal of kainate receptors (Selak et al., 2009). Moreover, acute down-regulation of SNAP-25 prevents LTP, possibly due to defective NMDA receptors trafficking (Jurado et al., 2013). In addition, it has been recently shown by our group that SNAP-25 has also a structural role in the morphogenesis of dendritic spines, through binding to the postsynaptic protein p140Cap (Tomasoni et al., 2013). These data open the possibility that SNAP-25 may play a dual role during postsynaptic maturation: one dealing with receptors trafficking and the other involved in the structural organization of the dendritic spines, possibly through the formation of a synaptic proteins network.

Based on these considerations, the main objectives of this project were:

1) To investigate whether changes in VGCC current densities affect neurotransmission in developing hippocampal cultures from SNAP-25 wild-type (wt), heterozygous (het) mice and upon acute down-regulation of the protein, through the analysis of spontaneous and evoked currents as well as short-term plasticity.

2) To evaluate whether reduced levels of SNAP-25 impact spine formation and morphology in vivo, and to assess whether this might result from an impairment in the

stability of fundamental postsynaptic components, which may possibly interact with SNAP-25 in a spine complex proteins network.

3) To define whether the occurrence of possible postsynaptic alterations result from presynaptic defects caused by the reduction of the protein expression or whether pre and postsynaptic defects occur independently one from the other.

EXPERIMENTAL PROCEDURES

Animals

All the experimental procedures followed the guidelines established by the Italian Council on Animal Care and were approved by the Italian Government decree No. 27/2010. All efforts were made to minimize the number of subjects used and their suffering. SNAP-25 wild type and SNAP-25 heterozygous male mice (Washbourne et al., 2001) were housed in cages with free access to food and water at 22°C and with a 12-h alternating light/dark cycle. Genotyping was performed by PCR as described in Washbourne et al., 2001.

Cell cultures

Mouse hippocampal or rat hippocampal and cortical neurons were prepared from E18 fetal SNAP-25 heterozygous (Het) or wild type (wt) littermates C57BL/6 mice as described by Banker & Cowan (1977) and Bartlett & Banker (1984) with slight modifications. Briefly, hippocampi were dissociated by treatment with trypsin (0.125% for 15 min at 37°C), followed by trituration with a polished Pasteur pipette. The dissociated cells were plated onto glass coverslips coated with poly-L-lysine at density of 400 cells/mm^2. The cells were maintained in Neurobasal (Invitrogen, San Diego, CA) with B27 supplement and antibiotics, 2mM glutamine, and 12.5µM glutamate (neuronal medium).

HEK293 cells are a kind gift from Dr.ssa G. Pietrini (CNR Institute of Neuroscience, Milan, Italy) and were manteined in culture medium (DMEM (Gibco) with antibiotics, 1% glutamine and 10%FCS).

Mixed cell cultures

Primary hippocampal GFP-positive neuronal cultures were prepared from the hippocampi of E18 fetal C57BL/6 GFP transgenic mice (Okabe et al., 1997), with the GFP gene controlled by the actin promoter. To isolate the neuronal type of interest among wild type or SNAP-25 heterozygous neurons GFP-positive neurons were co-cultured with SNAP-25 Het or wt neurons in a ratio of 1 to 10 or 10 to 1.

Lentiviral constructs

A short hairpin RNA construct directed against SNAP-25 was generated by PCR and subcloned into a lentiviral vector plasmid (pLKO.1-puro-CMV-tGFP™, Sigma-Aldrich, Israel). As a control, we generated in a similar way a scrambled shRNA sequence. The effective and scrambled U6-shRNA expression cassettes were co-expressed with EGFP driven by CMV promoter. High titer lentiviral vectors were produced by a transient transfection of the third generation transfer, packaging and envelope plasmid set into 293FT cell line (Invitrogen, Carlsbad, CA, USA), and allowed to express and form viral particles for 48h. The medium was collected; the viral particles were purified and concentrated by multiple centrifugation steps, dissolved in sterile PBS, aliquoted and stored at -80 °C until further use. Viral titer was determined using the FACS analysis. A titer higher than 10^8 TU/ML was used for future experiments.

DNA constructs and expression

Neuronal cultures were transfected at 17DIV with pEGFP-C1 (Clontech, Palo Alto, CA) or pSUPER-DsRed plasmid (obtained from pSUPER-GFP, Oligoengine, Seattle, USA) and FU(PSD95:EGFP)W (Minerbi et al., 2009). Silencing of SNAP-25 was achieved via transfection of a pSUPER construct (Verderio et al., 2004, Condliffe et al., 2010). A nonspecific siRNA duplex of the same nucleotides but in an irregular sequence (scrambled SNAP-25 siRNA) was prepared using oligonucleotides 5-GATCCCCGAGGAGTTATGCGATAGTATTCAAGAGAATGATAGCGTATTGAG GAGTTTTTGGAAA-3-and5-AGCTTTTCCAAAAACTCCTCAATACGCTATCATTCTCTTGAATACTATCGCA TAACTCCTCGGG- 3-that were annealed and ligated into the pSuper vector as described previously (Verderio et al., 2004; Condliffe et al., 2010). Botulinum toxin type E light chain cDNA is a kind gift from prof. Thierry Galli (ISERM, Paris, France). SNAP-25-GFP tagged construct was obtained as in Verderio et al., 2004.

For LUMIER assay, mouse SRCIN1 was PCR amplified using Phusion Hot Start II High-Fidelity DNA Polymerase (Thermo Scientific) and the following primers: 5-GGGGACAAGTTTGTACAAAAAAGCAGGCTTCATGGGGAACGCTCCGTCCCA AG-3 and 5-GGGACCACTTTGTACAAGAAAGCTGGGTCGGAAGGAGATGGAAGAATTCCT TGC-3. The PCR product was inserted into pDONR221 using the BP clonase, (Invitrogen), amplified and further shuttled into the LUMIER prey vector (FireV5DM).

Human full-length cDNA clones of SNAP-25, PSD-95 and CTTN where available as entry clones and shuttled into the respective LUMIER bait (PAReniDM) and prey (FireV5DM) vectors.

Real-Time PCR

Total RNA was extracted using TRI REAGENT (Sigma) according to the manufacturer's instructions, including *DNase* I genomic DNA degradation step. Total RNA was reverse-transcribed using high capacity cDNA reverse transcription kit (Applied Biosystems). Real-time PCR analysis was performed using the PCR System STEP-ONE plus (PE Applied Biosystems, Foster City, CA, USA). Q-PCR reactions were carried out in a total volume of 10μL on 10ng of cDNA using the following Taqman® assays (Applied Biosystems): synaptosomal-associated protein 25, SNAP-25 (Mm00456921_m1), glyceraldehyde-3-phosphate dehydrogenase. GAPDH (Rn01775763_g1). The relative mRNA levels were calculated using the comparative C_t method, using GAPDH as a normalizer. To test knock-down levels of SNAP25 mRNA, primary neuronal culture was transduced (MOI 20) with the indicated viral vectors at 8 DIV. Transduced cells were selected using puromycin (2μg/ml), mRNA was extracted and reversed triscribed into cDNA. Relative SNAP-25 expression level was determined by Q-PCR.

Mortality assay

Neuron viability was analyzed by simultaneous fluorescence staining of viable and dead cells with calcein-AM (0.5 mg/ml, Invitrogen, Life Technologies Ltd., Paisley, UK), propidium iodide (PI) (1μg/ml, Molecular Probes, Life Technologies Ltd., Paisley, UK) and Hoechst (8.1 μM, Molecular Probes, Life Technologies Ltd., Paisley, UK). Incubation was performed for 20 min in neuronal medium at 37°c and 5% C02. Calcein-AM emits green fluorescence signal in viable cells. Conversely, PI reaches nuclei of dead cells only, where emits red fluorescence. Fluorescence images were acquired by Leica DMI 4000B microscope. The percentage of neuronal death was calculated as the ratio of PI positive and calcein negative dead cells relative to the total number of Hoechst stained neurons.

Immunocytochemical staining

Neuronal cultures were fixed with 4% paraformaldehyde + 4% sucrose, or with 100% cold methanol, depending on the markers. The following antibodies were used: rabbit anti-SV2A (1:1000; Synaptic Systems, Goettingen, Germany), guinea pig anti-Bassoon (1:300; Synaptic Systems, Goettingen, Germany), guinea pig anti-vGLUT1 (1:1000; Synaptic Systems, Goettingen, Germany), mouse anti-PSD95 (1:400; UC Davis/NIH NeuroMab Facility, CA), rabbit anti-GFP (1:400; Invitrogen, San Diego, CA), mouse anti-beta III tubulin (1:400; Promega corporation, Madison, USA), rabbit anti-tubulin (1:80; Sigma-aldrich, Milan, Italy), rabbit anti-MAP2 (Millipore, Billerica, MA, USA), mouse anti-SNAP-25 (1:1000; SMI81 Sternberger Monoclonals, Baltimore MD). Antibody against the BonT/E cleaved portion of SNAP-25 is a kind gift from O. Rossetto (University of Padua, Italy). Secondary antibodies were conjugated with Alexa-488, Alexa-555 or Alexa-633 fluorophores (Invitrogen, San Diego, CA). Images were acquired using a Leica SPE confocal microscope equipped with an ACS APO 63X/1.30 Oil objective. Colocalization of two or three selected markers was measured using the boolean function "AND" for the selected channels. The resulting image was binarized and used as a colocalization mask to be subtracted to single channels. The number of the puncta resulting from colocalization mask subtraction were measured for each marker. A colocalization ratio was set as colocalizing puncta / total puncta number.

Immunohystochemical staining

Experiments were performed on C57BL/6 mice. Animals were anaesthetized with chloral hydrate (4%; 1 ml/100 g body weight, i.p.) and perfused with 4% paraformaldehyde. The brain was postfixed and coronally cut with a Vibratome in 50µm thick serial sections. Immunofluorescence staining was carried out on free-floating sections as described in Frassoni et al., 2005. Free-floating sections were processed for rabbit anti-GFP (1:400, Invitrogen, San Diego, CA) followed by incubation with secondary antibody Alexa-488 fluorophore (Invitrogen, San Diego, CA) and mounted in Fluorsave (Calbiochem, San Diego, CA, USA). Sections were examined by means of a Zeiss LSM 510 META confocal microscope (Leica Microsystems, Germany). The images were acquired using a 40X oil immersion lens (numerical aperture 1.0) with additional electronic zoom factor up to 4. Up to 10 different neurons were acquired and analysed for each animal.

Western blot

Homogenates from cortices, hippocampi and cerebellum from 8 months old wt and heterozygous mice or 3 months old mice injected with virus were analyzed by Western blotting using mouse anti-SNAP-25, 1:1000000 (SMI81, Abcam, Cambridge, UK), rabbit anti-vGlut1 (1:2000; Synaptic System, Gottingen, Germany), rabbit anti-p140Cap (1:4000; kind gift from prof. Paola Defilippi, University of Turin, Italy), rabbit anti-calnexin 1:2000 (Sigma-Aldrich, St Louis, MO), mouse anti-sintaxin 1A (1:1000, Synaptic System, Gottingen, Germany), mouse anti-PSD95 (1:10000; UC Davis/NIH NeuroMab Facility, CA), rabbit anti-GFP (1:4000, Invitrogen, San Diego, CA). Membranes were washed and incubated for 1 hour at room temperature with the secondary antibody IRDye 680-conjugated goat anti-mouse (LI-COR Biosciences, Lincoln, NE; diluted 1:10000). Blots were scanned using an Odyssey Infrared Imaging System (LI-COR Biosciences). The intensities of immunoreactive bands were measured using LI-COR Image Studio, version 2.0 with local background subtracted. For each sample, calnexin was used as a loading control.

Co-immunoprecipitation

Brain tissues were frozen in liquid nitrogen. Proteins were extracted from mice brain with lysis buffer (1% Triton X-100, 150mM sodium chloride, 50mM Tris–HCl pH 7.5, protease inhibitors (Roche, Basel, Switzerland), 1 mM phenylmethylsulphonyl fluoride, 1mM Sodium Vanadate, 1mM Sodium Fluoride, 1mM DTT). For Immunoprecipitation (IP) assays 5mg of total extract were immunoprecipitated for 2 hours at 4°C with specific or unrelated antibodies in presence of Dynabeads® Protein G (Invitrogen). The proteins were resolved by reducing SDS–polyacrylamide gel electrophoresis and transferred to nitro- cellulose filters, which were incubated with the indicated antibodies and developed with ECL system. The following antibodies were used: PSD-95 (1:4000, monoclonal; UC Davis/NIH NeuroMab Facility, CA); SNAP-25 (1:10000, polyclonal, Synaptic System, Gottingen, Germany); mouse monoclonal to p140Cap for western blot was homemade produced as described in Di Stefano et al., 2007.

LUMIER assay

The Lumier assay was performed as described previously (Petrakis et al., 2012). Briefly, PSD-95, SRCIN1, SNAP-25, CTTN were cloned into the bait PA-Renilla luciferase vector and/or into the prey firefly luciferase vector using the gateway

technology (Invitrogen). Vectors were co-transfected into HEK293 cells using jetPEI transfection reagent (Polyplus) and 48h after transfection lysed in HEPES-lysis buffer (50mM HEPES, 150mM NaCl, 10% glycerin, 1% NP-40, 20mM NaF, 1.5mM MgCl2, 1mM EDTA, 1mM DTT, 1x Benzonase, 1x Protease Inhibitor Cocktail –EDTA (Roche), 1mM PMSF). 384-well high-binding white microplates (Greiner) were coated with sheep-gamma globulin (Dianova) and rabbit anti-sheep IgG (Dianova). Bait and prey protein expression was confirmed by measuring Renilla and Firefly luciferease activity of the crude lysates. Baits were immunoprecipitated from cell extracts via the PA-tag and immunoprecipitation and co-immunoprecipitation evaluated by Renilla and Firefly activity, respectively. Luciferase activities were determined using the Dual-Glo Luciferase Kit (Promega) in a luminescence plate reader (TECAN Infinite M1000). To determine background protein binding, bait protein binding to empty prey vectors, as well as prey protein binding to empty bait vector were determined as well.

Proximity Ligation Assay

Proximity Ligation Assay was performed according to the manufactures protocol using custom blocking solutions during antibody incubations (Olink, Bioscience). Briefly, rat cortical neurons were grown at low density (34000 cells/cm^2) on coverslips for 2DIV before AraC (5µM, Sigma) was added to inhibit glial growth and enable signal quantification per neuronal cell. Cells were grown further till 14-DIV and then fixed with 4% PFA, washed with PBS and permeabilized with 0.2% TX-100 in PBS for 2 minutes. Afterwards, cells were washed with PBS-T (0.05% Tween-20) and blocked with 1% BSA PBS-T for 30 min. Primary antibodies were diluted in 1% BSA PBS-T and incubated for 60 min at 37°C before the cells were washed three times with PBS-T. PLA probes PLUS (anti-rabbit) and MINUS (anti-mouse) were diluted 1:5 in 1% BSA PBS-T and incubated for another 60 min at 37°C before the Ligation and Amplification Reactions were performed as described in the PLA assay protocol. PLA signals were detected using the 20x or 40x objective of a Zeiss Imager Z1 fluorescence microscope and quantified using the "find maxima" function of ImageJ. Cell numbers were determined from intact DAPI signal and fragmented nuclear signals resulting from dying glia cells excluded. To exclude an effect of AraC on protein interactions, PLA was performed initially on neuronal culture grown without the addition of AraC (not shown). The following antibodies were used for PLA: rabbit anti-PCLO (1:500, Synaptic Systems, Goettingen, Germany), mouse anti-PSD-95 (1:500, Synaptic

Systems, Goettingen, Germany) and rabbit anti-SNAP-25 (1:100, Synaptic Systems, Goettingen, Germany).

Cell culture electrophysiology

Whole-cell patch-clamp recordings of EPSCs were obtained from 13/14 or 20/21 -old neurons using a Multiclamp 700A amplifier (Molecular Devices) and pClamp-10 software (Axon Instruments, Foster City, CA). Recordings were performed in the voltage-clamp mode. Currents were sampled at 5 kHz and filtered at 2-5 kHz. External solution [Krebs' Ringer's-HEPES (KRH)] had the following composition (in mM): 125 NaCl, 5 KCl,1 .2 $MgSO_4$, 1.2 KH_2PO_4, 2 $CaCl_2$, 6 glucose, and 25 HEPES-NaOH, pH 7.4. Only cells obtained from wt and het embryos that had resting membrane potentials < -50 mV were considered for experiments. Resting membrane potentials were measured immediately upon breaking into whole-cell mode by setting the current to 0 pA. No differences were found between neuronal genotypes. Cells were then voltage-clamped at a holding potential of -70 mV, unless otherwise noted. Recordings of mEPSCs were obtained in presence of Tetrodotoxin (TTX, l µM, Tocris, Bristol, UK) to block spontaneous action potentials propagation. Recording pipettes, tip resistances of 3-5 M were filled with the intracellular solution of the following composition (in mM): 130 potassium gluconate, 10 KCl, 1 EGTA, 10 Hepes, 2 MgCl2, 4 MgATP, 0.3 Tris-GTP. Off-line analysis of miniature events was performed by the use of Clampfit-pClamp-10 software and events had to exceed a threshold of 10 pA to be taken into account.

For evoked currents, recording pipettes obtained as described above, were filled with the intracellular solution of the following composition (in mM): 130 K-gluconate, 10 KCl,1 EGTA, 10 HEPES, 2 MgCl2, 4 MgATP, and 0.3 Tris-GTP. The inhibitory or excitatory nature of the presynaptic neurons was routinely determined at the end of each experiment by application of selective receptor blockers (100µM APV+ 20µM CNQX or 20µM bicuculline) to unambiguously identify the presynaptic neuronal phenotype. Also reversal potential was kept in consideration to identify and distinguish excitatory vs inhibitory cells (closed to -50 mV for eIPSCs and + 5mV for eEPSCs). We tested synaptic connectivity by applying at least 15 sweeps, each of them separated by 5 sec.

Paired pulse ratio (PPR=P2/P1) was recorded by applying pairs of action potentials separated by inter-stimulus intervals (ISIs) of 50/100/150 ms and presented every 5 sec. RRP sizewas evaluated exposing neurons for 4 sec to hypertonic solution containing 4-5

M sucrose with a puffer pipette. The ionophore calcimycine (40µM) was applied for 90 seconds. In siRNA experiments, acute downregulation of SNAP-25 was carried out at DIV 10 and measurement of PPR was performed at DIV 14.

For chemical LTP experiments, recordings of EPSCs were performed using the same intracellular solution of miniature events while glycine (100 µM, Sigma-Aldrich, Milan, Italy) was applied for 3 minutes at room temperature in Mg^{2+}free KRH also containing TTX (0.5 µM), bicuculline (to block GABA-A receptors, 20 µM, Tocris, Bristol, UK) and strychnine (1 µM, Sigma-Aldrich, Milan, Italy).

Fluorescence recovery after photobleaching (FRAP)

FRAP experiments were performed by maintaining coverslips in a 37°C heated chamber with 5% CO_2 in their own growth medium. Live imaging was performed with a confocal microscopy Leica SP5 using a HCX PL APO 63X/ 1.4 OIL objective. Photobleaching was obtained using a 488nm laser light at 100%. Images were collected every 500ms. The region of interest (ROI) placed over the spine was used for both photobleaching and fluorescence recovery analysis. Analysis was performed on the first 40sec of acquisition. Each image at each time point was corrected for the background and for the ongoing bleaching and normalized according to this formula: $((F_t\text{-}F_b)/(F_r\text{-}F_b))/(F_a\text{-}F_b)$, where F_t is the fluorescence of a ROI at time t; F_b is the fluorescence of the background; F_r is the fluorescence of the reference ROI at time t and F_a is the fluorescence of the ROI immediately before photobleaching. The data obtained were fitted with a single exponential using the Leica SP5 software.

Golgi staining

Mice were deeply anesthetized with avertin (0.2ml/10g body weight, i.p.) and perfused transcardially with 0.9% saline solution. The brains were removed and stained by modified Golgi-Cox method described by Glaser and Van der Loos (1981). Coronal sections of 100µm thickness from the dorsal hippocampus were obtained using a vibratome (VT1000S, Leica, Wetzlar, Germany). These sections were collected on clean, gelatin-coated microscope slides and treated with ammonium hydroxide for 30 min, followed by 30 min in Kodak Film Fixer, and finally were rinsed with distilled water, dehydrated and mounted with a xylene-based medium.

Lentiviral injection

C57BL6 mice (Janvier labs) were deeply anaesthetized (100 mg/kg Ketamine (KETAVET, INTERVET), 10 mg/kg Xilazina (Rompun, BAYER) in physiologic solution) and placed on a stereotaxic frame (Kopf). The viral suspension was delivered via glass needle attached to a 10μl Hamilton syringe. Bilateral injection (2μl/each) was performed in the CA1 area of dorsal hippocampus (coordinates of injection: anteroposterior -2.0, lateral ±1.5, dorsoventral -1.1 from dura madre surface) at a rate of 1μl/min. Coordinates of injection were calculated from the Bregma level according to Paxinos and Franklin Mouse Brain Atlas (Paxinos and Franklin, 1997) under microscope guide (L-0940SD, INAMI). The needle remained in place for an additional 5 minutes to facilitate the controlled delivery of the virus. The titer of the SNAP-25-shRNA virus is $2.3*10^9$ tu/ml and for the scramble $5*10^8$ tu/ml. Stereotaxic injections into the gustatory cortex were performed as described in Elkobi et al., 2008.

CTA learning

Taste learning paradigms are discussed in details in Gal-Ben-Ari and Rosenblum, 2011. Briefly, rats were habituated to get their daily water ratio once a day for 20 min from two pipettes, each containing 5 ml of water for three days. On the fourth (conditioning) day, they were allowed to drink 0.3% NaCl (Sigma) solution (prepared in tap water-the water mice usually drink) instead of water from similar pipettes for 20 min, and 40 min later were injected with LiCl (0.14M for strong CTA; 2% b.w). They were given 20 min access to water on days 5 and 6. On day 7 (memory test) mice were subjected to a multiple choice test situation involving two pipettes with 5 ml each of conditioned taste solution (NaCl) and two with 5ml each of water. The mice tested again for one more day (Day1). The behavioral data are expressed in terms of preference- the volume of NaCl consumed divided by the total fluid consumed (NaCl/ml water plus ml taste).

Statistical analysis

Analysis was performed using ImageJ software (NIH, Bethesda, Maryland, USA). Statistical analysis was performed using SigmaStat 3.5 (Jandel Scientific), with statistical tests used based on initial testing distribution normality. Data are presented as mean ± SEM. Differences were considered to be significant if $p<0.05$ and are indicated by an asterisk; those at $p<0.01$ are indicated by double asterisks; those at $p<0.001$ are indicated by triple asterisks.

RESULTS

SECTION I:
REDUCED SNAP-25 LEVELS IMPACT NEUROTRANSMISSION IN DEVELOPING HIPPOCAMPAL CULTURES

Spontaneous and evoked synaptic currents in developing excitatory and inhibitory neurons

It has been demonstrated that SNAP-25 negatively modulates voltage-gated calcium channels (VGCC) (Pozzi et al., 2008, Condliffe et al., 2010). In a first study, to which I contributed, we aimed to investigate whether changes in VGCC current densities affect neurotransmission in developing (13-14 days in vitro, DIV) hippocampal cultures from SNAP-25 wild-type (wt) and heterozygous (het) mice. As indicated from previous studies (Washbourne et al., 2002, Sharma et al., 2011), we found no differences in miniature excitatory and inhibitory spontaneous synaptic currents (mEPSC or mIPSC) neither in frequency nor in amplitude in het neurons relative to wt (Fig.17 A and B).

Depolarization of presynaptic glutamatergic or GABAergic cells in synaptically connected neurons evoked unitary EPSCs or IPSCs, respectively. Evoked EPSCs were significantly larger in het cultures compared to wt. On the contrary, in gabaergic neurons a slight, but significant reduction in IPSCs has been observed (Fig. 17C). The small reduction in eIPSC amplitude recorded in het neurons could be endorsed to the SNARE properties of SNAP-25. Actually, SNAP-25, although being expressed at very low levels in most GABAergic terminals, appears to be part of the SNARE complex in GABAergic neurons.
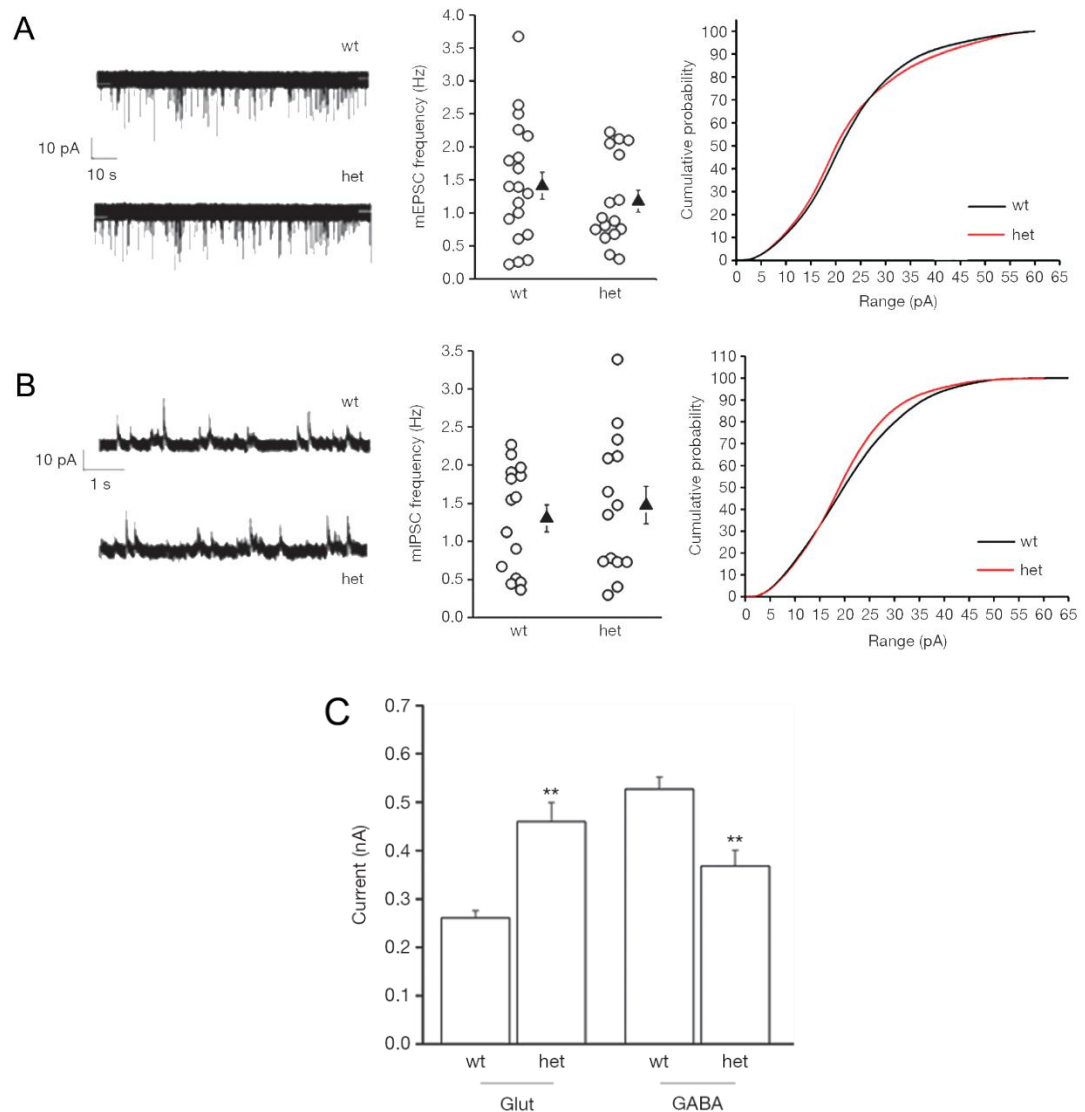
Fig. 17: A-B) Representative traces of mEPSC and mIPSC in wt and het neurons, followed by the analysis of frequency and amplitude. C) Analysis of EPSC and IPSC in wt and het cultures.

Increased glutamatergic transmission depends on an altered regulation of VGCC

We analysed various parameters to determine the basis of the enhanced glutamatergic transmission. We investigated possible modifications in the synapse number, which did not differ between wt and het cultures as revealed by the analysis of the density of the puncta positive for SV2A (i.e. SV2A puncta/μm), a vesicular protein presents either in excitatory or inhibitory synapses. We could also exclude an imbalance between excitatory and inhibitory synapses, because the ratio v-Glut1/v-GAT was the same between genotypes (Fig. 18A and B). v-Glut1 is the vesicular transporter of glutamate, instead v-GAT is the vesicular transporter of the neurotransmitter GABA, so they univocally mark excitatory or inhibitory synapses, respectively.

Moreover, enhanced EPSCs amplitude was not due to changes in the readily releasable pool of synaptic vesicles, as revealed by hypertonic sucrose application (Fig. 18C). When a hypertonic solution is first applied, the quantal release rate jumps rapidly to a relatively high level and then declines approximately exponentially to a low, steady level. The readily releasable pool is defined as those quanta that are released during the transient burst of exocytotic activity following application of hypertonic solution (Rosenmund and Stevens, 1996). Both in wt and het cultures there was no difference considering the RRP charge.

Finally, the charge transfer at glutamatergic synapses induced by 40mM calcimycin was lower, although not significantly, in het neurons with respect to wt (Fig. 18D). Calcimycin is a divalent cation ionophore, allowing ions to cross cell membranes, which are usually impermeable to them. It causes calcium dependent exocytosis bypassing voltage-gated Ca^{2+} channels thus allowing a direct evaluation of the efficacy of SV fusion machinery downstream of Ca^{2+} influx into the presynaptic boutons (Tokuoka and Goda, 2006). The reduction observed in het cultures suggests a requirement of presynaptic calcium channels in the SNAP-25-dependent effects.
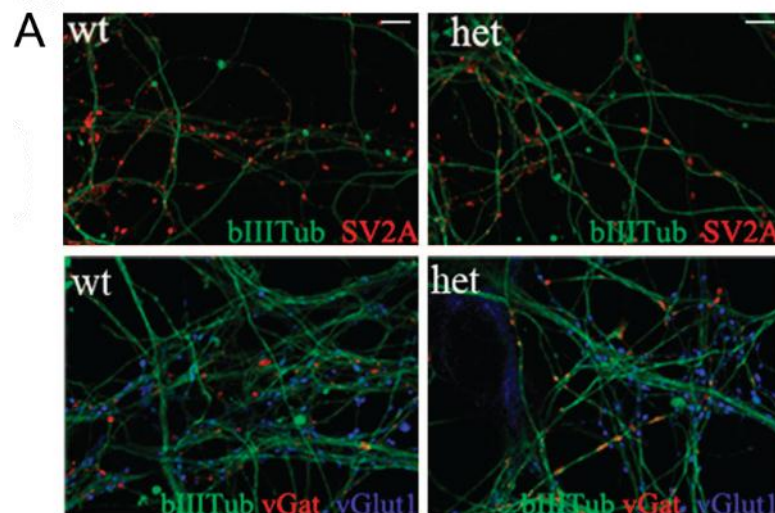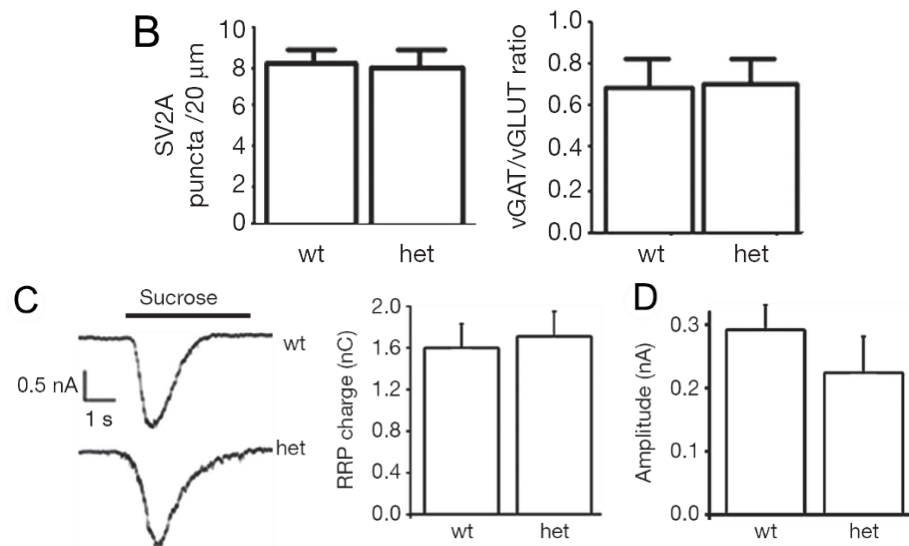
Fig. 18: A) Representative image of wt and het neurons stained for βIIItubulin (green) and SV2A (red) or v-Glut1 (blue) and v-GAT (red). Scale bar: 10μm. B) Quantification of SV2A puncta / μm and the v-Glut1/v-GAT ratio. C) Sucrose-evoked response and relative RRP charge in wt and het. D) Charge transfer in calcimycin experiment.

Altered short-term plasticity at SNAP-25 het synapses

Short-term synaptic plasticity regulates the activity of neural networks and information processing in the nervous system and typically reflects a presynaptic change in neurotransmitter release (Catterall el al., 2008). The direction of short-term plasticity (depression or facilitation) correlates with the initial efficacy with which synapses transduce action potentials into neurotransmitter release. Synapses with a high release probability are more likely to show depression (called pair-pulse depression, PPD), consistent with a depletion of vesicles from the readily releasable pool or an activity-dependent inhibition of the release machinery. Synapses with an initially low release probability do not exhaust their releasable pool of vesicles in response to the first action potential, so a lingering effect of the first stimulation can potentiate the response to subsequent stimuli (pair pulse facilitation, PPF) (Sippy et al., 2003). Calcium is heavily involved in this phenomenon because the source and regulation of the residual Ca^{2+} initiates the process and the effector mechanism responds to residual Ca^{2+} and enhances neurotransmitter release. Paired-pulse ratio (PPR) is the fraction between the entities of the response to the second respect to the first stimulus.

Given that alteration in presynaptic release in het neurons seemed to be ascribed to an alteration in calcium channels, we tested short-term plasticity in wt and het neurons.

Fig. 19 shows PPF occurring in wt, whereas in het the same protocol (two consecutive

stimuli delivered with an inter-spike interval of 50ms) resulted in PPD. In contrast, only a slight, although significant, reduction in PPR occurred at het inhibitory synapses, which were characterized, as their wt counterpart, by prevalence of PPD.
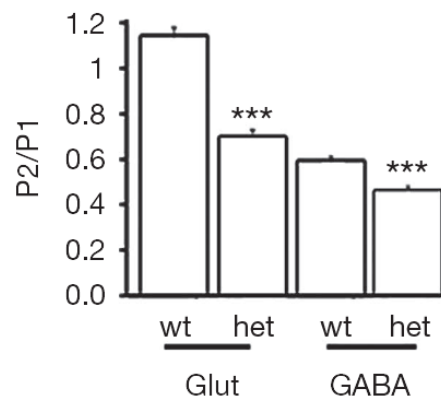

Fig. 19: PPR at glutamatergic and gabaergic synapses.

To further confirm that the actual presynaptic reduction of SNAP-25 was responsible for the shift from PPF to PPD, paired recordings were carried out from mixed cultures of wt hippocampal neurons, from genetically modified mice constitutively expressing GFP under the beta-actin promoter (Okabe et al., 1997), and neurons heterozygous for SNAP-25, originating from the same strain of mice, but not expressing GFP (Fig. 20A). In this set up wt-GFP neurons were plated with het neurons, thus, it is possible to stimulate a neuron of one genotype and see the effects on the synaptically-connected neuron of the other genotype, isolating the preysinaptic from the postsynaptic component (Fig. 20B).

Recordings revealed that PPR was strongly dependent on the genotype of the presynaptic neuron. In particular, wt-GFP presynaptic neurons invariably produced facilitating EPSCs, whereas presynaptic het neurons induced depressing glutamatergic responses (Fig. 20C).
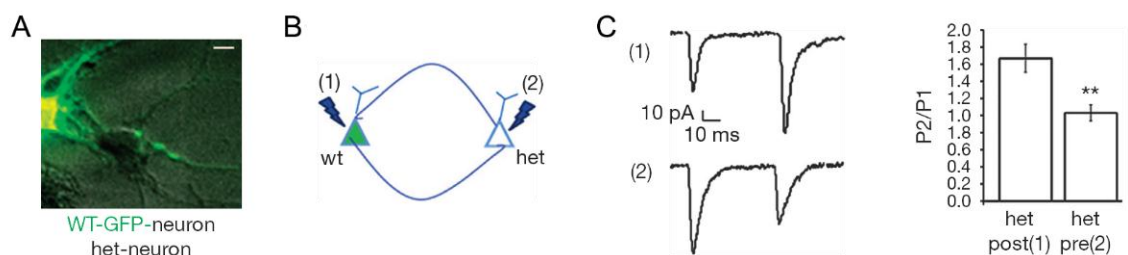

Fig. 20: A) Merged bright field and fluorescence image of a mixed culture (wt-GFP with het neurons). Scale bar:10μm. B) Short-term plasticity in pairs where either the presynaptic [2] or the postsynaptic [1]

neuron was het for SNAP-25. C) Representative traces and mesurement of PPR when the het neuron is at the postsynapse [1] or at the presynapse [2].

Evoked response and paired pulse facilitation are restored in mature cultures

During in vitro maturation, SNAP-25 levels increase in wt, as known by literature (Bark et al., 2004), but also in het cultures. Probably due to this fact, some of the electrophysiological alterations we observed disappeared in 21DIV het cultures. Consistently, no differences in evoked response (Fig. 21A) and PPR (Fig. 21B) have been found in 21 DIV in excitatory and inhibitory synapses.
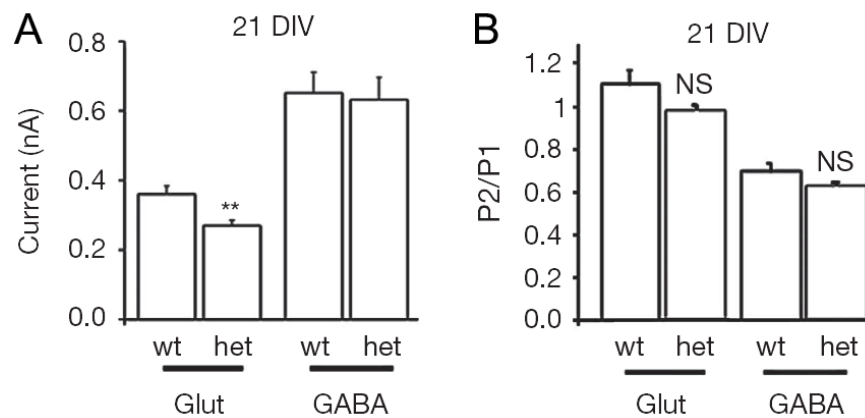

Fig. 21: Evoked response (A) and pair-pulse ratio (B) evaluated in excitatory and inhibitory terminals in wt and het cultures at 21DIV.

Interestingly, on the contrary, 21DIV SNAP-25 het networks showed a significant reduction in both frequency and amplitude of miniature excitatory postsynaptic current (mEPSC) relative to wt age-matched cultures (Fig. 22). These results suggested that reduced levels of SNAP-25 might affect synapse function at later stages of development. Two processes might therefore take place in neurons developing in the presence of reduced SNAP-25 levels, the first occurring at the presynaptic level at early developmental stages, when the protein is significantly reduced, and a second happening at later stages of maturation and mainly affecting the postsynapse.
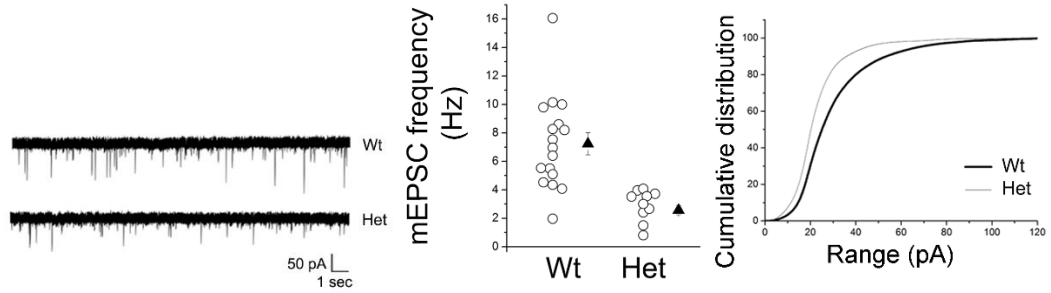
Fig. 22: Representative traces of mEPSCs from 21DIV wt or het neurons followed by the corresponding quantitative analysis of miniature frequency (frequency (Hz) wt=7.23±0.78; het=2.56±0.32; Student t-test, p= <0.001) and amplitude (Amplitude (pA) wt=37.67±2.3; het=29.61±0.99, cumulative probability; Kolmogorov-Smirnov test, p<0.05; number of neurons: wt=17, het=10; 2 independent experiments).

Acute down-regulation of SNAP-25 changes paired pulse ratio

So far, we have demonstrated that reduction of presynaptic SNAP-25 in developing cultures leads to an altered synaptic trasmission, i.e. an increase in evoked response and a shift from PPF to PPD. However, we also observed a recovery of normal excitatory neurotrasmission and short-term plasticity in mature cultures. We then aimed to demonstrate that the effects previously described are effectively dependent from a reduction of SNAP-25 at a presynaptic level.

To address this issue, SNAP-25 has been acutely downregulated by transfection of rat hippocampal neurons with a cDNA codifying a small RNA interference sequence (Condliffe et al., 2010) (siRNA) (Fig. 23A). This treatment reduces the protein expression of about 60% (Grumelli et al., 2010). Dual whole-cell recordings were performed from synaptically connected neurons. Results show that acute reduction of SNAP-25 in the presynaptic glutamatergic neuron leads to PPD instead of PPF (Fig. 23B) Importantly, no changes were present when scramble or SNAP-25 siRNA was transfected in the postsynaptic neuron (Fig. 23C). Therefore, even acute reductions of SNAP-25 in wt presynaptic neurons switch PPF to PPD at glutamatergic synapses.
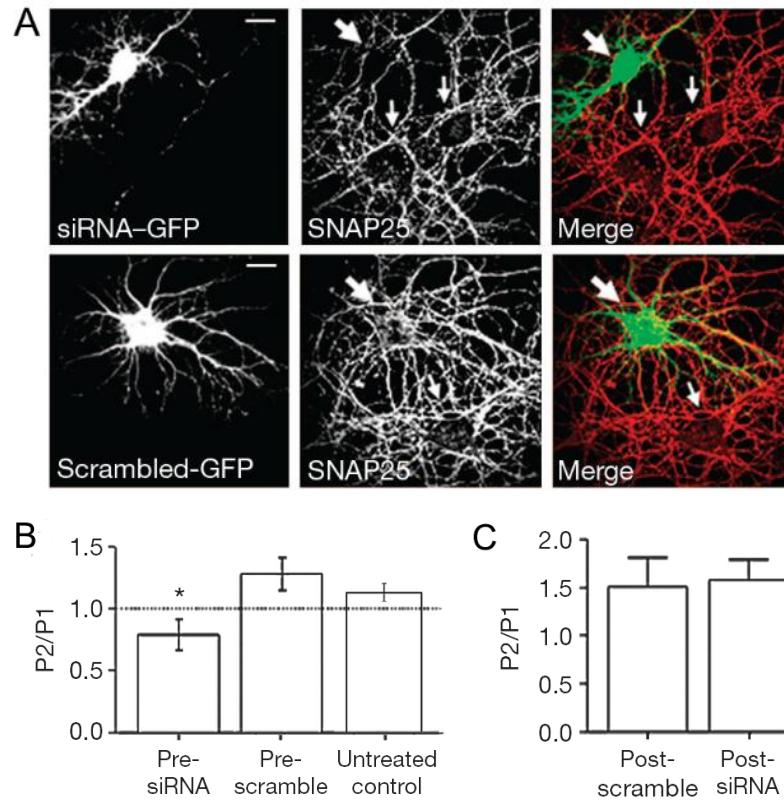
Fig. 23: A) SNAP-25 staining in neurons co-transfected with either SNAP-25 siRNA plus GFP or scramble sequence plus GFP. Large arrows point to neurons transfected with either siRNA (top panels) or scramble (bottom panels) constructs. Small arrows point to non-transfected neurons. Scale bar: 20μm. B) PPR in scramble presynaptic versus SNAP-25 siRNA presynaptic. C) PPR in SNAP-25 siRNA postsynaptic versus scramble siRNA postsynaptic.

Taken together, these data demonstrate that reductions of SNAP-25 in developing neurons (14DIV) alter neurotransmission, and it is a clear presynaptic, SNAP-25-dependent effect. Moreover, there is a hint that in more mature cultures (21DIV) the defect involves the postsynaptic compartment.

SECTION II:
REDUCED SNAP-25 INCREASES PSD-95 MOBILITY AND IMPAIRS SPINE MORPHOGENESIS

Acute reduction of SNAP-25 expression in CA1 alters spine morphology

As extensively described in §3.4 of the Introduction, new roles are emerging for SNAP-25 in the postsynaptic compartment. I have already mentioned that postsynaptic SNAP-25 regulates surface NMDAR levels and plays a role in LTP induction in the CA1

hippocampal neurons (Jurado et al., 2013). Given that activity-driven changes of synaptic efficacy underlying LTP require proper dendritic spine morphogenesis, we used a lentiviral approach to induce *in vivo* silencing of SNAP-25 by expressing short hairpin RNA (shRNA) specific for SNAP-25. The construct has EGFP as a marker, and as control we expressed scrambled shRNA-EGFP (Fig. 24A). At first, we validated the SNAP-25-shRNA lentiviral constructs either in mice primary neuronal cultures by real time-PCR analysis (Fig. 24B) or in vivo by evaluating CTA (conditioned taste aversion) memory which has been previously demonstrated to be impaired in SNAP-25 het mice (Corradini et al., 2012). CTA is a form of associative learning in which an animal rejects a food that has been paired previously with a toxic effect (e.g., a sucrose solution paired with a malaise-inducing injection of lithium chloride). The indicated vectors were injected into the gustatory cortex, which resides within the insular cortex, and the rats were tested for CTA memory. Rats injected with scrambled lentiviral vectors displayed a normal CTA, while the LV- SNAP-25 shRNA injected rats did not (Fig. 24C), thus indicating that acute down-regulation of SNAP-25 into the gustatory cortex is sufficient to affect CTA and that this shRNA sequence is specific in either mice or rats.
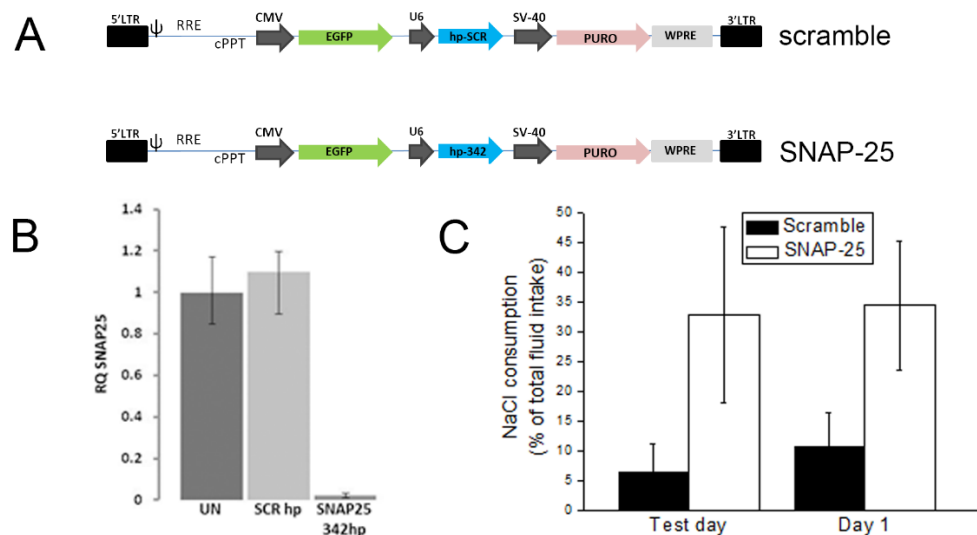
Fig. 24: A) Schematic representation of lentiviral constructs. B) Silencing efficiency of SNAP-25 shRNA determined by Q-PCR. C) Acute down-regulation of SNAP-25 in the gustatory cortex affects CTA memory. Control group (n=4) demonstrate low preference/high avoidance from the conditioned taste whereas the shRNA injected group (n=4) show high preference/low avoidance demonstrating an impaired CTA memory during two consecutive test days (Test day: wt=6.3±0.05, het=32.8±0.15; p=0.127 T-test. Day 1: wt=10.6±0.06, het=34.5±0.11; p=0.087 T-test).

Then to evaluate whether SNAP-25 is required for dendritic spine morphogenesis *in vivo*, we injected mice in the CA1 region of the hippocampus. We quantified by confocal microscopy the spine morphology of CA1 neurons positive for the fluorescent reporter GFP, which allows the unambiguous identification of cells expressing SNAP-25-shRNA. Mice were perfused 15 days after lentiviral vector injection and the brains were sectioned and immunostained for GFP (Fig. 25A low mag image). Spine density and morphology were analyzed on secondary and tertiary branches of apical dendrites in the stratum radiatum (SR; Fig 25A high mag image). SNAP-25 knockdown caused a significant decrease in spine density on CA1 dendrites in LV-shRNA-SNAP-25 neurons with respect to the LV-Scramble-SNAP-25 controls (Fig. 25B). Such a decrease was accompanied by a significant reduction in the number of mushroom spines and an increase in the number of thin spines (Fig. 25C), that suggest a reversal toward a more immature phenotype.
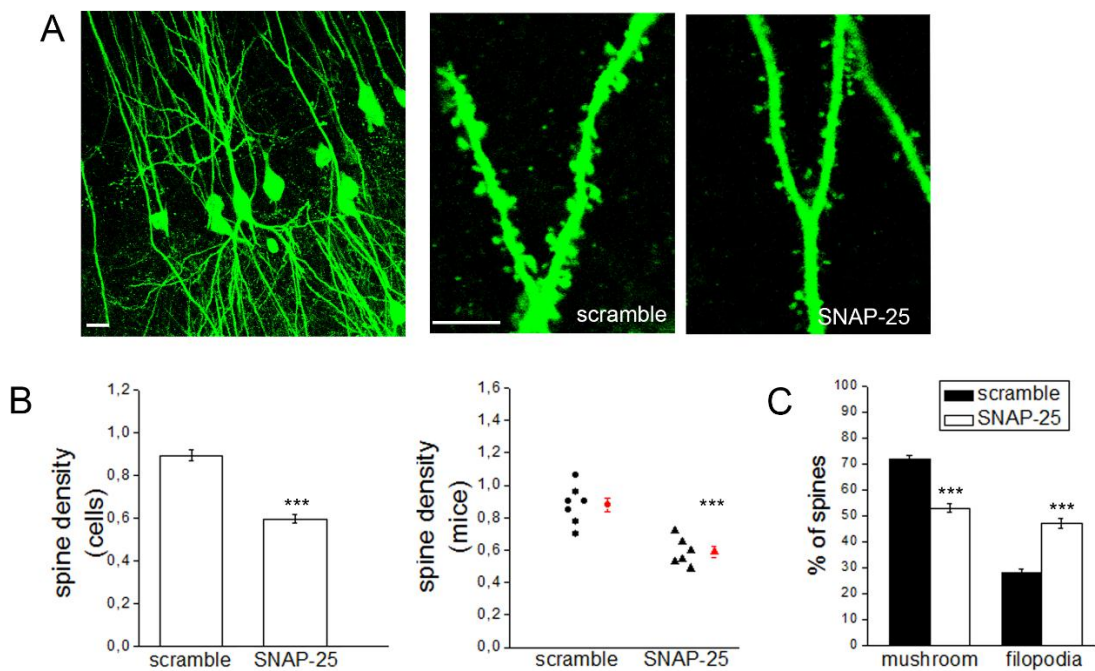

Fig. 25: A) Representative images of a coronal slice showing the CA1 area of an hippocampus injected with the lentiviral vector (low magnification, left) and the secondary branches of apical dendrites of scramble and shRNA SNAP-25 treated mice (high magnification, right). Scale bars 20µm, 10µm respectively. B) Quantification of spine density in the CA1 field of scramble and shRNA SNAP-25 treated mice. A reduction in spine densities was found (number of spines per µm: scramble=0.89±0.03; shRNA SNAP-25=0.60±0.02; p= <0.001; Student t-test; comparison between animals: scramble: 0.88±0.04, n=7; shSNAP-25:0.59±0.04, n=6, p<0.001, Student t-test). C) Quantitative analysis of mushroom-type and thin filopodia-like spines percentage. Of note, SNAP-25-shRNA neurons show a decrease in mature spine number (mushroom-type) which is accompanied by an increase in thin spine number (filopodia-like) (percentage of spines: mushroom: scramble=71.9±1.4; shRNA SNAP-25=53±1.7; p=<0.001, Student t-test. Filopodia: scramble=28.1±1.4; shRNA SNAP-25=47±1.7; p= <0.001; Student t-test). Number of examined cells: scramble=38, shRNA SNAP-25= 36. 7 scramble and 6 shRNA SNAP-25 animals were analyzed and all data are expressed as mean±SEM.

To characterize the underlying molecular mechanisms, we decided to investigate a panel of synaptic proteins from the LV-shRNA or LV-scramble SNAP-25 injected area. Quantitative western blotting analysis carried out on the dorsal hippocampus of LV-shRNA SNAP-25 mice showed a consistent reduction in the levels of expression of the postsynaptic protein PSD-95 along with SNAP-25 whereas no virtual changes occurred in vGlut-1 and syntaxin1A (Fig. 26).
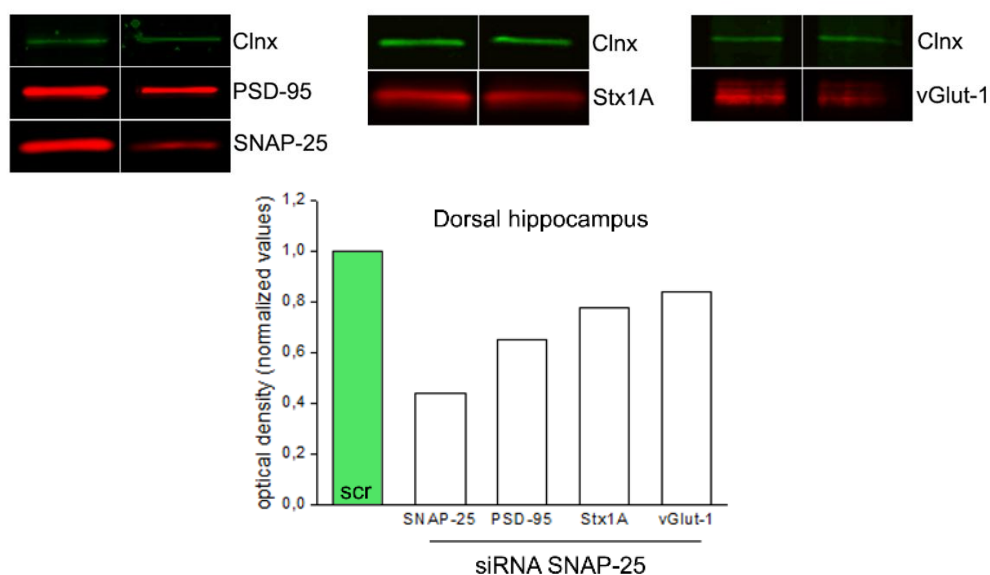
Fig. 26: Exemplificative western blot of synaptic proteins from the injected LV hippocampal area. Note the reduction of SNAP-25 and PSD-95 in SNAP-25-shRNA LV treated versus scramble treated animals. No change is evident in syntaxin1A and vGlut1 expression levels.

These results indicate that in vivo down-regulation of SNAP-25 directly affects spine morphology and PSD-95 expression.

Defective postsynaptic maturation of glutamatergic synapses in SNAP-25 heterozygous cultures

The alteration in spine morphology and the consequent reduction of a key postsynaptic protein such as PSD-95 prompted us to hypothesize an alteration in the maturation of the synapse itself. To investigate if reduced SNAP-25 expression impairs the proper maturation of glutamatergic synapses, we used primary hippocampal cultures prepared from SNAP-25 heterozygous (het) embryos. In these neurons, a 50% reduction of

SNAP-25 levels was detected by quantitative immunocytochemistry in the somato-dendritic region and around 30% at axonal varicosities (Fig. 27A and B).

Fig. 27: A) Representative images of 21 DIV wt and het neurons stained for SNAP-25 (upper panel), Map2 and Bsn (lower panel). Scale bar, 10µm (upper panel) and 5µm (lower panel). B) Quantitation of SNAP-25 signal has been carried out in the somatodendritic and axo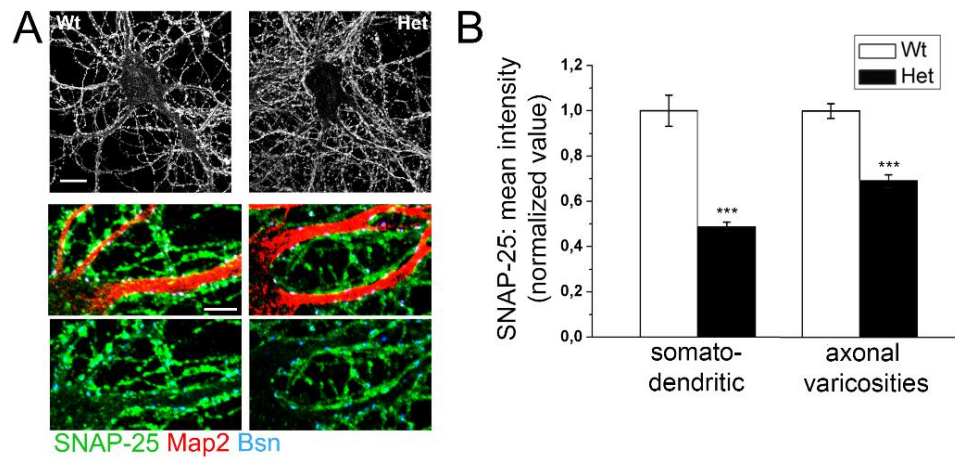nal compartments respectively. The histogram shows the reduction of SNAP-25 signal in both compartments (Somatodendritic area: wt 21DIV= 1±0,069; het 21DIV=0,48±0,022. Mann-Whitney Rank Sum Test, p= <0,001. Axonal varicosities: wt 21DIV= 1±0,032; het 21DIV=0,69±0,026. Student t test, p= <0,001. Data represents mean±SEM. Number of cell analyzed: 7 wt and 8 het).

Immunocytochemical stainings for the synaptic vesicle protein SV2A, for the active zone component Bassoon and for the postsynaptic scaffold protein PSD-95 were performed at 14 and 21DIV and percentages of colocalization among these proteins were quantified. Since the levels of SV2A do not differ between wt and het cultures we used this protein as a reference marker (Antonucci et al., 2013; see above). The percentage of juxtaposed pre- and postsynaptic terminals relative to the total presynaptic sites (SV2A&PSD-95/SV2A), the percentage of synapses showing immunoreactivity for the all three markers (SV2A&PSD-95&Bsn/SV2A) and the percentage of mature presynaptic terminals (SV2A&Bsn/SV2A) were quantified (Fig. 28A-C). The increase in the first two parameters occurring in wt cultures between 14 and 21DIV (Fig. 28B) is consistent with the physiological maturation of neuronal cultures and the increasing number of synaptic contacts, while the lack of increase in the percentage of SV2A&Bsn/SV2A colocalizing puncta is in line with the earlier maturation of presynaptic relative to postsynaptic terminals, which is completed already at 14DIV (Garner et al., 2006). A similar analysis carried out in het cultures revealed a lack of postsynaptic maturation between 14 and 21DIV (Fig. 28C).
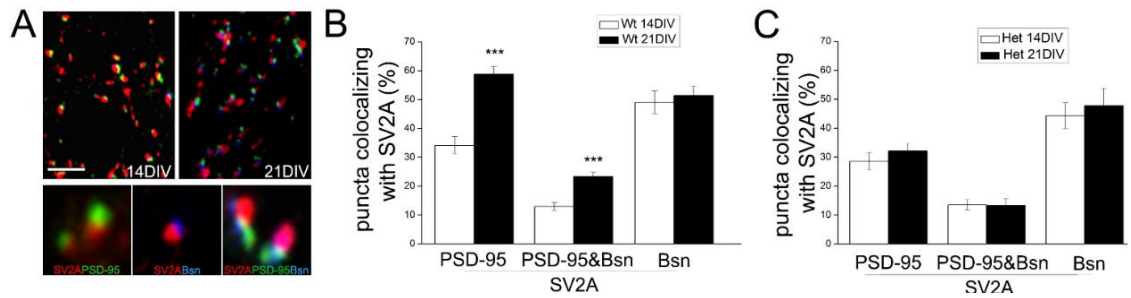
Fig. 28: A) Representative images of 14DIV and 21DIV wt cultures stained for the presynaptic markers SV2A (red), Bassoon (blue) and the postsynaptic protein PSD-95 (green). Scale bar: 5μm. B-C) Quantification of the percentage of colocalizing puncta of juxtaposed pre- and postsynaptic terminals relative to the total presynaptic sites (SV2A&PSD-95/SV2A), the percentage of synapses showing immunoreactivity for the all three markers (SV2A&PSD-95&Bsn/SV2A) and the percentage of mature presynaptic terminals (SV2A&Bsn/SV2A) during development, in wt (B) and het (C) cultures at 14 and 21 DIV. Postsynaptic maturation occurs in wt cultures between 14DIV and 21DIV (wt 14DIV= SV2A&PSD-95/SV2A: 34.1±3.0; SV2A&PSD-95&Bsn/SV2A: 12.9±1.4; SV2A&Bsn/SV2A: 49±4.0, number of fields analyzed: 31; 21DIV= SV2A&PSD-95/SV2A: 58.8±2.7; SV2A&PSD-95&Bsn/SV2A: 23.4±1.5; SV2A&Bsn/SV2A: 51.4±3.2; number of fields analyzed: 27; Mann-Whitney rank sum test p= <0.001; 3 independent experiments). A lack of postsynaptic maturation occurs in het cultures during development (het 14DIV= SV2A&PSD-95/SV2A: 28.5±3.0; SV2A&PSD-95&Bsn/SV2A: 13.5±1.8; SV2A&Bsn/SV2A: 44.3±4.5, number of fields analyzed: 20; 21DIV= SV2A&PSD-95/SV2A: 32.2±2.7, SV2A&PSD-95&Bsn/SV2A: 13.3±2.3; SV2A&Bsn/SV2A: 47.7±6.0, number of fields analyzed: 15; Mann-Whitney rank sum test p=0.397, p=0.881, p=0.726 respectively; 3 independent experiments).

In order to exclude the possibility that the alteration of PSD-95 density might result from a progressive decline of neuronal viability in culture, cell mortality was quantitatively assessed by propidium iodide (PI) and calcein staining. While calcein emits green fluorescence signal in viable cells, PI reaches nuclei of dead cells only. Quantification of PI-positive/calcein-negative cells relative to the overall nuclei (labeled with Hoechst) indicated no difference in the extent of cell death between wt and het cultures, at both 14DIV and 21DIV (Fig. 29).
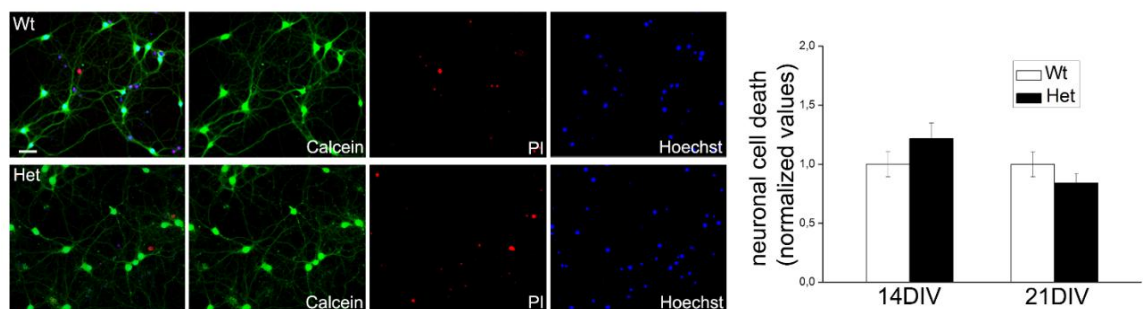
Fig. 29: Representative images of 14DIV wt and het cultures stained with propidium iodide (red), calcein (green) and Hoechst dye (blue). Propidium iodide positive cells relative to the overall Hoechst positive nuclei were counted (normalized data). The histogram shows no difference in the extent of cell death between wt and het cultures. (wt 14DIV=1.00±0.12, number of fields analyzed: 44; het 14DIV=1.22±0.13, number of fields analyzed: 52; p=0.429; wt 21DIV=1.00±0.11, number of fields analyzed: 37; het 21DIV=0.84±0.08, number of fields analyzed: 44; Mann-Whitney Rank Sum Test p=0.418, 4 independent experiments). Scale bar: 40μm.

As already presented, a difference in mEPSC frequency and amplitude occurs in primary hippocampal mature cultures (see above), thus confirming that morphological and functional postsynaptic defects become evident only at later stages during neuronal development.

We then performed a morphological analysis of dendritic spines also in culture, in wt and heterozygous GFP-transfected neurons at 21DIV. The results showed a significant reduction in the number of mushroom spines and a parallel increase in the density of thin, filopodia-like protrusions (Fig. 30A and B). Concomitantly, a significant reduction in the number of PSD-95 puncta per unit length (Fig. 30C and D) and a smaller PSD-95 cluster size (Fig. 30C and E) were detected in het cultures relative to wt.

This data indicate that neuronal cultures constitutively developing in the presence of reduced protein levels show a defective maturation of the glutamatergic postsynaptic compartment, which resembles the spine defect of CA1 interfered neurons.
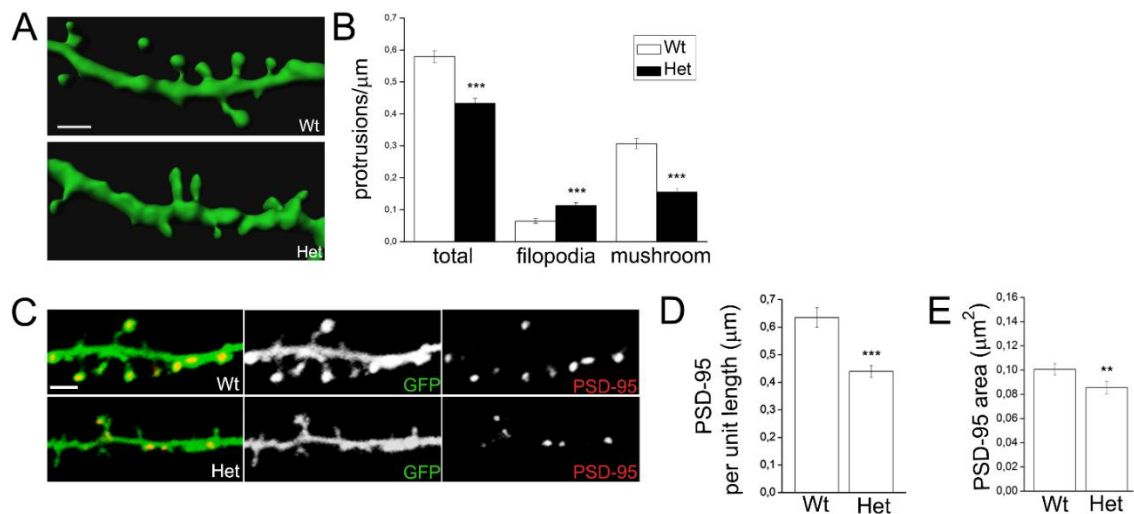
Fig. 30: A) 3D reconstruction of dendritic shaft of neurons from 21DIV wt or het cultures transfected with GFP. Scale bar 2μm. B) Quantification shows a reduction of the number of total protrusions in het neurons with respect to wt (number of protrusions per micron, wt=0.58±0.02, number of examined dendrites: 83, number of neurons: 37; het=0.43±0.02, number of examined dendrites: 87; number of neurons: 45; Mann-Whitney rank sum test p= <0.001; 3 independent experiments). The decrease in mature spine number (mushroom-type) is accompanied by an increase in thin spine number (filopodia-like) (number of mushroom spines per micron, wt: 0.31±0.02, number of examined dendrites: 63; number of neurons: 37; het: 0.16±0.01, number of examined dendrites: 84; number of neurons: 45; number of filopodia-like spines per micron, wt: 0.06±0.01; het: 0.11 ±0.01; Mann-Whitney rank sum test p= <0.001; 3 independent experiments). C) Representative images of 21 DIV wt and het cultures transfected with GFP and immunostained for PSD-95 (red). D) Quantification of PSD-95 positive puncta per unit length of parent dendrite (μm) (wt= 0.64±0.04, number of examined dendrites: 88, number of neurons: 34; het= 0.44±0.02, number of examined dendrites: 68, number of neurons: 33; Mann-Whitney rank sum test p<0.001; 3 independent experiments). E) Quantification of PSD-95 puncta size reveals a significant reduction in het neurons (in μm², wt=0.101±0.004, number of puncta: 433; number of analyzed neurons:

10; het=0.086±0.005, number of puncta: 354, number of analyzed neurons: 7; Mann-Whitney rank sum test p=0.003; 3 independent experiments). Data are expressed as mean±SEM. Scale bar 2μm.

As mentioned before, *SNAP25* gene has been associated with different psychiatric diseases and SNAP-25 levels are lower in the hippocampus and in the frontal lobe of patients with schizophrenia (Young et al. 1998; Thompson et al., 1998 and 2003). Moreover, a reduction in spine density and morphological alterations in dendritic spines of schizophrenic patients has been reported (Penzes et al., 2011; Bennett, 2011). We then aimed to assess whether reduction of SNAP-25 impacts spine morphogenesis also in brain of het mice. Spine density and length were measured from the second and third branches of apical dendrites in the CA1 area of wt and SNAP-25 het mice, using Golgi-Cox labeling (Glaser and Van der Loos, 1981, Fig. 31A). Indeed, a reduction of spine density, accompanied by morphological abnormalities, was observed in the hippocampi of adult SNAP-25 het mice (Fig. 31B-C), indicating that genetically reduced SNAP-25 levels lead to dendritic spines defects also in vivo.
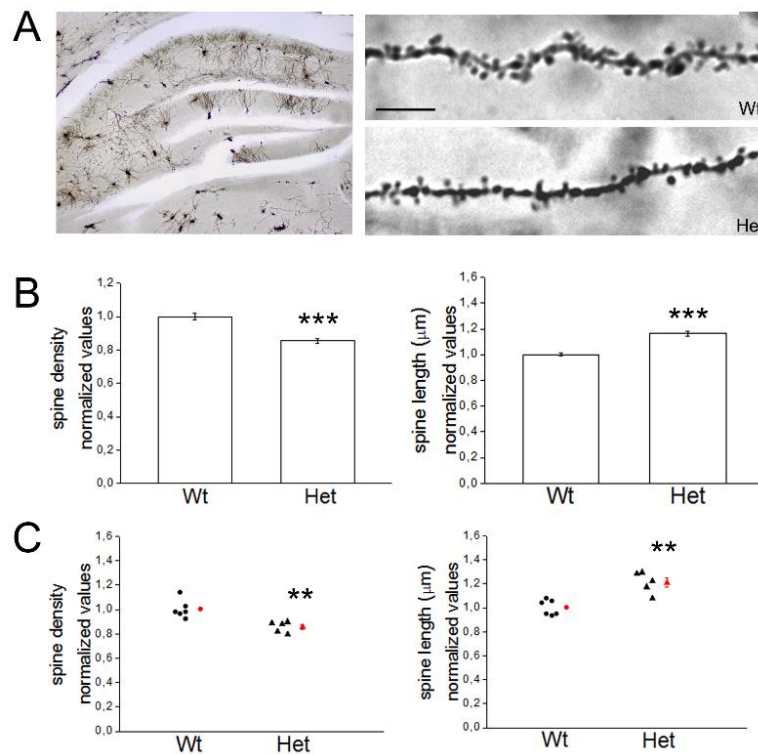
Fig. 31: A) Representative images of a coronal slice showing the dorsal hippocampus a wt mice (low magnification, left) and of secondary branches of apical dendrites of wt and het mice (high magnification, right) stained with the Golgi-Cox method. Scale bars: 100μm, 10μm respectively. B) Quantification of spine density and length in the CA1 field of wt and het mice and relatively single-mouse means distribution. A significant reduction in spine density accompanied by an increase in spine length was evident in heterozygous mice with respect to wt mice (number of spines per micron wt=1±0.02; number of examined dendrites: 292; het=0.85±0.01; number of examined dendrites: 259; p= <0.001; spines length: wt=1±0.01; number of examined dendrites: 547; het=1.16±0.02; number of examined spines: 446;

p= <0.001, Mann-Whitney rank sum test; 6 wt and 5 het mice).C) Mean spine density and length for each animal (spine density: wt=1±0.03, het=0.86±0.02; p= 0.004, T-test; spine length: wt=1±0.03, het=1.2±0.04; p= 0.001, T-test). All data normalized and expressed as mean±SEM.

The postsynaptic defect of SNAP-25 het neurons does not stem from a defective presynaptic function

Since SNAP-25 plays crucial roles in the presynapse, the possibility exists that the postsynaptic defects might have resulted from a functional alteration at the presynaptic level (see Section I), in turn leading to altered postsynaptic development. To address this possibility, we used mixed cultures of het and wt-GFP neurons. Cultures were then maintained for three weeks before functional and morphological analysis. We generated two complementary experimental conditions. By plating wt-GFP and SNAP-25 het neurons in a 1:10 ratio (wt-GFP/het), the formation of networks in which several het neurons impinged on a postsynaptic wt-GFP cell (Fig. 32A) was favored. Conversely, plating SNAP-25 het and wt-GFP neurons at an opposite ratio (het/wt-GFP), favored the formation of networks in which het neurons received most synaptic inputs from wt-GFP cells (Fig. 32A'). Given the large excess of presynaptic inputs from het neurons in the former setting, it would be reasonable to conclude that postsynaptic alterations in the wt-GFP neurons would be the result of defective presynaptic function of SNAP-25 het neurons. In contrast, in the latter setting, given the large excess of presynaptic inputs from wt neurons, it would be reasonable to conclude that a postsynaptic defect in SNAP-25 het neurons would point to a cell-autonomous, postsynaptic failure.

Interestingly, no difference in PSD-95 density has been detected in wt-GFP neurons surrounded by het neurons (Fig. 32B), whereas RFP transfected SNAP-25 het neurons receiving synaptic inputs from wt-GFP neurons (het-RFP/wt-GFP) showed a significant reduction of PSD-95 puncta density relative to RFP-transfected wt neurons receiving from wt-GFP cells (wt-RFP/wt-GFP) (Fig. 32B').
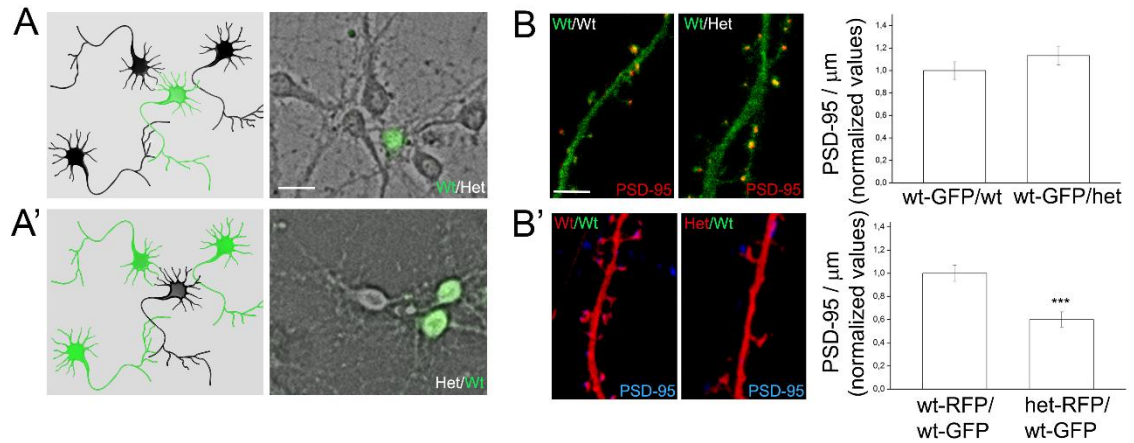
Fig. 32: A-A') Schematic representation and representative images of the two experimental settings used for mixed wt-GFP/het neurons. Scale bar: 20µm. B-B') Left, representative images of wt-GFP/het mixed cultures transfected with GFP or RFP as indicated and stained for PSD-95. Right, analysis of density of PSD-95 puncta in wt-GFP/het mixed cultures. Results show no difference in PSD-95 density in wt neurons surrounded by either het or wt neurons (B, PSD-95 puncta per unit length: wt-GFP/wt=1.00±0.08, number of examined dendrites: 45, number of neurons: 16 ; wt-GFP/het=1.13±0.08, number of examined dendrites: 63, number of neurons: 27; Mann-Whitney rank sum test p=0.481) whereas a significant decrease of the density of PSD-95 puncta is observed in het neurons surrounded by either wt or het neurons (B', PSD-95 puncta per unit length: wt-RFP/wt-GFP=1.00±0.07, number of examined dendrites: 9, number of neurons n=4; het-RFP/wt-GFP=0.6±0.07, number of examined dendrites: 21, number of neurons: 8; normalized values; Mann-Whitney rank sum test p= <0.001). Data are normalized and expressed as mean±SEM. Scale bar: 2µm.

Consistently, electrophysiological analysis showed that mEPSC frequency (Fig. 33A) and amplitude (Fig. 33B) of wt-GFP neurons grown together with a majority of het neurons (wt-GFP/het) did not differ with respect to control cultures of wt neurons. However, mEPSC frequency and amplitude of het neurons cultured together with a majority of wt-GFP neurons (het/wt-GFP) were significantly reduced with respect to control cultures.
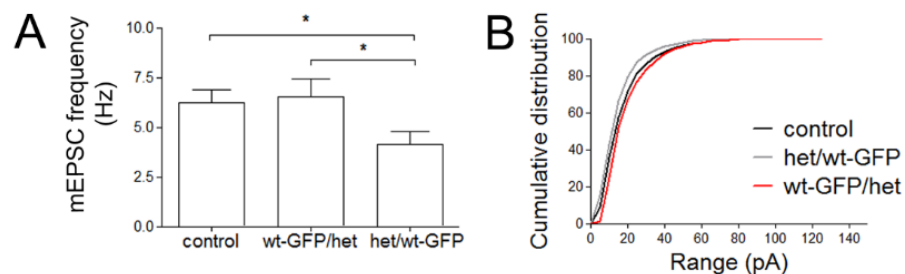
Fig. 33: A) mEPSC recordings of wt-GFP surrounded by het neurons or of het neurons surrounded by wt-GFP neurons reveal a significant reduction in mEPSC frequency in the latter condition. B) A reduction of mEPSC amplitude, is also evident (frequency (Hz) control=6.22±0.67, number of cells: 13; wt-GFP/het=6.53±0.92, number of cells: 10; het-/wt-GFP=4.14±0.64, number of cells: 9; control vs het/wt-GFP p= 0.02, wt-GFP/het vs het/wt-GFP p=0.03, Mann-Whitney rank sum test; amplitude (pA), control=19.78±1.01; wt-GFP/het=19.04±1.6; het/wt-GFP=17.01±1.08; control vs het/wt-GFP p= 0.005; wt-GFP/het vs het/wt-GFP p=0.005; Kolmogorov Smirnov test; 3 independent experiments).

These data fully recapitulate the postsynaptic functional defects of SNAP-25 heterozygous cultures and rule out the possibility that functional defects in spines are secondary to presynaptic alterations.

Lack of plasticity occurring in networks constitutively developing in the presence of reduced SNAP-25 levels

Synaptic plasticity is defective in neurons where the expression of SNAP-25 is acutely down regulated (Jurado et al., 2013). We then asked whether neuronal networks constitutively developing in the presence of reduced SNAP-25 were able to compensate for this failing or display defective plasticity as well and, in the latter case, whether this could be univocally ascribed to a postsynaptic failure. Neuronal cultures were subjected to a chemical LTP protocol (Lu et al., 2001) consisting of an application of high-dose glycine (100μM) for 3 min, which was followed by washout. Glycine acts as a co-activator of synaptic NMDA receptors, prolonging the opening time of the channel. To avoid glycine receptors activation strychnine has been added to all solutions. Stimulation with glycine leads to enhancement of NMDAR transmission without incurring in LTD phenomenon, as it happens giving extracellular NMDA (Liu et al., 2013). This protocol permits to study the structural rearrangements occurring during synaptic plasticity processes, the so-called activity-driven structural plasticity. To this end, we stained for PSD-95, v-Glut1 and βIIItubulin after a 1-hour recovery period. In line with previous reports, application of chemical LTP protocol results in a significant increase in the size of PSD-95 positive puncta and in a higher extent of colocalization of PSD-95 and v-Glut1 staining, in line with a potentiation of synaptic connections (Menna et al., 2013).

Notably, in neurons heterozygous for SNAP-25, this protocol did not induce any significant increases in either the size of PSD-95 positive puncta or the colocalization of pre and postsynaptic markers (Fig. 34A and B), whereas unmistakable increases were observed in wt neurons.
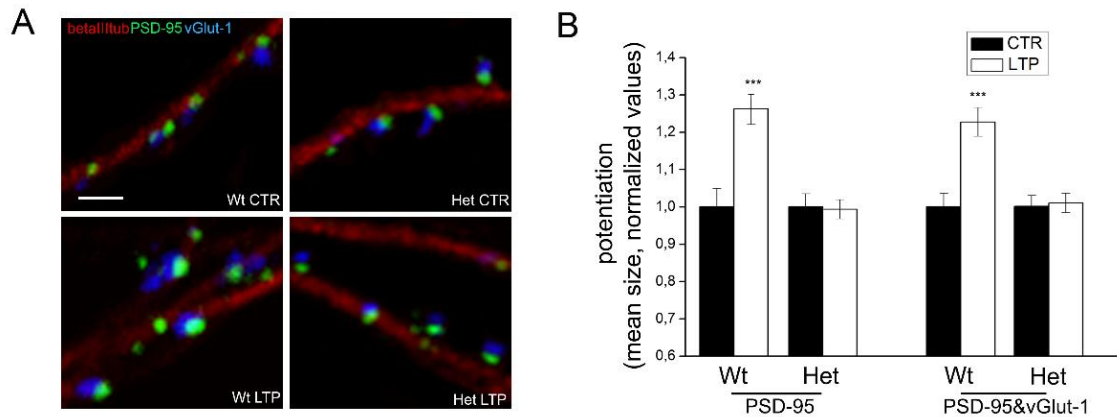
Fig. 34: A) Representative images of wt and het cultures before and after performing a chemical LTP procedure. Cultures were stained for βIIItubulin (red), PSD-95 (green) and v-Glut1 (blue). Scale bar depicts 2μm. B) Extent of potentiation is represented by the quantification of the mean size of PSD-95 positive clusters and by the PSD-95&vGlut1 colocalization area. Potentiation occurs in wt but not het cultures (PSD-95 size: wt ctr:1.00±0.05, wt LTP: 1,26±0.04, het ctr: 1.00±0.03, het LTP: 0.99±0.03. PSD-95&v-Glut1 size: wt ctr:1.00±0.03, wt LTP: 1,23±0.04, het ctr: 1.00±0.03, het LTP: 1.01±0.03. Number of analyzed fields: wt ctr: 46, wt LTP: 50, het ctr: 62, het LTP: 75. Mann-Whitney rank sum test, p= <0.001; 3 independent experiments). Data are expressed as mean±SEM; normalized values.

Electrophysiological recordings of mEPSCs also confirmed the lack of potentiation in SNAP-25 het cultures. Indeed, while both frequency (Fig. 35A and B) and amplitude (Fig. 35A and C) of mEPSCs significantly increased 35 minutes after glycine application in SNAP-25 wt neurons, no potentiation occurred in SNAP-25 het neurons (Fig. 35A-C).

Therefore, a clear deficit in the ability of SNAP-25 het neurons to undergo this form of LTP is also detectable in neuronal networks chronically developing in the presence of reduced SNAP-25.
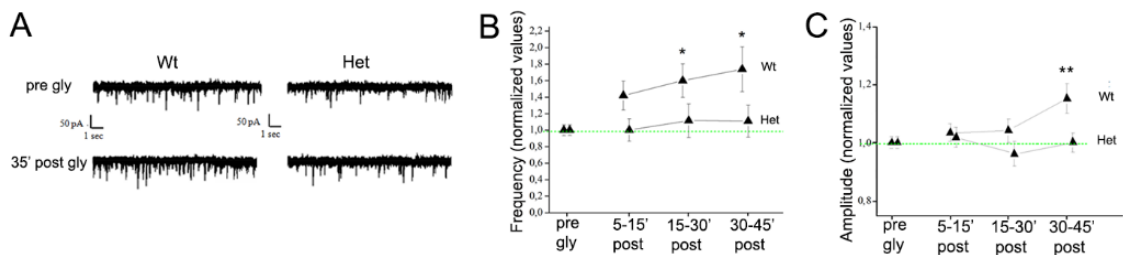
Fig. 35: A) Representative mEPSC traces. Differently from wt, het neurons are unable to undergo LTP. B) mEPSC frequency (normalized values): wt pre gly: 1± 0.06 (n=29), wt post 5': 1.4±0.17 (n=20); wt post 30': 1.59±0.20 (n=17); wt post 45': 1.73±0.27 (n=10); het pre gly: 1±0.06 (n=15); het post 5': 1.00±0.13 (n=14); het post 30': 1.11±0.20 (n=10); het post 45': 1.10±0.19 (n=10). wt pre gly vs wt post 5': p<0.021, wt pre gly vs wt post 30': p<0.012, wt pre gly vs wt post 45': p<0.014. Mann-Withney rank sum test. C) mEPSC amplitude (normalized values): wt pre gly: 1±0.02; wt post 5': 1.03±0.03; wt post 30': 1.04 ±0.04; wt post 45': 1.15±0.05; het pre gly: 1±0.02; het post 5': 1.02±0.03; het post 30': 0.96±0.04; het post 45': 1±0.03. wt pre gly vs wt post 45': p=0.001. Student t-test. n is the number of cells. 4 independent experiments.

We then tested the ability of wt-GFP neurons cultured together with het neurons (wt-GFP/het) or het neurons cultured together with wt-GFP neurons (het/wt-GFP) to undergo synaptic potentiation. These experiments indicated that wt-GFP neurons receiving synaptic inputs from SNAP-25 het neurons (red dots), when subjected to a chemical LTP protocol, display potentiation levels similar to their control counterparts (black dots). By contrast, SNAP-25 het neurons receiving synapses from wt neurons (grey dots) did not exhibit such potentiation (Fig. 36).
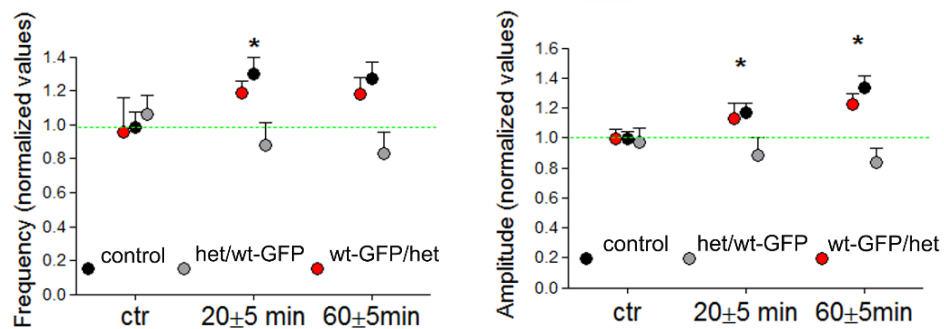
Fig. 36: mEPSC frequency and amplitude recorded from neurons in mixed cultures experimental settings were normalized to values obtained before glycine application. Note that wt-GFP neurons surrounded by het neurons undergo LTP, whereas het neurons surrounded by wt-GFP neurons fail to potentiate (frequency (Hz) pre-gly: control=0.99±0.09 (n=16), wt-GFP/het=0.96±0.2 (n=5), het/wt-GFP=1.06±0.11 (n=8); 20±5min: control=1.30±0.1 (n=15), wt-GFP/het=1.19±0.07 (n=3), het/wt-GFP=0.88±0.13 (n=8); 60±5min: control=1.27±0.1 (n=7), wt-GFP/het=1.18±0.10 (n=2), het/wt-GFP=0.83±0.13 (n=5); n is the number of cells; ctr vs ctr 20min: p=0.04, Mann-Withney rank sum test,. Amplitude (pA) pre-gly: control=0.99±0.04, wt-GFP/het=0.99±0.07, het/wt-GFP=0.97±0.09; 20±5min: control=1.17±0.06, wt-GFP/het=1.13±0.10, het/wt-GFP=0.88±0.12; 60±5min: control=1.34±0.08, wt-GFP/het=1.23±0.07, het/wt-GFP=0.84±0.09; ctr vs ctr 20min: p=0.03, ctr vs ctr 60min: p=0.2; Mann-Withney rank sum test; 3 independent experiments). Data are expressed as mean±SEM.

These results indicate that genetic, moderate reductions of SNAP-25 levels impair synaptic plasticity and that a cell autonomous, postsynaptic defect is responsible for this defect.

PSD-95-dependent spine formation requires postsynaptic SNAP-25

PSD-95 is a major organizer of the postsynaptic density, playing a crucial role in determining spine size and morphology (reviewed in Sheng and Kim, 2011; see §1.4 of the Introduction). Our data so far suggest that SNAP-25 reductions may affect the localization and/or stabilization of PSD-95 in dendritic protrusions, possibly impacting synapse morphology and strength during development and plasticity.

Consistent with this possibility, we performed, in primary cultures, acute down-regulation of SNAP-25 expression by a cDNA codifying a siRNA sequence (see above) resulting in a significant reduction of PSD-95 area (Fig. 37A and C) which is

accompanied by a prominent alteration in the morphology of dendritic spines (Fig. 37A, see also Tomasoni et al., 2013). Conversely, overexpression of PSD-95, a procedure which results in the marked increase in spine volume and the enlargement of the postsynaptic densities (Nikonenko et al., 2008), induced the formation of significantly smaller PSD-95 positive puncta in SNAP-25 siRNA-treated neurons relative to scramble-transfected neurons (Fig. 37B-C). Therefore, postsynaptic SNAP-25 is required for proper PSD-95 accumulation and spine morphogenesis.
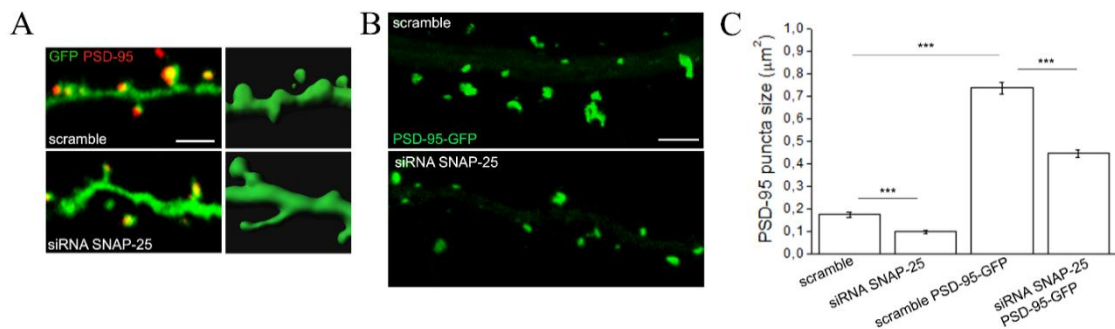
Fig. 37: A) Representative images of neurons transfected with GFP and a scramble construct or a construct silencing SNAP-25 (siRNA), fixed and stained for PSD-95 (red) and relative 3D reconstruction. Note the different spine morphology and PSD-95 size in neurons transfected with siRNA in comparison to scramble transfected neurons. B) Representative images of neurons transfected with a scramble construct or a construct silencing SNAP-25 (siRNA) co-transfected with PSD-95-GFP. C) The histogram shows a statistically significant decrease of PSD-95 puncta size in siRNA-, relative to scramble- treated neurons, and PSD-95-GFP transfection fails to rescue a normal size of PSD-95 (in μm^2, scramble=0.17 ± 0.01, number of analyzed puncta: 152, number of analyzed neurons: 21; siRNA SNAP-25=0.10 ± 0.01, number of analyzed puncta: 97, number of analyzed neurons: 20; scramble PSD-95-GFP=0.74 ± 0.02, number of analyzed puncta: 203, number of analyzed neurons: 24; siRNA SNAP-25 PSD-95-GFP=0.45 ± 0.02, number of analyzed puncta: 296, number of analyzed neurons: 28. Mann-Whitney rank sum test $p=$ <0.001; 3 independent experiments). Data are expressed as mean±SEM. Scale bar: 2µm for A and B.

Given the essential role of SNARE proteins in trafficking and fusion of secretory organelles we asked whether such a process could play a role during spine formation. To investigate this issue, neurons were co-transfected with GFP and a cDNA codifying for the botulinum neurotoxin type E (BoNT/E) light chain (LC), which cleaves SNAP-25 at its N-terminal side and prevents the protein entering in the fusion complex (Keller and Neale, 2001). Botulinum toxins (BoNTs) are produced by anaerobic Clostridium bacteria and include seven serotypes. BoNTs are composed of a light chain and a heavy chain connected via a disulphide bond. The heavy chain contains a receptor-binding domain that targets neurons and a membrane translocation domain that relocates the

LCs into the cytosol. LCs act as proteases cleaving proteins required for synaptic vesicle exocytosis (Peng et al., 2013).

We decided to transfect neurons with the cDNA for BoNT/E light chain, rather than using the toxin itself, because we aimed to define whether the SNARE function of dendritic SNAP-25 may play a role during spine formation and PSD-95 accumulation at the synaptic level. Treatment of neuronal cultures with BoNT/E would not discriminate between the specific dendritic effect at the level of single neuron rather than the generalized block of neuronal activity. First, we validated BoNT/E transfection and the specificity of the antibody recognizing the BoNT/E-cleaved SNAP-25 fragment in HEK cells co-transfected with a SNAP-25 full length cDNA, because these cells do not express the protein constitutively (Fig. 38A). Then, BoNT/E transfected neurons were stained with PSD-95 and the BoNT/E-cleaved specific SNAP-25 antibodies, and either the density and morphological parameters of dendritic spines were evaluated (Fig. 38B). Results show that the spine density and PSD-95 size did not change in BoNT/E transfected neurons with respect to controls. These data indicate that the fusion activity of SNAP-25 is not required for PSD-95 accumulation and spine morphogenesis and suggest that the protein may instead play a scaffolding role at the postsynapse (Fig. 38C-D, see also Tomasoni et al., 2013). However we cannot exclude the possibility that expressed BoNT/E did not completely shear off all the SNAP-25 protein into the cell. Residual protein might be indeed important for neuronal health (Peng et al., 2013), although the small residual amount is likely not sufficient to maintain the SNARE properties of SNAP-25 (Peng et al., 2013).
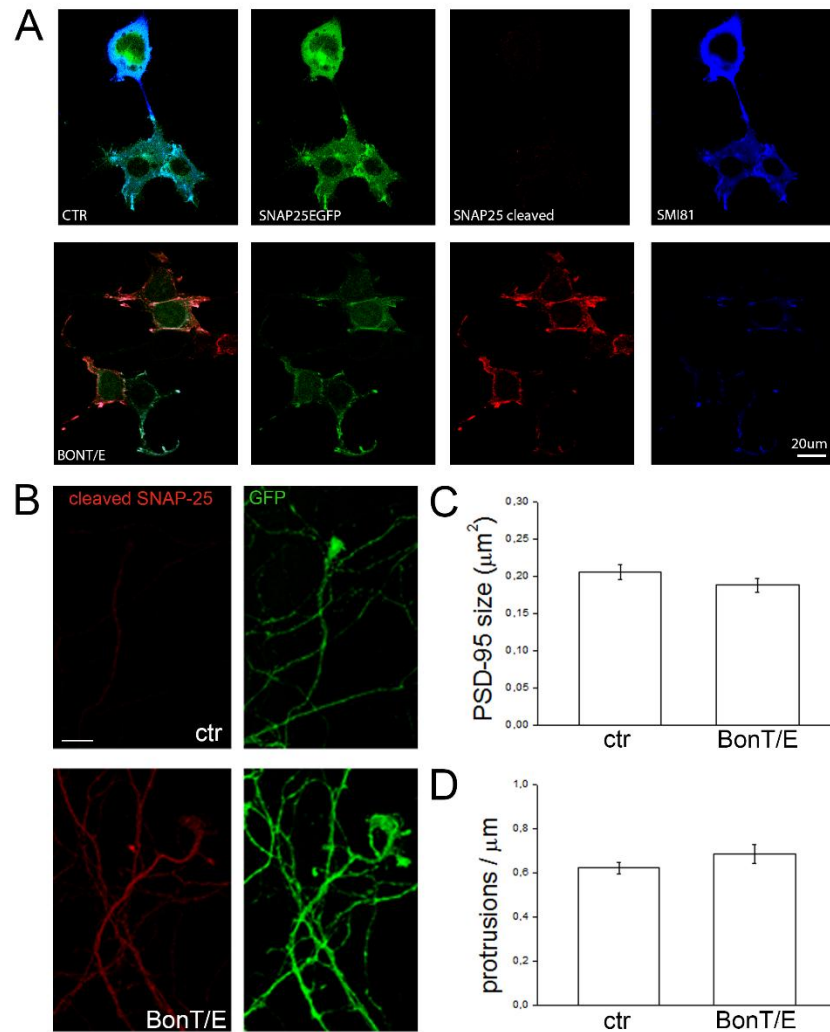
Fig. 38: A) Representative images of HEK cells transfected with SNAP-25-GFP alone or SNAP-25-GFP plus a cDNA codifying the light chain of the Botulinum toxin E (BonT/E) and stained with an antibody, which specifically recognizes the BonT/E-cleaved SNAP-25 (red), and an antibody that recognizes only the full length SNAP-25 (blue). B) Representative images of 21DIV neurons transfected with GFP alone (ctr) or with GFP plus a BonT/E cDNA and stained with an antibody which specifically recognize only the BonT/E-cleaved SNAP-25 (red). C) Quantification of the size of PSD-95 positive puncta of control or BonT/E transfected neurons (in μm^2, ctr=0.20±0.01, number of analyzed puncta: 100; BonT/E=0.19±0.01, number of analyzed puncta: 93; p=0.244, Mann-Whitney rank sum test). D) Quantification of the spine density in ctr and BonT/E transfected neurons (per μm, ctr=0.62±0.03, number of analyzed spines: 40,; BonT/E=0.68±0.04, number of analyzed spines: 36; p=0.374, Mann-Whitney rank sum test). These results indicate that the fusion activity of SNAP-25 is not required for PSD-95 accumulation and spine morphogenesis. Number of analyzed neurons: ctr=20; BonT/E=15; 3indipendent experiments, all data are expressed as mean±SEM.

Since PSD-95 continuously migrates between synaptic and extrasynaptic pools (Bresler et al., 2001; Gray et al., 2006), we then reasoned that SNAP-25 could operate at the spine by restricting, either directly or indirectly, PSD-95 mobility. We therefore measured the dynamics of synaptic PSD-95 upon acute reduction of SNAP-25 expression by siRNA, using fluorescence recovery after photobleaching (FRAP)

analysis. This technique employs irradiation of a fluorophore in a living sample with a short laser pulse to degrade it and thereby abolish fluorescence, followed by time-resolved image recording of the sample. If the protein of interest, which is conjugated to the fluorophore, moves through the sample, a recovery of fluorescence can be observed. To carry out PSD-95 FRAP experiments, four to five days after transfection, we selected spines with similar morphologies in siRNA- or scramble- treated cultures, in order to rule out the possibility that differences in PSD-95 mobility might have been due to the comparison of mature and immature thin, filopodia-like protrusions which were more abundant in the siRNA-treated neurons. PSD-95-GFP bleaching, followed by temporal analysis of fluorescence recovery over the next 40 seconds (Fig. 39A), revealed a significantly larger mobile fraction of PSD-95 in acutely SNAP25-downregulated cells compared to scramble control cells (Fig. 39B).
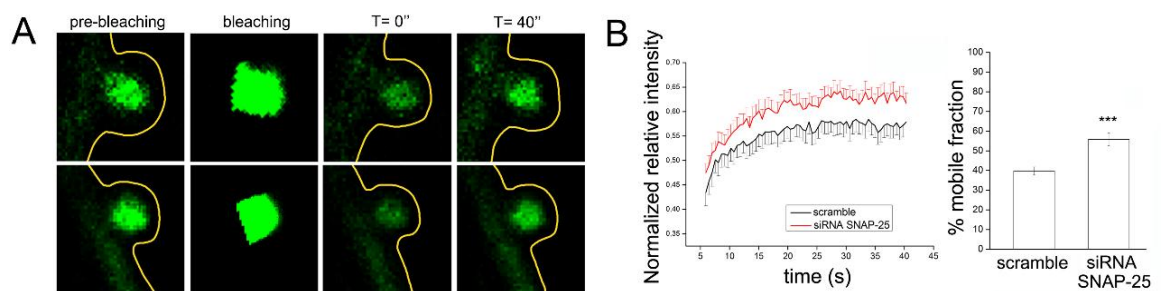
Fig. 39: A-B) FRAP measurements of PSD-95-GFP in spines of siRNA-treated or scramble-treated neurons. A) Representative images of the same area before photobleaching (Pre-bleaching), at t= 0sec and 40sec after photobleaching of scramble- and siRNA-treated neurons. Neurons were maintained at 37°C during the experiment. B) Left, FRAP curves of PSD-95-GFP in spines over a 40sec period. The curves were fit to single exponential equations. Right, histogram showing the increase of mobile fraction of PSD-95-GFP in siRNA-treated spines with respect to scramble-treated spines (Scramble=39.72±2.09, number of analyzed spines: 58; siRNA SNAP-25=55.81±3.30, number of analyzed spines: 52; Mann-Whitney rank sum test p= <0.001; 4 independent experiments). Data are normalized and expressed as mean±SEM.

These data point out that SNAP-25 affects PSD-95 localization and mobility through a mechanism that does not involve its fusion activity, but rather implicates a scaffolding, protein-protein interaction role.

SNAP-25 is part of the postsynaptic protein complex with p140Cap and PSD-95

To assess whether SNAP-25 controls PSD-95 mobility through direct participation to the PSD complex, immunoprecipitation of PSD-95 from brain lysates was performed. Fig. 40 shows that SNAP-25 and the spine protein p140Cap (Jaworski et al., 2009; Tomasoni et al., 2013) were coimmunoprecipitated with PSD-95.

65
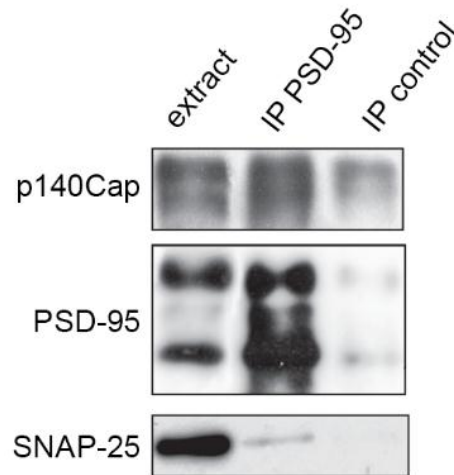
Fig. 40: Brain extracts immunoprecipitated with a PSD-95 antibody or an unrelated one, and run on SDS PAGE. Western blot was performed with antibodies to p140Cap, PSD-95 and SNAP-25. p140Cap clearly coimmunoprecipitates with PSD-95. It is also possible to see a faint band for SNAP-25, this suggests an indirect relation.

Proximity Ligation Assay (PLA) has next been performed in rat cultured neurons to evaluate an in-situ complex formation. The PLA assay principle relies in the use of primary antibodies raised in different species recognizing the target antigen or antigens of interest. Species-specific secondary antibodies, called PLA probes, each tagged with a unique short DNA strand, bind to the primary antibodies. When the PLA probes are in close proximity, the DNA strands can interact through a subsequent addition of two other circle-forming DNA oligonucleotides. After joining of the two added oligonucleotides by enzymatic ligation, they are amplified via rolling circle amplification using a polymerase. After the amplification reaction, several-hundredfold replication of the DNA circle has occurs, and labeled complementary oligonucleotide probes highlight the product. The resulting high concentration of fluorescence in each single-molecule amplification product is easily visible as a distinct bright spot when viewed with a fluorescence microscope. This technique is able to recognize proteins distant up to 40nm (Sodeberg et al., 2006).

PLA revealed indeed a significantly higher signal for SNAP-25 and PSD-95 compared to PSD-95 and the merely presynaptic protein Piccolo (Fig. 41). This suggests that PSD-95 and SNAP-25 can be part of the same complex in their natural cellular environment.
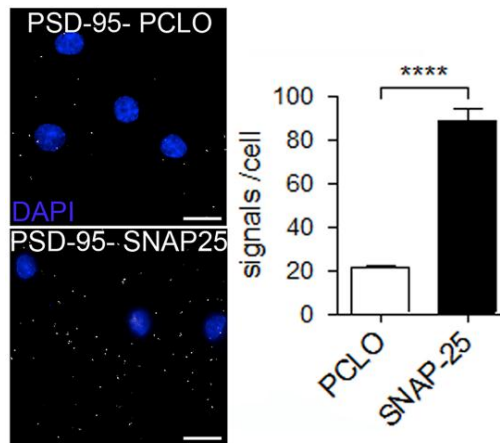
Fig. 41: Representative images obtained from Proximity Ligation Experiment. Rat neurons where incubated with primary antibodies against PSD-95/PCLO or PSD-95/SNAP-25 after which PLA probes where added, ligated, amplified and detected with a Cy3 probe. Right, quantification of PLA signals per neuron. PLA signals: 21.1±0.9 per nucleus in PSD-95/PCLO stained cells (34 analyzed cells); 88.3±6.3 per nucleus in PSD-95/SNAP-25 stained cells (32 analyzed cells); p=< 0.0001, unpaired t-test.

To further probe the possible existence of a postsynaptic protein network including SNAP-25, we applied a LUminescence-based Mammalian intERactome (LUMIER) assay (Barrios-Rodiles et al., 2005; Petrakis et al., 2012) to test the following protein-protein interactions: SNAP-25 and PSD-95; PSD-95 and p140Cap (SRCIN1); PSD-95 and cortactin (CTTN). The well characterized protein:protein interaction as Bcl2-BAD (Chen et al., 2005) served as a positive controls. The bait protein fused to a protein-A tag and linked to a Renilla Luciferase and the prey protein fused to a Firefly Luciferase were coexpressed in HEK293 cells for 48h. After cells lysis, protein complex formation was assessed by Firefly Luciferase activity of the co-immunoprecipitated prey fusion-protein (Fig. 42).

Results indicated that SNAP-25 and PSD-95 were unable to interact directly, whereas both p140Cap and cortactin specifically interact with PSD-95 (Fig. 42). Given p140Cap interacts with SNAP-25 (Jaworski et al., 2009) and cortactin (Damiano et al., 2012), an indirect association between SNAP-25 and PSD-95 potentially mediated by p140Cap may occur at the postsynaptic level.
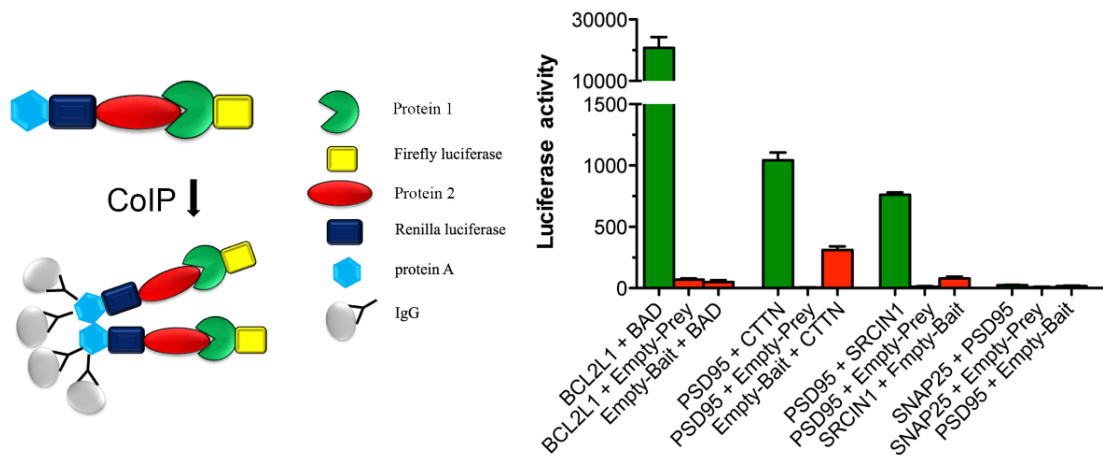
Fig. 42: Left, scheme representing the LUMIER co-immunoprecipitation assay. Right, interactions between the tested proteins in HEK293 cells as detected by LUMIER assay. The green bar indicates a specific interaction, evaluated in term of firefly luciferase activity. Red bars are controls.

Together, these data indicate that SNAP-25 is part of the postsynaptic density, where it associates with PSD-95, likely through the postsynaptic proteins p140Cap and cortactin, and that lowering its expression reduces the immobile fraction of PSD-95 at the spine and leads to defects in spine formation and function (Fig. 43).
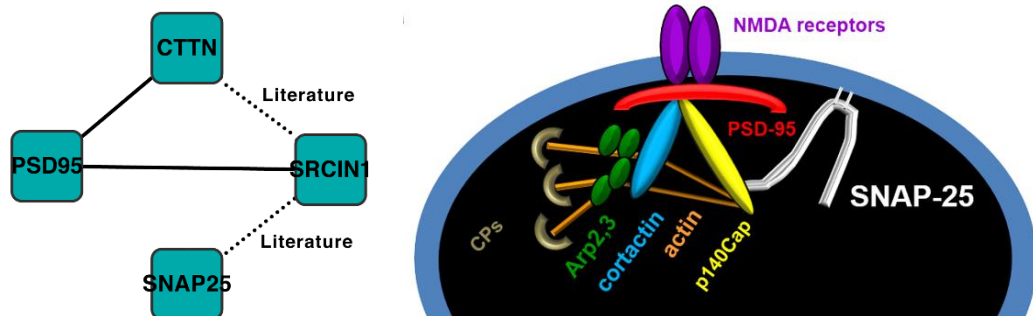
Fig. 43: Left, interaction hypothesis according to LUMIER assay results and literature. Right, our proposed model of interaction in the postsynaptic compartment: SNAP-25 and PSD-95 interact likely through another protein, such as p140Cap.

DISCUSSION

In this study, we have demonstrated that the SNARE protein SNAP-25 may exert a dual role during excitatory synapse development. Indeed, at earlier developmental stages it plays a crucial role at the presynaptic level by regulating short-term plasticity whereas later in development it is required for the proper formation of the postsynaptic compartment. These phenomena occur in vitro and in vivo. In particular, by using mixed neuronal cultures we have shown that reduced levels of SNAP-25 in the presynaptic compartment impair short-term plasticity, whereas reduction of protein levels in the postsynaptic compartment leads to a defective maturation of postsynaptic specializations, reduced densities of dendritic spines and defective PSD-95 clustering. In vivo acute down-regulation of SNAP-25 in CA1 hippocampal neurons affects spine number and morphology and causes a specific reduction of the postsynaptic protein PSD-95. We also found that SNAP-25, PSD-95 and p140Cap are part of the same molecular complex in the brain.

SNAP-25 is a regulator of neurotransmission in developing cultures

Control of neurotransmitter release is essential for communication in the nervous system and for preventing synaptic dysfunctions. Activity-dependent presynaptic processes producing various forms of short-term plasticity are believed to control several essential neural functions, such as information processing, working memory and decision-making (Deng and Klyachko, 2011).

SNAP-25 is a member of the SNARE protein superfamily that participates in synaptic vesicles exocytosis and in negative regulation of voltage gated calcium channels (Pozzi et al., 2008, Stein et al., 2009). We found an increased glutamatergic transmission and a reduction in the ability to undergo short-term plasticity due to reductions in SNAP‑25 expression. This defect could have direct consequences for brain function and for the progression of neuropsychiatric disorders. Indeed, presynaptic abnormalities were described at excitatory hippocampal synapses in a mouse model of Fragile X syndrome, leading to defects in short-term plasticity and information processing (El-Idrissi et al., 2010, Deng et al., 2011). Reduced SNAP-25 levels, leading to abnormal presynaptic short-term plasticity at glutamatergic terminals, at least at early developmental stages, might therefore contribute to cognitive impairments in intellectual disability syndromes.

Moreover, analysis of allele frequencies of two genetic variants in SNAP-25 indicated that SNAP-25 might be directly involved in intellectual disability syndromes (Rizzi et al., 2012).

SNAP-25, as other SNAREs, is abundant in neuronal cells but only a few of SNARE complexes are reported to be required to drive the fusion of a single synaptic vesicle (Mohrmann et al., 2010). One possible explanation of their abundance, as suggested in Kochlamazashvili and Haucke, 2013, might be that SNARE proteins, in addition to forming trans-SNARE complexes, assemble with other proteins, regulating neurotransmission in other ways than the fusion of vesicles. In fact, SNAP-25 can negatively modulate Cav2.1-type voltage-gated calcium channels (VGCC) (Pozzi et al., 2008; Condliffe et al., 2010); notably this effect can be reversed by overexpression of synaptotagmin1, which might associate with SNAP‑25 (Catterall and Fee, 2008). Conversely, the inhibitory effects of syntaxin1 on Cav2.2 channels can be reversed by co-expressing SNAP-25 (Catterall and Fee, 2008). Therefore, it is possible to speculate that differential distribution of SNAP‑25 between free, SNARE‑, synaptotagmin1‑ and VGCC-bound forms might regulate evoked neurotransmission.

Our data indicate that the augmented glutamate release is due to the lack of the regulation of VGCCs as revealed by recordings on neuronal cultures treated with calcimycin that permits calcium-dependent exocytosis bypassing VGCC. One might speculate that reduced SNAP‑25 expression in heterozygous animals as well as in schizophrenic or ADHD patients would be sufficient to sustain SNARE-mediated synaptic vesicle fusion but not to regulate efficiently VGCCs, thus leading to increased calcium influx at the presynaptic terminals, facilitated neurotransmission and alteration in short-term plasticity. Additional levels of regulation could be enforced by developmental switching between alternatively spliced 'a' and 'b' isoforms of SNAP‑25 (Bark et al., 2004), age-dependent alterations in the presynaptic protein turnover and post-translational modifications (Kochlamazashvili and Haucke, 2013).

Reduced levels of SNAP-25 in heterozygous cultures affect the maturation of postsynaptic terminals and PSD-95 dynamics

SNAP-25 levels increase during development both in wt (Bark et al., 2004) and in het neurons (Antonucci et al., 2013). Our data indeed suggest that a mere 20% reduction of protein content is sufficient to induce a change of PPF (Antonucci et al., 2013). The reasons of such an increase are not known, one might speculate that this phenomenon is

due to an augmented protein synthesis or a reduction in protein degradation, to homeostatically compensate the lack of one producing allele; otherwise, this could be due to post-translational mechanisms that improve the rate of mRNA translation. Nevertheless, the developmentally regulated increase of SNAP-25 protein content, which occurs in het cultures, could be the reason why evoked response and pair pulse facilitation are restored in mature cultures. Notably, we have some indications that the reduction of SNAP-25 levels in het cultures could not involve the axon termini and the somato-dendritic region at the same extent (see Fig. 27 of the Result section) with the somato-dendritic regions being more affected. In fact, mature het cultures display a reduction in both frequency and amplitude of mEPSCs and are unable to undergo a common form of experimentally induced potentiation. Morphologically, het neurons revealed a lower density of spines that display also an immature feature. These facts unmask an alteration at the postsynaptic terminal, which become evident at a later stage of development. We hypothesized a dual effect of a genetic reduction of SNAP-25, which leads to a presynaptic defect during early phases of development, at least in culture, and turns to be a postsynaptic impairment in more advanced stages of development. This hypothesis is confirmed by the analysis of synaptic markers in wt and het cultures at 14 or 21 days in vitro. At DIV14, there was no difference between the genotypes, but at DIV21 het neurons failed the physiological maturation of synaptic contacts, in particular we found a reduction of the postsynaptic protein PSD-95.

Variations in dendritic spine number and morphology occur both during development and in adulthood, allowing the establishment and remodeling of neuronal circuits. Spine structural plasticity is tightly coordinated with synaptic function, with spine enlargement occurring during long-term potentiation and spine shrinkage during long-term depression (reviewed in Kasai and Fukuda, 2010).

Although different models concerning the dynamic aspects of synaptogenesis have been proposed, presynaptic differentiation appears to occur slightly faster than postsynaptic development (Friedman et al., 2000; Okabe et al., 2001). Cycling of synaptic vesicle protein transport vesicles (STVs) at predefined sites along the axon appears to selectively attract dendritic filopodia and initiate synapse formation (Sabo et al., 2006). Furthermore, although it is clear that vesicular glutamate release is not required for excitatory synapse formation (Craig et al., 1994; Verhage et al., 2000; Varoqueaux et al., 2002; Harms and Craig 2005), the number of synapses formed in the absence of neurotransmitter release is dramatically decreased (Bouwman et al., 2004),

Given that SNAP-25 plays a critical role at the presynaptic terminal during synaptic vesicle fusion and considering the possible role of presynaptic function in the maturation of the postsynaptic compartment, the postsynaptic effects observed here might have been the result of SNAP-25–related alterations in presynaptic release (Washbourne et al., 2002). By taking advantage of mixed cultures of wt and het neurons, we demonstrated that postsynaptic defects in SNAP-25 het neurons do not stem from alterations in the presynaptic terminal, but are instead related to a cell-autonomous impairment at the postsynaptic compartment.

Genome-wide linkage scan analysis for schizophrenia susceptibility genes suggested the chromosomal region 20p12.3-11, containing *Snap25*, as a candidate region for the disease (Lewis et al., 2003) and SNAP-25 levels have been found to be lower in the hippocampus and in the frontal lobe of patients with schizophrenia (Thompson et al., 1998; Young et al., 1998; Thompson et al., 2003). Notably, a profound reduction in spine density on pyramidal neurons in the superior temporal gyrus and in subicular and CA3 dendrites has been described in schizophrenic patients (Kolomeets and Orlovskaya, 2005; Steen and Mull, 2006; Sweet and Henteleff, 2009; reviewed in Penzes et al., 2011). Consistently, heterozygous mice exhibit, at seven postnatal weeks, a moderate hyperactivity, which, however, disappears in adult animals, which are instead characterized by impairments in associative learning and memory (Corradini et al., 2012). Notably, mice injected with viral vector harboring shRNA to SNAP-25 to the gustatory cortex demonstrated an impaired taste memory similarly to injected with viral vector expressing shRNA to PSD-95 (Elkobi et al., 2008). It has been recently demonstrated that acute down-regulation of SNAP-25 leads to an impairment in long-term potentiation possibly due to altered NMDAR trafficking (Jurado et al., 2013). Activity-dependent changes of synaptic strength require not only receptors trafficking, but also structural changes at the postsynaptic level that were not addressed by Jurado and colleagues. Rescuing the phenotype by using lentiviral vectors encoding the full length SNAP-25 would further support the hypothesis.

During development and synaptic potentiation processes, synapse formation is directed by reciprocal signaling between pre- and postsynaptic neurons. Synaptic adhesion complexes and secreted factors act as synaptic organizing proteins that stabilize early synaptic contacts via recruitment of synaptic vesicles to the presynaptic active zone and NMDA receptors to the postsynaptic density. PSD-95 binds NMDA receptors

(Niethammer et al., 1996; O'Brien et al., 1998) and also interacts with AMPA receptors via TARPs (Chen et al., 2000; Nicoll et al., 2006). PSD-95 appears very early at nascent synapses (Friedman et al., 2000; Bresler et al., 2001) where it clusters NMDA receptors (O'Brien et al., 1998; Lee and Sheng, 2000) and controls synaptic AMPA receptors number, thus determining synaptic strength (Schnell et al., 2002; Stein et al., 2003; Ehrlich et al., 2004). SNAP-25, in particular, has been reported to play a role in the removal of kainate receptors from the postsynaptic membrane (Selak et al., 2009) as well as in the insertion of NMDA receptors in neuronal plasma membrane (Lau et al, 2010). However, the molecular mechanism through which SNAP-25 acts in receptor trafficking at the postsynaptic terminal is still not known. A possible mechanism involves a PKC dependent phosphorylation of SNAP-25 (Lau et al., 2010), another possibility may rely on other interacting proteins at the postsynapse. In particular, our group has recently reported that SNAP-25 directly interacts with p140Cap at spine level and acute down-regulation of p140Cap as well as of SNAP-25 leads to an alteration in spine structure (Tomasoni et al., 2013). Here we have shown that acute down-regulation of SNAP-25 leads to PSD-95 destabilization, thus suggesting that SNAP-25 may cooperate with p140Cap and PSD-95 to regulate spine formation and structural plasticity. As a further support to this hypothesis, we found that overexpression of PSD-95 in the absence of SNAP-25 failed to induce larger spines and PSD-95, p140Cap and SNAP-25 co-precipitate in brain homogenates suggesting that they form a synaptic protein network. Indeed, we have demonstrated by LUMIER assay that p140Cap is able to bind PSD-95, whereas SNAP-25 and PSD-95 do not interact directly. Given SNAP-25 interacts with p140Cap a possibility emerges that a synaptic protein network involving SNAP-25, p140Cap and PSD-95 is localized at the postsynaptic compartment. The integrity of this macromolecular complex appears to be fundamental for both structural and functional synaptic plasticity. An indisputable role of p140Cap in the formation of this protein network would be obtained by co-immunoprecipitation experiments from brain homogenates of p140Cap KO and wt mice. It also would be interesting to expand the number of protein interactions analyzed with LUMIER assay to better characterize the postsynaptic complex where SNAP-25 is located.

In recent years evidence has accumulated suggesting a role for SNAREs at the postsynapse (Ovsepian and Dolly, 2011). Given the essential role of SNAREs in trafficking and fusion of vesicles, we have used BONT/E to investigate if the SNARE properties of SNAP-25 could play a role during spine formation. Our data indicate that

BoNT/E cleavage of SNAP-25, which does not prevent SNAP-25:p140Cap interaction (Tomasoni et al., 2013), does not affect PSD-95 clustering and number, thus strongly suggesting that it is the protein interaction with p140Cap and not its SNARE activity that may account for the spine defect. Although it is not possible to quantify the residual full-length protein, it is likely that BoNT/E did not completely eliminate all the SNAP-25 present in the neuron. This small protein residue, which is not however able to sustain SV exocytosis, is important for the health of the neuron. In fact, a recent study demonstrate that a complete elimination of SNAP-25 after BoNT/E somministration causes neurodegeneration (Peng et al., 2013), a phenotype we did not observe.

These data provide new mechanistic insights as to SNAP-25 involvement in synaptopathies that go beyond the protein's known roles in presynaptic function, indicating a protein's role as a postsynaptic structural hub. Indeed, the activity-driven spine remodeling is defective in neuronal networks constitutively developing in the presence of reduced levels of SNAP-25, as it might presumably occur in human pathologies, such as schizophrenia, where both a reduction of SNAP-25 expression (Thompson et al., 2003) and reduction in dendritic spine density (Penzes et al., 2011) have been described.

ACKNOWLEDGEMENTS

Now I excuse myself with my readers, because this page is not about *science*, this is about *life* during my Ph.D. Therefore, I need all the complexity and the richness of my mother tongue, to properly express what I have to say.

Grazie a Michela, un esempio, una persona fantastica che mi ha dato la possibilità di svolgere il dottorato nel suo laboratorio. Grazie per la sua guida attenta e continua, nonostante i mille impegni, sia sul piano lavorativo che personale. E grazie per tutte le opportunità che in questi anni mi ha dato.

Grazie a Elisabetta, non solo per la sua onniscienza, cosa ben nota dai tempi della tesi, ma per esserci sempre, anche se divento grande, per i successi e per le "rogne".

Grazie alla Ste, perchè dopo le burrasche della tesi si è rivelata una persona preziosa.

E, ultimo, ma non ultimo, grazie al fantastico gruppo che è stato Filarete, per l'amicizia, gli insegnamenti, la condivisione, perché andare al lavoro era piacevole come andare a casa. Sono stati due anni indimenticabili. Non c'è bisogno di far nomi, chi c'era, lo sa.

BIBLIOGRAPHY

1. Andersen P (1990) Synaptic integration in hippocampal CA1 pyramids. *Progress in brain research* **83:** 215-222

2. Antonucci F, Corradini I, Morini R, Fossati G, Menna E, Pozzi D, Pacioni S, Verderio C, Bacci A, Matteoli M (2013) Reduced SNAP-25 alters short-term plasticity at developing glutamatergic synapses. *EMBO reports* **14:** 645-651

3. Arnsten AF (2011) Catecholamine influences on dorsolateral prefrontal cortical networks. *Biol Psychiatry* **69:** e89-99

4. Banker GA, Cowan WM (1977) Rat hippocampal neurons in dispersed cell culture. Brain research 126: 397-342

5. Bark IC (1993) Structure of the chicken gene for SNAP-25 reveals duplicated exon encoding distinct isoforms of the protein. *Journal of molecular biology* **233:** 67-76

6. Bark IC, Hahn KM, Ryabinin AE, Wilson MC (1995) Differential expression of SNAP-25 protein isoforms during divergent vesicle fusion events of neural development. *Proc Natl Acad Sci U S A* **92:** 1510-1514

7. Bark IC, Wilson MC (1994) Human cDNA clones encoding two different isoforms of the nerve terminal protein SNAP-25. *Gene* **139:** 291-292

8. Barnes KA, Howard JH, Jr., Howard DV, Kenealy L, Vaidya CJ (2010) Two forms of implicit learning in childhood ADHD. *Developmental neuropsychology* **35:** 494-505

9. Barr CL, Feng Y, Wigg K, Bloom S, Roberts W, Malone M, Schachar R, Tannock R, Kennedy JL (2000) Identification of DNA variants in the SNAP-25 gene and linkage study of these polymorphisms and attention-deficit hyperactivity disorder. *Mol Psychiatry* **5:** 405-409

10. Bartlett WP, Banker GA (1984) An electron microscopic study of the development of axons and dendrites by hippocampal neurons in culture. I. Cells which develop without intercellular contacts. J Neurosci 4: 1944-1953

11. Bartlett WP, Banker GA (1984) An electron microscopic study of the development of axons and dendrites by hippocampal neurons in culture. II. Synaptic relationships. J Neurosci 4: 1954-1965

12. Bayes A, van de Lagemaat LN, Collins MO, Croning MD, Whittle IR, Choudhary JS, Grant SG (2011) Characterization of the proteome, diseases and evolution of the human postsynaptic density. *Nat Neurosci* **14:** 19-21

13. Becker K, Sinzig JK, Holtmann M (2004) Attention deficits and subclinical epileptiform discharges: are EEG diagnostics in ADHD optional or essential? *Developmental medicine and child neurology* **46:** 431-432

14. Benarroch EE (2013) Synaptic vesicle exocytosis: molecular mechanisms and clinical implications. *Neurology* **80:** 1981-1988

15. Bennett MR (2011) Schizophrenia: susceptibility genes, dendritic-spine pathology and gray matter loss. *Progress in neurobiology* **95:** 275-300

16. Bertram L, Tanzi RE (2008) Thirty years of Alzheimer's disease genetics: the implications of systematic meta-analyses. *Nat Rev Neurosci* **9:** 768-778

17. Bezzi P, Volterra A (2001) A neuron-glia signalling network in the active brain. *Current opinion in neurobiology* **11:** 387-394

18. Bliss TV, Lomo T (1973) Long-lasting potentiation of synaptic transmission in the dentate area of the anaesthetized rabbit following stimulation of the perforant path. *J Physiol* **232:** 331-356

19. Boeckers TM (2006) The postsynaptic density. *Cell Tissue Res* **326:** 409-422

20. Boschert U, O'Shaughnessy C, Dickinson R, Tessari M, Bendotti C, Catsicas S, Pich EM (1996) Developmental and plasticity-related differential expression of two SNAP-25 isoforms in the rat brain. *The Journal of comparative neurology* **367:** 177-193

21. Bouwman J, Maia AS, Camoletto PG, Posthuma G, Roubos EW, Oorschot VM, Klumperman J, Verhage M (2004) Quantification of synapse formation and maintenance in vivo in the absence of synaptic release. *Neuroscience* **126:** 115-126

22. Bragina L, Candiracci C, Barbaresi P, Giovedi S, Benfenati F, Conti F (2007) Heterogeneity of glutamatergic and gabaergic release machinery in cerebral cortex. *Neuroscience* **146:** 1829-1840

23. Bragina L, Candiracci C, Barbaresi P, Giovedi S, Benfenati F, Conti F (2007) Heterogeneity of glutamatergic and GABAergic release machinery in cerebral cortex. *Neuroscience* **146:** 1829-1840

24. Brennand KJ, Simone A, Jou J, Gelboin-Burkhart C, Tran N, Sangar S, Li Y, Mu Y, Chen G, Yu D, McCarthy S, Sebat J, Gage FH (2011) Modelling schizophrenia using human induced pluripotent stem cells. *Nature* **473:** 221-225

25. Bresler T, Ramati Y, Zamorano PL, Zhai R, Garner CC, Ziv NE (2001) The dynamics of SAP90/PSD-95 recruitment to new synaptic junctions. *Mol Cell Neurosci* **18:** 149-167

26. Bresler T, Ramati Y, Zamorano PL, Zhai R, Garner CC, Ziv NE (2001) The dynamics of SAP90/PSD-95 recruitment to new synaptic junctions. *Mol Cell Neurosci* **18:** 149-167

27. Bresler T, Shapira M, Boeckers T, Dresbach T, Futter M, Garner CC, Rosenblum K, Gundelfinger ED, Ziv NE (2004) Postsynaptic density assembly is fundamentally different from presynaptic active zone assembly. *J Neurosci* **24:** 1507-1520

28. Brose N, O'Connor V, Skehel P (2010) Synaptopathy: dysfunction of synaptic function? *Biochem Soc Trans* **38:** 443-444

29. Carroll LS, Kendall K, O'Donovan MC, Owen MJ, Williams NM (2009) Evidence that putative ADHD low risk alleles at SNAP25 may increase the risk of schizophrenia. *Am J Med Genet B Neuropsychiatr Genet* **150B:** 893-899

30. Catsicas S, Larhammar D, Blomqvist A, Sanna PP, Milner RJ, Wilson MC (1991) Expression of a conserved cell-type-specific protein in nerve terminals coincides with synaptogenesis. *Proc Natl Acad Sci U S A* **88:** 785-789

31. Catterall WA, Few AP (2008) Calcium channel regulation and presynaptic plasticity. *Neuron* **59:** 882-901

32. Caylak E (2012) Biochemical and genetic analyses of childhood attention deficit/hyperactivity disorder. *Am J Med Genet B Neuropsychiatr Genet* **159B:** 613-627

33. Caylak E (2012) Biochemical and genetic analyses of childhood attention deficit/hyperactivity disorder. *Am J Med Genet B Neuropsychiatr Genet* **159B:** 613-627

34. Chang YT, Chen PC, Tsai IJ, Sung FC, Chin ZN, Kuo HT, Tsai CH, Chou IC (2011) Bidirectional relation between schizophrenia and epilepsy: a population-based retrospective cohort study. *Epilepsia* **52:** 2036-2042

35. Chen L, Chetkovich DM, Petralia RS, Sweeney NT, Kawasaki Y, Wenthold RJ, Bredt DS, Nicoll RA (2000) Stargazin regulates synaptic targeting of AMPA receptors by two distinct mechanisms. *Nature* **408:** 936-943

36. Chieregatti E, Chicka MC, Chapman ER, Baldini G (2004) SNAP-23 functions in docking/fusion of granules at low Ca2+. *Molecular Biology of the Cell* **15:** 1918-1930

37. Chua JJ, Kindler S, Boyken J, Jahn R The architecture of an excitatory synapse. *J Cell Sci* **123:** 819-823

38. Cingolani LA, Goda Y (2008) Actin in action: the interplay between the actin cytoskeleton and synaptic efficacy. *Nat Rev Neurosci* **9:** 344-356

39. Clinton SM, Haroutunian V, Davis KL, Meador-Woodruff JH (2003) Altered transcript expression of NMDA receptor-associated postsynaptic proteins in the thalamus of subjects with schizophrenia. *The American journal of psychiatry* **160:** 1100-1109

40. Clinton SM, Meador-Woodruff JH (2004) Abnormalities of the NMDA Receptor and Associated Intracellular Molecules in the Thalamus in Schizophrenia and Bipolar Disorder. *Neuropsychopharmacology : official publication of the American College of Neuropsychopharmacology* **29:** 1353-1362

41. Coenen AM, Van Luijtelaar EL (2003) Genetic animal models for absence epilepsy: a review of the WAG/Rij strain of rats. *Behavior genetics* **33:** 635-655

42. Condliffe SB, Corradini I, Pozzi D, Verderio C, Matteoli M (2010) Endogenous SNAP-25 regulates native voltage-gated calcium channels in glutamatergic neurons. *J Biol Chem* **285:** 24968-24976

43. Copits BA, Swanson GT (2013) Kainate receptor post-translational modifications differentially regulate association with 4.1N to control activity-dependent receptor endocytosis. *J Biol Chem* **288:** 8952-8965

44. Corradini I, Donzelli A, Antonucci F, Welzl H, Loos M, Martucci R, De Astis S, Pattini L, Inverardi F, Wolfer D, Caleo M, Bozzi Y, Verderio C, Frassoni C, Braida D, Clerici M, Lipp HP, Sala M, Matteoli M (2012) Epileptiform Activity and Cognitive Deficits in SNAP-25+/- Mice are Normalized by Antiepileptic Drugs. *Cereb Cortex*

45. Corradini I, Verderio C, Sala M, Wilson MC, Matteoli M (2009) SNAP-25 in neuropsychiatric disorders. *Ann N Y Acad Sci* **1152:** 93-99

46. Coutinho V, Knopfel T (2002) Metabotropic glutamate receptors: electrical and chemical signaling properties. *The Neuroscientist : a review journal bringing neurobiology, neurology and psychiatry* **8:** 551-561

47. Craig AM, Blackstone CD, Huganir RL, Banker G (1994) Selective clustering of glutamate and gamma-aminobutyric acid receptors opposite terminals releasing the corresponding neurotransmitters. *Proc Natl Acad Sci U S A* **91:** 12373-12377

48. Davis SM, Katusic SK, Barbaresi WJ, Killian J, Weaver AL, Ottman R, Wirrell EC (2010) Epilepsy in children with attention-deficit/hyperactivity disorder. *Pediatric neurology* **42:** 325-330

49. de Bartolomeis A, Latte G, Tomasetti C, Iasevoli F (2013) Glutamatergic Postsynaptic Density Protein Dysfunctions in Synaptic Plasticity and Dendritic Spines Morphology: Relevance to Schizophrenia and Other Behavioral Disorders Pathophysiology, and Implications for Novel Therapeutic Approaches. *Molecular neurobiology*

50. Deng PY, Sojka D, Klyachko VA (2011) Abnormal presynaptic short-term plasticity and information processing in a mouse model of fragile X syndrome. *J Neurosci* **31:** 10971-10982

51. Deng PY, Klyachko VA (2011) The diverse functions of short-term plasticity components in synaptic computations. Communicative & integrative biology 4: 543-548

52. Di Stefano P, Damiano L, Cabodi S, Aramu S, Tordella L, Praduroux A, Piva R, Cavallo F, Forni G, Silengo L, Tarone G, Turco E, Defilippi P (2007) p140Cap protein suppresses tumour cell properties, regulating Csk and Src kinase activity. *EMBO J* **26:** 2843-2855

53. Dingledine R, Borges K, Bowie D, Traynelis SF (1999) The glutamate receptor ion channels. *Pharmacol Rev* **51:** 7-61

54. Dosemeci A, Makusky AJ, Jankowska-Stephens E, Yang X, Slotta DJ, Markey SP (2007) Composition of the synaptic PSD-95 complex. *Molecular & cellular proteomics : MCP* **6:** 1749-1760

55. Ehrlich I, Klein M, Rumpel S, Malinow R (2007) PSD-95 is required for activity-driven synapse stabilization. *Proc Natl Acad Sci U S A* **104:** 4176-4181

56. Ehrlich I, Malinow R (2004) Postsynaptic density 95 controls AMPA receptor incorporation during long-term potentiation and experience-driven synaptic plasticity. *J Neurosci* **24:** 916-927

57. El Idrissi A, Neuwirth LS, L'Amoreaux W (2010) Taurine regulation of short term synaptic plasticity in fragile X mice. *Journal of biomedical science* **17 Suppl 1:** S15

58. El-Husseini AE, Schnell E, Chetkovich DM, Nicoll RA, Bredt DS (2000) PSD-95 involvement in maturation of excitatory synapses. *Science* **290:** 1364-1368

59. Elkobi A, Ehrlich I, Belelovsky K, Barki-Harrington L, Rosenblum K (2008) ERK-dependent PSD-95 induction in the gustatory cortex is necessary for taste learning, but not retrieval. *Nat Neurosci* **11:** 1149-1151

60. Faraone SV, Perlis RH, Doyle AE, Smoller JW, Goralnick JJ, Holmgren MA, Sklar P (2005) Molecular genetics of attention-deficit/hyperactivity disorder. *Biol Psychiatry* **57:** 1313-1323

61. Feng Y, Crosbie J, Wigg K, Pathare T, Ickowicz A, Schachar R, Tannock R, Roberts W, Malone M, Swanson J, Kennedy JL, Barr CL (2005) The SNAP25 gene as a susceptibility gene contributing to attention-deficit hyperactivity disorder. *Mol Psychiatry* **10:** 998-1005, 1973

62. Feyder M, Bonito-Oliva A, Fisone G (2011) L-DOPA-Induced Dyskinesia and Abnormal Signaling in Striatal Medium Spiny Neurons: Focus on Dopamine D1 Receptor-Mediated Transmission. *Frontiers in behavioral neuroscience* **5:** 71

63. Friedman HV, Bresler T, Garner CC, Ziv NE (2000) Assembly of new individual excitatory synapses: time course and temporal order of synaptic molecule recruitment. *Neuron* **27:** 57-69

64. Gal-Ben-Ari S, Rosenblum K (2011) Molecular mechanisms underlying memory consolidation of taste information in the cortex. *Frontiers in behavioral neuroscience* **5:** 87

65. Genoud S, Pralong W, Riederer BM, Eder L, Catsicas S, Muller D (1999) Activity-dependent phosphorylation of SNAP-25 in hippocampal organotypic cultures. *Journal of neurochemistry* **72:** 1699-1706

66. Giusti-Rodriguez P, Sullivan PF (2013) The genomics of schizophrenia: update and implications. *The Journal of clinical investigation* **123:** 4557-4563

67. Gonelle-Gispert C, Halban PA, Niemann H, Palmer M, Catsicas S, Sadoul K (1999) SNAP-25a and -25b isoforms are both expressed in insulin-secreting cells and can function in insulin secretion. *The Biochemical journal* **339 (Pt 1):** 159-165

68. Gray NW, Weimer RM, Bureau I, Svoboda K (2006) Rapid redistribution of synaptic PSD-95 in the neocortex in vivo. *PLoS Biol* **4:** e370

69. Grumelli C, Corradini I, Matteoli M, Verderio C (2010) Intrinsic calcium dynamics control botulinum toxin A susceptibility in distinct neuronal populations. *Cell Calcium* **47:** 419-424

70. Guilmatre A, Huguet G, Delorme R, Bourgeron T (2013) The emerging role of SHANK genes in neuropsychiatric disorders. *Developmental neurobiology*

71. Halassa MM, Fellin T, Haydon PG (2009) Tripartite synapses: roles for astrocytic purines in the control of synaptic physiology and behavior. *Neuropharmacology* **57:** 343-346

72. Harms KJ, Craig AM (2005) Synapse composition and organization following chronic activity blockade in cultured hippocampal neurons. *The Journal of comparative neurology* **490:** 72-84

73. Harris KM, Jensen FE, Tsao B (1992) Three-dimensional structure of dendritic spines and synapses in rat hippocampus (CA1) at postnatal day 15 and adult ages: implications for the maturation of synaptic physiology and long-term potentiation. *J Neurosci* **12:** 2685-2705

74. Harrison PJ, Weinberger DR (2005) Schizophrenia genes, gene expression, and neuropathology: on the matter of their convergence. *Mol Psychiatry* **10:** 40-68; image 45

75. Hawi Z, Matthews N, Wagner J, Wallace RH, Butler TJ, Vance A, Kent L, Gill M, Bellgrove MA (2013) DNA variation in the SNAP25 gene confers risk to ADHD and is associated with reduced expression in prefrontal cortex. *PloS one* **8:** e60274

76. Hayashi-Takagi A, Takaki M, Graziane N, Seshadri S, Murdoch H, Dunlop AJ, Makino Y, Seshadri AJ, Ishizuka K, Srivastava DP, Xie Z, Baraban JM, Houslay MD, Tomoda T, Brandon NJ, Kamiya A, Yan Z, Penzes P, Sawa A (2010) Disrupted-in-Schizophrenia 1 (DISC1) regulates spines of the glutamate synapse via Rac1. *Nat Neurosci* **13:** 327-332

77. Hess EJ, Jinnah HA, Kozak CA, Wilson MC (1992) Spontaneous locomotor hyperactivity in a mouse mutant with a deletion including the Snap gene on chromosome 2. *J Neurosci* **12:** 2865-2874

78. Honkura N, Matsuzaki M, Noguchi J, Ellis-Davies GC, Kasai H (2008) The subspine organization of actin fibers regulates the structure and plasticity of dendritic spines. *Neuron* **57:** 719-729

79. Hotulainen P, Hoogenraad CC Actin in dendritic spines: connecting dynamics to function. *J Cell Biol* **189:** 619-629

80. Iasevoli F, Tomasetti C, de Bartolomeis A (2013) Scaffolding proteins of the post-synaptic density contribute to synaptic plasticity by regulating receptor localization and distribution: relevance for neuropsychiatric diseases. *Neurochemical research* **38:** 1-22

81. Isaac JT, Ashby MC, McBain CJ (2007) The role of the GluR2 subunit in AMPA receptor function and synaptic plasticity. *Neuron* **54:** 859-871

82. Jacobsson G, Bark C, Meister B (1999) Differential expression of SNAP-25a and SNAP-25b RNA transcripts in cranial nerve nuclei. *The Journal of comparative neurology* **411:** 591-600

83. Jacobsson G, Bean AJ, Scheller RH, Juntti-Berggren L, Deeney JT, Berggren PO, Meister B (1994) Identification of synaptic proteins and their isoform mRNAs in compartments of pancreatic endocrine cells. *Proc Natl Acad Sci U S A* **91:** 12487-12491

84. Jacobsson G, Piehl F, Bark IC, Zhang X, Meister B (1996) Differential subcellular localization of SNAP-25a and SNAP-25b RNA transcripts in spinal motoneurons and plasticity in expression after nerve injury. *Brain research Molecular brain research* **37:** 49-62

85. Jahn R, Fasshauer D (2012) Molecular machines governing exocytosis of synaptic vesicles. *Nature* **490:** 201-207

86. Jaworski J, Kapitein LC, Gouveia SM, Dortland BR, Wulf PS, Grigoriev I, Camera P, Spangler SA, Di Stefano P, Demmers J, Krugers H, Defilippi P, Akhmanova A, Hoogenraad CC (2009) Dynamic microtubules regulate dendritic spine morphology and synaptic plasticity. *Neuron* **61:** 85-100

87.   Ji J, Yang SN, Huang X, Li X, Sheu L, Diamant N, Berggren PO, Gaisano HY (2002) Modulation of L-type Ca(2+) channels by distinct domains within SNAP-25. *Diabetes* **51:** 1425-1436

88.   Jourdain P, Fukunaga K, Muller D (2003) Calcium/calmodulin-dependent protein kinase II contributes to activity-dependent filopodia growth and spine formation. *J Neurosci* **23:** 10645-10649

89.   Jurado S, Goswami D, Zhang Y, Molina AJ, Sudhof TC, Malenka RC (2013) LTP Requires a Unique Postsynaptic SNARE Fusion Machinery. *Neuron* **77:** 542-558

90.   Kasai H, Fukuda M, Watanabe S, Hayashi-Takagi A, Noguchi J (2010) Structural dynamics of dendritic spines in memory and cognition. *Trends Neurosci* **33:** 121-129

91.   Kataoka M, Yamamori S, Suzuki E, Watanabe S, Sato T, Miyaoka H, Azuma S, Ikegami S, Kuwahara R, Suzuki-Migishima R, Nakahara Y, Nihonmatsu I, Inokuchi K, Katoh-Fukui Y, Yokoyama M, Takahashi M (2011) A single amino acid mutation in SNAP-25 induces anxiety-related behavior in mouse. *PloS one* **6:** e25158

92.   Kerrigan TL, Randall AD (2013) A new player in the "synaptopathy" of Alzheimer's disease - arc/arg 3.1. *Frontiers in neurology* **4:** 9

93.   Kerti K, Lorincz A, Nusser Z (2012) Unique somato-dendritic distribution pattern of Kv4.2 channels on hippocampal CA1 pyramidal cells. *European Journal of Neuroscience* **35:** 66-75

94.   Kim E, Sheng M (2004) PDZ domain proteins of synapses. *Nat Rev Neurosci* **5:** 771-781

95.   Kochlamazashvili G, Haucke V (2013) A dual role of SNAP-25 as carrier and guardian of synaptic transmission. *EMBO reports* **14:** 579-580

96.   Koleske AJ (2013) Molecular mechanisms of dendrite stability. *Nat Rev Neurosci* **14:** 536-550

97.   Kolomeets NS, Orlovskaya DD, Rachmanova VI, Uranova NA (2005) Ultrastructural alterations in hippocampal mossy fiber synapses in schizophrenia: a postmortem morphometric study. *Synapse* **57:** 47-55

98.   Korobova F, Svitkina T Molecular architecture of synaptic actin cytoskeleton in hippocampal neurons reveals a mechanism of dendritic spine morphogenesis. *Mol Biol Cell* **21:** 165-176

99.   Kovacs-Nagy R, Hu J, Ronai Z, Sasvari-Szekely M (2009) SNAP-25: a novel candidate gene in psychiatric genetics. *Neuropsychopharmacologia Hungarica : a Magyar Pszichofarmakologiai Egyesulet lapja = official journal of the Hungarian Association of Psychopharmacology* **11:** 89-94

100.   Lai KO, Ip NY (2013) Structural plasticity of dendritic spines: The underlying mechanisms and its dysregulation in brain disorders. *Biochimica et biophysica acta* **1832:** 2257-2263

101.   Lau CG, Takayasu Y, Rodenas-Ruano A, Paternain AV, Lerma J, Bennett MV, Zukin RS (2010) SNAP-25 is a target of protein kinase C phosphorylation critical to NMDA receptor trafficking. *J Neurosci* **30:** 242-254

102.   Lee SH, Sheng M (2000) Development of neuron-neuron synapses. *Current opinion in neurobiology* **10:** 125-131

103.   Lewis CM, Levinson DF, Wise LH, DeLisi LE, Straub RE, Hovatta I, Williams NM, Schwab SG, Pulver AE, Faraone SV, Brzustowicz LM, Kaufmann CA, Garver DL, Gurling HM, Lindholm E, Coon H, Moises HW, Byerley W, Shaw SH, Mesen A, Sherrington R, O'Neill FA, Walsh D, Kendler KS, Ekelund J, Paunio T, Lonnqvist J, Peltonen L, O'Donovan MC, Owen MJ, Wildenauer DB, Maier W, Nestadt G, Blouin JL, Antonarakis SE, Mowry BJ, Silverman JM, Crowe RR, Cloninger CR, Tsuang MT, Malaspina D, Harkavy-Friedman JM, Svrakic DM, Bassett AS, Holcomb J, Kalsi G, McQuillin A, Brynjolfson J, Sigmundsson T, Petursson H, Jazin E, Zoega T, Helgason T (2003) Genome scan meta-analysis of schizophrenia and bipolar disorder, part II: Schizophrenia. *Am J Hum Genet* **73:** 34-48

104. Liu DD, Yang Q, Li ST (2013) Activation of extrasynaptic NMDA receptors induces LTD in rat hippocampal CA1 neurons. *Brain research bulletin* **93:** 10-16

105. Lochman J, Balcar VJ, Stastny F, Sery O (2013) Preliminary evidence for association between schizophrenia and polymorphisms in the regulatory Regions of the ADRA2A, DRD3 and SNAP-25 Genes. *Psychiatry research* **205:** 7-12

106. Lu J, Helton TD, Blanpied TA, Racz B, Newpher TM, Weinberg RJ, Ehlers MD (2007) Postsynaptic positioning of endocytic zones and AMPA receptor cycling by physical coupling of dynamin-3 to homer. *Neuron* **55:** 874-889

107. Lu W, Man H, Ju W, Trimble WS, MacDonald JF, Wang YT (2001) Activation of synaptic NMDA receptors induces membrane insertion of new AMPA receptors and LTP in cultured hippocampal neurons. *Neuron* **29:** 243-254

108. Luscher C, Nicoll RA, Malenka RC, Muller D (2000) Synaptic plasticity and dynamic modulation of the postsynaptic membrane. *Nat Neurosci* **3:** 545-550

109. Malenka RC, Bear MF (2004) LTP and LTD: an embarrassment of riches. *Neuron* **44:** 5-21

110. Martin-Moutot N, Charvin N, Leveque C, Sato K, Nishiki T, Kozaki S, Takahashi M, Seagar M (1996) Interaction of SNARE complexes with P/Q-type calcium channels in rat cerebellar synaptosomes. *J Biol Chem* **271:** 6567-6570

111. Megias M, Emri Z, Freund TF, Gulyas AI (2001) Total number and distribution of inhibitory and excitatory synapses on hippocampal CA1 pyramidal cells. *Neuroscience* **102:** 527-540

112. Menna E, Fossati G, Scita G, Matteoli M (2011) From filopodia to synapses: the role of actin-capping and anti-capping proteins. *The European journal of neuroscience* **34:** 1655-1662

113. Menna E, Zambetti S, Morini R, Donzelli A, Disanza A, Calvigioni D, Braida D, Nicolini C, Orlando M, Fossati G, Cristina Regondi M, Pattini L, Frassoni C, Francolini M, Scita G, Sala M, Fahnestock M, Matteoli M (2013) Eps8 controls dendritic spine density and synaptic plasticity through its actin-capping activity. *EMBO J* **32:** 1730-1744

114. Minerbi A, Kahana R, Goldfeld L, Kaufman M, Marom S, Ziv NE (2009) Long-term relationships between synaptic tenacity, synaptic remodeling, and network activity. PLoS Biol 7: e1000136

115. Mohrmann R, de Wit H, Connell E, Pinheiro PS, Leese C, Bruns D, Davletov B, Verhage M, Sorensen JB (2013) Synaptotagmin interaction with SNAP-25 governs vesicle docking, priming, and fusion triggering. *J Neurosci* **33:** 14417-14430

116. Neher E, Sakaba T (2008) Multiple roles of calcium ions in the regulation of neurotransmitter release. *Neuron* **59:** 861-872

117. Nicoll RA, Tomita S, Bredt DS (2006) Auxiliary subunits assist AMPA-type glutamate receptors. *Science* **311:** 1253-1256

118. Niethammer M, Kim E, Sheng M (1996) Interaction between the C terminus of NMDA receptor subunits and multiple members of the PSD-95 family of membrane-associated guanylate kinases. *J Neurosci* **16:** 2157-2163

119. Nikonenko I, Boda B, Steen S, Knott G, Welker E, Muller D (2008) PSD-95 promotes synaptogenesis and multiinnervated spine formation through nitric oxide signaling. *J Cell Biol* **183:** 1115-1127

120. Nikonenko I, Jourdain P, Muller D (2003) Presynaptic remodeling contributes to activity-dependent synaptogenesis. *J Neurosci* **23:** 8498-8505

121. O'Brien RJ, Lau LF, Huganir RL (1998) Molecular mechanisms of glutamate receptor clustering at excitatory synapses. *Current opinion in neurobiology* **8:** 364-369

122. Okabe M, Ikawa M, Kominami K, Nakanishi T, Nishimune Y (1997) 'Green mice' as a source of ubiquitous green cells. *FEBS Lett* **407:** 313-319

123. Okabe S, Miwa A, Okado H (2001) Spine formation and correlated assembly of presynaptic and postsynaptic molecules. *J Neurosci* **21:** 6105-6114

124. Okamoto K, Nagai T, Miyawaki A, Hayashi Y (2004) Rapid and persistent modulation of actin dynamics regulates postsynaptic reorganization underlying bidirectional plasticity. *Nat Neurosci* **7:** 1104-1112

125. Osen-Sand A, Staple JK, Naldi E, Schiavo G, Rossetto O, Petitpierre S, Malgaroli A, Montecucco C, Catsicas S (1996) Common and distinct fusion proteins in axonal growth and transmitter release. *The Journal of comparative neurology* **367:** 222-234

126. Ovsepian SV, Dolly JO (2011) Dendritic SNAREs add a new twist to the old neuron theory. *Proc Natl Acad Sci U S A* **108:** 19113-19120

127. Owald D, Sigrist SJ (2009) Assembling the presynaptic active zone. *Current opinion in neurobiology* **19:** 311-318

128. Oyler GA, Higgins GA, Hart RA, Battenberg E, Billingsley M, Bloom FE, Wilson MC (1989) The identification of a novel synaptosomal-associated protein, SNAP-25, differentially expressed by neuronal subpopulations. *J Cell Biol* **109:** 3039-3052

129. Oyler GA, Polli JW, Wilson MC, Billingsley ML (1991) Developmental expression of the 25-kDa synaptosomal-associated protein (SNAP-25) in rat brain. *Proc Natl Acad Sci U S A* **88:** 5247-5251

130. Paoletti P, Bellone C, Zhou Q (2013) NMDA receptor subunit diversity: impact on receptor properties, synaptic plasticity and disease. *Nat Rev Neurosci* **14:** 383-400

131. Park M, Salgado JM, Ostroff L, Helton TD, Robinson CG, Harris KM, Ehlers MD (2006) Plasticity-induced growth of dendritic spines by exocytic trafficking from recycling endosomes. *Neuron* **52:** 817-830

132. Paxinos G and Franklin KGB (1997) The Mouse Brain in Stereotaxic Coordinates. San Diego: Academic Press

133. Penzes P, Cahill ME, Jones KA, VanLeeuwen JE, Woolfrey KM (2011) Dendritic spine pathology in neuropsychiatric disorders. *Nat Neurosci* **14:** 285-293

134. Perea G, Navarrete M, Araque A (2009) Tripartite synapses: astrocytes process and control synaptic information. *Trends Neurosci* **32:** 421-431

135. Peters A, Kaiserman-Abramof IR (1970) The small pyramidal neuron of the rat cerebral cortex. The perikaryon, dendrites and spines. *The American journal of anatomy* **127:** 321-355

136. Petrakis S, Rasko T, Russ J, Friedrich RP, Stroedicke M, Riechers SP, Muehlenberg K, Moller A, Reinhardt A, Vinayagam A, Schaefer MH, Boutros M, Tricoire H, Andrade-Navarro MA, Wanker EE (2012) Identification of human proteins that modify misfolding and proteotoxicity of pathogenic ataxin-1. *PLoS Genet* **8:** e1002897

137. Petrakis S, Rasko T, Russ J, Friedrich RP, Stroedicke M, Riechers SP, Muehlenberg K, Moller A, Reinhardt A, Vinayagam A, Schaefer MH, Boutros M, Tricoire H, Andrade-Navarro MA, Wanker EE (2012) Identification of human proteins that modify misfolding and proteotoxicity of pathogenic ataxin-1. *PLoS Genet* **8:** e1002897

138. Pozueta J, Lefort R, Shelanski ML (2012) Synaptic changes in Alzheimer's disease and its models. *Neuroscience*

139. Pozueta J, Lefort R, Shelanski ML (2013) Synaptic changes in Alzheimer's disease and its models. *Neuroscience* **251:** 51-65

140. Pozzi D, Condliffe S, Bozzi Y, Chikhladze M, Grumelli C, Proux-Gillardeaux V, Takahashi M, Franceschetti S, Verderio C, Matteoli M (2008) Activity-dependent phosphorylation of Ser187 is required for SNAP-25-negative modulation of neuronal voltage-gated calcium channels. *Proc Natl Acad Sci U S A* **105:** 323-328

141. Purves et al., (2008) Neuroscience, 3rd edition: Zanichelli.

142. Ramachandran B, Frey JU (2009) Interfering with the actin network and its effect on long-term potentiation and synaptic tagging in hippocampal CA1 neurons in slices in vitro. *J Neurosci* **29:** 12167-12173

143. Rettig J, Sheng ZH, Kim DK, Hodson CD, Snutch TP, Catterall WA (1996) Isoform-specific interaction of the alpha1A subunits of brain Ca2+ channels with the presynaptic proteins syntaxin and SNAP-25. *Proc Natl Acad Sci U S A* **93:** 7363-7368

144. Richer LP, Shevell MI, Rosenblatt BR (2002) Epileptiform abnormalities in children with attention-deficit-hyperactivity disorder. *Pediatric neurology* **26:** 125-129

145. Rizzi TS, Beunders G, Rizzu P, Sistermans E, Twisk JW, van Mechelen W, Deijen JB, Meijers-Heijboer H, Verhage M, Heutink P, Posthuma D (2012) Supporting the generalist genes hypothesis for intellectual ability/disability: the case of SNAP25. *Genes, brain, and behavior* **11:** 767-771

146. Rizzoli SO, Betz WJ (2003) Neurobiology: All change at the synapse. *Nature* **423:** 591-592

147. Rochefort NL, Konnerth A (2012) Dendritic spines: from structure to in vivo function. *EMBO reports* **13:** 699-708

148. Rodesch CK, Broadie K (2000) Genetic studies in Drosophila: vesicle pools and cytoskeleton-based regulation of synaptic transmission. *Neuroreport* **11:** R45-53

149. Russell VA (2007) Neurobiology of animal models of attention-deficit hyperactivity disorder. *Journal of neuroscience methods* **161:** 185-198

150. Sabo SL, Gomes RA, McAllister AK (2006) Formation of presynaptic terminals at predefined sites along axons. *J Neurosci* **26:** 10813-10825

151. Sala C, Cambianica I, Rossi F (2008) Molecular mechanisms of dendritic spine development and maintenance. *Acta Neurobiol Exp (Wars)* **68:** 289-304

152. Santello M, Cali C, Bezzi P (2012) Gliotransmission and the tripartite synapse. *Advances in experimental medicine and biology* **970:** 307-331

153. Scarr E, Gray L, Keriakous D, Robinson PJ, Dean B (2006) Increased levels of SNAP-25 and synaptophysin in the dorsolateral prefrontal cortex in bipolar I disorder. *Bipolar disorders* **8:** 133-143

154. Schnell E, Sizemore M, Karimzadegan S, Chen L, Bredt DS, Nicoll RA (2002) Direct interactions between PSD-95 and stargazin control synaptic AMPA receptor number. *Proc Natl Acad Sci U S A* **99:** 13902-13907

155. Selak S, Paternain AV, Aller MI, Pico E, Rivera R, Lerma J (2009) A role for SNAP25 in internalization of kainate receptors and synaptic plasticity. *Neuron* **63:** 357-371

156. Sharma M, Burre J, Bronk P, Zhang Y, Xu W, Sudhof TC (2012) CSPalpha knockout causes neurodegeneration by impairing SNAP-25 function. *EMBO J* **31:** 829-841

157. Sheng ZH, Rettig J, Cook T, Catterall WA (1996) Calcium-dependent interaction of N-type calcium channels with the synaptic core complex. *Nature* **379:** 451-454

158. Shirasu M, Kimura K, Kataoka M, Takahashi M, Okajima S, Kawaguchi S, Hirasawa Y, Ide C, Mizoguchi A (2000) VAMP-2 promotes neurite elongation and SNAP-25A increases neurite sprouting in PC12 cells. *Neuroscience research* **37:** 265-275

159. Sorra KE, Harris KM (2000) Overview on the structure, composition, function, development, and plasticity of hippocampal dendritic spines. *Hippocampus* **10:** 501-511

160. Steen RG, Mull C, McClure R, Hamer RM, Lieberman JA (2006) Brain volume in first-episode schizophrenia: systematic review and meta-analysis of magnetic resonance imaging studies. *Br J Psychiatry* **188:** 510-518

161. Stein A, Weber G, Wahl MC, Jahn R (2009) Helical extension of the neuronal SNARE complex into the membrane. *Nature* **460:** 525-528

162. Stein V, House DR, Bredt DS, Nicoll RA (2003) Postsynaptic density-95 mimics and occludes hippocampal long-term potentiation and enhances long-term depression. *J Neurosci* **23:** 5503-5506

163. Steiner P, Higley MJ, Xu W, Czervionke BL, Malenka RC, Sabatini BL (2008) Destabilization of the postsynaptic density by PSD-95 serine 73 phosphorylation inhibits spine growth and synaptic plasticity. *Neuron* **60:** 788-802

164. Sturgill JF, Steiner P, Czervionke BL, Sabatini BL (2009) Distinct domains within PSD-95 mediate synaptic incorporation, stabilization, and activity-dependent trafficking. *J Neurosci* **29:** 12845-12854

165. Sudhof TC (2004) The synaptic vesicle cycle. *Annu Rev Neurosci* **27:** 509-547

166. Sudhof TC (2008) Neuroligins and neurexins link synaptic function to cognitive disease. *Nature* **455:** 903-911

167. Sudhof TC (2012) The presynaptic active zone. *Neuron* **75:** 11-25

168. Suh YH, Terashima A, Petralia RS, Wenthold RJ, Isaac JTR, Roche KW, Roche PA (2010) A neuronal role for SNAP-23 in postsynaptic glutamate receptor trafficking. *Nature Neuroscience* **13:** 338-U316

169. Sweet RA, Henteleff RA, Zhang W, Sampson AR, Lewis DA (2009) Reduced dendritic spine density in auditory cortex of subjects with schizophrenia. *Neuropsychopharmacology : official publication of the American College of Neuropsychopharmacology* **34:** 374-389

170. Takamori S, Holt M, Stenius K, Lemke EA, Gronborg M, Riedel D, Urlaub H, Schenck S, Brugger B, Ringler P, Muller SA, Rammner B, Grater F, Hub JS, De Groot BL, Mieskes G, Moriyama Y, Klingauf J, Grubmuller H, Heuser J, Wieland F, Jahn R (2006) Molecular anatomy of a trafficking organelle. *Cell* **127:** 831-846

171. Thompson PM, Egbufoama S, Vawter MP (2003) SNAP-25 reduction in the hippocampus of patients with schizophrenia. *Prog Neuropsychopharmacol Biol Psychiatry* **27:** 411-417

172. Thompson PM, Sower AC, Perrone-Bizzozero NI (1998) Altered levels of the synaptosomal associated protein SNAP-25 in schizophrenia. *Biol Psychiatry* **43:** 239-243

173. Tomasoni R, Repetto D, Morini R, Elia C, Gardoni F, Di Luca M, Turco E, Defilippi P, Matteoli M (2013) SNAP-25 regulates spine formation through postsynaptic binding to p140Cap. *Nature communications* **4:** 2136

174. Toro C, Deakin JF (2005) NMDA receptor subunit NRI and postsynaptic protein PSD-95 in hippocampus and orbitofrontal cortex in schizophrenia and mood disorder. *Schizophrenia research* **80:** 323-330

175. Tsakiridou E, Bertollini L, de Curtis M, Avanzini G, Pape HC (1995) Selective increase in T-type calcium conductance of reticular thalamic neurons in a rat model of absence epilepsy. *J Neurosci* **15:** 3110-3117

176. Varoqueaux F, Sigler A, Rhee JS, Brose N, Enk C, Reim K, Rosenmund C (2002) Total arrest of spontaneous and evoked synaptic transmission but normal synaptogenesis in the absence of Munc13-mediated vesicle priming. *Proc Natl Acad Sci U S A* **99:** 9037-9042

177. Verderio C, Pozzi D, Pravettoni E, Inverardi F, Schenk U, Coco S, Proux-Gillardeaux V, Galli T, Rossetto O, Frassoni C, Matteoli M (2004) SNAP-25 modulation of calcium dynamics underlies differences in GABAergic and glutamatergic responsiveness to depolarization. *Neuron* **41:** 599-610

178. Verhage M, Maia AS, Plomp JJ, Brussaard AB, Heeroma JH, Vermeer H, Toonen RF, Hammer RE, van den Berg TK, Missler M, Geuze HJ, Sudhof TC (2000) Synaptic assembly of the brain in the absence of neurotransmitter secretion. *Science* **287:** 864-869

179. Vickers CA, Stephens B, Bowen J, Arbuthnott GW, Grant SG, Ingham CA (2006) Neurone specific regulation of dendritic spines in vivo by post synaptic density 95 protein (PSD-95). *Brain research* **1090:** 89-98

180. von Bohlen Und Halbach O (2009) Structure and function of dendritic spines within the hippocampus. *Ann Anat* **191:** 518-531

181. Wang GY, Witkin JW, Hao GM, Bankaitis VA, Scherer PE, Baldini G (1997) Syndet is a novel SNAP-25 related protein expressed in many tissues. *Journal of Cell Science* **110:** 505-513

182. Washbourne P, Thompson PM, Carta M, Costa ET, Mathews JR, Lopez-Bendito G, Molnar Z, Becher MW, Valenzuela CF, Partridge LD, Wilson MC (2002) Genetic ablation of the t-SNARE SNAP-25 distinguishes mechanisms of neuroexocytosis. *Nat Neurosci* **5:** 19-26

183. Wilson MC (2000) Coloboma mouse mutant as an animal model of hyperkinesis and attention deficit hyperactivity disorder. *Neuroscience and biobehavioral reviews* **24:** 51-57

184. Wiser O, Bennett MK, Atlas D (1996) Functional interaction of syntaxin and SNAP-25 with voltage-sensitive L- and N-type Ca2+ channels. *EMBO J* **15:** 4100-4110

185. Young CE, Arima K, Xie J, Hu L, Beach TG, Falkai P, Honer WG (1998) SNAP-25 deficit and hippocampal connectivity in schizophrenia. *Cereb Cortex* **8:** 261-268

186. Young JZ (1973) Receptive fields of the visual system of the squid. *Nature* **241:** 469-471

187. Zamponi GW (2003) Regulation of presynaptic calcium channels by synaptic proteins. *Journal of pharmacological sciences* **92:** 79-83

188. Zhang J, Lewis SM, Kuhlman B, Lee AL (2013) Supertertiary structure of the MAGUK core from PSD-95. *Structure* **21:** 402-413

189. Zhang Y, Vilaythong AP, Yoshor D, Noebels JL (2004) Elevated thalamic low-voltage-activated currents precede the onset of absence epilepsy in the SNAP25-deficient mouse mutant coloboma. *J Neurosci* **24:** 5239-5248

190. Zhong H, Yokoyama CT, Scheuer T, Catterall WA (1999) Reciprocal regulation of P/Q-type Ca2+ channels by SNAP-25, syntaxin and synaptotagmin. *Nat Neurosci* **2:** 939-941

ANNEXES

1) Antonucci F, Corradini I, Morini R, **Fossati G**, Menna E, Pozzi D, Pacioni S, Verderio C, Bacci A, Matteoli M (2013) Reduced SNAP-25 alters short-term plasticity at developing glutamatergic synapses. EMBO reports **14:** 645-651

2) Menna E, Zambetti S, Morini R, Donzelli A, Disanza A, Calvigioni D, Braida D, Nicolini C, Orlando M, **Fossati G**, Cristina Regondi M, Pattini L, Frassoni C, Francolini M, Scita G, Sala M, Fahnestock M, Matteoli M (2013) Eps8 controls dendritic spine density and synaptic plasticity through its actin-capping activity. EMBO J **32:** 1730-1744

3) Menna E, **Fossati G**, Scita G, Matteoli M (2011) From filopodia to synapses: the role of actin-capping and anti-capping proteins. The European journal of neuroscience **34:** 1655-1662

scientific report

Reduced SNAP-25 alters short-term plasticity at developing glutamatergic synapses

Flavia Antonucci[1,2], *Irene Corradini*[1,3], *Raffaella Morini*[1,4], *Giuliana Fossati*[1,4], *Elisabetta Menna*[2,4], *Davide Pozzi*[5], *Simone Pacioni*[6], *Claudia Verderio*[2], *Alberto Bacci*[6,7] *& Michela Matteoli*[1,4+]

[1]Department of Biotechnology and Translational Medicine, University of Milan, Milano, [2]CNR Institute of Neuroscience, Milano, [3]Fondazione Filarete viale Ortles 22/4, Milano, [4]Istituto Clinico Humanitas, IRCCS, Rozzano, Milano, [5]Fondazione IRCCS Don Gnocchi, Milano, [6]European Brain Research Institute (EBRI), Roma, Italy, and [7]Centre National de la Recherche Scientifique, Unité Mixte de Recherche 7225, Institut du Cerveau et de la Moelle épinière (ICM), Paris, France

SNAP-25 is a key component of the synaptic-vesicle fusion machinery, involved in several psychiatric diseases including schizophrenia and ADHD. SNAP-25 protein expression is lower in different brain areas of schizophrenic patients and in ADHD mouse models. How the reduced expression of SNAP-25 alters the properties of synaptic transmission, leading to a pathological phenotype, is unknown. We show that, unexpectedly, halved SNAP-25 levels at 13–14 DIV not only fail to impair synaptic transmission but instead enhance evoked glutamatergic neurotransmission. This effect is possibly dependent on presynaptic voltage-gated calcium channel activity and is not accompanied by changes in spontaneous quantal events or in the pool of readily releasable synaptic vesicles. Notably, synapses of 13–14 DIV neurons with reduced SNAP-25 expression show paired-pulse depression as opposed to paired-pulse facilitation occurring in their wild-type counterparts. This phenotype disappears with synapse maturation. As alterations in short-term plasticity represent a new mechanism contributing to cognitive impairments in intellectual disabilities, our data provide mechanistic clues for neuronal circuit alterations in psychiatric diseases characterized by reduced expression of SNAP-25.

[1]Department of Biotechnology and Translational Medicine, University of Milan, Via Vanvitelli 32, 20129 Milano
[2]CNR Institute of Neuroscience, 20129 Milano
[3]Fondazione Filarete viale Ortles 22/4, 20139 Milano
[4]Istituto Clinico Humanitas, IRCCS, Via Manzoni 56, Rozzano, 20089 Milano
[5]Fondazione IRCCS Don Gnocchi, 20162 Milano
[6]European Brain Research Institute (EBRI), Via del Fosso di Fiorano 64, 00143 Roma, Italy
[7]Centre National de la Recherche Scientifique, Unité Mixte de Recherche 7225, Institut du Cerveau et de la Moelle épinière (ICM), 75013 Paris, France
[+]Corresponding author. Tel: +39 2 50317097; Fax: +39 2 7490574;
E-mail: michela.matteoli@unimi.it

INTRODUCTION

SNAP-25 (synaptosomal-associated protein of 25 kDa) is a SNARE protein that participates in the regulation of synaptic-vesicle (SV) exocytosis [1–3] and negatively modulates voltage-gated ion channels (VGCCs) [4–7]. Consistently, silencing endogenous SNAP-25 results in increased VGCC activity in glutamatergic neurons [8,9].

The *SNAP-25* gene has been associated with schizophrenia [10,11], as SNAP-25 protein levels are lower in hippocampi and frontal lobes of schizophrenic patients [12–14]. Also, case control or family-based studies indicated that the *SNAP-25* gene is associated with attention deficit hyperactivity disorder [15,11] and, indeed, reduced SNAP-25 expression has been found to mediate hyperactivity in mice [16,17]. Furthermore, reduction of SNAP-25 levels is responsible for the massive neurodegeneration in mice genetically devoid of the SV protein cystein spring protein alpha [18].

Despite the involvement of reduced SNAP-25 in psychiatric defects, the underlying cellular mechanisms are at present unknown. We then investigated whether halved SNAP-25 expression results in altered neurotransmission and plasticity in neuronal networks. We demonstrate that in developing hippocampal neurons of SNAP-25 heterozygous mice glutamate release probability is increased, heavily impacting short-term plasticity phenomena.

RESULTS AND DISCUSSION
Glutamatergic currents in developing neurons

SNAP-25 modulates VGCC current density in glutamatergic neurons [8]. To investigate whether the changes in VGCC current densities in neuronal cell bodies affect neurotransmission, synaptic properties were investigated in SNAP-25$^{+/+}$ and SNAP-25$^{+/-}$ hippocampal cultures (here in defined as wild type (wt) and het, respectively) at 13–14 days *in vitro* (DIV). We recorded miniature excitatory (mEPSCs) or inhibitory (mIPSCs) currents (Fig 1A–B), holding neurons at the reversal potential for GABA (γ-aminobutyric acid)- and glutamate-mediated responses
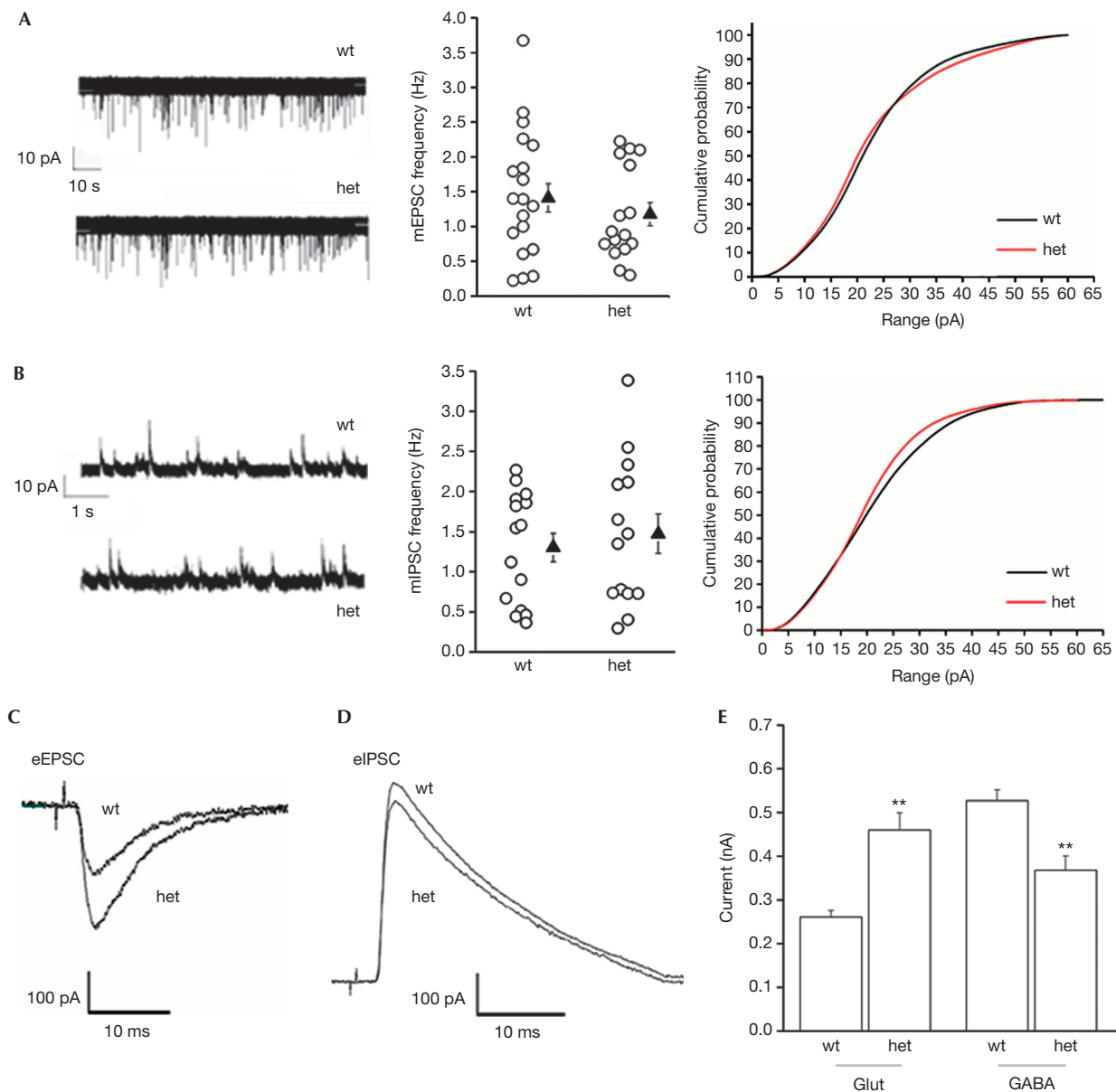
Fig 1 | Enhanced evoked glutamatergic transmission in het cultures at 14 div. (A–B) Traces of mEPSCs and mIPSCs from wt or het neurons followed by the analysis of frequency and amplitude ((A) frequency, t-test, $P = 0.399$; $N = 4$; amplitude: KS-test not significant; (B) frequency, t-test, $P = 0.49$, $N = 4$; amplitude: KS-test not significant). (C–D) Traces of eEPSCs (C) and eIPSC (D) from wt or het neurons. (E) Analysis of eEPSCs: wt ($n = 10$) versus het ($n = 10$), t-test, $P < 0.01$, $N = 4$; eIPSCs: wt ($n = 13$) versus het ($n = 8$), t-test, $P < 0.01$, $N = 3$). Error bars indicate s.e.m. KS-test, Kolmogorov–Smirnov test; wt, wild type. **$P < 0.01$.

(–70 and $+5$ mV, respectively) in the presence of $1 \, \mu M$ tetrodotoxin. Frequency and amplitudes of both mEPSCs and mIPSCs were not significantly different in het neurons relative to wt, in line with previous reports [19,3,18] (mEPSC frequency: 1.41 ± 0.20 versus $1.17 \pm 0.16 \, Hz$, wt versus het; mIPSC frequency: 1.30 ± 0.17 versus $1.47 \pm 0.24 \, Hz$, wt versus het. mEPSC and mIPSC amplitude distributions were not significantly different).

Depolarizations of presynaptic glutamatergic or GABAergic cells in synaptically connected neurons evoked unitary EPSCs or IPSCs, respectively. Notably, evoked EPSCs were

significantly larger in het cultures as compared with wt (eEPSCs: 0.26 ± 0.01 versus $0.45 \pm 0.04 \, nA$, wt versus het; $P < 0.05$; Fig 1C,E). Conversely, a slight, although significant, reduction of evoked IPSC amplitude was recorded in het neurons relative to wt (0.52 ± 0.03 versus $0.36 \pm 0.03 \, nA$, wt versus het, $P < 0.05$; Fig 1D,E).

Glutamate-receptor sensitivity was not affected by reduced SNAP-25, as indicated by unaltered mEPSC amplitudes (Fig 1A) and by similar intracellular Ca^{2+} transients in response to $30 \, \mu M$ AMPA (α-amino-3-hydroxy-5-methyl-4-isoxazolepropio-
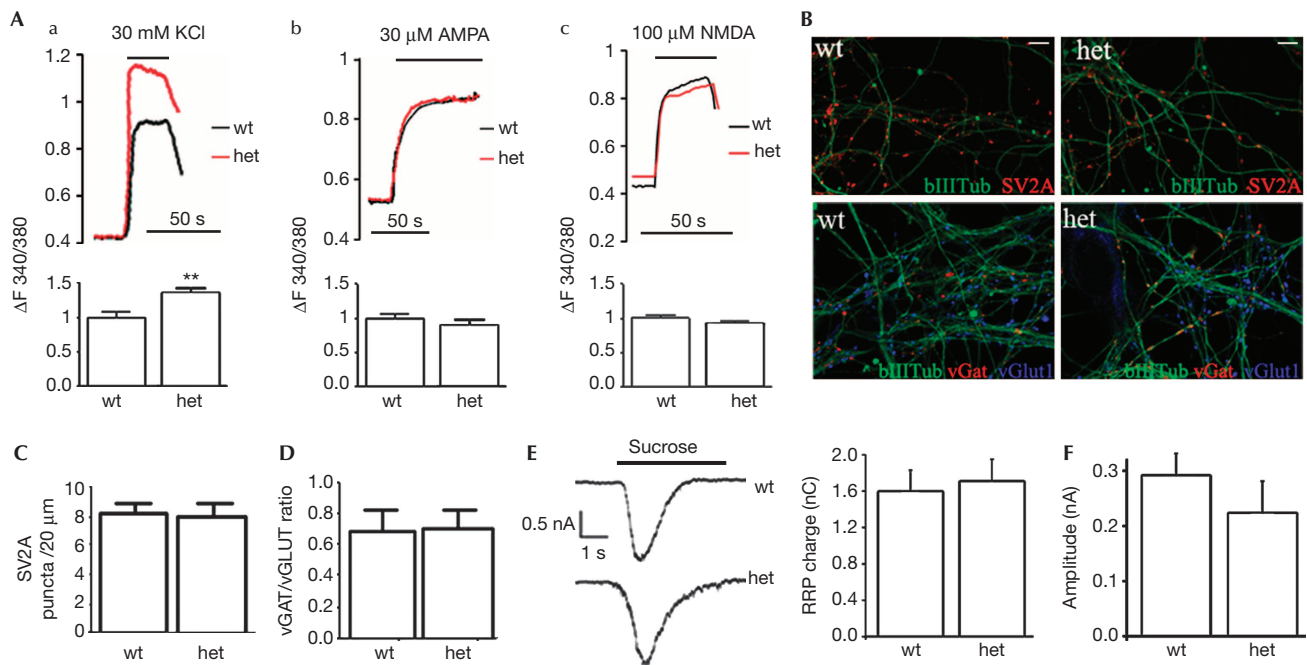
Fig 2 | Enhanced glutamatergic transmission in het cultures does not depend on synapse number or RRP size. (A) Traces and quantification of calcium responses on: (a) KCl: wt ($n = 76$) versus het ($n = 63$), t-test, $P = 0.007$; (b) AMPA: wt ($n = 22$) versus het ($n = 22$), t-test, $P = 0.33$; (c) NMDA: wt ($n = 84$) versus het ($n = 52$) t-test, $P = 0.15$; $N = 3$. (B) Staining of neurons for SV2A (red) and β_{III} tubulin (green) (top panels) and for β_{III} tubulin (green), vGAT (red) and vGlut (blue). Calibration bar = 10 μm. (C) SV2 puncta/20 μm: wt ($n = 24$) versus het ($n = 26$), t-test, $P = 0.82$. (D) Measurement of vGAT/vGlut puncta: wt ($n = 34$) versus het ($n = 54$), t-test, $P = 0.89$. (E) Sucrose-evoked responses from wt and het neurons and charge response: wt ($n = 12$) versus het ($n = 12$), t-test, $P = 0.55$, $N = 3$. (F) Charge transfer in calcimycin experiment: wt ($n = 13$) versus het ($n = 11$) t-test, $P = 0.06$, $N = 3$. Error bars indicate s.e.m. AMPA, α-amino-3-hydroxy-5-methyl-4-isoxazolepropionic acid; NMDA, N-methyl-D-aspartic acid; wt, wild type.

nic acid) or 100 μM NMDA (N-methyl-D-aspartic acid) stimulation (AMPA: wt $= 1 \pm 0.066$, het $= 0.899 \pm 0.078$; NMDA: wt $= 1 \pm 0.039$, het $= 0.919 \pm 0.046$, normalized value; Fig 2A). Conversely, stimulation with 30 mM KCl induced a higher Ca^{2+} response in het neurons compared with wt (normalized het F340/380: 1.2 ± 0.06, $P < 0.05$).

Increased glutamatergic neurotransmission in het neurons did not result from a higher number of synaptic contacts, as indicated by the comparable density of excitatory or inhibitory synapses formed along dendrites (SV2 puncta/20 μm: wt $= 8.20 \pm 0.66$; het $= 7.96 \pm 0.82$; % of SV2; vGAT/vGlut puncta: wt $= 0.68 \pm 0.14$, het $= 0.70 \pm 0.10$; Fig 2B–D). Moreover, enhanced EPSC amplitudes were not owing to changes of the readily releasable pool of SVs, as revealed by hypertonic sucrose applications, inducing Ca^{2+}-independent release [20] (charge transfer, wt $= 1.59 \pm 0.23$ nC; het $= 1.71 \pm 0.23$ nC, Fig 2E). Finally, the charge transfer at glutamatergic synapses induced by 40 μM calcimycin, which causes calcium-dependent exocytosis bypassing activation of VGCCs [21], was lower, although not significantly, in het neurons with respect to wt (wt $= 0.29 \pm 0.38$ nC, het $= 0.22 \pm 0.57$ nC, Fig 2F), suggesting a requirement of presynaptic calcium channels in the SNAP-25-dependent effects.

The observation that reductions of SNAP-25 levels do not significantly affect neurotransmission in inhibitory neurons (see also Sharma et al [18]) is in line with the finding that het excitatory, but not inhibitory, neurons show enhanced voltage-gated calcium

currents [8]. The small reduction in eIPSC amplitude recorded in het neurons could be ascribed to the SNARE properties of SNAP-25. Indeed SNAP-25, although being expressed at very low levels in most GABAergic terminals *in situ* [22–25], appears to be part of the GABAergic SNARE complex [26,27].

Short-term plasticity at SNAP25$^{+/-}$ synapses

A simple form of short-term synaptic plasticity associated to presynaptic release properties is the paired-pulse ratio (PPR) of two consecutive synaptic responses. Paired-pulse facilitation (PPF) occurs at low-probability synapses, requiring accumulation of intra-terminal Ca^{2+} to reliably induce SV fusion. Conversely, paired-pulse depression (PPD) results from a prompt depletion of the readily releasable pool of transmitter at high-probability synapses. Both PPF and PPD rely on Ca^{2+}-dependent mechanisms triggering fusion of docked SVs [5] and indeed neurons might change use-dependent plasticity depending on extracellular calcium concentration, presynaptic calcium accumulations and expression of calcium-binding proteins [28–30].

At 13–14 DIV, when excitatory synapses in wt cultures were stimulated by two consecutive stimuli delivered with an inter-spike interval of 50 ms, PPF prevailed. Conversely, in neurons obtained from het mice, identical protocols induced PPD of EPSCs (PPR: 1.14 ± 0.04 versus 0.68 ± 0.03, wt versus het; Fig 3A,C). Notably, a similar reduction in PPR was obtained in wt glutamatergic neurons following elevation of extracellular calcium
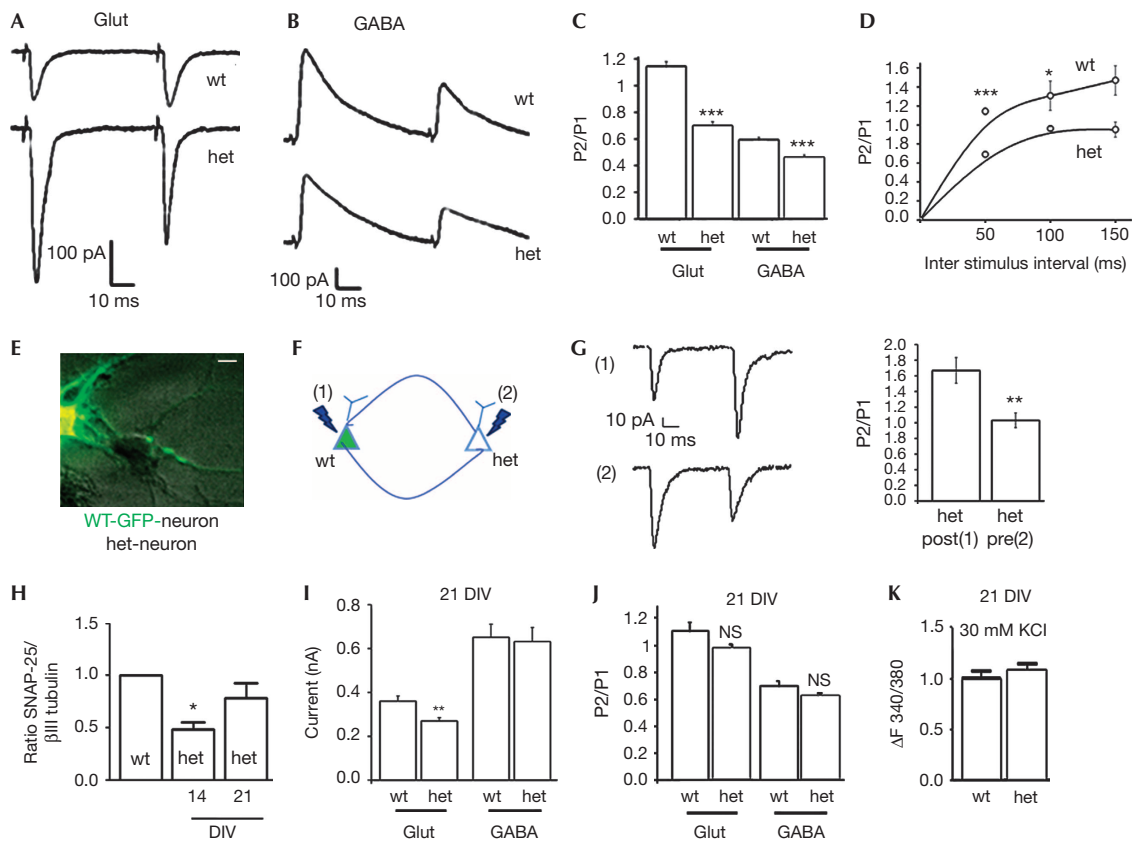
Fig 3 | Shift from paired-pulse facilitation to paired-pulse depression at 14 DIV hippocampal het synapses. (A–B) Traces of short-term plasticity experiments. **(C)** PPR at glutamatergic synapses: wt ($n = 10$) versus het ($n = 10$), t-test, $P < 0.001$, $N = 4$; GABAergic synapses: wt ($n = 13$) versus het ($n = 8$), t-test, $P < 0.001$, $N = 4$. **(D)** PPR plotted against different interpulse intervals. PPR ISI 100: t-test, $P = 0.048$; PPR ISI 150: t-test $P = 0.619$. **(E)** Merged bright field and fluorescence image of a mixed culture (wt-GFP with het neurons). Calibration bar $= 10 \, \mu m$. **(F)** Short-term plasticity in pairs where either the presynaptic [2] or the postsynaptic [1] neuron was het for SNAP-25. **(G)** PPR: (pre)-wt-GFP $= 1.44 \pm 0.21$, ($n = 5$); (pre)-het $= 0.85 \pm 0.2$ ($n = 5$) t-test, $P = 0.001$. **(H)** Quantive western blotting for SNAP-25 expression: wt versus het 14 DIV, t-test, $P = 0.042$. **(I)** eEPSC: wt ($n = 4$) versus het ($n = 9$), t-test, $P = 0.01$, $N = 3$. **(J)** PPR: glut: wt ($n = 4$) versus het ($n = 9$), t-test, $P = 0.058$; GABA: wt ($n = 4$), het ($n = 5$), t-test, $P = 0.06$, $N = 2$. **(K)** Calcium responses: wt ($n = 62$) versus het ($n = 55$), t-test, $P = 0.83$, $N = 3$. Error bars indicate s.e.m. DIV, days in vitro; GABA, γ-aminobutyric acid; GFP, green fluorescent protein; NS, not significant; PPR, paired-pulse ratio; SNAP-25, synaptosomal-associated protein of 25 kDa; wt, wild type. *$P < 0.05$; **$P < 0.01$; ***$P < 0.005$.

concentration to 4 mM (PPR: wt, 4 mM $Ca^{2+} = 0.82 \pm 0.021$; $N = 3$ independent experiments; one-way analysis of variance Kruskal–Wallis one-way analysis of variance on Ranks, $P < 0.01$). In contrast, only a slight, although significant, reduction in PPR occurred at het inhibitory synapses, which were characterized, as their wt counterpart, by prevalence of PPD (wt $= 0.54 \pm 0.025$, het $= 0.46 \pm 0.017$, Fig 3B,C). Plotting PPRs as a function of inter-stimulus interval showed that the inter-spike interval of 50 ms is the most effective in inducing PPD (PPR ISI 100: wt $= 1.30 \pm 0.16$, het $= 0.96 \pm 0.02$; PPR ISI 150: wt $= 1.46 \pm 0.25$, het $= 0.95 \pm 0.08$, $N = 2$ independent experiments; Fig 3D).

In acute hippocampal slices from adult wt or het mice, 10 EPSCs at 30 Hz evoked in CA1 pyramidal neurons by Schaffer-collateral stimulation revealed the absence of a shift from PPF to PPD. However, at 30 Hz EPSCs facilitated significantly less in het neurons (area of normalized EPSC amplitudes versus stimulus number: 14.6 ± 0.7 and 12.6 ± 0.6 wt and SNAP-25$^{+/-}$,

respectively; supplementary Fig 1 online), going in the same direction of cultured hippocampal neurons.

As a further confirmation that presynaptic reduction of SNAP-25 is responsible for the shift from PPF to PPD, paired recordings carried out from mixed cultures of het and wt green fluorescent protein (GFP) neurons (Fig 3E) revealed that the direction of PPR depended on the genotype of presynaptic neurons (Fig 3E-G). Indeed, wt (GFP+) presynaptic neurons invariably produced facilitating EPSCs, whereas presynaptic het neurons induced depressing glutamatergic responses (Fig 3F(1),(2), respectively; (pre)-wt-GFP-positive $= 1.44 \pm 0.2$; (pre)-het $= 0.85 \pm 0.2$; Fig 3G).

SNAP-25 expression increases in wt [31] and in SNAP-25 het cultures during maturation in vitro (Fig 3H). Notably, at 21 DIV, when SNAP-25 expression was significantly increased, differences in evoked responses (eEPSC and eIPSC) and in short-term plasticity disappeared (eEPSC (nA): wt $= 0.360 \pm 0.023$,
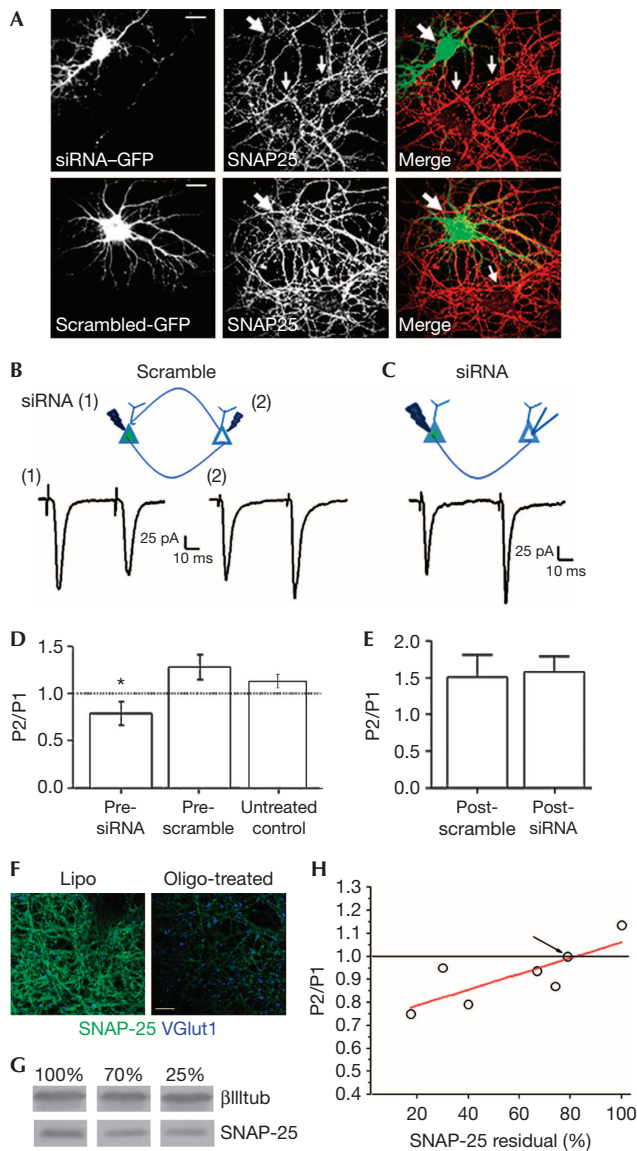
Fig 4 | Paired-pulse depression after acute downregulation of SNAP-25 expression in the presynaptic neuron. (A) SNAP-25 labelling of rat neurons co-transfected with either SNAP-25 siRNA plus GFP or scramble siRNA plus GFP. Large arrows point to neurons transfected with either siRNA (top panels) or scramble (bottom panels) constructs. Small arrows point to non-transfected neurons. Calibration bar = 20 μm. (B–C) top: cartoons of recording configurations. (B) (1) stimulation of presynaptic siRNA-treated neuron; (2) stimulation of presynaptic scramble neuron. Bottom: traces of experiments described above; (C) bottom: traces of recordings experiments in scramble siRNA-treated postsynaptic neuron. (D) PPR in scramble siRNA presynaptic (n = 6) versus SNAP-25 siRNA presynaptic (n = 7), t-test, P = 0.018. (E) PPR in SNAP-25 siRNA postsynaptic (n = 3) versus scramble siRNA postsynaptic (n = 5), t-test, P = 0.87, N = 4. (F) Examples of 14 DIV rat hippocampal cultures immunostained for SNAP-25 (green) and vGlut1 (blue) on reduction of SNAP-25 expression through stealth oligonucleotides. Calibration bar = 10 μm. (G) Western blotting showing varied reduction of SNAP-25 levels following stealth oligonucleotide treatment. (H) Plot of PPR versus residual levels of SNAP-25 in rat hippocampal cultures treated with stealth oligonucleotides. The value of PPR relative to SNAP-25 levels recorded in 21 DIV het neurons is pointed by the arrow. Error bars indicate s.e.m. DIV, days in vitro; GFP, green fluorescent protein; PPR, paired-pulse ratio; siRNA, small interfering RNA; SNAP-25, synaptosomal-associated protein of 25 kDa. *P < 0.05.

het = 0.266 ± 0.0157; PPR in EPSCs: wt = 1.10 ± 0.06, het = 0.97 ± 0.03; PPR of IPSCs: wt = 0.70 ± 0.02; het = 0.62 ± 0.01, Fig 3I–J). Accordingly, depolarization-induced Ca^{2+} responses in het neurons were comparable to those of wt neurons (ΔF340/380: wt = 1 ± 0.041, het = 1.012 ± 0.042, Fig 3K, compare with Fig 2A), indicating that neurotransmission and short-term plasticity defects can be fully recovered in parallel with increases in protein expression. The milder phenotype observed in het hippocampal slices, as compared with cultured neurons, might be owing therefore to upregulation of protein expression, which occurs also in vivo during postnatal development [32].

Notably, the recovery of the presynaptic altered phenotype in het neurons at 21 DIV is associated with the development of postsynaptic defects as indicated by the significantly lower amplitude of eEPSCs at 21 DIV (Fig 3I), which is accompanied by reduced PSD-95 density and altered spine maturation (Fossati et al, unpublished work). Two processes might therefore take place in neurons developing in the presence of reduced SNAP-25

levels, the first occurring at the presynaptic level at early developmental stages, when the protein is substantially reduced, and a second occurring at later stages of maturation and mainly impacting the postsynapse. Notably, het mice, at the age of 7 weeks, show motor hyperactivity, a phenotype that is rescued in the adult animal [32], while adult SNAP-25 heterozygous mice seem defective in different forms of associative learning [32].

Downregulation of SNAP-25 changes PPR

Recovery of normal excitatory neurotransmission and short-term plasticity on SNAP-25 developmental increase prompted us to provide a direct demonstration that the switch from PPF to PPD is a direct consequence of SNAP-25 reduction at the presynaptic level. Acute protein downregulation by double-stranded small interfering RNA oligonucleotides (siRNAs) was carried out and dual whole-cell recordings were performed from connected neurons. siRNA, but not scramble oligonucleotide, application reduced SNAP-25 levels, leaving ~40% residual (Fig 4A and Grumelli et al [33]). Notably, acute reduction of SNAP-25 by siRNAs in the presynaptic glutamatergic neuron reduced PPR (scramble siRNA, presynaptic = 1.28 ± 0.13, Fig 4B (2), SNAP-25 siRNA, presynaptic = 0.79 ± 0.12, Fig 4B (1), untreated control = 1.11 ± 0.069, Fig 4B,D). Importantly, no reductions were present when scramble or SNAP-25 siRNA was transfected in the postsynaptic neuron (scramble siRNA, postsynaptic = 1.508 ± 0.29, SNAP-25 siRNA, postsynaptic = 1.57 ± 0.21, Fig 4C,E). Therefore, even acute reductions of SNAP-25 in wt presynaptic neurons switch PPF to PPD at glutamatergic synapses.

To directly assess whether varied levels of SNAP-25 expression correlate with different PPR ratio, we used three different siRNA oligonucleotides to achieve controlled SNAP-25 downregulation (Fig 4F,G). Different concentrations of oligonucleotides were

transfected in rat hippocampal neurons at DIV 10 and the extent of protein reduction was assessed by quantitative western blotting, after electrophysiological recording at DIV 14. A correlation between PPR values and levels of residual SNAP-25 was present, with 20–25% reductions of SNAP-25 being sufficient to shift PPF to PPD (Fig 4H).

CONCLUSIONS

Activity-dependent presynaptic processes producing various forms of short-term plasticity are believed to control several essential neural functions, such as information processing, working memory and decision making. Presynaptic abnormalities were reported at excitatory hippocampal synapses in a mouse model of Fragile X syndrome, leading to defects in short-term plasticity and information processing [34,35]. These changes were associated with exaggerated calcium influx in presynaptic neurons during high-frequency stimulation [34]. Reduced SNAP-25 levels, leading to abnormal presynaptic short-term plasticity at glutamatergic terminals, at least during early developmental stages, might therefore contribute to cognitive impairments in intellectual disability syndromes. Interestingly, analysis of allele frequencies of two genetic variants in SNAP-25 indicated that SNAP-25 might be directly involved in intellectual disability syndromes [36].

METHODS

Animals. All the experimental procedures followed the guidelines established by the Italian Council on Animal Care and were approved by the Italian Government decree No. 27/2010 (supplementary Information online).

Cell cultures. Hippocampal neurons were established from E18 fetal het or wt littermates C57BL/6 mice or from E18 fetal rats as described by Bartlett [37] with slight modifications (supplementary Information online). Primary hippocampal GFP-positive neuronal cultures were prepared from the hippocampi of C57BL/6 GFP transgenic mice at embryonic day 18.

Acute downregulation of SNAP-25 expression. Silencing of SNAP-25 was achieved via transfection of a pSUPER construct [8,25]. A nonspecific siRNA duplex of the same nucleotides but in an irregular sequence (scrambled iSNAP-25 siRNA) was prepared (supplementary Information online). In a different set of experiments, three different double-stranded siRNA oligonucleotides were used to achieve controlled SNAP-25 downregulation.

Immunocytochemical staining. Immunofluorescence staining was carried out using the following antibodies: rabbit anti-SV2A, rabbit anti-vGAT guinea pig anti-vGLUT1, mouse anti-SNAP-25, mouse anti-β_{III}tubulin. Secondary antibodies were conjugated with Alexa-488, Alexa-555 or Alexa-633 fluorophores.

Quantitative western blotting. Homogenates from hippocampal cultures were separated by electrophoresis, blotted on nitro-cellulose membrane and analysed by western blot by using monoclonal antibodies against SNAP-25 and beta-III-tubulin. Membranes were washed and incubated for 1 h at room temperature with the secondary antibody IRDye 680-conjugated goat anti-mouse (1:10,000). Blots were scanned using an Odyssey Infrared Imaging System (LI-COR Biosciences).

Calcium imaging. Hippocampal cultures of 13 or 21 DIV were loaded with 5 µM Fura-2 pentacetoxymethylester in KRH for 45 min at 37 °C, washed in the same solution and transferred to the recording chamber of an inverted microscope (Axiovert 100; Zeiss, Oberkochen, Germany) equipped with a calcium imaging unit. After a period for baseline acquisition, neurons were stimulated with different drugs (supplementary Information online).

Cell culture electrophysiology. Whole-cell patch-clamp recordings of EPSCs and IPSCs were obtained from 13–14-day-old neurons using a Multiclamp 700A amplifier (Molecular Devices) and pClamp-10 software (Axon Instruments, Foster City, CA). Currents were sampled at 5 kHz and filtered at 2–5 kHz. mEPSCs or mIPSCs were recorded in presence of tetrodotoxin (l µM). Evoked currents were recorded in isolated pairs of neurons in low-density cultures. Neurons were held at − 70 mV, and eEPSC or eIPSC evoked by a 100-mV depolarization pulse in the presynaptic cell lasting 1 ms. Readily releasable pool size was evaluated exposing neurons for 4 s to hypertonic solution of sucrose. The ionophore calcimycine was applied for 90 s.

Supplementary information is available at EMBO *reports* online (http://www.emboreports.org).

REFERENCES
1. Jahn RSR (2006) SNAREs–engines for membrane fusion. *Nat Rev Mol Cell Biol* **7:** 631–643
2. Sudhof TC, Rothman JE (2009) Membrane fusion: grappling with SNARE and SM proteins. *Science* **323:** 474–477
3. Washbourne P et al (2002) Genetic ablation of the t-SNARE SNAP-25 distinguishes mechanisms of neuroexocytosis. *Nat Neurosci* **5:** 19–26
4. Atlas DWO, Trus M (2001) The voltage-gated Ca2 + channel is the Ca2 + sensor of fast neurotransmitter release. *Cell Mol Neurobiol* **21:** 717–731
5. Catterall WA, Few AP (2008) Calcium channel regulation and presynaptic plasticity. *Neuron* **59:** 882–901
6. Zamponi GW (2003) The L-type calcium channel C-terminus: sparking interest beyond its role in calcium-dependent inactivation. *J Physiol* **552:** 333
7. Pozzi DCS, Bozzi Y, Chikhladze M, Grumelli C, Proux-Gillardeaux V, Takahashi M, Franceschetti S, Verderio C, Matteoli M (2008) Activity-dependent phosphorylation of Ser187 is required for SNAP-25-negative modulation of neuronal voltage-gated calcium channels. *Proc Natl Acad Sci USA* **105:** 323–328
8. Condliffe SB, Corradini I, Pozzi D, Verderio C, Matteoli M (2010) Endogenous SNAP-25 regulates native voltage-gated calcium channels in glutamatergic neurons. *J Biol Chem* **285:** 24968–24976
9. Condliffe SBMM (2011) Inactivation kinetics of voltage-gated calcium channels in glutamatergic neurons are influenced by SNAP-25. *Channels* **5:** 304–307

10. Lewis CM *et al* (2003) Genome scan meta-analysis of schizophrenia and bipolar disorder, part II: schizophrenia. *Am J Hum Genet* **73:** 34–48
11. Corradini I, Verderio C, Sala M, Wilson MC, Matteoli M (2009) SNAP-25 in neuropsychiatric disorders. *Ann N Y Acad Sci* **1152:** 93–99
12. Young CE, Arima K, Xie J, Hu L, Beach TG, Falkai P, Honer WG (1998) SNAP-25 deficit and hippocampal connectivity in schizophrenia. *Cereb Cortex* **8:** 261–268
13. Thompson PM, Kelley M, Yao J, Tsai G, van Kammen DP (2003) Elevated cerebrospinal fluid SNAP-25 in schizophrenia. *Biol Psychiatry* **53:** 1132–1137
14. Thompson PM, Sower AC, Perrone-Bizzozero NI (1998) Altered levels of the synaptosomal associated protein SNAP-25 in schizophrenia. *Biol Psychiatry* **43:** 239–243
15. Barr CLFY, Wigg K, Bloom S, Roberts W, Malone M, Schachar R, Tannock R, Kennedy JL (2000) Identification of DNA variants in the SNAP-25 gene and linkage study of these polymorphisms and attention-deficit hyperactivity disorder. *Mol Psychiatry* **5:** 405–409
16. Hess EJ, Rogan PK, Domoto M, Tinker DE, Ladda RL, Ramer JC (1995) Absence of linkage of apparently single gene mediated ADHD with the human syntenic region of the mouse mutant Coloboma. *Am J Med Genet* **60:** 573–579
17. Faraone SV, Perlis RH, Doyle AE, Smoller JW, Goralnick JJ, Holmgren MA, Sklar P (2005) Molecular genetics of attention-deficit/hyperactivity disorder. *Biol Psychiatry* **57:** 1313–1323
18. Sharma M, Burre J, Sudhof TC (2011) CSPalpha promotes SNARE-complex assembly by chaperoning SNAP-25 during synaptic activity. *Nat Cell Biol* **13:** 30–39
19. Bronk P, Deak F, Wilson MC, Liu X, Sudhof TC, Kavalali ET (2007) Differential effects of SNAP-25 deletion on Ca2 + -dependent and Ca2 + -independent neurotransmission. *J Neurophysiol* **98:** 794–806
20. Rosenmund CSC (1996) Definition of the readily releasable pool of vesicles at hippocampal synapses. *Neuron* **16:** 1197–1207
21. Tokuoka HGY (2006) Myosin light chain kinase is not a regulator of synaptic vesicle trafficking during repetitive exocytosis in cultured hippocampal neurons.. *J Neurosci* **26:** 11606–11614
22. Benagiano VLL, Flace P, Girolamo F, Rizzi A, Bosco L, Cagiano R, Nico B, Ribatti D, Ambrosi G (2011) VAMP-2, SNAP-25A/B and syntaxin-1 in glutamatergic and GABAergic synapses of the rat cerebellar cortex. *BMC Neurosci* **12:** 118
23. Bragina L, Melone M, Fattorini G, Conti F (2007) Clozapine upregulates the expression of the vesicular GABA transporter (VGAT) in rat frontal cortex. *Mol Psychiatry* **12:** 612–613
24. Mandolesi G, Vanni V, Cesa R, Grasselli G, Puglisi F, Cesare P, Strata P (2009) Distribution of the SNAP25 and SNAP23

25. Verderio C *et al* (2004) SNAP-25 modulation of calcium dynamics underlies differences in GABAergic and glutamatergic responsiveness to depolarization. *Neuron* **41:** 599–610
26. Tafoya LCMM, Miyashita T, Guzowski JF, Valenzuela CF, Wilson MC (2006) Expression and function of SNAP-25 as a universal SNARE component in GABAergic neurons. *J Neurosci* **26:** 7826–7838
27. Boyken JGM, Riedel D, Urlaub H, Jahn R, Chua JJ (2013) Molecular profiling of synaptic vesicle docking sites reveals novel proteins but few differences between glutamatergic and GABAergic synapses. *Neuron* **78:** 285–297
28. Saviane CSL, Raffaelli G, Voronin LL, Cherubini E (2002) Frequency-dependent shift from paired-pulse facilitation to paired-pulse depression at unitary CA3-CA3 synapses in the rat hippocampus. *J Physiol* **544:** 469–476
29. Rettig J, Sheng ZH, Kim DK, Hodson CD, Snutch TP, Catterall WA (1996) Isoform-specific interaction of the alpha1A subunits of brain Ca2 + channels with the presynaptic proteins syntaxin and SNAP-25. *Proc Natl Acad Sci USA* **93:** 7363–7368
30. Sippy TC-MA, Jeromin A, Schweizer FE (2003) Acute changes in short-term plasticity at synapses with elevated levels of neuronal calcium sensor-1. *Nat Neurosci* **6:** 1031–1038
31. Bark CBF, Kaushal A, Mathews JR, Partridge LD, Wilson MC (2004) Developmentally regulated switch in alternatively spliced SNAP-25 isoforms alters facilitation of synaptic transmission. *J Neurosci* **24:** 8796–8805
32. Corradini IDA *et al* (2012) Epileptiform Activity and cognitive deficits in SNAP-25 +/− mice are normalized by antiepileptic drugs. *Cereb Cortex* **12:** [Epub ahead of print] doi:10.1093/cercor/bhs316
33. Grumelli C, Corradini I, Matteoli M, Verderio C (2010) Intrinsic calcium dynamics control botulinum toxin A susceptibility in distinct neuronal populations. *Cell Calcium* **47:** 419–424
34. Deng PY, Sojka D, Klyachko VA (2011) Abnormal presynaptic short-term plasticity and information processing in a mouse model of fragile X syndrome. *J Neurosci* **31:** 10971–10982
35. El Idrissi A, Neuwirth LS, L'Amoreaux W (2010) Taurine regulation of short term synaptic plasticity in fragile X mice. *J Biomed Sci* **17**(Suppl 1): S15
36. Rizzi TS *et al* (2012) Supporting the generalist genes hypothesis for intellectual ability/disability: the case of SNAP25. *Genes Brain Behav* **11:** 767–771
37. Bartlett WPBG (1984) An electron microscopic study of the development of axons and dendrites by hippocampal neurons in culture. I. Cells which develop without intercellular contacts. *J Neurosci* **4:** 1944–1953

synaptosomal-associated protein isoforms in rat cerebellar cortex. *Neuroscience* **164:** 1084–1096

THE EMBO JOURNAL

Eps8 controls dendritic spine density and synaptic plasticity through its actin-capping activity

Elisabetta Menna[1,2,8,*],
Stefania Zambetti[1,3,8], Raffaella Morini[2,3],
Andrea Donzelli[3], Andrea Disanza[4],
Daniela Calvigioni[1,3], Daniela Braida[3],
Chiara Nicolini[5], Marta Orlando[3],
Giuliana Fossati[2,3],
Maria Cristina Regondi[6], Linda Pattini[7],
Carolina Frassoni[6], Maura Francolini[1,3],
Giorgio Scita[4], Mariaelvina Sala[1,3],
Margaret Fahnestock[5] and
Michela Matteoli[2,3,*]

[1]CNR Institute of Neuroscience, Milano, Italy, [2]Humanitas Clinical and Research Center, Milan, Italy, [3]Department of Medical Biotechnology and Translational Medicine, University of Milano, Milan, Italy, [4]IFOM Foundation—FIRC (Italian Foundation for Cancer Research) Institute of Molecular Oncology, Milan, Italy, [5]Department of Psychiatry and Behavioural Neurosciences, McMaster University, Hamilton, Ontario, Canada, [6]Fondazione I.R.C.C.S. Istituto Neurologico Carlo Besta, Clinical Epileptology and Experimental Neurophysiology Unit, Milan, Italy and [7]Dipartimento di Elettronica, Informazione e Bioingegneria—Politecnico di Milano, Milan, Italy

Actin-based remodelling underlies spine structural changes occurring during synaptic plasticity, the process that constantly reshapes the circuitry of the adult brain in response to external stimuli, leading to learning and memory formation. A positive correlation exists between spine shape and synaptic strength and, consistently, abnormalities in spine number and morphology have been described in a number of neurological disorders. In the present study, we demonstrate that the actin-regulating protein, Eps8, is recruited to the spine head during chemically induced long-term potentiation in culture and that inhibition of its actin-capping activity impairs spine enlargement and plasticity. Accordingly, mice lacking Eps8 display immature spines, which are unable to undergo potentiation, and are impaired in cognitive functions. Additionally, we found that reduction in the levels of Eps8 occurs in brains of patients affected by autism compared to controls. Our data reveal the key role of Eps8 actin-capping activity in spine morphogenesis and plasticity and indicate that reductions in actin-capping proteins may characterize forms of intellectual disabilities associated with spine defects.

*Corresponding authors. M Matteoli, Department of Medical Biotechnology and Translational Medicine, University of Milan, Via Vanvitelli 32, 20129, Milan, Italy or Humanitas Clinical and Research Center, Via Manzoni 56, Rozzano, Milan, Italy. Tel.: +39 02 82245202; Fax: +39 02 82245101; E-mail: michela.matteoli@unimi.it or E Menna, CNR Institute of Neuroscience and Department of Medical Biotechnology and Translational Medicine, University of Milano, Via Vanvitelli 32, 20129, Milan, Italy. Tel.: +39 02 50317009; Fax: +39 02 50317132; E-mail: e.menna@in.cnr.it
[8]These authors contributed equally to this work.

Introduction

The establishment of synaptic contacts between appropriate neurons is the basis for the formation of neural networks. Filopodia are thought to play an active role in synaptogenesis, guiding the co-ordinated growth of pre- and postsynaptic partners and functioning as initial bridges between neurons (Dailey and Smith, 1996; Ziv and Smith, 1996; Fiala et al, 1998; Dunaevsky et al, 1999; Okabe et al, 2001; Evers et al, 2006). Subsequently, through the actions of synapse-inducing factors and neuronal activity, filopodia switch to more stable structures, the dendritic spines, which gradually gain a typical mushroom-like structure with a prominent head and a thin neck, and ultimately become the dominant forms in adults (Harris et al, 1992; Fiala et al, 1998; Jontes and Smith, 2000; Bhatt et al, 2009; Hotulainen et al, 2009; Hotulainen and Hoogenraad, 2010). This process is associated with the assembly of pre- and postsynaptic components (Craig et al, 2006; Arikkath and Reichardt, 2008; Yoshihara et al, 2009; Hotulainen and Hoogenraad, 2010). There is a positive correlation between spine shape and dimensions and synaptic strength (Yuste and Bonhoeffer, 2001; Kasai et al, 2003); also, abnormalities in spine number and morphology have been observed in a number of neurological disorders (van Spronsen and Hoogenraad, 2010), thus linking spine morphogenesis with plasticity processes eventually leading to memory formation. Consistently, spine abnormalities and excessive synaptic growth have been reported in subjects with autism (Hutsler and Zhang, 2010; Toro et al, 2010; Penzes et al, 2011).

The process of spinogenesis is controlled by actin, which, besides providing the structural basis for spine formation and elimination, also regulates spine shape (Matus, 2000; Cingolani and Goda, 2008). During development and plasticity, the stabilization of filopodia to form new synaptic contacts is based on a rapid and persistent reorganization of the spine actin cytoskeleton (Luscher et al, 2000; Jourdain et al, 2003; Nikonenko et al, 2003; Honkura et al, 2008). This mainly consists of a reduced depolymerization rate from the pointed end of the filament at the core of the spine, with polymerization continuing at the barbed end in the spine periphery (Fukazawa et al, 2003; Okamoto et al, 2004; Ramachandran and Frey, 2009).

It has been proposed recently that spine formation and enlargement of spine heads may rely on actin remodelling processes similar to those occurring in lamellipodia (Hotulainen and Hoogenraad, 2010). The latter process

mainly involves the activity of the branched actin filament nucleator Arp2/3 complex, working in concert with actin-capping proteins. These latter proteins, by binding to the barbed ends of densely packed, plasma membrane-localized actin filaments, control not only their lifetime but also the architecture of the resulting meshwork (Akin and Mullins, 2008). Indeed, when capping activity is high, newly nucleated branched filaments become rapidly capped; this also causes a local increase in the concentration of available actin monomers, which further feeds Arp2/3 nucleation/branching activity, ultimately promoting the generation of a dense and highly branched dendritic array of short actin filaments. Conversely, when capping activity is low, local monomer availability is reduced, as G-actin becomes incorporated into long and uncapped actin filaments (Mogilner and Rubinstein, 2005; Akin and Mullins, 2008; Korobova and Svitkina, 2008).

In support of this possibility, a branched actin filament network is detectable in the distal regions of the spine head (Korobova and Svitkina, 2010); furthermore, the Arp2/3 complex is concentrated within spines (Racz and Weinberg, 2008), where it appears to be an important molecular signal for regulating spine size and synaptic plasticity (Wegner *et al*, 2008; Nakamura *et al*, 2011). Platinum replica electron microscopy analysis has revealed that spine heads also contain large amounts of capping proteins (Korobova and Svitkina, 2010). Also, the actin-capping protein CP has been found to be essential for spine development (Fan *et al*, 2011). However, since CP forms a complex with other proteins, such as twinfilin (Falck *et al*, 2004), and also mediates membrane attachment of actin (Amatruda *et al*, 1992; Schafer *et al*, 1992), the direct demonstration that the actin-capping activity is, in fact, a crucial function required for spine formation is still missing.

Eps8 is a multimodular protein involved in actin remodelling through several activities, including regulation of Rac, a pivotal GTPase involved in the control of actin dynamics and direct interaction with actin. Through the latter property, in particular, Eps8 exerts both actin barbed end capping and actin bundling activities (Disanza *et al*, 2004, 2006). Eps8 is reported to be expressed at elevated levels in a range of human malignancies (Welsch *et al*, 2010; Abdel-Rahman *et al*, 2012), while loss of Eps8 causes intestinal defects and improved metabolic status in mice (Tocchetti *et al*, 2010). Notably, Eps8 plays a unique and nonredundant role in the polarized migration of dendritic cells. Consequently, Eps8 KO dendritic cells are delayed in reaching the draining lymph node after inflammatory challenge and Eps8 KO mice are unable to mount a contact hypersensitivity response (Frittoli *et al*, 2011). In brain, Eps8 has been localized postsynaptically in the dendritic articulations of cerebellar granule neurons (Offenhäuser *et al*, 2006; Sekerková *et al*, 2007) and in axons of cultured hippocampal neurons, where it controls filopodia formation (Menna *et al*, 2009). Here we show that the actin-capping protein, Eps8, is recruited to the spine head during chemically induced LTP and that inhibition of its capping activity impairs spine enlargement and plasticity. Accordingly, mice lacking Eps8 display immature spines, are impaired in cognitive function and show an abnormal EEG profile characterized by spike activity. Finally, we show that reduced levels of Eps8 are present in the brain of patients affected by autism.

Results

Eps8 knockout (Eps8 KO) mice are impaired in learning and memory

Eps8 KO mice were subjected to a series of behavioural tests to evaluate learning and memory.

Radial maze performance, in terms of mean total number of errors, days to reach the criterion and percentage of animals that reached the criterion over 30 days, is shown in Figure 1A.

Eps8 KO mice exhibited a worse performance, in comparison with the wild-type (wt) group, as indicated by the higher number of errors and by the calculated area under the curve (AUC), which revealed a significant increase of this parameter. Consistently, Eps8 KO mice needed significantly more days than controls to reach the criterion (Figure 1A, right).

In the T-maze task, wt mice performed statistically better during acquisition compared to Eps8 KO mice (Figure 1B, left). Conversely, no significant difference was detected in the reversal phase (Figure 1B, right).

When tested for novel object recognition (Figure 1C), no significant difference was detected in the amount of time that the mice spent exploring the two objects during the familiarization (T1) phase, indicating that both genotypes had the same motivation to explore the object. However, during T2 (novel object recognition phase), Eps8 KO mice spent significantly less time exploring the novel object compared to the familiar one, as shown by a significant decrease in the discrimination index (Figure 1C). This was not due to altered sensorial parameters, as all mice appeared healthy, displaying normal motor activity and sensory abilities (Supplementary Table 1). Long-term memory was altered in Eps8 KO mice, as shown by the significant reduction of the mean value of step through latency compared to wt mice in the passive avoidance task (Figure 1D).

Furthermore, when tested for sociability, differently from wt mice, which spent longer time to explore the compartment with the stranger mouse than the empty cage, Eps8 KO mice were significantly less social and spent the same amount of time in the two compartments (Figure 1E).

Finally, 2-h cortical EEG recordings revealed that Eps8 KO mice displayed frequent spikes of high amplitude (Figure 1F), which, however, did not lead to spontaneous seizures, either spontaneously or even after mice handling. The mean number and the mean amplitude of spikes were significantly higher than in wt mice (Figure 1F).

These data indicate that Eps8 KO mice show defects in learning and memory, social behaviour and EEG.

No alterations of the gross anatomy were observed in the brain of Eps8 KO mice. Indeed, the cortex, hippocampus and cerebellum displayed normal architecture and all layers were preserved (Supplementary Figure 1A–L). Therefore, excluding developmental defects (e.g., cortical displacement of neurons, lamination defects), no compensatory elevation of Eps8L family members has ever been detected in different tissues of Eps8-null mice (Frittoli *et al*, 2011; Zampini *et al*, 2011) and, accordingly, was not detected in the hippocampus (Supplementary Figure 1M).

Excessive synaptic growth and abnormal spine morphology in the hippocampus of Eps8 KO mice

We have previously shown that Eps8 controls filopodia formation during neuronal development and that the lack
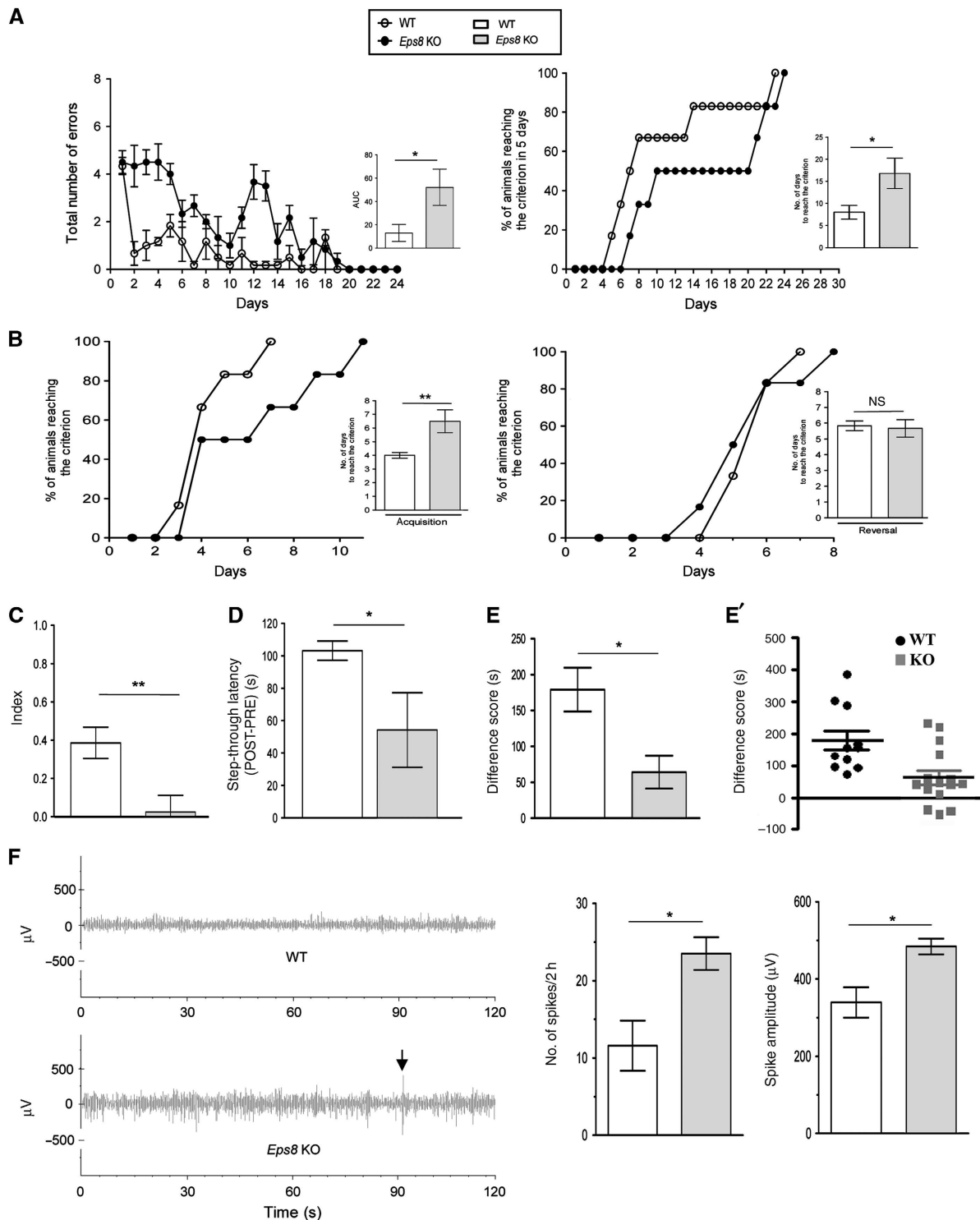
Figure 1 Eps8 KO mice are impaired in learning and sociability. (**A** and **B**) Eps8 KO mice are impaired in spatial learning. (**A**) Eight-arm radial maze. (Left) Eps8 KO mice show a delayed learning in terms of increased number of errors statistically evaluated as the area under the curve (AUC); (Right) A lower number of Eps8 KO mice reaches the criterion within 5 days evaluated as number of days taken to reach the criterion. (**B**) T-maze task. During the acquisition phase (left), Eps8 KO mice exhibit a delayed learning in terms of increased number of days to reach the criterion but normal learning during reversal phase (right). The number of days to reach the criterion during both phases is illustrated in the flanking graph. (**C**) Novel object recognition test. Eps8 KO mice show no net preference between novel and familiar objects, as shown by the lower discrimination index. (**D**) Passive avoidance task. A reduced step-through latency is detected in Eps8 KO mice compared to wt animals. (**E**, **E**′) Sociability test. Eps8 KO mice spend significantly less time exploring a conspecific than an empty cage in a social choice paradigm, as shown by the significantly lower difference score. (**F**) EEG. Eps8 KO mice display abnormal EEG profile. (Left) EEG recordings of two representative mice (one for each genotype) for 120 s. KO mouse shows higher spike activity. The mean number of spikes recorded for 2 h in Eps8 KO mice is higher compared to wt (centre) and the spike amplitude was larger than wt (right). Increments above a threshold determined according to the increments distribution through an unsupervised approach (Manfredi *et al*, 2009) and whose amplitude was greater than twice the background were considered as spikes. Data are shown as mean ± s.e.m. of ten animals for each genotype and each test. Statistical assessments were performed by Student's *t*-test comparing wt and KO mice (*$P < 0.05$, **$P < 0.01$). n.s., not significant.

of Eps8 results in increased formation of protrusions from both the axon and dendrites (Menna *et al*, 2009). Since filopodia represent the precursors of pre- and postsynaptic compartments during the process of hippocampal synaptogenesis (Fiala *et al*, 1998), we investigated whether Eps8 KO adult brain is characterized by a higher number of synaptic contacts compared to wt. Figure 2A shows the CA1 hippocampal region of wt and Eps8 KO mouse brain, stained for the synaptic vesicle protein synaptobrevin/VAMP2 and the glutamatergic postsynaptic protein PSD-95. A significantly higher number of both pre- and postsynaptic puncta were detected in the hippocampi of Eps8 KO mice relative to control (Figure 2B).

Ultrastructural analysis of synaptic terminals revealed normal numbers and dimensions of synaptic vesicles (SVs) and a normal size of synaptic boutons (Supplementary Figure 1N–P), thus indicating that lack of Eps8, although affecting synapse number, does not prominently impact the structural organization of the presynaptic compartment. Conversely, analysis of dendritic spines by Golgi-Cox staining revealed that Eps8 KO mice displayed a clear alteration in the morphology of spines, which appeared thinner and were significantly longer relative to wt (Figure 2C and D). A significantly higher number of protrusions per unit length was detected on secondary branches of CA1 neuronal dendrites in the Eps8
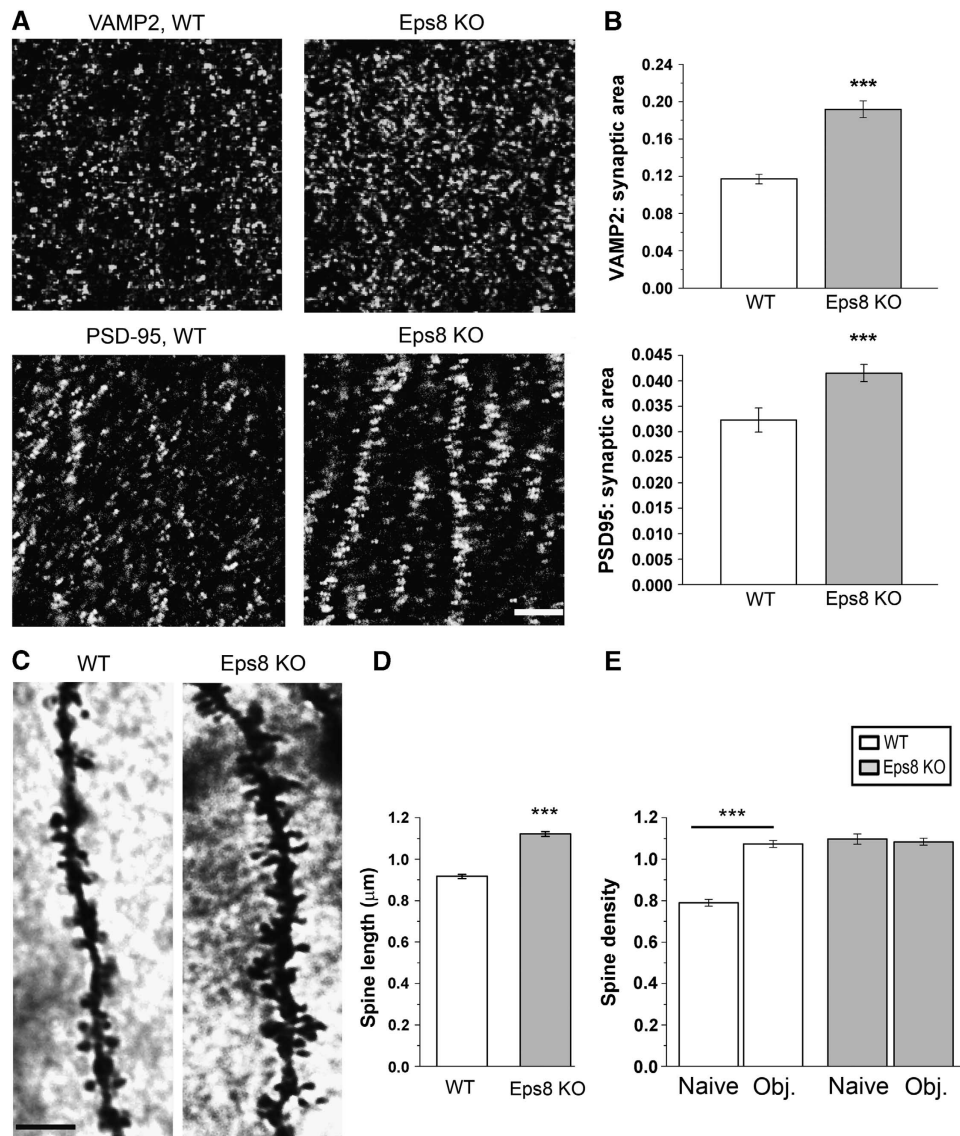

Figure 2 Excessive synaptic growth and spine abnormalities in the hippocampus of Eps8 KO mice. (**A, B**) Representative fields of the CA1 hippocampal region of a wt and Eps8 KO mouse brains, stained for the synaptic vesicle protein synaptobrevin/VAMP2 and the glutammatergic postsynaptic protein, PSD-95. Quantitation of either pre- or postsynaptic areas reveals a larger number of synaptic contacts in Eps8 KO hippocampus. Scale bar, 5 μm. (**C**) Details of CA1 apical dendrites from wt and Eps8 KO hippocampi stained with Golgi-Cox technique. Scale bars, 10 μm. (**D, E**) Quantitation of spine length and density in wt or KO animals under control conditions (naïve) or after application of the novel object recognition test (obj) (length, **D**, wt spines = 0.91 ± 0.010 μm; KO spines = 1.12 ± 0.012 μm; total number of examined spines: 551, wt and 506, Eps8 KO; number of independent experiments: 3) (density, **E**, wt naïve = 0.789 ± 0.017 spines per μm of parent dendrite; wt obj. = 1.07 ± 0.016 spines per μm; KO naïve = 1.09 ± 0.024 spines per μm; KO obj. = 1.08 ± 0.016 spines per μm total number of examined dendritic branches: 321 wt ctr, 242 wt obj, 105 KO ctr, 361 KO obj; number of independent experiments: 3). Note that Eps8 KO mice display denser and longer spines, which fail in undergoing further increase in number after the object recognition test. Mann–Whitney rank sum test $P < 0.001$. All data are expressed as mean ± s.e.m. Six animals for each condition have been analysed.

KO group compared with the wt (Figure 2E, compare the first and third columns).

Given that mutant mice are impaired in learning and memory and in consideration of the abnormal spine features, we investigated whether learning-dependent spinogenesis processes occur properly in Eps8 KO mice. We found that Eps8 KO mice lacked structural dendritic plasticity, i.e., increases in spine density, which typically develop in the hippocampus during memory formation (Restivo *et al*, 2006). Figure 2E shows that mutant mice, trained for object recognition and processed for Golgi-Cox 24 h after training, did not display any increase in spine number, which was instead clearly detectable in wt mice. These results indicated that Eps8-null mice have a defect in spine formation and learning-dependent spinogenesis in the hippocampus.

Excessive synaptic growth and abnormal spine morphology in Eps8 KO hippocampal cultures

To gain insights into the cellular and molecular mechanisms at the basis of abnormal spine morphology and plasticity defects occurring in Eps8 KO mice, we analysed synapse density and dendritic morphology in primary hippocampal cultures established from E18 wt or mutant mice. Quantification of pre- and postsynaptic puncta in 21 DIV cultures revealed that, similar to what occurred *in vivo*, Eps8 KO cultures displayed a significantly higher synapse density than wt cultures, measured as number of vGlut1 or PSD-95 positive contacts per unit length of tubulin-positive dendrites (Supplementary Figure 2A). Similarly to the *in vivo* situation (Supplementary Figure 1), ultrastructural analysis of 21 DIV old wt and Eps8 KO cultures did not reveal any gross alteration of the presynaptic compartment, including SV size and number (not shown). Transfection of cultures with a vector coding for red fluorescence protein, which fills all neuronal processes and allows a direct examination of dendritic morphology, revealed that Eps8 KO neurons, similar to Eps8 KO brain sections, are characterized by a higher density of spines, which appeared significantly longer than wt (Figure 3A). Indeed, the morphology of spines changes, as the number of thin spines is significantly increased while the number of mushroom type decreases (Figure 3A). Notably, however, most of these protrusions, although appearing immature and filopodia like, displayed PSD-95 and bassoon staining, thus indicating that they represent *bona fide* synaptic contacts (Figure 3A).

Fluorescence recovery after photobleaching (FRAP) measurements of PSD-95-GFP in wt or mutant neurons revealed a significantly higher PSD-95 mobile fraction in Eps8 KO spines with respect to wt, thus indicating that the dynamics of PSD-95 are altered in mutant neurons (Supplementary Figure 2B). Consistent with the possibility of a functional defect, miniature excitatory postsynaptic currents (mEPSCs), recorded in the presence of 1 μM TTX, displayed a significantly reduced amplitude in Eps8-null neurons with respect to wt (Supplementary Figure 2C). Despite the increase in synapse density, no changes in mEPSC frequency were detected (Supplementary Figure 2C). This could result from the reduced mEPSC amplitude, which would cause many of the events falling below detection. We cannot, however, exclude a role of Eps8 in reducing presynaptic release probability.

A branched actin filament network containing the Arp2/3 complex and capping proteins, the conventional lamellipodial markers, is a dominant feature of spine heads

(Svitkina *et al*, 2010). The possibility, therefore, has been raised that high capping and branching activity may be required for spine head enlargement during development and plasticity (Hotulainen and Hoogenraad, 2010). We, therefore, hypothesized that the ability of Eps8 to cap actin filaments in the spine head may be required for spine formation. It has been previously shown that the capping activity of Eps8 is primarily mediated by the amphipathic H1 helix, while the globular H2–H5 core is responsible for bundling (Hertzog *et al*, 2010). We then took advantage of the Eps8 capping mutant Eps8H1, in which the hydrophobic residues in the amphipathic helix, H1, critical for actin capping, were mutated while leaving intact the actin bundling activity (Hertzog *et al*, 2010). A total of 10–11 DIV hippocampal cultures were transfected with constructs expressing either the Eps8 wt protein or its actin-capping mutant, Eps8H1. Figure 3B shows that overexpression of Eps8 induced a potent increase in mature spine density, also promoting the formation of larger spines. Conversely, expression of the H1 actin-capping mutant did not result in spine enlargement, clearly indicating that the actin-capping activity is required for the process. No changes of spine length are observed (data not shown). Notably, Eps8-induced spines appeared positive for the presynaptic active zone protein Bassoon (Bsn) (Figure 3B) and displayed significantly larger PSD-95 puncta compared to neurons transfected with either RFP or the H1 mutant, as indicated by immuno-fluorescence staining and by IMARIS reconstruction (Supplementary Figure 3A and A′). These results indicate that the actin-capping activity of Eps8 is required for proper mushroom-type spine formation. However, we cannot exclude that the bundling activity of Eps8 might play a role in the filopodia protrusion from the dendritic shaft, a step that precedes the transition from filopodia to mature spines.

Lack of Eps8 precludes synaptic potentiation in hippocampal cultures

We then aimed to define whether Eps8 KO neurons in culture are able to undergo synaptic potentiation, or, like their *in vivo* counterpart, show defects in structural plasticity. To address this issue, a chemically-induced form of LTP was applied to cultures. Selective activation of synaptic NMDA receptors was achieved by briefly (3 min) elevating the concentration of the NMDA receptor co-agonist glycine in the perfusion solution to suprasaturating levels (100 μM, Lu *et al*, 2001). The potential activation of glycine receptors was avoided by including strychnine in all of the solutions. Following washout of glycine, insertion of AMPA receptors in the spine head accompanied by LTP of mEPSCs occurs (Lu *et al*, 2001). In line with previous reports, application of the protocol to wt neurons resulted in a significant increase in both density and size of the PSD-95 positive puncta and density of synaptic contacts (Figure 4A and B). Furthermore, a significant increase in the extent of colocalization between PSD-95 and vGlut1 staining was detected, in line with synaptic strengthening occurring during potentiation phenomena (Fortin *et al*, 2010). Notably, in neurons devoid of Eps8, application of the same protocol did not induce any significant increase in either the density or the size of PSD-95 positive puncta, or any increase in the colocalization extent of pre- and postsynaptic markers (Figure 4A and B). Both wt and Eps8 KO cultures displayed normal input
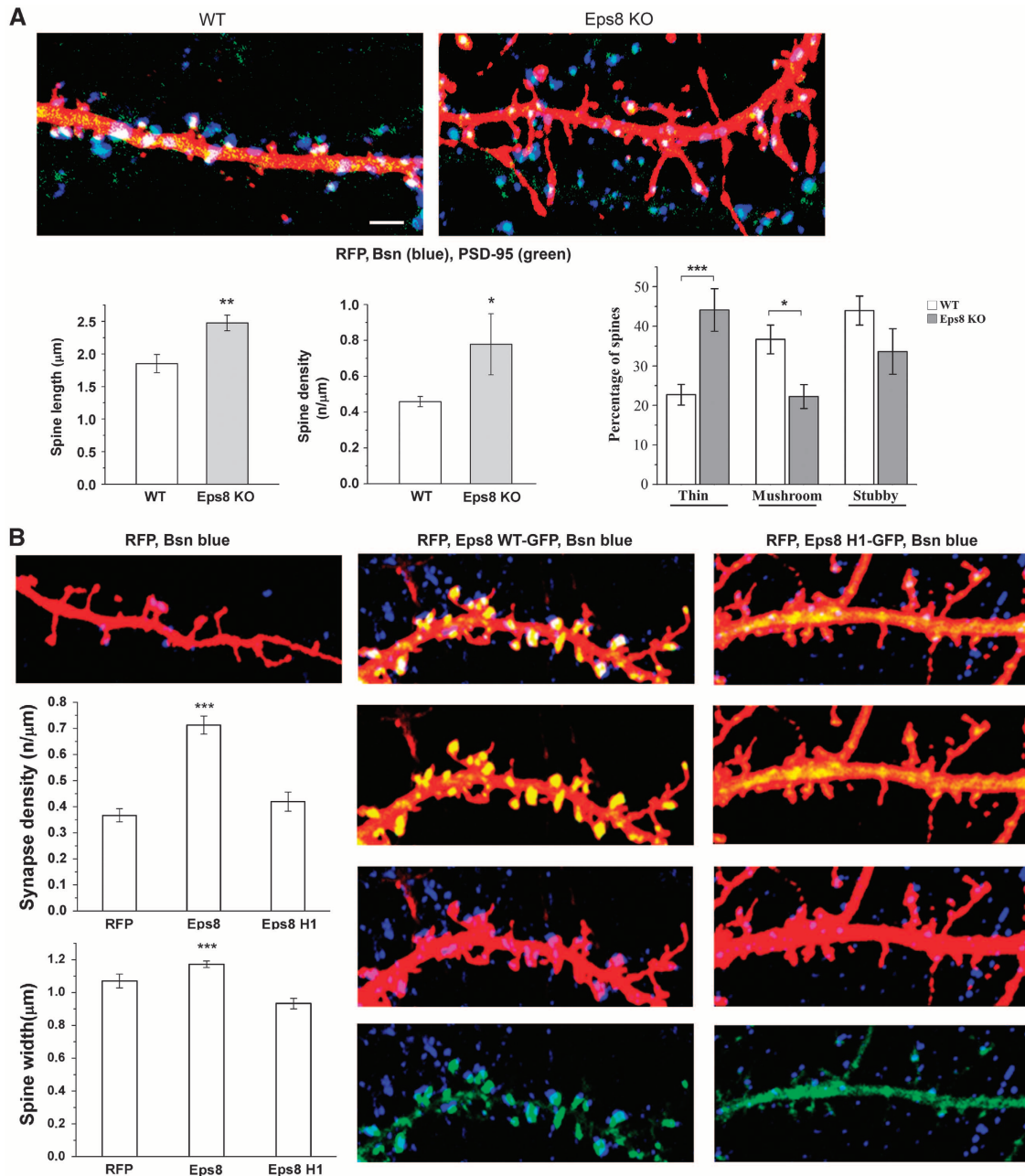
Figure 3 The actin-capping activity of Eps8 is required for spine formation. (**A**) Eps8 wt and KO neurons transfected with RFP and stained for the presynaptic protein Bassoon (Bsn, blue) and for the postsynaptic marker PSD-95 (green). Eps8 KO neurons display more abundant and longer protrusions (total number of examined protrusions: 260 wt, 146 Eps8 KO; number of independent experiments: 3). (**B**) Analysis of spine width and density in neurons transfected with RFP, with the cDNA for wt Eps8 (Eps8WT-EGFP) or with the construct for Eps8 devoid of capping activity (Eps8 H1-EGFP) reveals that Eps8wt but not Eps8H1 increases spine number and size (total number of examined neurons: 15 for RFP, 29 for Eps8 wt and 18 for Eps8 H1; total number of examined spines: 145 for RFP, 553 for Eps8 wt and 105 for Eps8 H1; number of independent experiments: 5). Scale bars depict 5 μm in all panels.

resistance before and after LTP protocol application, thus confirming that the protocol did not impact neuronal health (input resistance: wt = 224 ± 7 MΩ; KO = 210 ± 3 MΩ; access resistance: wt = 15 ± 2 MΩ; KO = 13 ± 2 MΩ; membrane capacitance: wt = 42 ± 3 pF; KO = 41 ± 10 pF. Number of cells examined, 12 wt and 10 KO).

The lack of potentiation in Eps8 KO neurons was also confirmed by electrophysiological recordings of mEPSCs after the application of the glycine protocol. Figure 4C and D show that, differently from wt neurons,

which display a significant increase of mEPSCs frequency and amplitude (Lu *et al*, 2001), mutant neurons fail to undergo potentiation (mEPSC frequency, during GLY: wt = 1.561 ± 0.1054, $n = 13$ Eps8, KO = 0.8319 ± 0.07001, $n = 16$, ***$P < 0.001$; 10-min wash: wt = 1.559 ± 0.1604, $n = 9$ Eps8, KO = 0.7738 ± 0.1193, $n = 8$, **$P = 0.0016$; 20-min wash: wt = 1.300 ± 0.1449, $n = 5$ Eps8, KO = 0.7250 ± 0.1750, $n = 6$, $P = 0.217$; 30-min wash: wt = 1.356 ± 0.1410, $n = 5$ Eps8, KO = 0.7460 ± 0.3230, $n = 5$, *$P = 0.036$; 40-min wash: wt = 1.390 ± 0.1860, $n = 5$ EPS8, KO = 0.7220 ± 0.2215, $n = 5$,
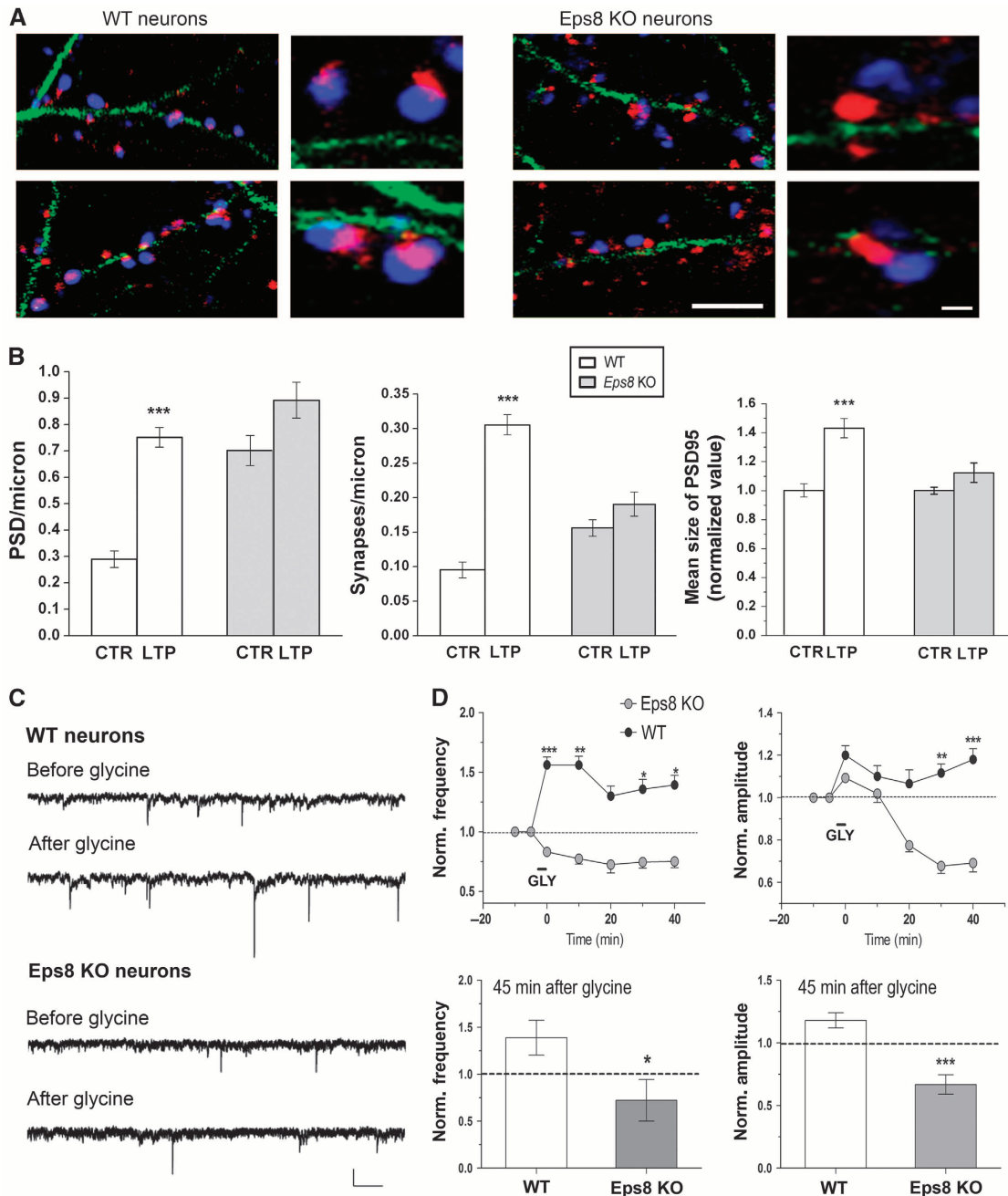
Figure 4 Lack of Eps8 impairs long-term potentiation. (**A**) Representative images of wt and KO cultured neurons before and after application of chemical LTP. Neurons are stained for tubulin (green), PSD-95 (red) and v-Glut1 (blue). Scale bars 10 and 2 μm for higher-magnification images. (**B**) Quantification of potentiation, as represented by number per unit length of PSD-95 (left), synapse density (middle), mean size of PSD-95 (right). Potentiation occurs in wt but not Eps8 KO cultures (Mann–Whitney rank sum test, $P < 0.001$). Data are expressed as mean ± s.e.m.; normalized values (total number of examined neurons for analysis of PSD-95 or synapse density: 35 wt ctr and 36 wt LTP; 33 KO ctr and 75 KO LTP; total number of fields for analysis of PSD-95: 46 wt ctr and 59 wt LTP; 72 KO ctr and 90 KO LTP; size number of independent experiments 5). (**C, D**) Electrophysiological analysis of LTP. (**C**) Representative mEPSCs traces before and after the induction of chemical LTP, in wt and KO neurons. (**D**) Analysis of mEPSC frequency and amplitude at different recording times (5 min before LTP application, 5, 10, 20, 30 and 40 min after LTP application) shows that KO neurons are unable to undergo LTP. Graphs indicate the mEPSC mean frequency and amplitude 45 min after the application of LTP. Scale bars, 10 pA and 250 ms (total number of examined neurons: 13 wt and 16 KO; number of independent experiments: 5).

*$P = 0.0491$; mEPSC amplitude, during GLY: wt = 1.200 ± 0.07783, $n = 13$ Eps8, KO = 1.093 ± 0.04924, $n = 15$, $P = 0.2418$; 10-min wash: wt = 1.100 ± 0.0773, $n = 9$ Eps8, KO = 1.019 ± 0.1084, $n = 7$, $P = 0.5414$; 20-min wash: wt = 1.066 ± 0.1054, $n = 7$ Eps8, KO = 0.7750 ± 0.075, $n = 5$, $P = 0.0893$; 30-min wash: wt = 1.116 ± 0.0457, $n = 5$ Eps8, KO = 0.6775 ± 0.08664, $n = 5$, **$P = 0.0021$; 40-min wash:

wt 1.180 ± 0.06042, $n = 5$ Eps8, KO = 0.6680 ± 0.07761, $n = 5$, ***$P = 0.0008$). The lack of potentiation was also confirmed by two independent paired recordings experiments, where stimulation of the presynaptic neuron (three 50-Hz, 2-s trains of depolarizations at 20-s intervals) during brief perfusion with Mg^{2+}-free solution (Arancio *et al*, 1996) induced potentiation of the excitatory current in wt but

not Eps8 KO neurons (eEPSC amplitude, wt = 1.350 ± 0.05 Eps8, KO = 0.7750 ± 0.0125).

Acute downregulation of Eps8 expression by siRNA similarly prevented synaptic potentiation (Supplementary Figure 3B and B′). These data indicate that Eps8 is required for LTP expression in hippocampal cultures and suggest that the protein may play a role in stabilizing the actin cytoskeleton during spine remodelling. In further support of this hypothesis, endogenous Eps8 is recruited to the spine head upon application of LTP, as indicated by increased protein localization in RFP-labelled dendritic protrusions (Figure 5A and B).

Inhibition of Eps8 capping activity impairs spine enlargement and plasticity

Since Eps8 is recruited to the spine head after chemical LTP induction (Figure 5A and B) and the actin-capping activity of Eps8 is required for proper spine formation during neuronal development (Figure 3B), one could hypothesize that the capping activity of Eps8 is crucial for the process of structural plasticity. The Eps8 wt protein or its actin-capping mutant, Eps8H1, was then exogenously expressed in hippocampal neurons and cultures were exposed to chemical LTP. Representative images of this experiment are shown
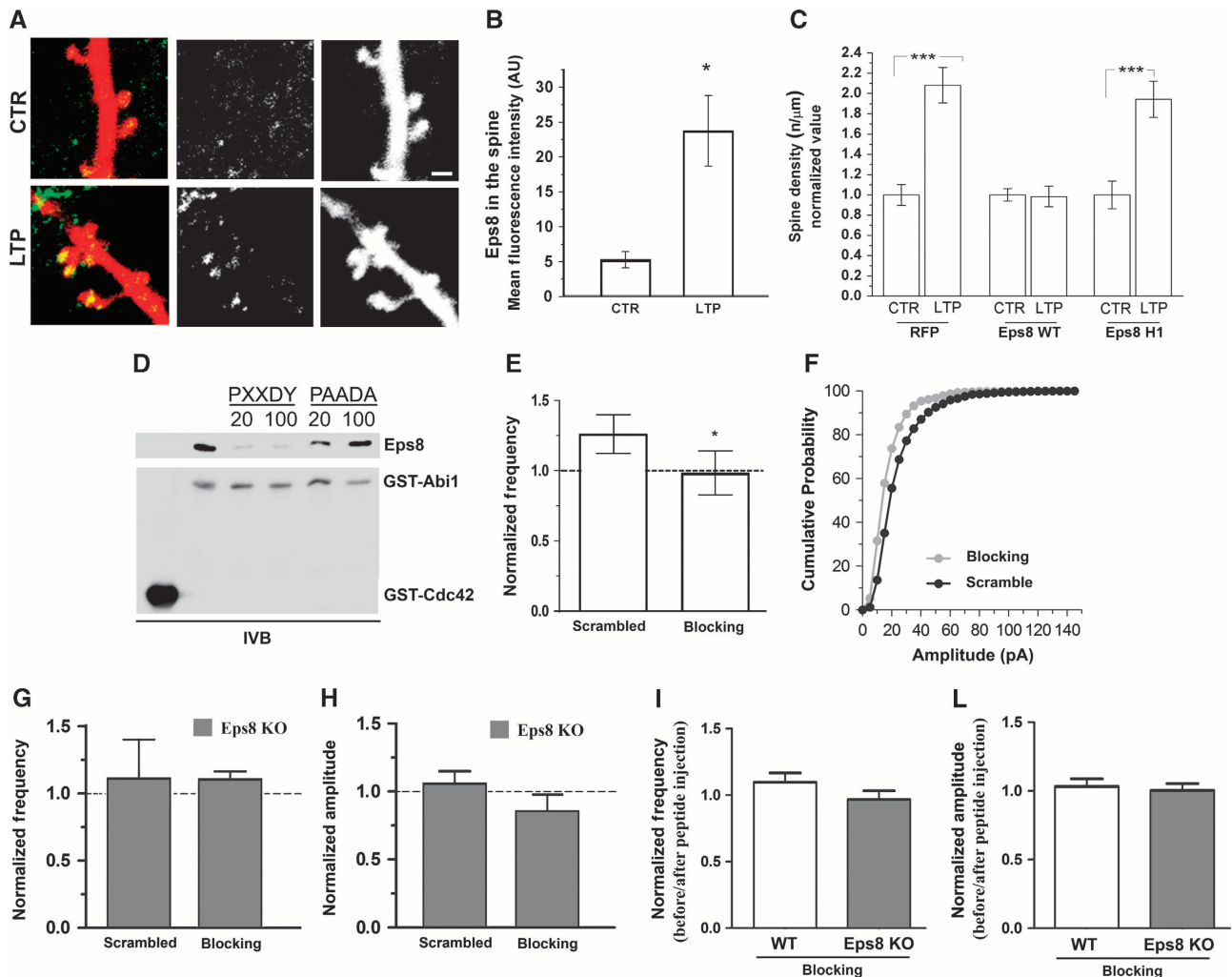

Figure 5 The acute inhibition of Eps8 actin-capping activity precludes potentiation. (**A**) Representative examples of dendrites of mice hippocampal neurons transfected with RFP, exposed to chemical LTP and stained for Eps8. Note that Eps8 immunoreactivity at the spine head increases after potentiation. Scale bar, 2 μm. (**B**) Quantitation of Eps8 immunofluorescence at the spine head in vehicle-treated and glycine-treated (100 μM) neurons (Mann–Whitney Rank Sum Test, $P = 0.013$) (total number of examined neurons: 16 untreated neurons and 12 gly-treated neurons; number of independent experiments: 3). (**C**) Quantitation of spine density under the different experimental conditions shows that potentiation is prevented by overexpression of Eps8 but not by its actin-capping mutant (total number of examined neurons: 15 ctr and 18 LTP for RFP, 29 ctr and 25 LTP for Eps8 wt and 18 ctr and 24 LTP for Eps8 H1; number of independent experiments: 5). (**D**) The proline rich consensus site of Abi1 (PXXDY) competes with Abi1 for binding to Eps8. Equal amounts of His-Eps8 (0.2 μM) were incubated with 0.2 μM immobilized GST-Abi1 in the absence or in the presence of 20 and 100 μM of either PXXDY or PAADA synthesized peptides. 2 μM GST-Cdc42 was used as a control. Proteins were analysed by immunoblotting with the indicated antibodies. (**E**, **F**) mEPSC frequency (**E**) and amplitude (**F**) in neurons exposed to chemical LTP and intracellularly perfused via the patch pipette with either the scrambled or the blocking peptide (the blocking peptide competes with Abi1 for binding to Eps8 and therefore inhibits the Eps8 capping activity). Note that neurons intracellularly perfused with the blocking peptide (grey column, white dots) are defective in potentiation, measured as mEPSC frequency or amplitude. Synaptic potentiation occurs in neurons intracellularly perfused with a scramble peptide (black dots) (total number of examined neurons: 6 for both conditions; number of independent experiments: 3). (**G**, **H**) mEPSC frequency (**G**) and amplitude (**H**) in Eps8 KO neurons exposed to chemical LTP and intracellularly perfused with either the scrambled or the blocking peptide. Note that mEPSC frequency and amplitude of KO neurons do not change upon glycine administration with or without injection of the blocking peptide. (**I–L**) Normalized mEPSC frequency (**I**) and amplitude (**L**) in WT and KO neurons before and after blocking peptide injection. Note that injection of the blocking peptide does not affect *per se* basal synaptic activity.

in Supplementary Figure 4A–C. Quantitative analysis (Figure 5C) demonstrates that high Eps8 capping activity impaired actin cytoskeleton remodelling and spine formation, possibly due to the blockade of actin barbed ends and altered actin dynamics. Indeed, exogenous expression of the Eps8 actin-capping-deficient mutant, Eps8H1, which has no effect on actin polymerization (Menna *et al*, 2009), did not prevent spine remodelling (Figure 5C).

To demonstrate more directly that the actin-capping activity of Eps8 is required for plasticity, we injected the postsynaptic neuron with a synthetic peptide (blocking peptide), which prevents Eps8 from capping actin filaments by competing with Abi1 for binding to Eps8 (Mongioví *et al*, 1999). Direct competition could be observed in *in vitro* binding assay using recombinant purified proteins (Figure 5D). LTP was induced 10 min after injection, while mEPSCs were recorded during the entire procedure. Injection of the blocking, but not of a scrambled peptide, impaired synaptic potentiation induced by glycine treatment (Figure 5E and F, mEPSC frequency, 40-min wash: wt = 1.260 ± 0.1060, blocking peptide = 0.9833 ± 0.2215 unpaired *t*-test, *$P = 0.0486$; mEPSC amplitude, 40-min wash: wt = 1.180 ± 0.06042, blocking peptide = 0.6680 ± 0.07761, Kolmogorov–Smirnov test **$P = 0.0028$; number of cells examined: 6 for both conditions; number of independent experiments: 3). Injection of either the blocking or the scrambled peptides in Eps8 KO neurons following glycine administration does not have any effect (Figure 5G and H). Furthermore, injection of these peptides does not change *per se* the mEPSC frequency and amplitude in either wt or Eps8 KO neurons (Figure 5I and L).

Notably, the lack of Eps8 had no effect on rac activation in 15 DIV hippocampal neurons (Supplementary Figure 4D) and in the brain (Menna *et al*, 2009), suggesting that Eps8 primarily functions as a capper in this system (Vaggi *et al*, 2011) and ruling out the possibility that the LTP impairment in Eps8 KO neurons could be due to a deregulation of rac activity or its downstream pathway, WAVE/SCAR and Arp2/3.

Altogether, these results univocally demonstrate that the capping activity of Eps8 is essential for LTP-mediated synapse formation and strengthening.

Eps8 is expressed at lower levels in brains of patients affected by autism

Eps8 capping activity is regulated by the neurotrophic factor BDNF (Menna *et al*, 2009). BDNF has been demonstrated to be required for spine maturation and dendritic LTP (An *et al*, 2008; Tanaka *et al*, 2008), and is critical for synaptogenesis, synaptic plasticity and memory formation (Chapleau *et al*, 2009; Cunha *et al*, 2010). Furthermore, the balance between the BDNF precursor, proBDNF, and mature BDNF, which controls spine formation (Koshimizu *et al*, 2009), has been found to be disrupted in the brain tissue of autism patients (Garcia *et al*, 2012). Given the established spine pathology in autism spectrum disorder (Hutsler and Zhang, 2010; Penzes *et al*, 2011), we examined Eps8 levels by quantitative western blotting in postmortem fusiform gyrus tissues from 11 patients with autism and 13 controls. We found a substantial reduction of Eps8 in autism patients compared to controls (Figure 6A–C). No differences in the expression of the SNARE protein, SNAP-25, were detected in the same samples (Figure 6D–F), supporting the specificity of the Eps8 deficit. By leading to changes in spine density and dynamics, a decrease in Eps8
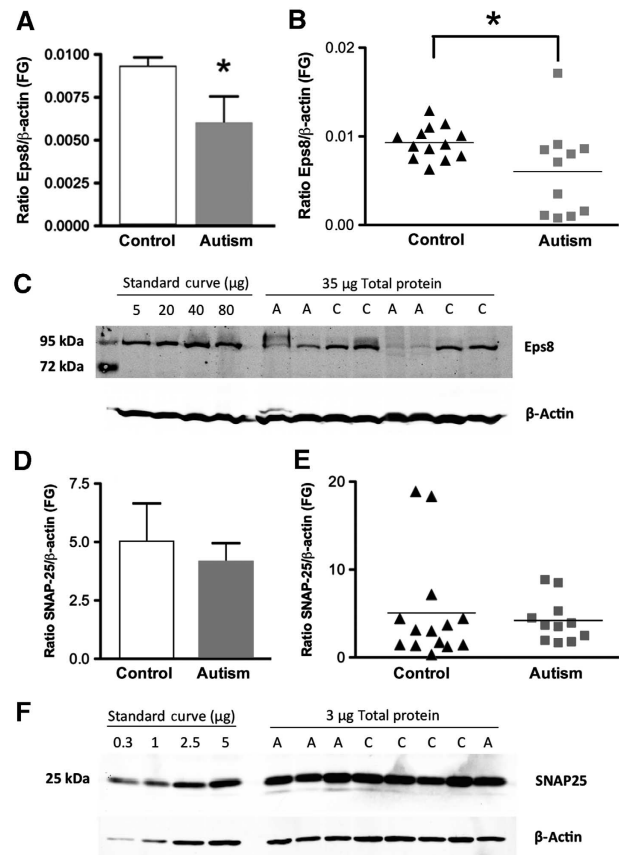

Figure 6 Eps8 expression levels are reduced in brains of patients affected by Autism. (**A**, **B**) Quantification of Eps8 protein expression in fusiform gyrus (FG) of autism and control samples by Western blotting. Each sample was normalized to β-actin. *$P < 0.05$, two-tailed Student's *t*-test. Bars indicate mean ± s.e. Autism, $n = 11$; control, $n = 13$. (**C**) Representative western blot of fusiform gyrus showing autism (A) and control (C) cases. Lanes 2–5: standard curve consisting of different amounts of total protein from a single normal human cortex sample. Lanes 6–13: 35 μg of total protein from each autism and control sample. Blots were run twice with two different Eps8 antibodies and gave similar results. (**D**, **E**) No change in SNAP-25 levels in fusiform gyrus of autism subjects compared to controls. Quantification of SNAP-25 protein expression in fusiform gyrus (FG) of autism and control samples determined by western blotting. Each sample was normalized to β-actin. $P = 0.67$, two-tailed *t*-test. Bars indicate mean ± s.e. Autism, $n = 11$; control, $n = 13$. (**F**) Representative western blot of fusiform gyrus showing autism (A) and control (C) cases. Lanes 1–4: standard curve consisting of different amounts of total protein from a single normal human cortex sample. Lanes 5–12: 3 μg of total protein from each autism and control sample.

expression in the brain of autism patients could contribute to the morphological, cognitive and behavioural defects of this disorder. The cognitive and social impairments and the alterations in spine number and morphology we observed in Eps8 KO mice support this hypothesis.

Discussion

There is substantial evidence that actin-based remodelling underlies spine structural changes and memory stabilization (Lamprecht and LeDoux, 2004; Hotulainen and Hoogenraad 2010). For instance, blockers of actin polymerization suppress LTP (Krucker *et al*, 2000; Fukazawa *et al*, 2003; Okamoto *et al*, 2004; Ramachandran and Frey, 2009); also, LIMK1

knockout mice, which do not regulate the activity of the actin-severing protein cofilin, have enhanced hippocampal LTP (Meng et al, 2002); finally, mice lacking the actin-regulating protein WAVE-1 displayed changes in spine density and abnormalities in synaptic plasticity (Soderling et al, 2007), while Abi2 knockout mice exhibit deficits in learning and memory (Grove et al, 2004). Here, we provide a direct demonstration that the actin-regulating protein Eps8, required for optimal actin-based motility and intestinal morphogenesis (Croce et al, 2004; Disanza et al, 2004; Disanza et al, 2006), critically involved in the formation of axonal and dendritic actin filopodia during neuronal development (Menna et al, 2009; Vaggi et al, 2011), is required for the process of spine morphogenesis during neuronal development and synaptic plasticity.

Dendritic protrusions vary in shape and length. Filopodia, thin and mobile structures, are more abundant at early developmental stages, when they sample potential presynaptic partners, eventually mediating the formation of synaptic contacts. This process coincides with the transition from filopodia to spiny protrusions occurring during development (Ziv and Smith, 1996; Yoshihara et al, 2009; Hotulainen and Hoogenraad, 2010). Further modifications of spine size and shape occur during synaptic plasticity, a process that constantly reshapes the circuitry of the adult brain in response to external stimuli, leading to learning and memory formation. It is known that the morphology of dendritic protrusions is directly linked to their function, with the spine head size being directly correlated with the density of glutamate AMPA receptors, and, therefore, with synaptic strength. Accordingly, immature spines are characterized by highly dynamic and less stable PSD-95 clusters (Tsuriel et al, 2009; Zheng et al, 2010). Notably, Eps8 knockdown leads to the formation of thinner and longer spines, characterized by a decreased synaptic strength and less stable PSD-95 dynamics, thus suggesting that the capping protein Eps8 is required for spine maturation and function involving both scaffolding proteins and receptors. Given that immature spines have impaired synaptic signalling and display defects in synaptic plasticity, the ratio of mature to immature spines could play a crucial role in neuronal function and connectivity. In line with this, dendritic spines in Eps8 KO neurons are unable to undergo potentiation.

It has been recently proposed that the mechanisms underlying spine head expansion during synaptic plasticity may share similarities with the process controlling lamellipodia formation, which involves a concomitant action of actin-capping proteins and Arp2/3-mediated actin nucleation and branching, eventually leading to spine head expansion (Hotulainen and Hoogenraad, 2010). The only evidence suggesting that actin-capping proteins may regulate synaptic plasticity comes from the study of Kitanishi and coworkers, who identified the F-actin-capping protein CapZ (Schafer et al, 1995), previously shown to regulate growth cone morphology and neurite outgrowth (Davis et al, 2009), among the proteins whose expression is regulated by neuronal activity (Kitanishi et al, 2010). Activity-dependent CapZ accumulation at the spine supported the possible role of the protein in the regulation of actin dynamics in response to synaptic inputs and eventually in synaptic plasticity. Despite this evidence, a direct demonstration that the capping activity of actin-regulating

protein is in fact required for the process of spine expansion occurring during synaptic plasticity was totally missing.

In the present study, we demonstrate that Eps8, through its actin-capping activity, controls spine morphogenesis and synaptic potentiation. Eps8 is the founding member of a unique family of capping proteins capable of side binding and bundling actin filaments. The protein has been detected in many regions of the grey matter, including the olfactory bulb, anterior olfactory nuclei, basal forebrain, cerebral cortex, hippocampus, septal nuclei, amygdala, thalamus, hypothalamus, colliculi, pontine nuclei, cerebellum, cochlear nuclear complex and inferior olive, while the white matter was generally unstained (Sekerková et al, 2007). Besides the cerebellum, Eps8 is expressed at higher levels in neurons in layers II and III of the cerebral cortex and in the hippocampus, two areas classically implicated in higher cognitive functions (Offenhäuser et al, 2006). Eps8 has been detected by western blotting in synaptosomal fractions from hippocampus (Menna et al, 2009) and cerebellum (Offenhäuser et al, 2006). By immunoelectron microscopy, Eps8 was localized postsynaptically in the dendritic articulations of cerebellar granule neurons (Offenhäuser et al, 2006; Sekerková et al, 2007), although the protein expression in axons of cultured hippocampal neurons (Menna et al, 2009) in situ and of granule cells in situ (Sekerková et al, 2007) suggests probable multiplicity of Eps8 functions at the synapse. In line with a role of Eps8 in spine morphogenesis and plasticity, mice lacking Eps8 display immature spines and are impaired in cognitive functions.

The identification of Eps8 capping activity as necessary for the process of spine morphogenesis comes from two lines of evidence. The first relies on the demonstration that a well-characterized Eps8H1 mutant, specifically devoid of actin-capping activity, is unable to support proper spine formation. The Eps8H1 mutant allowed us to dissociate the Eps8 capping from bundling activity: indeed, while the Eps8 bundling activity is mainly mediated by a compact four-helix bundle, which contacts three actin subunits along the filament, the actin-capping activity of Eps8 is mainly mediated by a amphipathic helix that binds within the hydrophobic pocket at the barbed ends of actin, thus blocking further addition of actin monomers (Hertzog et al, 2010). In the Eps8H1 mutant, the hydrophobic residues critical for actin capping were mutated, while leaving intact the actin bundling activity. As a further support, acute inhibition of the protein capping activity, obtained through neuronal intracellular perfusion with a blocking peptide, resulted in impairment of plasticity phenomena, thus univocally demonstrating that Eps8 controls spine formation and activity-driven potentiation through the capping of actin filaments. While the present manuscript was under revision, a paper has been published (Stamatakou et al, 2013) showing that acute Eps8 reduction in primary cultures impacts spine formation and plasticity, the former, in particular, through the protein capping activity. Stamatakou et al did not observe any changes in mEPSC amplitude upon LTP, leading them to conclude that Eps8 is required for LTP-mediated synapse formation, but not LTP-induced synaptic strengthening. Our in vitro and in vivo data support that Eps8 is needed for LTP-induced synaptic strengthening. The differences observed may be due to residual Eps8 levels in the experimental conditions of the Stamatakou's study.

End capping of cytoskeletal filaments is a key mechanism for regulating filaments' elongation and disassembly, as well as the organization of the cytoskeletal architecture. It is therefore conceivable that the lack of Eps8, either genetic or consequent to siRNA knockdown, impairs actin organization and remodelling in the dendritic spines. As a further support to the view that a proper process of spine morphogenesis is required both during development and during plasticity phenomena, alterations of the spine actin structure and its dynamic regulation have been observed in a number of neurological disorders characterized by intellectual disability (ID), such as autism spectrum disorder (ASD), mental retardation and fragile X syndrome (van Spronsen and Hoogenraad, 2010; Penzes *et al*, 2011). Mutations in specific synaptic genes including the Akt/mTOR pathway (Kelleher and Bear, 2008; Bourgeron, 2009) involved in regulation of spine protein synthesis, the Neurexin–Neuroligin–Shank pathway (Jamain *et al*, 2003; Durand *et al*, 2007) associated with synaptogenesis and excitation-inhibition imbalance, and Ras/Rho GTPase pathway (Pinto *et al*, 2010) implicated in spine formation and stabilization have been identified in subjects with ASD. Furthermore, overabundant and immature spines have been reported in ASD (Hutsler and Zhang, 2010). Taken together, these findings suggest a major role for dendritic spine abnormalities in the pathogenesis of these diseases. We show here that reduced levels of the actin-capping protein, Eps8, occur in brains of patients affected by autism. Together with previous evidence that capping protein (CP) levels are significantly lower in fetal brains of Down syndrome than in controls (Gulesserian *et al*, 2002), our data suggest that reduction in actin-capping proteins may characterize cognitive impairments associated with spine defects. Interestingly, alterations in BDNF isoform levels have been found in autism patients (Garcia *et al*, 2012). Since the actin-capping activity of Eps8 in neurons is regulated by BDNF (Menna *et al*, 2009), the possibility arises that BDNF controls actin-capping and spine morphogenesis via Eps8 during synaptic plasticity and learning and that defects in this network may be involved in the pathogenesis of autism.

Materials and methods

See also Supplementary data for '*In vitro* binding assay', 'Immunofluorescent staining on sections' and 'Golgi staining'.

Animals
All the experimental procedures followed the guidelines established by the Italian Council on Animal Care and were approved by the Italian Government Decree No. 27/2010. All efforts were made to minimize the number of subjects used and their suffering. Eps8 wild-type (WT) and Eps8 knockout (KO) mice (Croce *et al*, 2004) were housed in cages with free access to food and water at 22°C and with a 12-h alternating light/dark cycle. Genotyping was performed by PCR.

Behavioural tests
All behavioural tests are shortly described below. Full details are available in details in the Supplementary Methods.

T-maze. Animals (10 Eps8 KO and 10 Eps8 wt) were food deprived until reaching 85–90% of their free-feeding body weight. Mice were habituated to a black wooden T-maze (stem length 41 cm; arm length 91 cm) and processed as described in Braida *et al* (2004).

Radial maze. Working memory was studied in 10 Eps8 KO and 10 Eps8 wt mice using a computerized wooden eight-arm radial maze according to Braida *et al* (2004).

Passive avoidance. Passive avoidance task was carried out in 10 Eps8 KO and 10 Eps8 wt mice as previously described (Braida *et al*, 2004) and described in detail in Supplementary data.

Object recognition. The test was conducted on 10 Eps8 KO and 10 Eps8 WT over a two-day period in an open plastic arena ($60 \times 50 \times 30$ cm), as previously described (Pan *et al*, 2008; Corradini *et al*, 2012 (see Supplementary data for details).

Sociability test. The test was performed on 11 wt and 15 Eps8 KO animals as described in Sala *et al*, 2011.

EEG
Electroencephalogram (EEG) activity was recorded, in a Faraday chamber, using a PowerLab digital acquisition system (AD Instruments, Bella Vista, Australia; sampling rate 100 Hz) in freely moving mice ($n = 10$ mice per genotype) previously submitted to surgical implantation of electrodes (See for details Supplementary data).

Cell cultures
Primary cultures of mouse hippocampal neurons were established from E18 fetal, Eps8 KO or wild type (wt) littermates C57BL/6 mice as described by Banker and Cowan (1977) and Bartlett and Banker (1984) with slight modifications. Briefly, hippocampi were dissociated by treatment with trypsin (0.125% for 15 min at 37°C), followed by trituration with a polished Pasteur pipette. The dissociated cells were plated onto glass coverslips coated with poly-L-lysine at density of 400 cells/mm². The cells were maintained in Neurobasal (Invitrogen, San Diego, CA) with B27 supplement and antibiotics, 2 mM glutamine and 12.5 μM glutamate (neuronal medium).

cDNA constructs and expression
Neuronal cultures were transfected at 10DIV with pEGFP-C1 (Clontech, Palo Alto, CA, USA) or pSUPER-DsRed plasmid (obtained from pSUPER-GFP, Oligoengine, Seattle, USA). The Eps8 WT or the capping mutant H1 are cloned in pEGFP vector as described (Disanza *et al*, 2006; Hertzog *et al*, 2010). Two different double-strand small interfering RNA (siRNA) oligonucleotides (Stealth RNAi; called 1525 and 1158) against mouse Eps8 were used according to Menna *et al* (2009). Hippocampal neurons were transfected by using Lipofectamine 2000 (Invitrogen).

Immunofluorescence staining of dissociated neurons
Neuronal cultures were fixed with 4% paraformaldehyde and 4% sucrose or with 100% cold methanol. The following antibodies were used: mouse anti-VAMP2 (1:1000; Synaptic System, Goettingen, Germany), guinea pig anti-Bassoon (1:300; Synaptic System, Goettingen, Germany), guinea pig anti-vGLUT1 (1:1000; Synaptic System, Germany), mouse anti-PSD-95 (1:400; UC Davis/NIH NeuroMab Facility, CA, USA), rabbit anti-GFP (1:400; Invitrogen, San Diego, CA), mouse anti-beta III tubulin (1:400; Promega Corporation, Madison, USA). Secondary antibodies were conjugated with Alexa-488, Alexa-555 or Alexa-633 fluorophores (Invitrogen, San Diego, CA, USA). Images were acquired using a Zeiss LSM 510 META confocal microscope producing image stacks. Pixel size was 110 nm × 110 nm, and acquisition parameters (i.e., laser power, gain and offset) were kept constant among different experimental settings. For the analysis of synaptic puncta only clusters lying along secondary dendritic branches were counted. The detection threshold was set to 2.5-fold the level of background fluorescence referring to diffuse fluorescence within dendritic shafts. The minimum puncta size was set at four pixels (0.048 μm²). Colocalization of two or three selected markers was measured using the boolean function 'and' for the selected channels. The resulting image was binarized and used as a colocalization mask to be subtracted to single channels. The number of puncta resulting from colocalization mask subtraction were measured for each marker. A colocalization ratio was set as colocalizing puncta/total puncta number. The total area of the measured synaptic puncta represents synaptic area. For each cell, three or four dendrites were analysed from maximum projection images. Filopodia were defined as thin protrusions without a distinguishable head, stubby spines as short protrusions without a neck, and mushroom spines as protrusions with a short neck and a

distinguishable head. Synapses were defined by the apposition of presynaptic and postsynaptic markers, such as vGlut1 or Bsn and PSD-95. Fluorescence images processing and analyses were performed with ImageJ Software (National Institutes of Health).

Cell culture electrophysiology

Whole-cell voltage-clamp recordings were performed on rat embryonic hippocampal neurons or on wt and Eps8 mice null hippocampal neurons maintained in culture for 13–15 DIV. Miniature activity was recorded as described in Antonucci *et al* (2012) (see Supplementary data for details).

For glycine-induced LTP experiments, recordings from each neuron lasted at least 60 min and each cell was continuously perfused (1 ml/min) from a computer-controlled perfusion system with a solution containing (in mM) 125 NaCl, 5 KCl, 1.2 KH_2PO_4, 2 $CaCl_2$, 6 glucose, and 25 HEPES-NaOH, TTX 0.001, Strychnine 0.001 and bicuculline methiodide 0.02 (pH 7.4). Solution with glycine (100 μM) was applied for 3 min and then washed out for at least 45 min. The patch pipette electrode contained the following solution (in mM): 130 CsGluconate, 8 CsCl, 2 NaCl, 10 HEPES, 4 EGTA, 4 MgATP and 0.3 Tris-GTP.

The Eps8-capping inhibitor peptide (blocking peptide) was dissolved in the intracellular solution and injected into neurons via the patch pipette. Glycine was applied at least 10 min after the injection of inhibitor peptide or its inactive control.

Analysis of human brain tissue samples

Eleven postmortem brain samples from subjects with autism and thirteen control brain samples were provided to us by the Autism Speaks' Tissue Program (Princeton, NJ, USA) via the Harvard Brain Bank (Belmont, MA, USA) and the University of Maryland Brain and Tissue Bank (Baltimore, MD, USA). Clinical information about each tissue sample was obtained through the Autism Tissue Program online portal (http://www.atpportal.org). There were no statistically significant differences between groups for age at death or PMI. Fusiform gyrus brain tissue was chosen, because this area is hypoactivated during face discrimination tasks in subjects with autism (Schultz *et al*, 2000). The diagnosis of autistic disorder was confirmed using the Autism Diagnostic Interview-Revised (Lord *et al*, 1994) postmortem through interviews with the parents and/or caregivers. Samples were stored at − 80°C before use. Protein extraction was performed as previously described with minor modifications (Fahnestock *et al*, 2001; Garcia *et al*, 2012). Approximately 100 mg of tissue was homogenized on ice without thawing using a sonic dismembrator in homogenization buffer (HB) (0.05 M Tris pH 7.5, 0.5% Tween-20, 10 mM EDTA, 1 complete, Mini, EDTA-free tablet (Roche, Cat. no. 11 836 170 001) per 10 ml of HB, 2 μg/ml pepstatin, 2 μg/ml aprotinin, 50 mM sodium fluoride, 2 mM sodium orthovanadate, 2.5 mM sodium pyrophosphate, 1 mM β-glycerophosphate, 0.5% sodium deoxycholate). The homogenate was incubated for 15 min on ice and then centrifuged at $12\,000 \times g$ for 20 min at 4°C. Supernatants containing solubilized protein were aliquoted and stored at − 80°C before use. Protein concentrations were determined using a DC protein assay kit as described by the manufacturer (Bio-Rad Laboratories, Mississauga, Ontario, Canada).

Western blotting analysis on human brain tissue samples

Western blotting was carried out as previously described with slight modifications (Fahnestock *et al*, 2001; Kawaja *et al*, 2011; Garcia *et al*, 2012). Samples containing 35 μg protein were resolved in 10% sodium dodecyl sulphate-polyacrylamide gels under reducing conditions. After transfer onto polyvinylidene diflouride membranes

for 2 h at 250 mA at 4°C, blots were blocked for 1 h at room temperature in a 1:1 solution of phosphate-buffered saline (PBS) pH 7.4 and Odyssey Blocking Buffer (BB) (Cedarlane, Burlington, Ontario, Canada) and then incubated with rabbit polyclonal or mouse monoclonal Eps8 primary antibodies (dilution 1:1000) and β-actin antibodies (Sigma, diluted 1:5000) at 4°C overnight in BB:PBS (1:1), 0.5% Tween-20 (PBS-T). Subsequently, membranes were washed and incubated for 1 h at room temperature in PBS-T with the secondary antibodies IRDye 680-conjugated goat anti-rabbit and IRDye 800CW-conjugated goat anti-mouse (LI-COR Biosciences, Lincoln, NE, USA; diluted 1:8000). All blots were scanned using an Odyssey Infrared Imaging System (LI-COR Biosciences). Blots were run twice with two different Eps8 antibodies. Each western blot contained a standard curve consisting of different amounts of protein per lane (from 5 to 80 μg) to ensure that the sample loading amount was in the linear range of detection for Eps8 (Fahnestock *et al*, 2001; Kawaja *et al*, 2011; Garcia *et al*, 2012). The intensities of immunoreactive bands were measured using LI-COR Odyssey Software, version 2.0 with local background subtracted. Eps8 pixel values were normalized to β-actin values for each sample.

Statistical analysis

Morphological analysis of spine parameters and synapse density was performed using ImageJ software (NIH, Bethesda, MD, USA).

n refers to the number of elements analysed. Statistical analysis was performed using SigmaStat 3.5 (Jandel Scientific) or PRISM 5 software (GraphPad, Software Inc., San Diego, CA, USA). After testing whether data were normally distributed or not, the appropriate statistical test has been used, see figure legends. Data are presented as mean ± s.e.m. from the indicated number of elements analysed. For behaviour, the continuous data were analysed using a paired Student's *t*-test and the categorical data were analysed using Fisher's exact probability test. The AUC was calculated for the total number of errors in completing the maze. The differences were considered to be significant if $P < 0.05$ and are indicated by an asterisk; those at $P < 0.01$ are indicated by double asterisks; those at $P < 0.001$ are indicated by triple asterisks.

Supplementary data

Supplementary data are available at *The EMBO Journal* Online (http://www.embojournal.org).

Conflict of interest

The authors declare that they have no conflict of interest.

References

Abdel-Rahman WM, Ruosaari S, Knuutila S, Peltomäki P (2012) Differential roles of EPS8 in carcinogenesis: loss of protein expression in a subset of colorectal carcinoma and adenoma. *World J Gastroenterol* **18**: 3896–3903

Akin O, Mullins RD (2008) Capping protein increases the rate of actin-based motility by promoting filament nucleation by the Arp2/3 complex. *Cell* **133**: 841–851

Amatruda JF, Gattermeir DJ, Karpova TS, Cooper JA (1992) Effects of null mutations and overexpression of capping protein on

morphogenesis, actin distribution and polarized secretion in yeast. *J Cell Biol* **119**: 1151–1162

An JJ, Gharami K, Liao GY, Woo NH, Lau AG, Vanevski F, Torre ER, Jones KR, Feng Y, Lu B, Xu B (2008) Distinct role of long 3' UTR BDNF mRNA in spine morphology and synaptic plasticity in hippocampal neurons. *Cell* **134**: 175–187

Antonucci F, Alpár A, Kacza J, Caleo M, Verderio C, Giani A, Martens H, Chaudhry FA, Allegra M, Grosche J, Michalski D, Erck C, Hoffmann A, Harkany T, Matteoli M, Härtig W (2012)

Cracking down on inhibition: selective removal of GABAergic interneurons from hippocampal networks. *J Neurosci* **32:** 1989–2001

Arancio O, Kiebler M, Lee CJ, Lev-Ram V, Tsien RY, Kandel ER, Hawkins RD (1996) Nitric oxide acts directly in the presynaptic neuron to produce long-term potentiation in cultured hippocampal neurons. *Cell* **87:** 1025–1035

Arikkath J, Reichardt LF (2008) Cadherins and catenins at synapses: roles in synaptogenesis and synaptic plasticity. *Trends Neurosci* **31:** 487–494

Banker GA, Cowan WM (1977) Rat hippocampal neurons in dispersed cell culture. *Brain Res* **126:** 397-442

Bartlett WP, Banker GA (1984) An electron microscopic study of the development of axons and dendrites by hippocampal neurons in culture. I. Cells which develop without intercellular contacts. *J Neurosci* **4:** 1944–1953

Bhatt DH, Zhang S, Gan WB (2009) Dendritic spine dynamics. *Annu Rev Physiol* **71:** 261–282

Bourgeron T (2009) A synaptic trek to autism. *Curr Opin Neurobiol* **19:** 231–234

Braida D, Sacerdote P, Panerai AE, Bianchi M, Aloisi AM, Iosuè S, Sala M (2004) Cognitive function in young and adult IL (interleukin)-6 deficient mice. *Behav Brain Res* **153:** 423–429

Chapleau CA, Larimore JL, Theibert A, Pozzo-Miller L (2009) Modulation of dendritic spine development and plasticity by BDNF and vesicular trafficking: fundamental roles in neurodevelopmental disorders associated with mental retardation and autism. *J Neurodev Disord* **1:** 185–196

Cingolani LA, Goda Y (2008) Actin in action: the interplay between the actin cytoskeleton and synaptic efficacy. *Nat Rev Neurosci* **9:** 344–356

Corradini I, Donzelli A, Antonucci F, Welzl H, Loos M, Martucci R, De Astis S, Pattini L, Inverardi F, Wolfer D, Caleo M, Bozzi Y, Verderio C, Frassoni C, Braida D, Clerici M, Lipp HP, Sala M, Matteoli M (2012) Epileptiform activity and cognitive deficits in SNAP-25 + / − mice are normalized by antiepileptic drugs. *Cereb Cortex* (advance online publication, 12 October 2012)

Craig AM, Graf ER, Linhoff MW (2006) How to build a central synapse: clues from cell culture. *Trends Neurosci* **29:** 8–20

Croce A, Cassata G, Disanza A, Gagliani MC, Tacchetti C, Malabarba MG, Carlier MF, Scita G, Baumeister R, Di Fiore PP (2004) A novel actin barbed-end-capping activity in EPS-8 regulates apical morphogenesis in intestinal cells of *Caenorhabditis elegans*. *Nat Cell Biol* **6:** 1173–1179

Cunha C, Brambilla R, Thomas KL (2010) A simple role for BDNF in learning and memory? *Front Mol Neurosci* **3:** 1

Dailey ME, Smith SJ (1996) The dynamics of dendritic structure in developing hippocampal slices. *J Neurosci* **16:** 2983–2994

Davis DA, Wilson MH, Giraud J, Xie Z, Tseng HC, England C, Herscovitz H, Tsai LH, Delalle I (2009) Capzb2 interacts with beta-tubulin to regulate growth cone morphology and neurite outgrowth. *PLoS Biol* **7:** e1000208

Disanza A, Carlier MF, Stradal TE, Didry D, Frittoli E, Confalonieri S, Croce A, Wehland J, Di Fiore PP, Scita G (2004) Eps8 controls actin-based motility by capping the barbed ends of actin filaments. *Nat Cell Biol* **6:** 1180–1188

Disanza A, Mantoani S, Hertzog M, Gerboth S, Frittoli E, Steffen A, Berhoerster K, Kreienkamp HJ, Milanesi F, Di Fiore PP, Ciliberto A, Stradal TE, Scita G (2006) Regulation of cell shape by Cdc42 is mediated by the synergic actin-bundling activity of the Eps8-IRSp53 complex. *Nat Cell Biol* **8:** 1337–1347

Dunaevsky A, Tashiro A, Majewska A, Mason C, Yuste R (1999) Developmental regulation of spine motility in the mammalian central nervous system. *Proc Natl Acad Sci USA* **96:** 13438–13443

Durand CM, Betancur C, Boeckers TM, Bockmann J, Chaste P, Fauchereau F, Nygren G, Rastam M, Gillberg IC, Anckarsäter H, Sponheim E, Goubran-Botros H, Delorme R, Chabane N, Mouren-Simeoni MC, de Mas P, Bieth E, Rogé B, Héron D, Burglen L *et al* (2007) Mutations in the gene encoding the synaptic scaffolding protein SHANK3 are associated with autism spectrum disorders. *Nat Genet* **39:** 25–27

Evers JF, Muench D, Duch C (2006) Developmental relocation of presynaptic terminals along distinct types of dendritic filopodia. *Dev Biol* **297:** 214–227

Falck S, Paavilainen VO, Wear MA, Grossmann JG, Cooper JA, Lappalainen P (2004) Biological role and structural mechanism of twinfilin-capping protein interaction. *EMBO J* **23:** 3010–3019

Fahnestock M, Michalski B, Xu B, Coughlin MD (2001) The precursor pro-nerve growth factor is the predominant form of nerve growth factor in brain and is increased in Alzheimer's disease. *Mol Cell Neurosci* **18:** 210–220

Fan Y, Tang X, Vitriol E, Chen G, Zheng JQ (2011) Actin capping protein is required for dendritic spine development and synapse formation. *J Neurosci* **31:** 10228–10233

Fiala JC, Feinberg M, Popov V, Harris KM (1998) Synaptogenesis via dendritic filopodia in developing hippocampal area CA1. *J Neurosci* **18:** 8900–8911

Fortin DA, Davare MA, Srivastava T, Brady JD, Nygaard S, Derkach VA, Soderling TR (2010) Long-term potentiation-dependent spine enlargement requires synaptic Ca2 + -permeable AMPA receptors recruited by CaM-kinase I. *J Neurosci* **30:** 11565–11575

Frittoli E, Matteoli G, Palamidessi A, Mazzini E, Maddaluno L, Disanza A, Yang C, Svitkina T, Rescigno M, Scita G (2011) The signaling adaptor Eps8 is an essential actin capping protein for dendritic cell migration. *Immunity* **35:** 388–399

Fukazawa Y, Saitoh Y, Ozawa F, Ohta Y, Mizuno K, Inokuchi K (2003) Hippocampal LTP is accompanied by enhanced F-actin content within the dendritic spine that is essential for late LTP maintenance *in vivo*. *Neuron* **38:** 447–460

Garcia KLP, Guanhua Y, Nicolini C, Michalski B, Garzon D, Chiu VS, Tongiorgi E, Szatmari P, Fahnestock M (2012) Altered balance of proteolytic forms of pro-brain-derived-neurotrophic factor in autism. *J Neuropathol Exp Neurol* **71:** 289–297

Garcia KL, Yu G, Nicolini C, Michalski B, Garzon DJ, Chiu VS, Tongiorgi E, Szatmari P, Fahnestock M (2012) Altered balance of proteolytic isoforms of pro-brain derived neurotrophic factor in autism. *J Neuropathol Exp Neurol* **71:** 289–297

Grove M, Demyanenko G, Echarri A, Zipfel PA, Quiroz ME, Rodriguiz RM, Playford M, Martensen SA, Robinson MR, Wetsel WC, Maness PF, Pendergast AM (2004) ABI2-deficient mice exhibit defective cell migration, aberrant dendritic spine morphogenesis, and deficits in learning and memory. *Mol Cell Biol* **24:** 10905–10922

Gulesserian T, Kim SH, Fountoulakis M, Lubec G (2002) Aberrant expression of centractin and capping proteins, integral constituents of the dynactin complex, in fetal down syndrome brain. *Biochem Biophys Res Commun* **291:** 62–67

Harris KM, Jensen FE, Tsao B (1992) Three-dimensional structure of dendritic spines and synapses in rat hippocampus (CA1) at postnatal day 15 and adult ages: implications for the maturation of synaptic physiology and long-term potentiation. *J Neurosci* **12:** 2685–2705

Hertzog M, Milanesi F, Hazelwood L, Disanza A, Liu H, Perlade E, Malabarba MG, Pasqualato S, Maiolica A, Confalonieri S, Le Clainche C, Offenhauser N, Block J, Rottner K, Di Fiore PP, Carlier MF, Volkmann N, Hanein D, Scita G (2010) Molecular basis for the dual function of Eps8 on actin dynamics: bundling and capping. *PLoS Biol* **8:** e1000387

Honkura N, Matsuzaki M, Noguchi J, Ellis-Davies GC, Kasai H (2008) The subspine organization of actin fibers regulates the structure and plasticity of dendritic spines. *Neuron* **57:** 719–729

Hotulainen P, Hoogenraad CC (2010) Actin in dendritic spines: connecting dynamics to function. *J Cell Biol* **189:** 619–629

Hotulainen P, Llano O, Smirnov S, Tanhuanpaa K, Faix J, Rivera C, Lappalainen P (2009) Defining mechanisms of actin polymerization and depolymerization during dendritic spine morphogenesis. *J Cell Biol* **185:** 323–339

Hutsler JJ, Zhang H (2010) Increased dendritic spine densities on cortical projection neurons in autism spectrum disorders. *Brain Res* **1309:** 83–94

Jamain S, Quach H, Betancur C, Råstam M, Colineaux C, Gillberg IC, Soderstrom H, Giros B, Leboyer M, Gillberg C, Bourgeron T (2003) Mutations of the X-linked genes encoding neuroligins NLGN3 and NLGN4 are associated with autism. Paris Autism Research International Sibpair Study. *Nat. Genet* **34:** 27–29

Jontes JD, Smith SJ (2000) Filopodia, spines and the generation of synaptic diversity. *Neuron* **27:** 11–14

Jourdain P, Fukunaga K, Muller D (2003) Calcium/calmodulin-dependent protein kinase II contributes to activity-dependent filopodia growth and spine formation. *J Neurosci* **23:** 10645–10649

Kasai H, Matsuzaki M, Noguchi J, Yasumatsu N, Nakahara H (2003) Structure-stability-function relationships of dendritic spines. *Trends Neurosci* **26:** 360–368

Kawaja MD, Smithson LJ, Elliot J, Trinh G, Crotty AM, Michalski B, Fahnestock M (2011) Nerve growth factor promoter activity revealed in mice expressing enhanced green fluorescent protein. *J Comp Neurol* **519:** 2522–2545

Kelleher RJ, Bear MF (2008) The autistic neuron: troubled translation? *Cell* **135:** 401–406

Kitanishi T, Sakai J, Kojima S, Saitoh Y, Inokuchi K, Fukaya M, Watanabe M, Matsuki N, Yamada MK (2010) Activity-dependent localization in spines of the F-actin capping protein CapZ screened in a rat model of dementia. *Genes Cells* **15:** 737–747

Korobova F, Svitkina T (2008) Arp2/3 complex is important for filopodia formation, growth cone motility, and neuritogenesis in neuronal cells. *Mol Biol Cell* **19:** 1561–1574

Korobova F, Svitkina T (2010) Molecular architecture of synaptic actin cytoskeleton in hippocampal neurons reveals a mechanism of dendritic spine morphogenesis. *Mol Biol Cell* **21:** 165–176

Koshimizu H, Kiyosue K, Hara T, Hazama S, Suzuki S, Uegaki K, Nagappan G, Zaitsev E, Hirokawa T, Tatsu Y, Ogura A, Lu B, Kojima M (2009) Multiple functions of precursor BDNF to CNS neurons: negative regulation of neurite growth, spine formation and cell survival. *Mol Brain* **2:** 27

Krucker T, Siggins GR, Halpain S (2000) Dynamic actin filaments are required for stable long-term potentiation (LTP) in area CA1 of the hippocampus. *Proc Natl Acad Sci USA* **97:** 6856–6861

Lamprecht R, LeDoux J (2004) Structural plasticity and memory. *Nat Rev Neurosci* **5:** 45–54

Lord C, Rutter M, Le Couteur A (1994) Autism diagnostic interview-revised. A revised version of a diagnostic interview for caregivers of individuals with possible pervasive developmental disorders. *Autism Dev Dis* **24:** 659–685

Lu W, Man H, Ju W, Trimble WS, MacDonald JF, Wang YT (2001) Activation of synaptic NMDA receptors induces membrane insertion of new AMPA receptors and LTP in cultured hippocampal neurons. *Neuron* **29:** 243–254

Luscher C, Nicoll RA, Malenka RC, Muller D (2000) Synaptic plasticity and dynamic modulation of the postsynaptic membrane. *Nat Neurosci* **3:** 545–550

Manfredi I, Zani AD, Rampoldi L, Pegorini S, Bernascone I, Moretti M, Gotti C, Croci L, Consalez GG, Ferini-Strambi L, Sala M, Pattini L, Casari G (2009) Expression of mutant beta2 nicotinic receptors during development is crucial for epileptogenesis. *Hum Mol Genet* **18:** 1075–1088

Matus A (2000) Actin-based plasticity in dendritic spines. *Science* **290:** 754–758

Meng Y, Zhang Y, Tregoubov V, Janus C, Cruz L, Jackson M, Lu WY, MacDonald JF, Wang JY, Falls DL, Jia Z (2002) Abnormal spine morphology and enhanced LTP in LIMK-1 knockout mice. *Neuron* **35:** 121–133

Menna E, Disanza A, Cagnoli C, Schenk U, Gelsomino G, Frittoli E, Hertzog M, Offenhauser N, Sawallisch C, Kreienkamp HJ, Gertler FB, Di Fiore PP, Scita G, Matteoli M (2009) Eps8 regulates axonal filopodia in hippocampal neurons in response to brain-derived neurotrophic factor (BDNF). *PLoS Biol* **7:** e1000138

Mogilner A, Rubinstein B (2005) The physics of filopodial protrusion. *Biophys J* **89:** 782–795

Mongiovì AM, Romano PR, Panni S, Mendoza M, Wong WT, Musacchio A, Cesareni G, Di Fiore PP (1999) A novel peptide-SH3 interaction. *EMBO J.* **18:** 5300–5309

Nakamura Y, Wood CL, Patton AP, Jaafari N, Henley JM, Mellor JR, Hanley JG (2011) PICK1 inhibition of the Arp2/3 complex controls dendritic spine size and synaptic plasticity. *EMBO J* **30:** 719–730

Nikonenko I, Jourdain P, Muller D (2003) Presynaptic remodeling contributes to activity-dependent synaptogenesis. *J Neurosci* **23:** 8498–8505

Offenhäuser N, Castelletti D, Mapelli L, Soppo BE, Regondi MC, Rossi P, D'Angelo E, Frassoni C, Amadeo A, Tocchetti A, Pozzi B, Disanza A, Guarnieri D, Betsholtz C, Scita G, Heberlein U, Di Fiore PP (2006) Increased ethanol resistance and consumption in Eps8 knockout mice correlates with altered actin dynamics. *Cell* **127:** 213–226

Okabe S, Miwa A, Okado H (2001) Spine formation and correlated assembly of presynaptic and postsynaptic molecules. *J Neurosci* **21:** 6105–6114

Okamoto K, Nagai T, Miyawaki A, Hayashi Y (2004) Rapid and persistent modulation of actin dynamics regulates postsynaptic reorganization underlying bidirectional plasticity. *Nat Neurosci* **7:** 1104–1112

Pan D, Sciascia 2nd A, Vorhees CV, Williams MT (2008) Progression of multiple behavioral deficits with various ages of onset in a murine model of Hurler syndrome. *Brain Res* **1188:** 241–253

Penzes P, Cahill ME, Jones KA, VanLeeuwen JE, Woolfrey KM (2011) Dendritic spine pathology in neuropsychiatric disorders. *Nat Neurosci* **14:** 285–293

Pinto D, Pagnamenta AT, Klei L, Anney R, Merico D, Regan R, Conroy J, Magalhaes TR, Correia C, Abrahams BS, Almeida J, Bacchelli E, Bader GD, Bailey AJ, Baird G, Battaglia A, Berney T, Bolshakova N, Bölte S, Bolton PF *et al* (2010) Functional impact of global rare copy number variation in autism spectrum disorders. *Nature* **466:** 368–372

Racz B, Weinberg RJ (2008) Organization of the Arp2/3 complex in hippocampal spines. *J Neurosci* **28:** 5654–5659

Ramachandran B, Frey JU (2009) Interfering with the actin network and its effect on long-term potentiation and synaptic tagging in hippocampal CA1 neurons in slices *in vitro*. *J Neurosci* **29:** 12167–12173

Restivo L, Roman FS, Ammassari-Teule M, Marchetti E (2006) Simultaneous olfactory discrimination elicits a strain-specific increase in dendritic spines in the hippocampus of inbred mice. *Hippocampus* **16:** 472–479

Sala M, Braida D, Lentini D, Busnelli M, Bulgheroni E, Capurro V, Finardi A, Donzelli A, Pattini L, Rubino T, Parolaro D, Nishimori K, Parenti M, Chini B (2011) Pharmacologic rescue of impaired cognitive flexibility, social deficits, increased aggression, and seizure susceptibility in oxytocin receptor null mice: a neurobehavioral model of autism. *Biol Psychiatry* **69:** 875–882

Schafer DA, Hug C, Cooper JA (1995) Inhibition of CapZ during myofibrillogenesis alters assembly of actin filaments. *J Cell Biol* **128:** 61–70

Schafer DA, Mooseker MS, Cooper JA (1992) Localization of capping protein in chicken epithelial cells by immunofluorescence and biochemical fractionation. *J Cell Biol* **118:** 335–346

Schultz RT, Gauthier I, Klin A, Fulbright RK, Anderson AW, Volkmar F, Skudlarski P, Lacadie C, Cohen DJ, Gore JC (2000) Abnormal ventral temporal cortical activity during face discrimination among individuals with autism and Asperger syndrome. *Arch Gen Psychiatry* **57:** 331–340

Sekerková G, Diño MR, Ilijic E, Russo M, Zheng L, Bartles JR, Mugnaini E (2007) Postsynaptic enrichment of Eps8 at dendritic shaft synapses of unipolar brush cells in rat cerebellum. *Neuroscience* **145:** 116–129

Soderling SH, Guire ES, Kaech S, White J, Zhang F, Schutz K, Langeberg LK, Banker G, Raber J, Scott JD (2007) A WAVE-1 and WRP signaling complex regulates spine density, synaptic plasticity, and memory. *J Neurosci* **27:** 355–365

Stamatakou E, Marzo A, Gibb A, Salinas PC (2013) Activity-dependent spine morphogenesis: a role for the actin-capping protein Eps8. *J Neurosci* **33:** 2661–2670

Svitkina T, Lin WH, Webb DJ, Yasuda R, Wayman GA, Van Aelst L, Soderling SH (2010) Regulation of the postsynaptic cytoskeleton: roles in development, plasticity, and disorders. *J Neurosci* **30:** 14937–14942

Tanaka J, Horiike Y, Matsuzaki M, Miyazaki T, Ellis-Davies GC, Kasai H (2008) Protein synthesis and neurotrophin-dependent structural plasticity of single dendritic spines. *Science* **319:** 1683–1687

Tocchetti A, Soppo CB, Zani F, Bianchi F, Gagliani MC, Pozzi B, Rozman J, Elvert R, Ehrhardt N, Rathkolb B, Moerth C, Horsch M, Fuchs H, Gailus-Durner V, Beckers J, Klingenspor M, Wolf E, Hrabé de Angelis M, Scanziani E, Tacchetti C *et al* (2010) Loss of the actin remodeler Eps8 causes intestinal defects and improved metabolic status in mice. *PLoS One* **5:** e9468

Toro R, Konyukh M, Delorme R, Leblond C, Chaste P, Fauchereau F, Coleman M, Leboyer M, Gillberg C, Bourgeron T (2010) Key role for gene dosage and synaptic homeostasis in autism spectrum disorders. *Trends Genet* **26:** 363–372

Tsuriel S, Fisher A, Wittenmayer N, Dresbach T, Garner CC, Ziv NE (2009) Exchange and redistribution dynamics of the cytoskeleton of the active zone molecule bassoon. *J Neurosci* **29:** 351–358

Vaggi F, Disanza A, Milanesi F, Di Fiore PP, Menna E, Matteoli M, Gov NS, Scita G, Ciliberto A (2011) The Eps8/IRSp53/VASP network differentially controls actin capping and bundling in filopodia formation. *PLoS Comput Biol* **7:** e1002088

van Spronsen M, Hoogenraad CC (2010) Synapse pathology in psychiatric and neurologic disease. *Curr Neurol Neurosci Rep* **10:** 207–214

Wegner AM, Nebhan CA, Hu L, Majumdar D, Meier KM, Weaver AM, Webb DJ (2008) N-wasp and the arp2/3 complex are critical regulators of actin in the development of dendritic spines and synapses. *J Biol Chem* **283:** 15912–15920

Welsch T, Younsi A, Disanza A, Rodriguez JA, Cuervo AM, Scita G, Schmidt J (2010) Eps8 is recruited to lysosomes and subjected to chaperone-mediated autophagy in cancer cells. *Exp Cell Res* **316:** 1914–1924

Yoshihara Y, De Roo M, Muller D (2009) Dendritic spine formation and stabilization. *Curr Opin Neurobiol* **19:** 146–153

Yuste R, Bonhoeffer T (2001) Morphological changes in dendritic spines associated with long-term synaptic plasticity. *Annu Rev Neurosci* **24:** 1071–1089

Zampini V, Rüttiger L, Johnson SL, Franz C, Furness DN, Waldhaus J, Xiong H, Hackney CM, Holley MC, Offenhauser N, Di Fiore PP, Knipper M, Masetto S, Marcotti W (2011) Eps8 regulates hair bundle length and functional maturation of mammalian auditory hair cells. *PLoS Biol* **9:** e1001048

Zheng CY, Petralia RS, Wang YX, Kachar B, Wenthold RJ (2010) SAP102 is a highly mobile MAGUK in spines. *J Neurosci* **30:** 4757–4766

Ziv NE, Smith SJ (1996) Evidence for a role of dendritic filopodia in synaptogenesis and spine formation. *Neuron* **17:** 91–102

EUROPEAN JOURNAL OF NEUROSCIENCE

From filopodia to synapses: the role of actin-capping and anti-capping proteins

Elisabetta Menna,[1] Giuliana Fossati,[1] Giorgio Scita[2] and Michela Matteoli[1,3]

[1]Department of Medical Pharmacology and CNR Institute of Neuroscience, University of Milan, Milano, Italy
[2]IFOM, FIRC Institute of Molecular Oncology Foundation at IFOM-IEO Campus, Milano, Italy
[3]IRCCS Don Gnocchi, Milano, Italy

Abstract

Actin-capping and anti-capping proteins are crucial regulators of actin dynamics. Recent studies have indicated that these proteins may be heavily involved in all stages of synaptogenesis, from the emergence of filopodia, through neuritogenesis and synaptic contact stabilization, to the structural changes occurring at the synapse during potentiation phenomena. In this review, we focus on recent evidence pointing to an active role of actin-capping and anti-capping proteins in orchestrating the processes controlling neuronal connectivity and plasticity.

Introduction

Neural circuits are defined by the structure of axons and dendrites, with single axons contacting and controlling the function of multiple targets, and individual dendrites integrating inputs from several sources. The molecular processes involved in establishing proper neuronal connectivity are not exclusively activated during brain development, because, even in the adult brain, continuous remodelling, accompanied by synapse formation and elimination, underlies the process of memory formation (Chklovskii *et al.*, 2004; Bruel-Jungerman *et al.*, 2007; Fu & Zuo, 2011). Deciphering the molecular mechanisms by which neurite extension and synaptogenesis occur is therefore critical to our understanding of brain ontogenesis, synaptic remodelling, and plasticity.

It is widely accepted that filopodia, which are highly motile, narrow extensions containing bundles of filamentous actin, play important roles at initial stages of synaptogenesis (Fiala *et al.*, 1998; Craig *et al.*, 2006; Geraldo & Gordon-Weeks, 2009). Also, growth and stabilization of filopodia for the formation of new synaptic contacts occur during long-term potentiation (Luscher *et al.*, 2000; Jourdain *et al.*, 2003; Nikonenko *et al.*, 2003). Filopodia emerge from all neuronal compartments: those extending at the tips of axonal growth cones mainly mediate neurite navigation and axonal pathfinding (Koleske, 2003). Filopodia emerging from developing axons, which are characterized by the presence of actively recycling synaptic vesicles, are thought, instead, to represent precursors of presynaptic boutons (Chang & De Camilli, 2001; Matteoli *et al.*, 2004). On the other hand, dendritic filopodia may serve as precursors of new spines in the context of activity-dependent synaptogenesis (Jontes & Smith, 2000; Wong *et al.*, 2000; Portera-Cailliau *et al.*, 2003; Yuste & Bonhoeffer, 2004; Knott & Holtmaat, 2008). The transition from filopodia to spines upon contact with a presynaptic bouton has been directly demonstrated (Ziv & Smith, 1996; Kayser *et al.*, 2008; Heiman & Shaham, 2010; Arstikaitis *et al.*, 2011).

It is generally thought that filopodial actin filaments originate from the lamellipodium, a flat membrane protrusion that is almost invariably seen at the leading edge of migratory cells. The diverse morphological features of lamellipodia and filopodia are mirrored by their architecturally diverse actin backbones. An extended meshwork of actin filaments of variable length and orientation supports the former protrusions, whereas filopodia are composed of bundles of long and linear actin filaments.

A number of actin-binding proteins have been implicated in regulating the equilibrium between filopodia and lamellipodia (Gupton *et al.*, 2007; Drees & Gertler, 2008; Le Clainche & Carlier, 2008). In particular, the formation of lamellipodia mainly involves the activity of a minimal key set of actin regulatory proteins (see below), and of the Arp2/3 complex, a branched actin filament nucleator that works in concert with actin-capping proteins. These latter proteins, by binding to the barbed ends of densely packed, plasma membrane-localized actin filaments, control not only their lifetime, but also the architecture of the resulting meshwork (Akin & Mullins, 2008). Filopodial initiation and extension requires, instead, the coordinated and balanced activities of actin-capping and anti-capping proteins that, together with linear filament elongators, including formin and vasodilator-stimulated phosphoprotein (VASP) family proteins, promote the formation of long filaments; the latter then converge to form bundles, which subsequently become tightly cross-linked through the action of proteins such as fascin (Mejillano *et al.*, 2004; Mogilner & Rubinstein, 2005; Drees & Gertler, 2008; Mattila & Lappalainen, 2008; Ridley, 2011) (Fig. 1).

Given that the mechanisms regulating the formation of neuronal filopodia directly impact on neuronal connectivity and network plasticity, we focus here on recent evidence pointing to an active role of actin-capping and anti-capping proteins in orchestrating the formation of neuronal filopodia, as well as in controlling neuritogenesis and spine morphology.

ADP-actin
ATP-actin
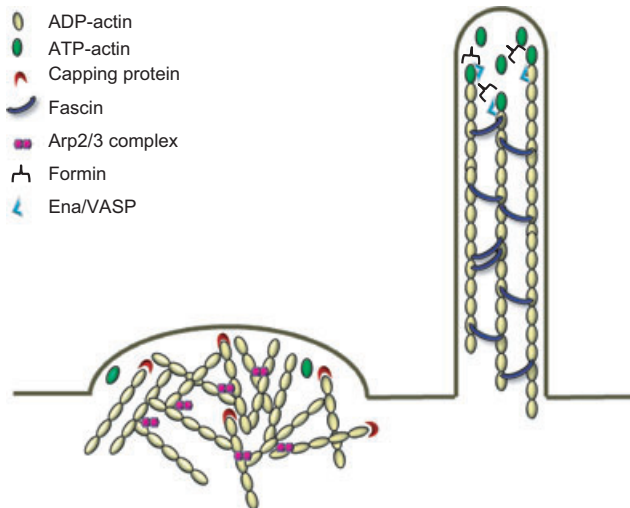Capping protein
Fascin
Arp2/3 complex
Formin
Ena/VASP

FIG. 1. Actin-binding proteins regulate the equilibrium between lamellipodia and filopodia. Left: the lamellipodial structure is maintained by the concerted actions of actin-capping and branching proteins. Right: filopodia formation is favoured by the removal of capping proteins and by the concomitant activity of actin-cross-linking (bundling) proteins.

The formation of filopodia in neurons: a role for actin-capping and anti-capping proteins

The core structural and dynamic components of filopodia are actin filaments, whose dynamic formation and topological organization are controlled by ensembles of actin-binding proteins. The actin regulatory machinery responsible for filopodia consists of different classes of proteins, such as F-actin nucleators (e.g. Arp2/3, formins), filament bundlers (e.g. fascin), membrane-deforming factors (e.g. BAR domain proteins), regulators of actin polymerization (e.g. Ena/VASP family proteins, profilin, and actin-capping proteins) or disassembly (e.g. ADF/cofilin), and actin-associated motors (e.g. myosin II and myosin X) (Ono, 2007; Le Clainche & Carlier, 2008; Chesarone & Goode, 2009).

The mechanism of filopodia formation is a controversial topic (Svitkina *et al.*, 2003; Vignjevic *et al.*, 2006; Gupton *et al.*, 2007; Mattila & Lappalainen, 2008; Faix *et al.*, 2009; Mellor, 2010). Two alternative models have been suggested: the convergent elongation model proposes that Arp2/3-seeded actin filaments are elongated by factors, such as Ena/VASP family proteins, that also protect them from capping, and are assembled into filopodial bundles by fascin; in contrast, the *de novo* nucleation model proposes that linear filament nucleators and elongators, such as formin and Ena/VASP family proteins, assemble into submembranous complexes, thereby promoting the processive elongation of parallel actin filaments, which are cross-linked into filopodial actin bundles. It must be pointed out that these two models are not necessarily exclusive, as both mechanisms may operate in cells in response to distinct sets of conditions, such as the abundance of specific cytoskeletal components, different signalling pathways, and diverse microenvironmental conditions, including the composition of the extracellular matrix in which cells are embedded.

The activity of actin-capping proteins, according to the convergent elongation model, is crucial for controlling the resultant architectural organization of actin in these protrusions. When the capping activity is high, newly nucleated branched filaments become rapidly capped; this also causes a local increase in the concentrations of available actin monomers, which further feed Arp2/3 nucleation/branching activity, ultimately promoting the generation of a dense and highly branched dendritic array of short actin filaments at the leading edge of lamellipodia. Conversely, when capping activity is low, local monomer availability is reduced, as G-actin becomes incorporated into long and uncapped actin filaments (Mogilner & Rubinstein, 2005; Akin & Mullins, 2008; Korobova & Svitkina, 2008). Factors such as VASP family members or ill-defined components of the filopodia tip complex may then promote the transient association of actin filaments, which can be further stabilized by other bundlers, such as fascin, thus permitting the formation of actin bundles and filopodia (Mogilner & Rubinstein, 2005). According to the *de novo* nucleation model, formins (Pellegrin & Mellor, 2005; Schirenbeck *et al.*, 2005; Yang *et al.*, 2007; Block *et al.*, 2008) or VASP tetramers, particularly when clustered along the plasma membrane (Breitsprecher *et al.*, 2008, 2011; Hansen & Mullins, 2010), may be responsible for promoting filopodial initiation. Also in this case, however, filaments must be protected from cappers, which have been shown, in the case of the capping protein (CP), to compete, either directly or indirectly, with VASP as well as with formins for barbed-end binding (Breitsprecher *et al.*, 2008).

Actin-capping proteins appear to play a role in regulating lamellipodia and filopodia formation in neurons. Gelsolin, for example, which severs actin filaments in a calcium-dependent manner and caps the plus ends of severed filaments, preventing the addition of actin monomers, appears to function in the initiation of filopodial retraction and in its smooth progression (Lu *et al.*, 1997). Another example is the actin-capping and regulatory protein Eps8, which is regulated, unlike gelsolin, not by calcium levels, but by protein–protein interactions and phosphorylation (see below). Eps8 is the prototype of a family of proteins involved in the regulation of actin remodelling (Offenhauser *et al.*, 2004). It is able to activate Rac, which in turn regulates the actin cytoskeleton. Moreover, Eps8 directly controls actin dynamics and the architecture of actin structures by capping barbed ends and cross-linking actin filaments, respectively (Croce *et al.*, 2004; Disanza *et al.*, 2006). The barbed-end-capping activity of Eps8 resides in its conserved C-terminal effector domain, and it is functional when the protein is associated with Abi1 (Disanza *et al.*, 2004). Conversely, Eps8 must associate with insulin receptor tyrosine kinase substrate of 53 kDa (IRSp53), also known as binding partner of the brain-specific angiogenesis inhibitor 1 (Abbott *et al.*, 1999; Oda *et al.*, 1999), to efficiently cross-link actin filaments (Disanza *et al.*, 2006). These multiple actin regulatory roles of Eps8 *in vitro* are reflected by the observation that, *in vivo*, Eps8 is required for optimal actin-based motility, intestinal morphogenesis, and filopodia-like extension (Croce *et al.*, 2004; Disanza *et al.*, 2004 and 2006). In hippocampal neurons, overexpression of Eps8 causes the formation of flat, actin-rich protrusions along axons, which resemble lamellipodia extensions; on the other hand, protein silencing leads to increased filopodia formation in the axonal and dendritic compartments (Menna *et al.*, 2009; Fig. 2A). Using fluorescence recovery after photobleaching measurements of actin in developing neurons, which allows measurement of fluorescence recovery as an indication of the movement of fluorophores after perturbation by photobleaching, we show here that the process of Eps8 removal is accompanied by an alteration in actin dynamics at the growth cone, as indicated by the reduction in the half-time of recovery ($t_{1/2}$) after photobleaching (Fig. 2B and C). Interestingly, the increased axonal filopodia formation in Eps8 null hippocampal neurons is significantly reduced upon interference with VASP functions through dominant-negative approaches, suggesting functional competition between the capping activity of Eps8 and the actin-regulatory properties of VASP (Menna *et al.*, 2009).
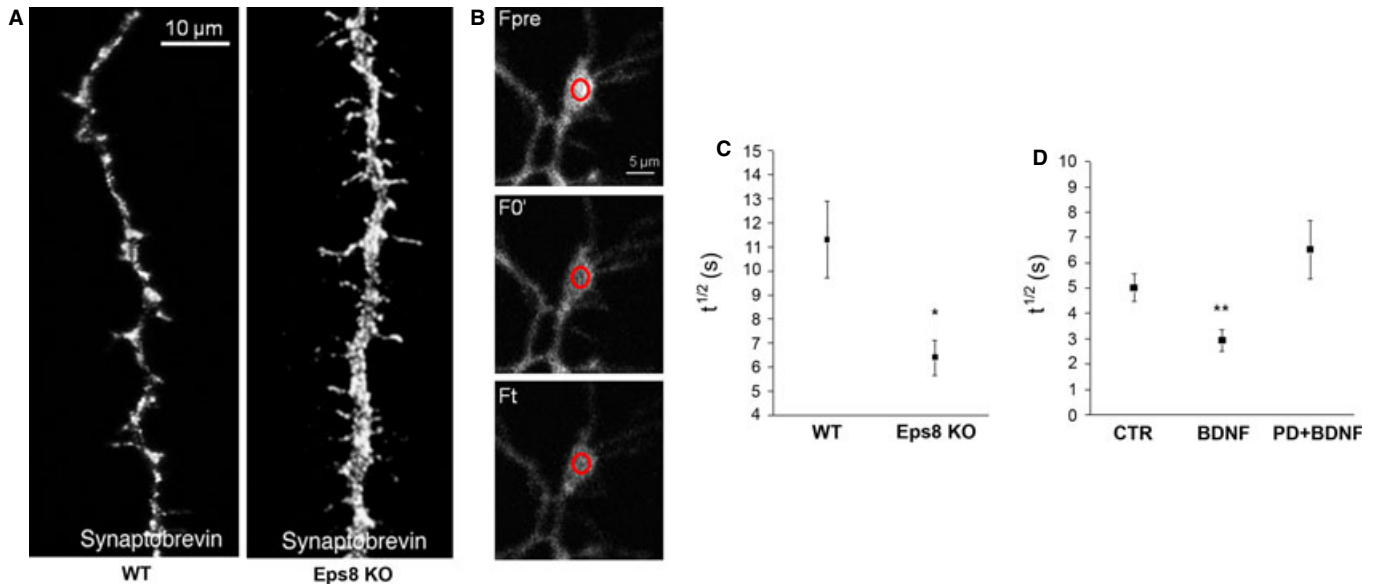
FIG. 2. Removal of capping proteins favours filopodia formation in neurons: the case of Eps8. (A) Increased number of filopodia in neurons from Eps8 knockout (KO) mice relative to wild-type (WT) mice. Staining for the synaptic vesicle synaptobrevin is shown. Reprinted from Menna *et al.* (2009). (B) An axonal growth cone of 6 days *in vitro* hippocampal neurons expressing yellow fluorescent protein–actin selectively photobleached by high-intensity laser light (514 nm). Fluorescence recovery was followed by collecting images at rates of one image every 500 ms for 2.5 min. Scale bar: 5 μm. The red circle represents the region of interest used for both the photobleaching and the fluorescence recovery analysis. For interpretation of color references in figure legend, please refer to the Web version of this article. (C) Actin dynamics at the axonal growth cone are significantly accelerated in the absence of the actin-capping protein Eps8. Number of growth cones: WT, 31; and and Eps8 KO, 25. (Mann–Whitney rank sum test, $P = 0.017$.) (D) Actin dynamics, measured at the axonal growth cone, are significantly accelerated after BDNF treatment, which increases filopodia formation (see text for details). The increase in actin dynamics is prevented by treatment with the MAPK blocker PD98059 (PD). Number of growth cones: control (CTR), 18; BDNF, 18; PD + BDNF, 16. (Kruskal–Wallis one way ANOVA on ranks, $P = 0.002$.) *$P < 0.05$; **$P < 0.01$.

The regulation of capping activity in filopodia formation: intrinsic and extrinsic cues

In a simplified view, actin-capping proteins can be seen as inhibitors, whereas bundling proteins are among the necessary components for filopodia formation. Consistent with this picture, removal of CP, even in non-neuronal cells, causes an increase in the number of filopodia (Mejillano *et al.*, 2004; Applewhite *et al.*, 2007), whereas cells devoid of the actin cross-linker fascin show a reduced amount of filopodia (Vignjevic *et al.*, 2006). Eps8 can efficiently cap barbed ends when bound to Abi-1 (Disanza *et al.*, 2004), whereas it cross-links actin filaments, particularly when it associates with IRSp53, a potent inducer of filopodia via its ability to bind actin filaments and deform the plasma membrane (Scita *et al.*, 2008). Consistent with its dual function, the role of Eps8 in filopodia formation is cell context-dependent. In HeLa and other epithelial cell lines, overexpression of Eps8 promotes the formation of filopodia (Disanza *et al.*, 2006), whereas in primary hippocampal neurons, genetic removal of Eps8 increases the formation of axonal and dendritic filopodia (Menna *et al.*, 2009). By the use of a combination of *in vivo* and *in vitro* experiments, together with a system of ordinary differential equations, a mathematical model was recently generated that allowed us to explain how filopodia are formed in different cellular contexts (Vaggi *et al.*, 2011). This study showed that the biochemical activities of Eps8 as a capper and bundler are a function of the dynamic interactions established by Eps8, IRSp53 and VASP with actin filaments. Eps8 therefore represents a molecular switch in the transduction of signalling, directing the cells towards either reduced or increased formation of filopodia, mainly depending on the relative concentrations of the components of the protein network underlying filopodia formation (Vaggi *et al.*, 2011).

One open question is how extracellular cues are translated into changes in the protein network, which operate in a dynamic interplay to control the actin cytoskeleton remodelling that is important for filopodia formation. Different cues in the extracellular environment have been found to modulate the dynamics of lamellipodia and filopodia, inducing either increased protrusions or collapse (McAllister, 2007; Lundquist, 2009; Mai *et al.*, 2009; Valiente & Martini, 2009). However, the signalling pathways by which these stimuli impact on actin dynamics are largely unknown. In sensory neurons, nerve growth factor (NGF) promotes the formation of axonal filopodia and branches. With the use of chicken sensory neurons and live imaging of enhanced yellow fluorescent protein–actin dynamics, it has been found that NGF induces the formation of microdomains of phosphatidylinositol 3,4,5-trisphosphate and actin patches from which filopodia could emerge. However, NGF does not directly promote the emergence of filopodia from patches themselves (Ketschek & Gallo, 2010). The cytoskeletal proteins downstream of NGF–phosphoinositide 3-kinase signalling are presently not characterized, although the bundling protein fascin might be implicated (Ketschek *et al.*, 2011).

More detailed insights into the signal transduction process by which an extracellular cue may regulate the formation of axonal filopodia have been obtained for the neurotrophin brain-derived neurotrophic factor (BDNF), a protein secreted by synaptic targets to modulate neuronal survival and differentiation, and which induces filopodia formation (Fass *et al.*, 2004; Gehler *et al.*, 2004; Chen *et al.*, 2006). In particular, a direct link between extracellular BDNF and axonal filopodia formation was shown to involve Eps8 capping activity. BDNF, through the activation of Trk receptor tyrosine kinases and activation of mitogen-activated protein kinase (MAPK) signalling, was found to induce phosphorylation of Eps8, thus inhibiting the
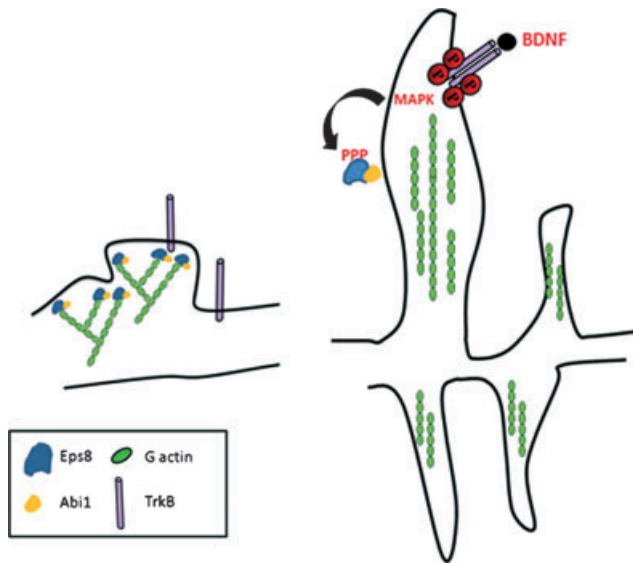
FIG. 3. Neurotrophic factors may control filopodia formation by regulating actin-capping proteins. A model depicting the effect of BDNF in regulating filopodia formation is shown. The neurotrophin, through MAPK activation, phosphorylates Eps8, inducing its detachment from actin barbed ends. This leads to actin elongation and filopodia formation. PPP, phosphorylation.

capping activity of the protein and causing its subcellular redistribution away from actin-rich structures (Menna *et al.*, 2009) (Fig. 3A). Also, neuronal exposure to BDNF led to an alteration in actin dynamics, that is, a reduction in the half-time of recovery, as revealed by fluorescence recovery after photobleaching. The MAPK inhibitor PD98059 completely prevented this effect (Fig. 2D). Therefore, inhibition of actin-capping proteins and consequent alterations in actin dynamics appear to represent key events in filopodia formation. These data also open the possibility that, in response to an external signal such as BDNF, asymmetric deactivation of Eps8 by MAPK on one side of the cell or growth cone may lead to the formation of polarized filopodial protrusions, resulting in altered outgrowth and guidance (Lundquist, 2009). Interestingly, the NGF and BDNF pathways might work in concert, promoting, respectively, the matching between the formation of actin patches and the rate of emergence of filopodia from patches. On the other hand, lack of MAPK activation could decrease the possibility of filopodial extension from actin patches that are formed through the action of phosphoinositide 3-kinase (Ketschek *et al.*, 2011).

Loss of filopodia impairs neuritogenesis: involvement of actin-capping and anti-capping proteins

In recent years, the concept has clearly emerged that the formation of axonal filopodia represents the first step in neuritogenesis. Neuritogenesis and collateral branching, that is, the processes by which postmitotic neurons extend long primary axons towards targets to form appropriate connections, are crucial processes for correct wiring of the brain and for the generation of appropriate synaptic networks (Garner *et al.*, 2006; Korobova & Svitkina, 2008). Ena/VASP family proteins bind actin and regulate the assembly of F-actin networks by antagonizing actin-capping proteins, by enhancing processive elongation, and by promoting the clustering and convergence of filaments at their barbed ends (Bear *et al.*, 2002; Krause *et al.*, 2003; Applewhite *et al.*, 2007; Breitsprecher *et al.*, 2008, 2011; Hansen & Mullins, 2010). Notably, loss of the anti-capping proteins Ena and VASP

causes a striking reduction in filopodia formation in stage 1 cortical neurons. Failure to form filopodia in Ena/VASP-deficient neurons induces a neurite initiation defect and blocks axon fibre tract formation in the cortex (Kwiatkowski *et al.*, 2007). Therefore, reduction of filopodial extension, resulting from loss of Ena/VASP, may be the primary cause of the block in neuritogenesis. Interestingly, neuritogenesis in Ena/VASP-null neurons could be rescued by restoring filopodia formation through ectopic expression of the motor protein myosin X or the actin-nucleating protein mDia2, or by plating cells on the extracellular matrix protein laminin, which promotes the formation of filopodia-like actin-rich protrusions (Dent *et al.*, 2007). These latter observations indicate that there are multiple and possibly independent molecular mechanisms to promote filopodial extension. In the same study, the authors also showed that neurite initiation requires microtubule extension into filopodia, suggesting that interactions between actin filament bundles and dynamic microtubules within filopodia are crucial for neuritogenesis (Dent *et al.*, 2007). This is in line with the concept that actin bundles within filopodia serve as tracks for microtubule exploration (Schaefer *et al.*, 2002) and that neurite formation occurs when actin filaments are destabilized, filopodia are extended, and microtubules invade filopodia (Georges *et al.*, 2008). Therefore, a failure in filopodia formation may lead to a secondary defect in the microtubule-dependent functions required for neuritogenesis. At least one of the molecular components mediating the interaction between microtubules and filopodial F-actin has been identified as drebrin, an F-actin-associated protein that binds directly to the microtubule-binding protein EB3. Indeed, when this interaction is disrupted, the formation of growth cones and the extension of neurites are impaired (Geraldo *et al.*, 2008). Whereas loss of anti-capping proteins impairs neuritogenesis, the genetic absence of actin-capping proteins enhances neuritogenesis. This has been shown in Eps8-deficient neurons, which, in culture, show a significantly higher number of neurites (Fig. 4). Thus, actin-capping and anti-capping proteins, through modulation of filopodia formation, appear to play a crucial role in neuritogenesis.

From filopodia to synapses: actin-capping and anti-capping proteins at neuronal contacts

Filopodia are thought to play an active role in synaptogenesis; in fact, they appear to guide the coordinated growth of presynaptic and postsynaptic partners (Dailey & Smith, 1996; Ziv & Smith, 1996; Fiala *et al.*, 1998; Dunaevsky *et al.*, 1999; Okabe *et al.*, 2001; Evers *et al.*, 2006). This concept is particularly well established in the case of dendritic filopodia, which participate in synaptic contact formation. These protrusions switch to more stable dendritic spines through the actions of synapse-inducing factors and neuronal activity (Jontes & Smith, 2000; Bhatt *et al.*, 2009; Hotulainen *et al.*, 2009; Hotulainen and Hoogenraad, 2010). Although less well investigated, axonal filopodia, which emerge from the shaft of axonal branches and contain small synaptic vesicle clusters, are also thought to be involved in initiating synapse formation (Chang & De Camilli, 2001). Accordingly, the actin-based motility of axonal filopodia is inversely correlated with contact with postsynaptic targets (Tashiro *et al.*, 2003), whereas the emergence of axonal filopodia from varicosities enriched in synaptic vesicles favours assembly of the neuromuscular junction (Li *et al.*, 2011).

Recent data have provided further evidence to support the long-standing concept that control of filopodia motility and number is only one aspect of establishing a synapse. Indeed, the extension of filopodial protrusions must be followed by the establishment of a
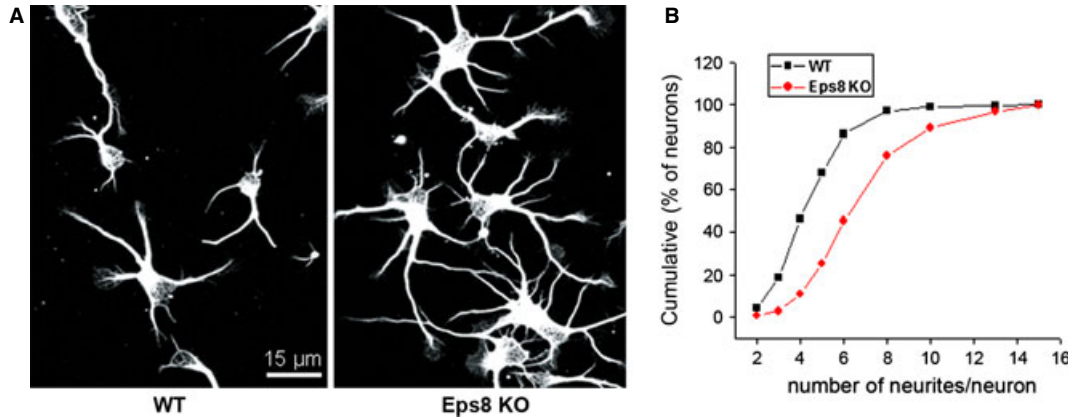
FIG. 4. Removal of the capping protein Eps8 enhances neuritogenesis. (A) βIII-tubulin staining of wild type (WT) and Eps8 knockout (KO) neurons reveals that protein removal induces a significant increase in neurite formation (reprinted from Menna *et al.*, 2009). (B) Cumulative analysis of neurite number in WT and Eps8 KO mice (Kolmogorov–Smirnov test, *P* = 0.001).

transcellular interaction to stabilize the nascent contact. The two processes may be concomitantly controlled, as in the case of EphB, which, by increasing dendritic filopodia motility to initiate presynaptic and postsynaptic contact and by stabilizing nascent synapses through trans-synaptic interactions, mediates a filopodia-based synaptogenesis process (Ethell *et al.*, 2001; Kayser *et al.*, 2008). Arstikaitis *et al.* (2011), using a filopodia-inducing motif that is found in growth-associated protein-43, found enhanced filopodia numbers and motility, but a reduced probability of the formation of a stable axon–dendrite contact; conversely, expression of neuroligin-1 results in a decrease in filopodia motility, but an increase in the number of stable axonal contacts. Hence, enhancing filopodia formation and mobility may not necessarily lead to more stable axon–dendrite contacts. Rather, the production of stable synapses seems to be dependent on key members of the postsynaptic scaffolding complex (Arstikaitis *et al.*, 2011).

It is presently not clear whether actin-capping and anti-capping proteins control the process of synaptogenesis from filopodia, modulating either their density or stability. Notably, however, actin-capping and anti-capping proteins have been recently detected in dendritic spines. Platinum replica electron microscopy analysis has recently revealed that spine heads are characterized by a branched actin filament network containing the Arp2/3 complex and actin-capping proteins, a cytoskeletal organization resembling the conventional lamellipodial structure (Hotulainen & Hoogenraad, 2010). Notably, the actin-capping protein CP, a regulator of actin filament growth, has been found recently to be essential for spine development and maturation, leading to functional synapses (Fan *et al.*, 2011). Presynaptic boutons, as well as spine necks and bases, also contain a very similar branched network of actin cytoskeleton (Korobova & Svitkina, 2010). Furthermore, it has been found that the anti-capping protein VASP is enriched in spine heads and synapses (Lin *et al.*, 2010). VASP expression increases the size of the spine head and results in a significant increase in the amount of actin filaments and uncapped barbed ends available for further actin polymerization in spines (Lin *et al.*, 2010). Ena/VASP was identified as a protein kinase A effector downstream of syndecan-2; in particular, syndecan-2 was found to activate, via neurofibromin, protein kinase A, which in turn phosphorylates Ena/VASP, thus promoting filopodium and spine formation (Lin *et al.*, 2007). Interestingly, in spines, VASP elevates the amount of postsynaptic density scaffolding proteins, including PSD95, Homer, and Shank, and increases the number and retention of glutamate receptor type 1-containing AMPA receptors, thus ultimately
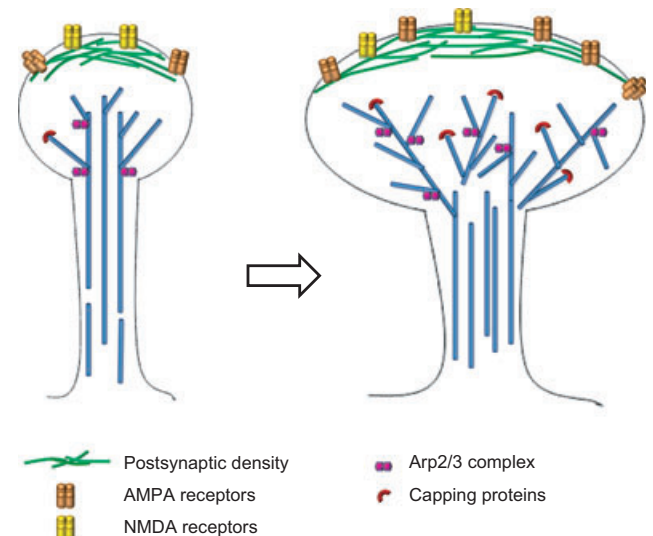

FIG. 5. Actin-capping and branching proteins in spine enlargement. The model depicts the possible involvement of actin-capping and branching proteins in favouring the spine head enlargement that occurs during long-term potentiation (based on Tada and Sheng, 2006; Hotulainen and Hoogenraad, 2010).

potentiating AMPA receptor-mediated synaptic transmission (Takahashi *et al.*, 2003; Lin *et al.*, 2010).

Notably, using fimbria–fornix transection as a model of memory deficit, coupled with a proteomic approach, Kitanishi and coworkers identified the F-actin-capping protein CapZ (Schafer & Cooper, 1995) among the candidate proteins showing a reduction in level after fimbria–fornix transection. CapZ, which has been previously shown to regulate growth cone morphology and neurite outgrowth in cultured hippocampal neurons (Davis *et al.*, 2009), was detected in dendritic spines of neurons *in vitro*, where its expression was reduced after silencing of neuronal activity by tetrodotoxin. Accordingly, unilateral administration of high-frequency stimuli to the medial perforant path in awake rats increased CapZ immunoreactivity (Kitanishi *et al.*, 2010). Activity-dependent CapZ accumulation supported a possible role for the protein in the regulation of actin dynamics in response to synaptic inputs and eventually in synaptic plasticity. All together, these data suggest that regulation of capping activity is involved in

synapse formation and postsynaptic stabilization, as well as in spine plasticity processes (Fig. 5).

Conclusions and perspectives

Actin-capping and anti-capping proteins are crucial regulators of actin dynamics. Recent studies have indicated that these proteins may be heavily involved in all stages of synaptogenesis, from the emergence of filopodia in developing neurons, through the processes of neuritogenesis and contact stabilization, to the structural changes occurring at the synapse during plasticity phenomena. In recent years, it has become evident that many psychiatric disorders, in particular autism and mental retardation, are accompanied by alterations in spine morphology and synapse number (Comery *et al.*, 1997; Irwin *et al.*, 2001; Bourgeron, 2009; Pfeiffer & Huber, 2009; Hutsler & Zhang, 2010; Pfeiffer *et al.*, 2010). It is expected that future genetic studies will identify new mutations in actin-capping and anti-capping proteins that, by altering either the process of filopodia-driven synaptogenesis and / or spine actin regulation, may result in abnormalities of spine morphology and synapse dysfunction.

Acknowledgements

Abbreviations

BNDF, brain-derived neurotrophic factor; CP, capping protein; IRSp53, insulin receptor tyrosine kinases substrate of 53 kDa; MAPK, mitogen-activated protein kinase; NGF, nerve growth factor; VASP, vasodilator-stimulated phosphoprotein.

References

Abbott, M.A., Wells, D.G. & Fallon, J.R. (1999) The insulin receptor tyrosine kinase substrate p58/53 and the insulin receptor are components of CNS synapses. *J. Neurosci.*, **19**, 7300–7308.

Akin, O. & Mullins, R.D. (2008) Capping protein increases the rate of actin-based motility by promoting filament nucleation by the Arp2/3 complex. *Cell*, **133**, 841–851.

Applewhite, D.A., Barzik, M., Kojima, S., Svitkina, T.M., Gertler, F.B. & Borisy, G.G. (2007) Ena/VASP proteins have an anti-capping independent function in filopodia formation. *Mol. Biol. Cell*, **18**, 2579–2591.

Arstikaitis, P., Gauthier-Campbell, C., Huang, K., El-Husseini, A. & Murphy, T.H. (2011) Proteins that promote filopodia stability, but not number, lead to more axonal-dendritic contacts. *PLoS ONE*, **6**, e16998.

Bear, J.E., Svitkina, T.M., Krause, M., Schafer, D.A., Loureiro, J.J., Strasser, G.A., Maly, I.V., Chaga, O.Y., Cooper, J.A., Borisy, G.G. & Gertler, F.B. (2002) Antagonism between Ena/VASP proteins and actin filament capping regulates fibroblast motility. *Cell*, **109**, 509–521.

Bhatt, D.H., Zhang, S. & Gan, W.B. (2009) Dendritic spine dynamics. *Annu. Rev. Physiol.*, **71**, 261–282.

Block, J., Stradal, T.E., Hanisch, J., Geffers, R., Kostler, S.A., Urban, E., Small, J.V., Rottner, K. & Faix, J. (2008) Filopodia formation induced by active mDia2/Drf3. *J. Microsc.*, **231**, 506–517.

Bourgeron, T. (2009) A synaptic trek to autism. *Curr. Opin. Neurobiol.*, **19**, 231–234.

Breitsprecher, D., Kiesewetter, A.K., Linkner, J., Urbanke, C., Resch, G.P., Small, J.V. & Faix, J. (2008) Clustering of VASP actively drives processive, WH2 domain-mediated actin filament elongation. *EMBO J.*, **27**, 2943–2954.

Breitsprecher, D., Kiesewetter, A.K., Linkner, J., Vinzenz, M., Stradal, T.E., Small, J.V., Curth, U., Dickinson, R.B. & Faix, J. (2011) Molecular mechanism of Ena/VASP-mediated actin-filament elongation. *EMBO J.*, **30**, 456–467.

Bruel-Jungerman, E., Davis, S. & Laroche, S. (2007) Brain plasticity mechanisms and memory: a party of four. *Neuroscientist*, **13**, 492–505.

Chang, S. & De Camilli, P. (2001) Glutamate regulates actin-based motility in axonal filopodia. *Nat. Neurosci.*, **4**, 787–793.

Chen, T.J., Gehler, S., Shaw, A.E., Bamburg, J.R. & Letourneau, P.C. (2006) Cdc42 participates in the regulation of ADF/cofilin and retinal growth cone filopodia by brain derived neurotrophic factor. *J. Neurobiol.*, **66**, 103–114.

Chesarone, M.A. & Goode, B.L. (2009) Actin nucleation and elongation factors: mechanisms and interplay. *Curr. Opin. Cell Biol.*, **21**, 28–37.

Chklovskii, D.B., Mel, B.W. & Svoboda, K. (2004) Cortical rewiring and information storage. *Nature*, **431**, 782–788.

Comery, T.A., Harris, J.B., Willems, P.J., Oostra, B.A., Irwin, S.A., Weiler, I.J. & Greenough, W.T. (1997) Abnormal dendritic spines in fragile X knockout mice: maturation and pruning deficits. *Proc. Natl. Acad. Sci. USA*, **94**, 5401–5404.

Craig, A.M., Graf, E.R. & Linhoff, M.W. (2006) How to build a central synapse: clues from cell culture. *Trends Neurosci.*, **29**, 8–20.

Croce, A., Cassata, G., Disanza, A., Gagliani, M.C., Tacchetti, C., Malabarba, M.G., Carlier, M.F., Scita, G., Baumeister, R. & Di Fiore, P.P. (2004) A novel actin barbed-end-capping activity in EPS-8 regulates apical morphogenesis in intestinal cells of Caenorhabditis elegans. *Nat. Cell Biol.*, **6**, 1173–1179.

Dailey, M.E. & Smith, S.J. (1996) The dynamics of dendritic structure in developing hippocampal slices. *J. Neurosci.*, **16**, 2983–2994.

Davis, D.A., Wilson, M.H., Giraud, J., Xie, Z., Tseng, H.C., England, C., Herscovitz, H., Tsai, L.H. & Delalle, I. (2009) Capzb2 interacts with beta-tubulin to regulate growth cone morphology and neurite outgrowth. *PLoS Biol.*, **7**, e1000208.

Dent, E.W., Kwiatkowski, A.V., Mebane, L.M., Philippar, U., Barzik, M., Rubinson, D.A., Gupton, S., Van Veen, J.E., Furman, C., Zhang, J., Alberts, A.S., Mori, S. & Gertler, F.B. (2007) Filopodia are required for cortical neurite initiation. *Nat. Cell Biol.*, **9**, 1347–1359.

Disanza, A., Carlier, M.F., Stradal, T.E., Didry, D., Frittoli, E., Confalonieri, S., Croce, A., Wehland, J., Di Fiore, P.P. & Scita, G. (2004) Eps8 controls actin-based motility by capping the barbed ends of actin filaments. *Nat. Cell Biol.*, **6**, 1180–1188.

Disanza, A., Mantoani, S., Hertzog, M., Gerboth, S., Frittoli, E., Steffen, A., Berhoerster, K., Kreienkamp, H.J., Milanesi, F., Di Fiore, P.P., Ciliberto, A., Stradal, T.E. & Scita, G. (2006) Regulation of cell shape by Cdc42 is mediated by the synergic actin-bundling activity of the Eps8–IRSp53 complex. *Nat. Cell Biol.*, **8**, 1337–1347.

Drees, F. & Gertler, F.B. (2008) Ena/VASP: proteins at the tip of the nervous system. *Curr. Opin. Neurobiol.*, **18**, 53–59.

Dunaevsky, A., Tashiro, A., Majewska, A., Mason, C. & Yuste, R. (1999) Developmental regulation of spine motility in the mammalian central nervous system. *Proc. Natl. Acad. Sci. USA*, **96**, 13438–13443.

Ethell, I.M., Irie, F., Kalo, M.S., Couchman, J.R., Pasquale, E.B. & Yamaguchi, Y. (2001) EphB/syndecan-2 signaling in dendritic spine morphogenesis. *Neuron*, **31**, 1001–1013.

Evers, J.F., Muench, D. & Duch, C. (2006) Developmental relocation of presynaptic terminals along distinct types of dendritic filopodia. *Dev. Biol.*, **297**, 214–227.

Faix, J., Breitsprecher, D., Stradal, T.E. & Rottner, K. (2009) Filopodia: complex models for simple rods. *Int. J. Biochem. Cell Biol.*, **41**, 1656–1664.

Fan, Y. & Tang, X., Vitriol, E., Chen, G. & Zheng, J.Q. (2011) Actin capping protein is required for dendritic spine development and synapse formation. *J. Neurosci.*, **31**, 10228–10233.

Fass, J., Gehler, S., Sarmiere, P., Letourneau, P. & Bamburg, J.R. (2004) Regulating filopodial dynamics through actin-depolymerizing factor/cofilin. *Anat. Sci. Int.*, **79**, 173–183.

Fiala, J. C., Feinberg, M., Popov, V. & Harris, K.M. (1998) Synaptogenesis via dendritic filopodia in developing hippocampal area CA1. *J. Neurosci.*, **18**, 8900–8911.

Fu, M. & Zuo, Y. (2011) Experience-dependent structural plasticity in the cortex. *Trends Neurosci.*, **34**, 177–187.

Garner, C.C., Waites, C.L. & Ziv, N.E. (2006) Synapse development: still looking for the forest, still lost in the trees. *Cell Tissue Res.*, **326**, 249–262.

Gehler, S., Shaw, A.E., Sarmiere, P.D., Bamburg, J.R. & Letourneau, P.C. (2004) Brain-derived neurotrophic factor regulation of retinal growth cone

filopodial dynamics is mediated through actin depolymerizing factor/cofilin. *J. Neurosci.*, **24**, 10741–10749.

Georges, P.C., Hadzimichalis, N.M., Sweet, E.S. & Firestein, B.L. (2008) The yin-yang of dendrite morphology: unity of actin and microtubules. *Mol. Neurobiol.*, **38**, 270–284.

Geraldo, S. & Gordon-Weeks, P.R. (2009) Cytoskeletal dynamics in growth-cone steering. *J. Cell Sci.*, **122**, 3595–3604.

Geraldo, S., Khanzada, U.K., Parsons, M., Chilton, J.K. & Gordon-Weeks, P.R. (2008) Targeting of the F-actin-binding protein drebrin by the microtubule plus-tip protein EB3 is required for neuritogenesis. *Nat. Cell Biol.*, **10**, 1181–1189.

Gupton, S.L., Eisenmann, K., Alberts, A.S. & Waterman-Storer, C.M. (2007) mDia2 regulates actin and focal adhesion dynamics and organization in the lamella for efficient epithelial cell migration. *J. Cell Sci.*, **120**, 3475–3487.

Hansen, S.D. & Mullins, R.D. (2010) VASP is a processive actin polymerase that requires monomeric actin for barbed end association. *J. Cell Biol.*, **191**, 571–584.

Heiman, M.G. & Shaham, S. (2010) Twigs into branches: how a filopodium becomes a dendrite. *Curr. Opin. Neurobiol.*, **20**, 86–91.

Hotulainen, P. & Hoogenraad, C.C. (2010). Actin in dendritic spines: connecting dynamics to function. *J. Cell Biol.*, **189**, 619–629.

Hotulainen, P., Llano, O., Smirnov, S., Tanhuanpaa, K., Faix, J., Rivera, C. & Lappalainen, P. (2009) Defining mechanisms of actin polymerization and depolymerization during dendritic spine morphogenesis. *J. Cell Biol.*, **185**, 323–339.

Hutsler, J.J. & Zhang, H. (2010) Increased dendritic spine densities on cortical projection neurons in autism spectrum disorders. *Brain Res.*, **1309**, 83–94.

Irwin, S.A., Patel, B., Idupulapati, M., Harris, J.B., Crisostomo, R.A., Larsen, B.P., Kooy, F., Willems, P.J., Cras, P., Kozlowski, P.B., Swain, R.A., Weiler, I.J. & Greenough, W.T. (2001) Abnormal dendritic spine characteristics in the temporal and visual cortices of patients with fragile-X syndrome: a quantitative examination. *Am. J. Med. Genet.*, **98**, 161–167.

Jontes, J.D. & Smith, S.J. (2000) Filopodia, spines, and the generation of synaptic diversity. *Neuron*, **27**, 11–14.

Jourdain, P., Fukunaga, K. & Muller, D. (2003) Calcium/calmodulin-dependent protein kinase II contributes to activity-dependent filopodia growth and spine formation. *J. Neurosci.*, **23**, 10645–10649.

Kayser, M.S., Nolt, M.J. & Dalva, M.B. (2008) EphB receptors couple dendritic filopodia motility to synapse formation. *Neuron*, **59**, 56–69.

Ketschek, A. & Gallo, G. (2010) Nerve growth factor induces axonal filopodia through localized microdomains of phosphoinositide 3-kinase activity that drive the formation of cytoskeletal precursors to filopodia. *J. Neurosci.*, **30**, 12185–12197.

Ketschek, A., Spillane, M. & Gallo, G. (2011) Mechanism of NGF-induced formation of axonal filopodia: NGF turns up the volume, but the song remains the same? *Commun. Integr. Biol.*, **4**, 55–58.

Kitanishi, T., Sakai, J., Kojima, S., Saitoh, Y., Inokuchi, K., Fukaya, M., Watanabe, M., Matsuki, N. & Yamada, M.K. (2010) Activity-dependent localization in spines of the F-actin capping protein CapZ screened in a rat model of dementia. *Genes Cells*, **15**, 737–747.

Knott, G. & Holtmaat, A. (2008) Dendritic spine plasticity – current understanding from *in vivo* studies. *Brain Res. Rev.*, **58**, 282–289.

Koleske, A.J. (2003) Do filopodia enable the growth cone to find its way? *Sci. STKE*, **183**, pe20.

Korobova, F. & Svitkina, T. (2008) Arp2/3 complex is important for filopodia formation, growth cone motility, and neuritogenesis in neuronal cells. *Mol. Biol. Cell*, **19**, 1561–1574.

Korobova, F. & Svitkina, T. (2010) Molecular architecture of synaptic actin cytoskeleton in hippocampal neurons reveals a mechanism of dendritic spine morphogenesis. *Mol. Biol. Cell*, **21**, 165–176.

Krause, M., Dent, E.W., Bear, J.E., Loureiro, J.J. & Gertler, F.B. (2003) Ena/VASP proteins: regulators of the actin cytoskeleton and cell migration. *Annu. Rev. Cell Dev. Biol.*, **19**, 541–564.

Kwiatkowski, A.V., Rubinson, D.A., Dent, E.W., Edward van Veen, J., Leslie, J.D., Zhang, J., Mebane, L.M., Philippar, U., Pinheiro, E.M., Burds, A.A., Bronson, R.T., Mori, S., Fassler, R. & Gertler, F.B. (2007) Ena/VASP is required for neuritogenesis in the developing cortex. *Neuron*, **56**, 441–455.

Le Clainche, C. & Carlier, M.F. (2008) Regulation of actin assembly associated with protrusion and adhesion in cell migration. *Physiol. Rev.*, **88**, 489–513.

Li, P.P., Chen, C., Lee, C.W., Madhavan, R. & Peng, H.B. (2011) Axonal filopodial asymmetry induced by synaptic target. *Mol. Biol. Cell*, **22**, 2480–2490.

Lin, Y.L., Nehban, C.A., Hong, C.J. & Hsueh, Y.P. (2007) Syndecan-2 induces filopodia and dendritic spine formation via the neurofibromin–PKA–Ena/VASP pathway. *J. Cell Biol.*, **177**, 829–841.

Lin, Y.L., Lei, Y.T., Anderson, B.R. & Webb, D.J. (2011) Vasodilator-stimulated phosphoprotein (VASP) induces actin assembly in dendritic spines to promote their development and potentiate synaptic strength. *J. Biol. Chem.*, **285**, 36010–36020.

Lu, M., Witke, W., Kwiatkowski, D.J. & Kosik, K.S. (1997) Delayed retraction of filopodia in gelsolin null mice. *J. Cell Biol.*, **138**, 1279–1287.

Lundquist, E.A. (2009) The finer points of filopodia. *PLoS Biol.*, **7**, e1000142.

Luscher, C., Nicoll, R.A., Malenka, R.C. & Muller, D. (2000) Synaptic plasticity and dynamic modulation of the postsynaptic membrane. *Nat. Neurosci.*, **3**, 545–550.

Mai, J., Fok, L., Gao, H., Zhang, X. & Poo, M.M. (2009) Axon initiation and growth cone turning on bound protein gradients. *J. Neurosci.*, **29**, 7450–7458.

Matteoli, M., Coco, S., Schenk, U. & Verderio, C. (2004) Vesicle turnover in developing neurons: how to build a presynaptic terminal. *Trends Cell Biol.*, **14**, 133–140.

Mattila, P.K. & Lappalainen, P. (2008) Filopodia: molecular architecture and cellular functions. *Nat. Rev. Mol. Cell Biol.*, **9**, 446–454.

McAllister, A.K. (2007) Dynamic aspects of CNS synapse formation. *Annu. Rev. Neurosci.*, **30**, 425–450.

Mejillano, M.R., Kojima, S., Applewhite, D.A., Gertler, F.B., Svitkina, T.M. & Borisy, G.G. (2004) Lamellipodial versus filopodial mode of the actin nanomachinery: pivotal role of the filament barbed end. *Cell*, **118**, 363–373.

Mellor, H. (2010) The role of formins in filopodia formation. *Biochim. Biophys. Acta*, **1803**, 191–200.

Menna, E., Disanza, A., Cagnoli, C., Schenk, U., Gelsomino, G., Frittoli, E., Hertzog, M., Offenhauser, N., Sawallisch, C., Kreienkamp, H.J., Gertler, F.B., Di Fiore, P.P., Scita, G. & Matteoli, M. (2009) Eps8 regulates axonal filopodia in hippocampal neurons in response to brain-derived neurotrophic factor (BDNF). *PLoS Biol.*, **7**, e1000138.

Mogilner, A. & Rubinstein, B. (2005) The physics of filopodial protrusion. *Biophys. J.*, **89**, 782–795.

Nikonenko, I., Jourdain, P. & Muller, D. (2003) Presynaptic remodeling contributes to activity-dependent synaptogenesis. *J. Neurosci.*, **23**, 8498–8505.

Oda, K., Shiratsuchi, T., Nishimori, H., Inazawa, J., Yoshikawa, H., Taketani, Y., Nakamura, Y. & Tokino, T. (1999) Identification of BAIAP2 (BAI-associated protein 2), a novel human homologue of hamster IRSp53, whose SH3 domain interacts with the cytoplasmic domain of BAI1. *Cytogenet. Cell Genet.*, **84**, 75–82.

Offenhauser, N., Borgonovo, A., Disanza, A., Romano, P., Ponzanelli, I., Iannolo, G., Di Fiore, P.P. & Scita, G. (2004) The eps8 family of proteins links growth factor stimulation to actin reorganization generating functional redundancy in the Ras/Rac pathway. *Mol. Biol. Cell*, **15**, 91–98.

Okabe, S., Miwa, A. & Okado, H. (2001) Spine formation and correlated assembly of presynaptic and postsynaptic molecules. *J. Neurosci.*, **21**, 6105–6114.

Ono, S. (2007) Mechanism of depolymerization and severing of actin filaments and its significance in cytoskeletal dynamics. *Int. Rev. Cytol.*, **258**, 1–82.

Pellegrin, S. & Mellor, H. (2005) The Rho family GTPase Rif induces filopodia through mDia2. *Curr. Biol.*, **15**, 129–133.

Pfeiffer, B.E. & Huber, K.M. (2009) The state of synapses in fragile X syndrome. *Neuroscientist*, **15**, 549–567.

Pfeiffer, B.E., Zang, T., Wilkerson, J.R., Taniguchi, M., Maksimova, M.A., Smith, L.N., Cowan, C.W. & Huber, K.M. (2010) Fragile X mental retardation protein is required for synapse elimination by the activity-dependent transcription factor MEF2. *Neuron*, **66**, 191–197.

Portera-Cailliau, C., Pan, D.T. & Yuste, R. (2003) Activity-regulated dynamic behavior of early dendritic protrusions: evidence for different types of dendritic filopodia. *J. Neurosci.*, **23**, 7129–7142.

Ridley, A.J. (2011) Life at the leading edge. *Cell*, **145**, 1012–1022.

Schaefer, A.W., Kabir, N. & Forscher, P. (2002) Filopodia and actin arcs guide the assembly and transport of two populations of microtubules with unique dynamic parameters in neuronal growth cones. *J. Cell Biol.*, **158**, 139–152.

Schafer, D.A. & Cooper, J.A. (1995) Control of actin assembly at filament ends. *Annu. Rev. Cell Dev. Biol.*, **11**, 497–518.

Schirenbeck, A., Bretschneider, T., Arasada, R., Schleicher, M. & Faix, J. (2005) The Diaphanous-related formin dDia2 is required for the formation and maintenance of filopodia. *Nat. Cell Biol.*, **7**, 619–625.

Scita, G., Confalonieri, S., Lappalainen, P. & Suetsugu, S. (2008) IRSp53: crossing the road of membrane and actin dynamics in the formation of membrane protrusions. *Trends Cell Biol.*, **18**, 52–60.

Svitkina, T.M., Bulanova, E.A., Chaga, O.Y., Vignjevic, D.M., Kojima, S., Vasiliev, J.M. & Borisy, G.G. (2003) Mechanism of filopodia initiation by reorganization of a dendritic network. *J. Cell Biol.*, **160**, 409–421.

Tada, T. & Sheng, M. (2006) Molecular mechanisms of dendritic spine morphogenesis. *Curr. Opin. Neurobiol.*, **16**, 95–101.

Takahashi, T., Svoboda, K. & Malinow, R. (2003) Experience strengthening transmission by driving AMPA receptors into synapses. *Science*, **299**, 1585–1588.

Tashiro, A., Dunaevsky, A., Blazeski, R., Mason, C.A. & Yuste, R. (2003) Bidirectional regulation of hippocampal mossy fiber filopodial motility by kainate receptors: a two-step model of synaptogenesis. *Neuron*, **38**, 773–784.

Vaggi, F. & Disanza, A., Milanesi, F., Di Fiore, P.P., Menna, E., Matteoli, M., Gov, N.S., Scita, G. & Ciliberto, A. (2011) The Eps8 ⁄ IRSp53 ⁄ VASP network differentially controls actin capping and bundling in filopodia formation. *PLoS Comput Biol.*, **7**, e1002088, doi:10.1371/journal.pcbi.1002088.

Valiente, M. & Martini, F.J. (2009) Migration of cortical interneurons relies on branched leading process dynamics. *Cell Adh. Migr.*, **3**, 278–280.

Vignjevic, D., Peloquin, J. & Borisy, G.G. (2006) *In vitro* assembly of filopodia-like bundles. *Methods Enzymol.*, **406**, 727–739.

Wong, W.T., Faulkner-Jones, B.E., Sanes, J.R. & Wong, R.O. (2000) Rapid dendritic remodeling in the developing retina: dependence on neurotransmission and reciprocal regulation by Rac and Rho. *J. Neurosci.*, **20**, 5024–5036.

Yang, C., Czech, L., Gerboth, S., Kojima, S., Scita, G. & Svitkina, T. (2007) Novel roles of formin mDia2 in lamellipodia and filopodia formation in motile cells. *PLoS Biol.*, **5**, e317.

Yuste, R. & Bonhoeffer, T. (2004) Genesis of dendritic spines: insights from ultrastructural and imaging studies. *Nat. Rev. Neurosci.*, **5**, 24–34.

Ziv, N.E. & Smith, S.J. (1996) Evidence for a role of dendritic filopodia in synaptogenesis and spine formation. *Neuron*, **17**, 91–102.